Discovery and Evaluation of Catalytic Allylation and Amination Reactions

By

Simon Bouyea Lang

Submitted to the graduate degree program in Chemistry and the Graduate Faculty of the University of Kansas in partial fulfillment of the requirements for the degree of Doctor of Philosophy.

_____

Chairperson Jon A. Tunge

_____

Michael D. Clift

_____

Paul R. Hanson

_____

Michael Rubin

_____

Ryan A. Altman

Date Defended: May 11 2016

The Dissertation Committee for Simon B Lang

certifies that this is the approved version of the following dissertation:

Discovery and Evaluation of Catalytic Allylation and Amination Reactions

_____

Chairperson Jon A. Tunge

Date approved: June, 3, 2016

Abstract

Simon B. Lang and Jon. A. Tunge

Department of Chemistry, May 2016

University of Kansas

Presented herein is the development and evaluation of several palladium-catalyzed allylic alkylation reactions and a method for visible light-mediated radical decarboxylative amination. These atom economical, environmentally friendly reactions generate molecular complexity via reactive intermediates formed *in situ* via the loss of carbon dioxide. In Chapter One an overview of the state-of-the-art regarding the combination of transition metal and photocatalysis is presented.

In Chapter Two efforts to combine Palladium and photoredox catalysis to effect the radical decarboxylative allylation (DcA) of amino acids and esters are detailed. This reaction extends the scope of the traditional DcA reaction to carboxylic acids that do not typically undergo two electron decarboxylation and produces CO_2 as the only stoichiometric byproduct. The substrate scope was evaluated and several salient mechanistic observations were made based on a variety of experiments.

Alkyl and phenylacetic carboxylic acids were also used as traceless activating groups for site-selective radical aminodecarboxylation reactions in Chapter Three. This direct functional group interconversion of non-activated carboxylic acids was achieved using mild reaction conditions and tolerated a variety of desirable functionalities.

In Chapter Four typically unreactive allylic alcohols were activated towards palladium-catalyzed Tsuji–Trost reactions by the addition of carbon dioxide. Oxidative addition toward palladium occurred after reversible carbonate formation to provide an electrophilic palladium-π-allyl species and a potent base for the activation of a variety of pronucleophiles *in situ*. Ultimately,

this method allowed for the topologically obvious C–C bond formation while forming water and carbon dioxide as waste.

Chapter 1. Metallaphotoredox catalysis: a review of synthetic applications of dual catalytic systems

Chapter 2. Dual catalytic decarboxylative allylation of amino acids and esters

Chapter 3. Photocatalytic aminodecarboxylation of carboxylic acids

Chapter 4. Activation of alcohols with carbon dioxide: intermolecular allylation of nitroalkanes, nitriles, and aldehydes

Abbreviations

Ac	acetate
Acr	acridinium
Ar	aryl
BINAP	2,2'-bis(diphenylphosphino)-1,1'-binaphthyl
Bn	benzyl
Boc	di-tert-butyl dicarbonate
bpy	bipyridine
Cbz	barboxybenzyl
COD	1,5 cyclooctadiene
COPC	cobaloxime pyridine chloride
Cp	cyclopentadienyl
Cy	cyclohexyl
Dba	dibenzylideneacetone
DBU	1,8-Diazabicycloundec-7-ene
DBC	dicyanobenzene
DCC	*N,N′*-Dicyclohexylcarbodiimide
DCE	dichloroethane
DCM	dichloromethane
DMAP	4-Dimethylaminopyridine
Dme	dimethoxyethane
DMF	dimethylformamide
DMSO	dimethylsulfoxide
dppf	1,1′-Ferrocenediyl-bis(diphenylphosphine
dtbbpy	di-*tert*-butyl-bipyridine
DuPhos	(+)-1,2-Bis[(2*S*,5*S*)-2,5-dimethylphospholano]benzene
EtOH	ethanol
EWG	electron withdrawing group
Ph	phenyl
ppy	phenylpyridine

MeCN	acetonitrile
MeOH	methanol
Mes	mesityl
OTMS	trimethylsiloxy
TBADT	tetrabutylammonium decatungstate
TBAI	tetrabutylammonium iodide
TEMPO	(2,2,6,6-Tetramethylpiperidin-1-yl)oxyl
Tf	triflyl
TFP	Tri(2-furyl)phosphine
THF	tetrahydrofuran
tppts	3,3′,3″-Phosphanetriyltris(benzenesulfonic acid) trisodium salt
TunePhos	(*R*)-1,13-Bis(diphenylphosphino)-7,8-dihydro-6*H*-dibenzo[f,h][1,5]dioxonin
Xantphos	4,5-Bis(diphenylphosphino)-9,9-dimethylxanthene
XPhos	2-Dicyclohexylphosphino-2′,4′,6′-triisopropylbiphenyl

Chapter 1. Metallaphotoredox catalysis: a review of synthetic applications of dual catalytic systems.

1.1 Introduction to photocatalysis

An essential step in the catalysis of organic reactions is the predictable formation of reactive intermediates. One activation pathway is the generation of the electronically excited state of an organic molecule, which can impart unique reactivity. An obstacle to this approach is that most organic molecules require high energy, short wavelength light to access their excited state which can also cause other deleterious side reactions to occur. An alternative is to use a visible light photocatalyst, a molecule that readily absorbs longer wavelengths and converts the energy to chemical potential, which can be transferred to organic molecules. The structures of popular organic and transition metal-containing photocatalysts are depicted in figure 1. Upon the absorption of visible light, the photocatalyst enters the excited state, from which it may interact with organic molecules via electron, atom, or energy transfer. Recent efforts towards the realization of new chemical transformations have utilized photocatalysts to generate

Figure 1. Common visible light photocatalysts

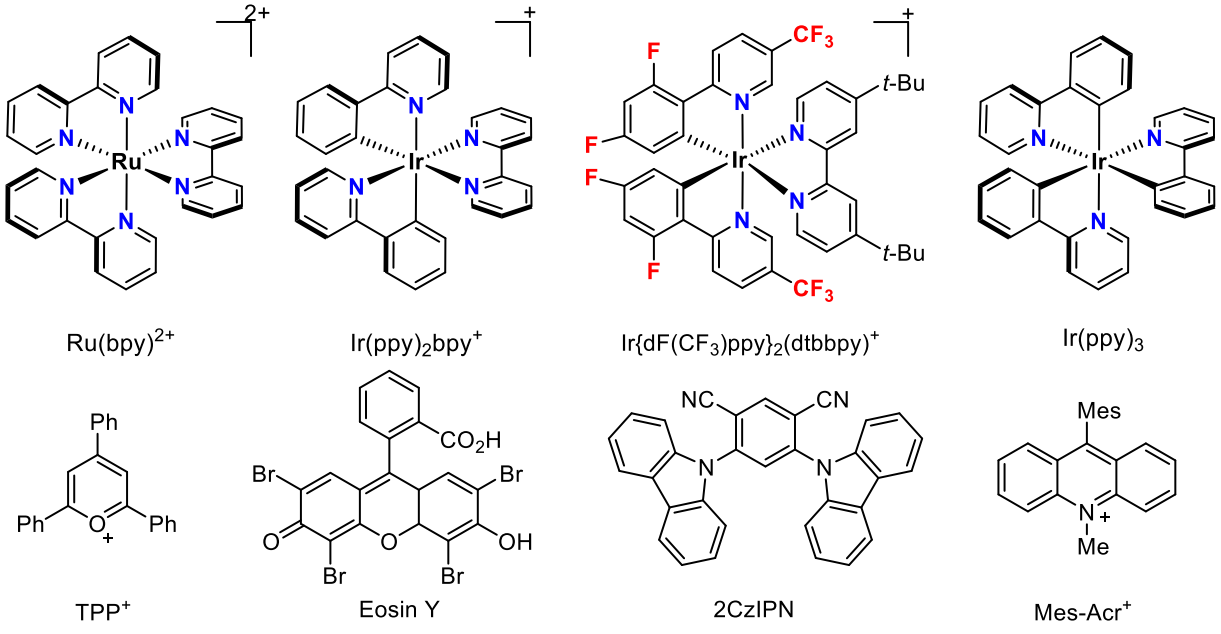

Scheme 1. Photochemistry of $Ir(ppy)_2(bpy)^+$

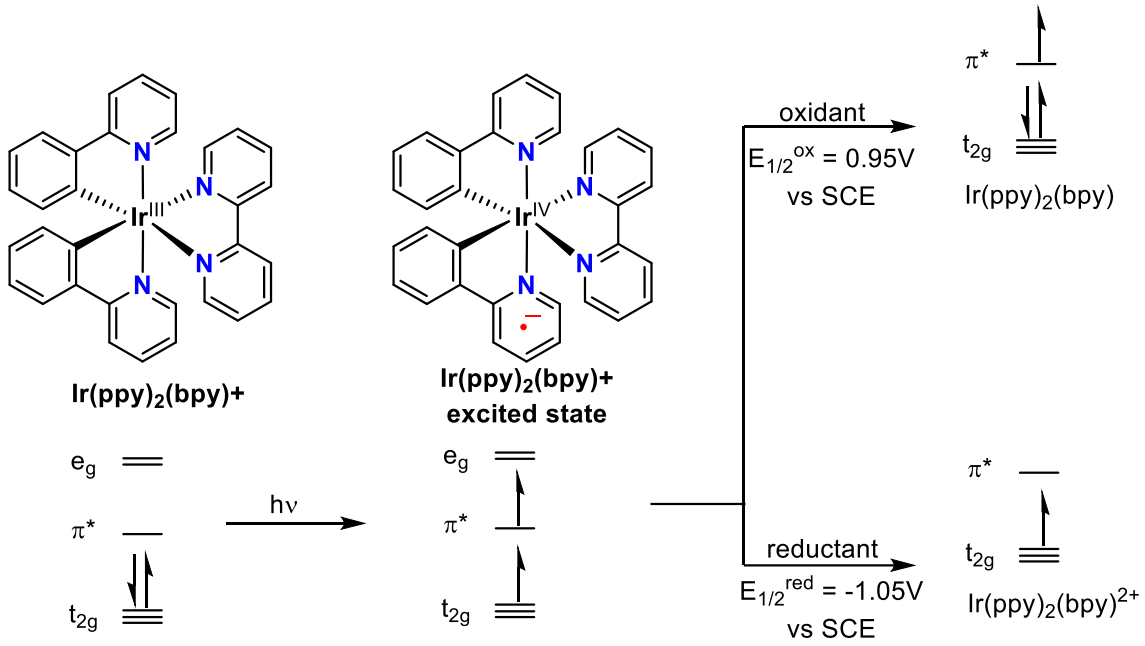

intermediates readily incorporated into traditional catalytic cycles (dual catalysis). Currently, the majority of dual catalytic systems utilize the excited state photocatalyst to modify the oxidation state of an organic molecule by one electron, imparting unique reactivity. The excited state of a photocatalyst is both more oxidizing and more reducing compared to the ground state. The chemistry of the iridium photocatalyst Ir(ppy)2(bpy)$^+$ is illustrative of this phenomenon. Absorption of visible light promotes a metal to ligand charge transfer, which results in the formal oxidation of Ir^{III} to Ir^{IV} (now a potent oxidant) and a reduction of a 2-phenylpyridine ligand by one electron to a radical anion (now a potent reductant). The catalyst can now participate in either a reductive or oxidative quenching cycle based on the propensity of the organic substrate to donate or accept an electron (Scheme 1). In an effort to discover novel environmentally friendly ways to construct bonds, chemists have begun to utilize a separate transition metal catalyst to further manipulate the reactive intermediates in a dual catalytic cycle.

1.2 Dual catalytic cycles involving photoinduced electron transfer

1.2.1 Dual catalytic Sonogashira coupling

One of the first examples of the successful merger of transition metal and photoredox catalysis was reported by Osawa, Nagai, and Akita in 2006. They found that a mixture of

Scheme 2. Pd/Ru metallaphotoredox catalysis of the Sonogashira reaction

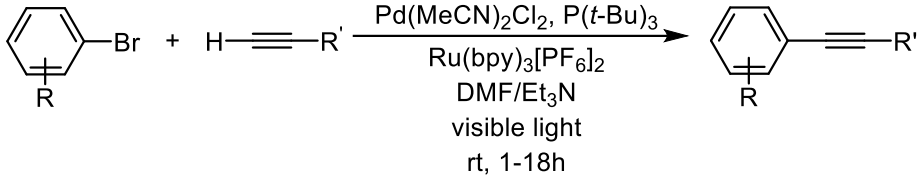

$Pd(CH_3CN)_2/P(t\text{-}Bu)_3$ and $Ru(bpy)_3[PF_6]_2$ promoted the copper-free Sonogashira coupling reaction of aryl bromides and acetylenes at room temperature under visible light irradiation (Scheme 2). The authors postulated that the Pd(II) precursor could be reduced by either the excited state Ru(II)* species or by the reduced Ru(I) species following oxidation of trimethylamine by Ru(II)*. They also speculated that the excited ruthenium complex may affect the oxidative addition of palladium to the aryl bromide, but did not provide specific rationale. Significantly lower yields were observed when the photocatalyst or light were omitted, and when alternating intervals of light and dark were applied, formation of product only occurred under irradiation.[1]

1.2.2 Room temperature arylation and trifluoromethylation

The combination of photoredox and palladium catalysis was also employed by the Stanford group to overcome rate limiting steps in traditional transition metal-catalyzed reactions.[3] Mechanistic analysis of a Pd-catalyzed ligand-directed C–H arylation of amides and aryl pyridines with diaryl iodonium salts by the Sanford group revealed that C–H activation was facile, and that oxidation of a dimeric Pd(II) intermediate to Pd(IV) was the rate-determining step, which required elevated temperatures. When the reactions were performed at room temperature low isolated yields were obtained. They postulated that aryl radicals, which have been demonstrated to participate in Pd catalyzed C–H arylation reaction by the Yu group,[2] could be generated at room temperature via the reduction of aryl diazonium salts by the hydrate of $Ru(bpy)_3Cl_2$ (Scheme 3).[3]

The reaction mechanism involves dual catalysis by a palladium and photoredox cycle. First, C–H activation of the substrate occurs to generate a Pd(II) intermediate, which is then intercepted by an aryl radical provided by the reduction of a aryl diazonium salt with the photoexcited Ru(II) catalyst. The transient Pd(III) aryl species is then oxidized by the resulting Ru(III) catalyst to provide a Pd(IV) intermediate, which provides the desired product after reductive elimination.

Scheme 3. Room Temperature C-H Arylation

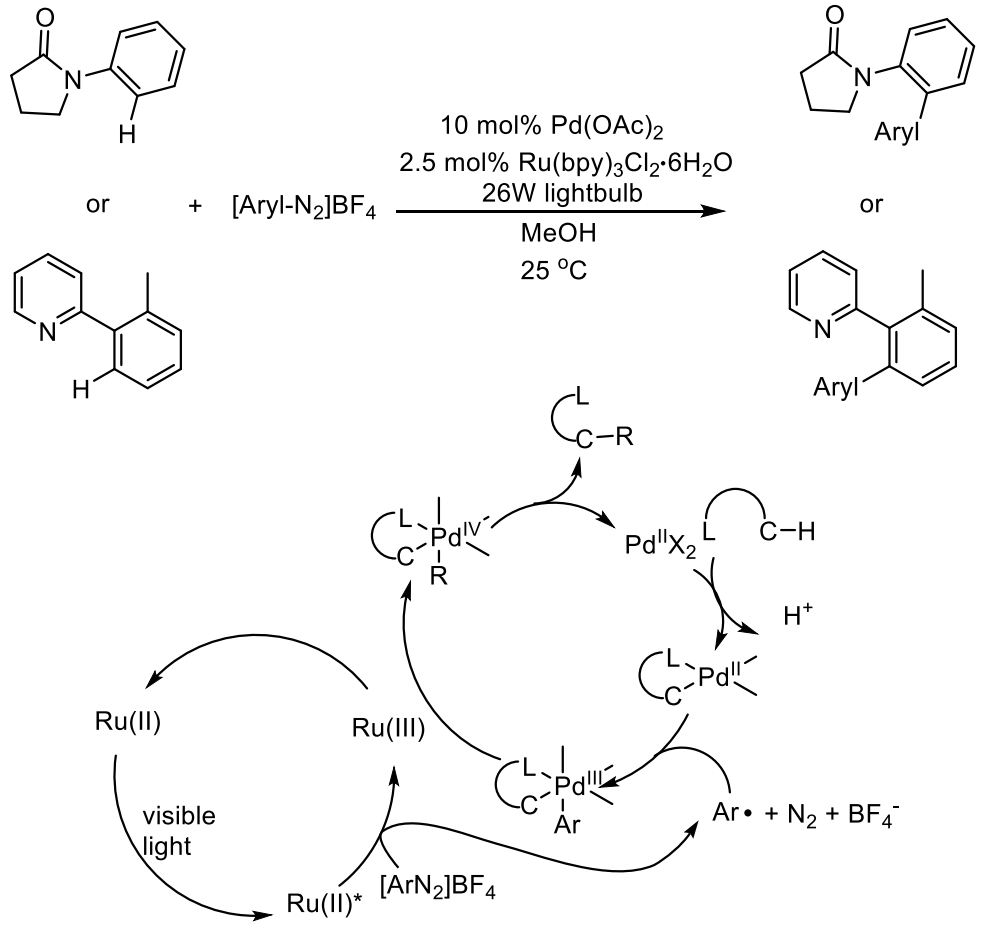

The Sanford group also employed a similar strategy to effect the trifluoromethylation of aryl boronic acids with copper and CF_3I under mild conditions via a radical pathway. In this case an external base was required to facilitate transmetalation, and Cu^{I} salts performed better than Cu^{II} salts. The same $Ru(bpy)_3^{2+}$ photocatalyst facilitated the electron transfer. However, based

upon redox potentials reported in the literature, they suggested that the excited state of the catalyst first oxidizes Cu^{I} to Cu^{II} and the resulting Ru(I) species reduces CF_3I to I^- and the corresponding trifluoromethyl radical (Scheme 4).[4] Interception of the radical by a Cu(III) species followed by transmetalation with the boronic acid and reductive elimination produces the desired product.

Scheme 4. Cu/Ru-Catalyzed Trifluoromethylation of Boronic Acids

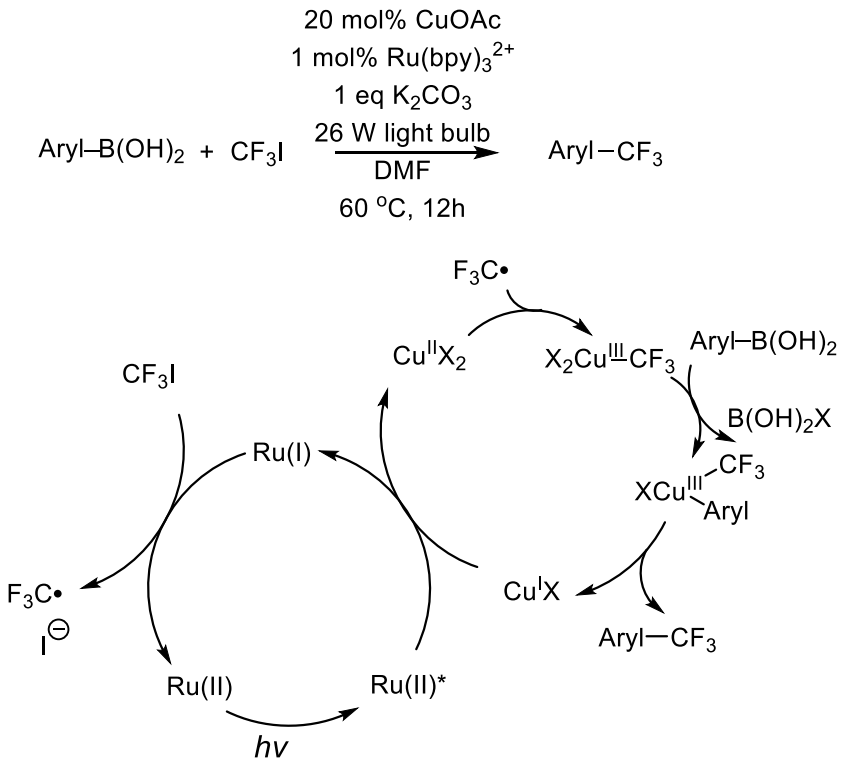

1.2.3 Oxidative Alkynylation of Tetrahydroisoquinolines

Photocatalysts can oxidize tertiary amines to the corresponding radical cation triggering the formation of electrophilic iminium ions, which subsequently undergo attack by organometallic nucleophiles. The cross dehydrogenative coupling of tetrahydroisoquinolines and acetylenes illustrates this mode of reactivity. In 2012, the Rueping group reported a light-induced aerobic oxidation reaction and a metal-catalyzed C–C bond forming that afforded propargylic

tetrahydroisoquinolines (Scheme 5).[5] After exposure to visible light, the photoexcited catalyst $[Ru(bpy)_2(dtbbpy)](PF_6)_2$ oxidizes a nitrogen atom by one electron. Further, removal of an electron and H atom forms an iminium cation. Molecular oxygen is proposed as the terminal oxidant to return the photocatalyst back to the Ru(II) ground state. Subsequently, the copper salt activated the alkyne to form a copper acetylide, which added to the resulting iminium to furnish the desired product. An asymmetric variant with a chiral QUINAP ligated copper species has also been developed.[6]

Scheme 5. Cu/Ru-Catalyzed Photooxidation-Alkynylation

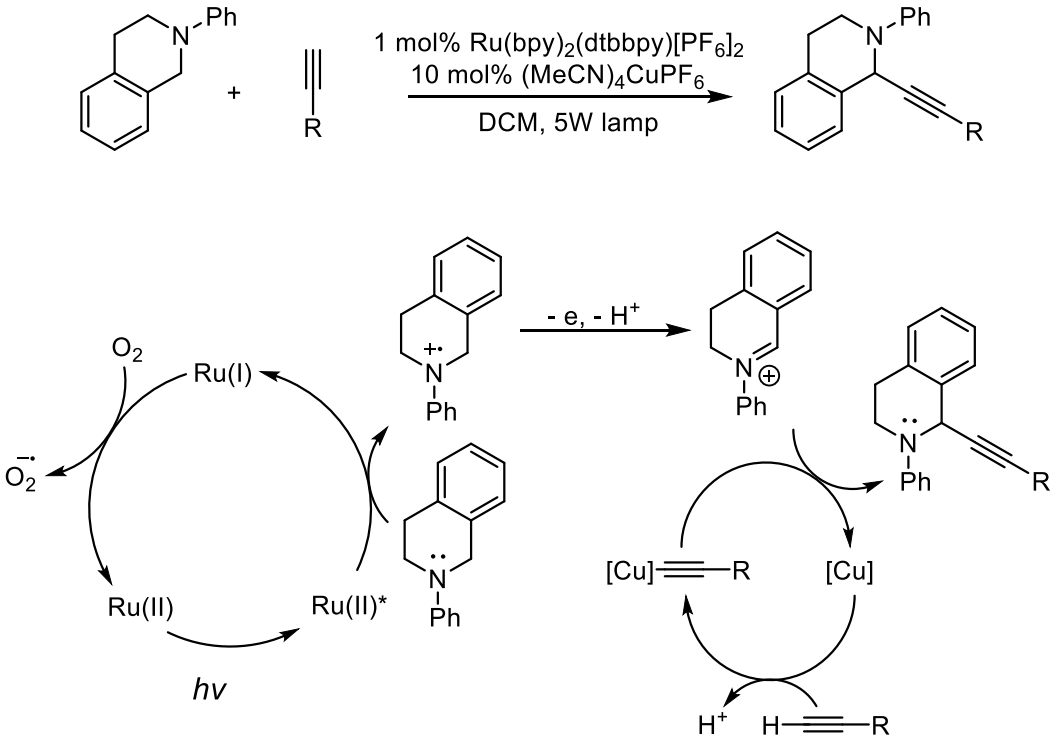

1.2.4 Visible Light-Mediated Oxy- and Aminoarylation of Alkenes

In 2013, the Glorius group sought to extend the scope of Au-catalyzed functionalization of alkenes by avoiding proto-deauration that typically occurs after nucleophilic attack on an Au-activated π system. Instead, they postulated that the Au(I) intermediate, post cyclization, could be intercepted by an aryl radical followed by reductive elimination to provide net oxy- or aminoarylation of alkenes. Optimization studies revealed that the cationic Gagosz catalyst

Scheme 6. Intramolecular oxy- and aminoarylation

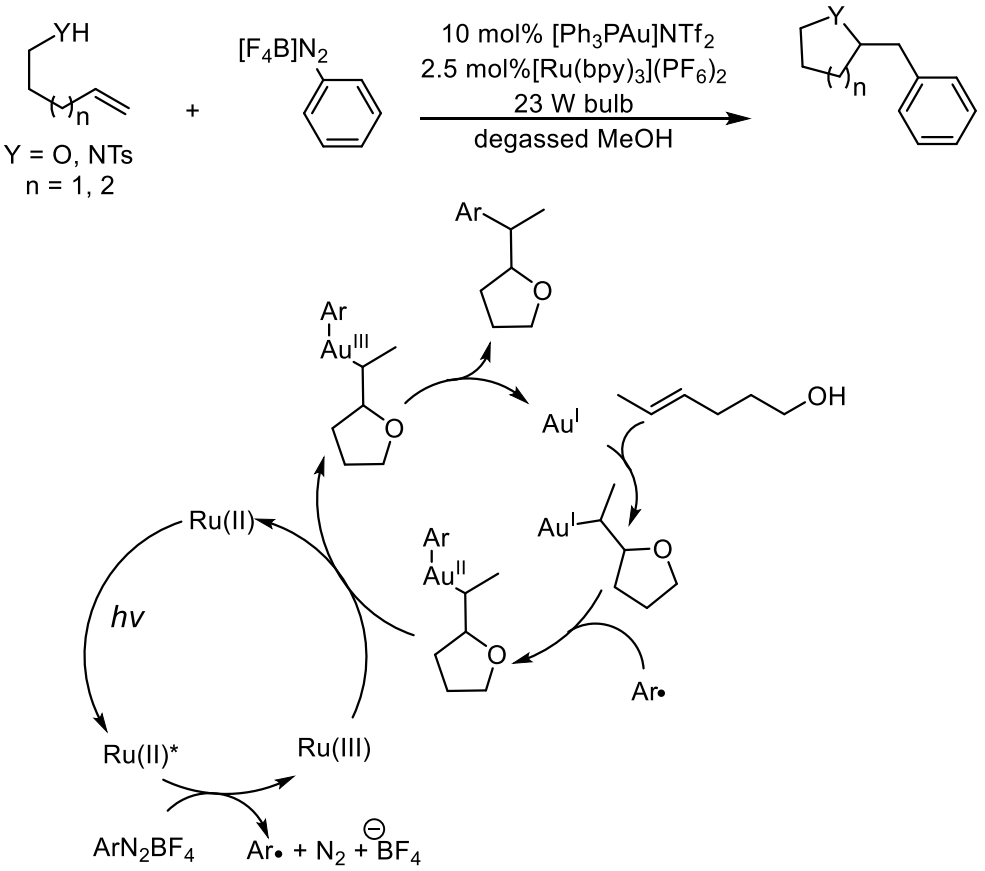

([Ph_3PAu]NTf_2) combined with $Ru(bpy)_3^{2+}$ and aryl diazonium salts previously employed by Sanford promoted the intramolecular cyclization of nucleophiles tethered to alkenes (Scheme 6).[7]

In the proposed mechanism, the excited state Ru(II) photocatalyst reduces the aryl diazonium salt. The resulting aryl radical is then intercepted by the Au(I) complex that forms after intramolecular cyclization. The intermediate Au(II) species is oxidized by one electron by the Ru(III) photocatalyst, and then undergoes reductive elimination to provide the product and regenerate the Au(I) catalyst.

1.2.5 Photoredox and Gold-Catalyzed Arylative Ring Expansion

The Toste group also utilized a combination of gold and photoredox catalysis with aryl diazonium salts to effect an arylative ring expansion of vinyl cyclopropanols and vinyl cyclobutanols. Mechanistic interrogation of the ring expansion revealed that various Au(I)

Scheme 7. Dual catalytic ring expansion

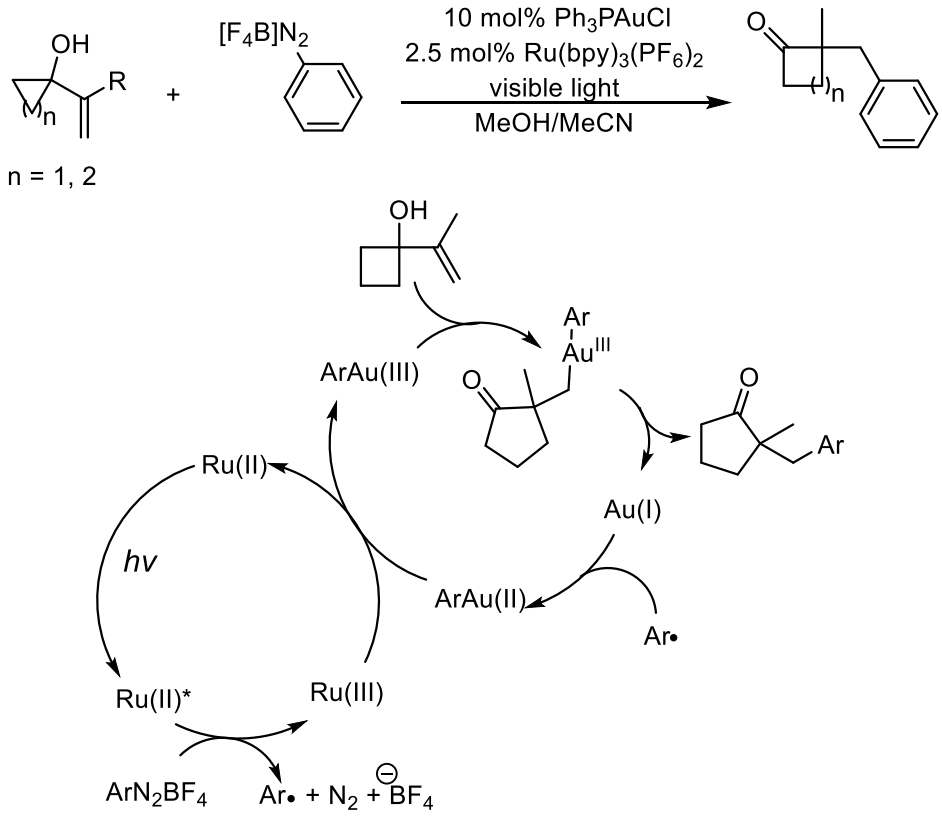

complexes by themselves did not promote the ring expansion event. Based on this observation and the detection of $[PPh_3\text{-}Ph]^+$ salts in the reaction mixture after alkene was consumed, they proposed that a Au(III)Ph species coordinated to the alkene and promoted ring expansion (Scheme 7).[8] The cycle begins with the reduction of the aryl diazonium salt by photoexcited Ru(II)*. This generates an aryl radical which is trapped by Au(I) to provide a transient Au(II) species, which is oxidized by Ru(III) to the electrophilic Au(III) species. Coordination to the alkene triggers the ring expansion metalation reaction followed by reductive elimination to provide the desired product and regenerate the Au(I) catalyst.

1.2.6 The Oxidative Heck Reaction with Visible Light

Photoredox catalysis can also recycle a transition metal catalyst in oxidative olefination reactions. In 2014, the Rueping group sought to replace superstoichiometric oxidants such as $Cu(OAc)_2$, in rhodium-catalyzed oxidative Heck reactions. Specifically, they examined the

rhodium-catalyzed, amide directed, C–H olefination of arenes. It was found that the reaction of rhodium catalyst, alkene, and photocatalyst produced < 5% desired product when conducted under an inert atmosphere. However, when the reaction was run open to air, yields >80% were obtained. Thus, molecular oxygen is involved was in completing the catalytic cycle. The authors found that the reduction potential of the photocatalyst had a direct impact on how efficiently the rhodium photocatalyst was recycled via oxidative formation of hydrogen peroxide as a by-product. Based on these findings, they proposed a dual catalytic cycle, where reduction of molecular oxygen by the photocatalyst is the key step (Scheme 8).[9]

Scheme 8. Oxidative Heck Reactions with Visible Light

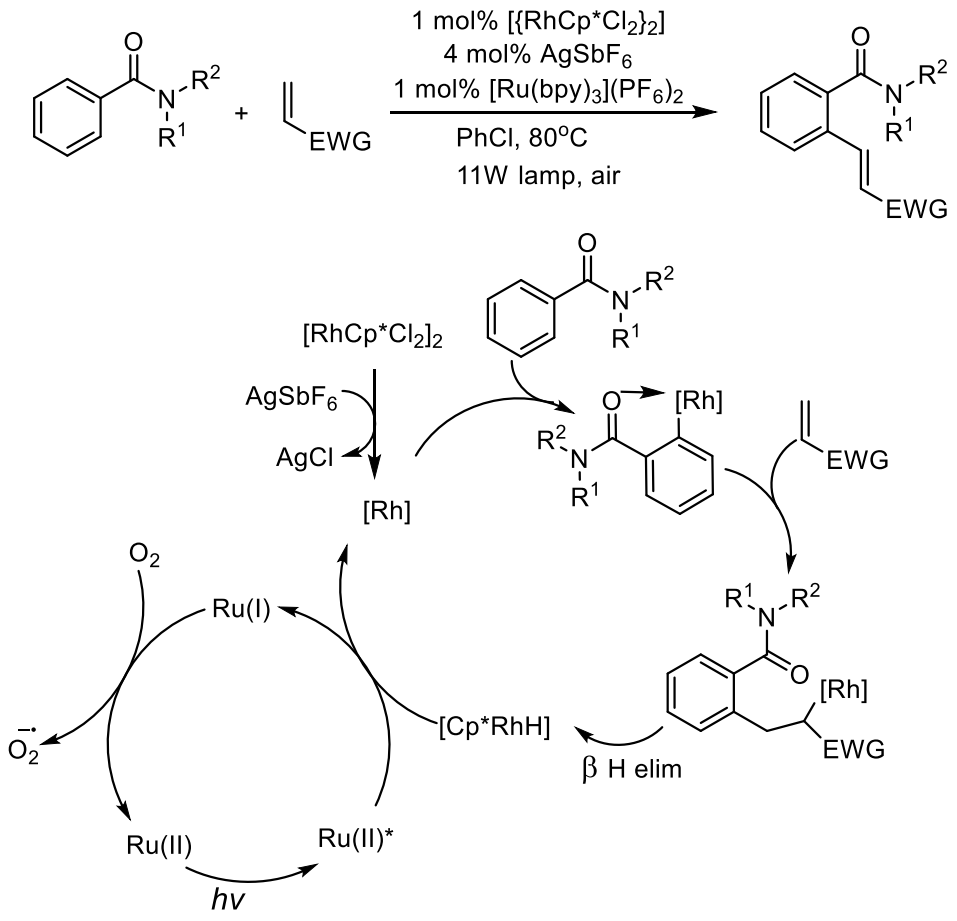

Amide directed C–H activation followed by carborhodation and β hydride elimination affords a rhodium hydride species which is then oxidized back to the active catalyst by the photoexcited

Ru(II)* catalyst. Reduction of molecular oxygen returns the Ru(I) photocatalyst back to the ground state.

A related approach was also reported by the Rueping group for the synthesis of indoles via the palladium-catalyzed C–H activation of aromatic enamines. Again, replacing the superstoichiometric $Cu(OAc)_2$ oxidant with 1 mol% of photocatalyst led to efficient regeneration of the palladium catalyst. Optimization studies revealed that the $Ir(bpy)(ppy)_2[PF_6]$ photocatalyst and the inorganic base K_2CO_3 along with $Pd(OAc)_2$ best facilitated the desired oxidative cyclization (Scheme 9).[10]

Scheme 9. Pd-catalyzed Intramolecular Olefination

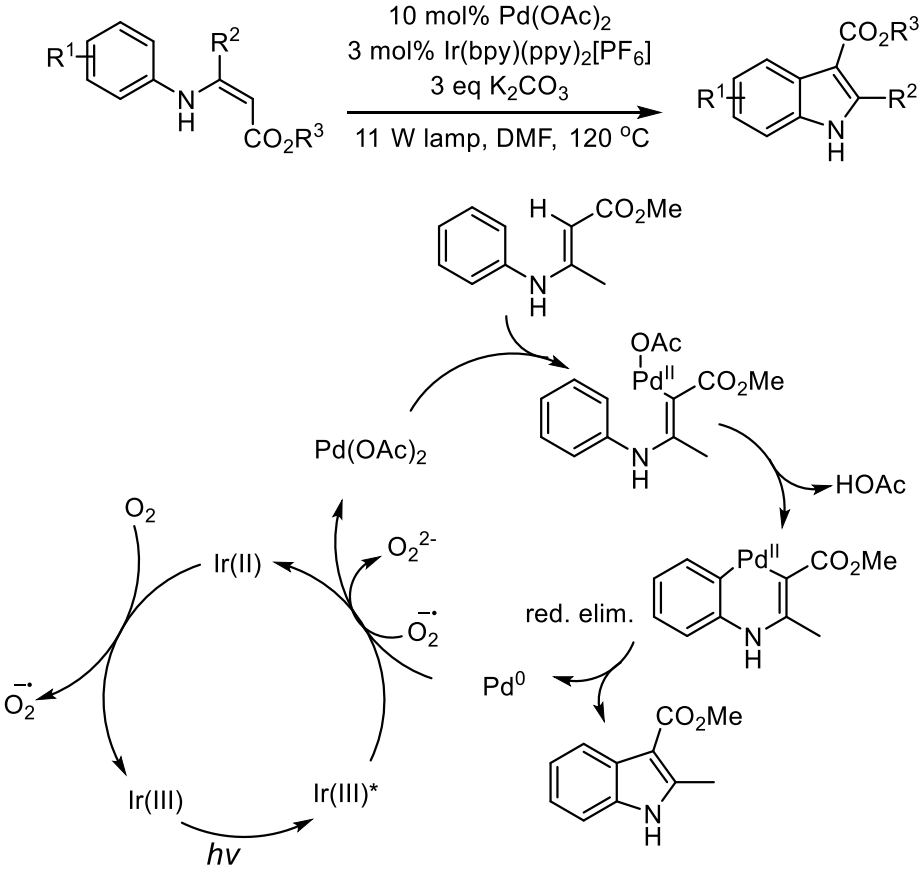

The authors showed that the reaction still reached completion, when potassium superoxide replaced the photocatalyst under an oxygen atmosphere. This result indicated that

the peroxy species that are formed by the reduction of molecular oxygen by the photocatalyst could facilitate the re-oxidation of palladium. Additionally, the reaction was performed under an oxygen atmosphere without photocatalyst to rule out participation by molecular oxygen. The authors propose C–H activation of the olefin, followed by activation of the arene ring. Reductive elimination affords the desired indole and a Pd(0) species, which can either be oxidized back to Pd(II) by the excitied Ir(III)* photocatalyst or by the superoxide formed *in situ*. The reduction of molecular oxygen returns the Ir(II) species back to the Ir(III) ground state. In this reaction, the electronic and steric character for the C2 and C3 positions did not have a significant effect on the product yield.

1.2.7 Single-electron Transmetalation in Organoboron Cross-Coupling

In 2014, the Molander group reported a method to engage C_{sp}^3-hybridized nucleophiles in cross-coupling reactions. The lower rates of oxidative addition and transmetalation along with the alkylmetallic intermediate's propensity to undergo β-hydride elimination are all challenges with employing C_{sp}^3-hybrizined organometallic reagents in traditional cross-coupling reactions.[11] They postulated that accessing a distinct single-electron transfer strategy for activation of organoborons towards transmetalation using a combination of photoredox and transition metal catalysis may provide access to a broad scope of coupling partners. Nickel was chosen due to its high reactivity towards organic halides and the fact it has several redox-accessible oxidation states. The authors found that the combination of Ni(0) ligated by 4,4-di-*tert*-butyl-2,2'-bipyridine (dtbbpy) and the iridium photocatalyst $Ir[dFCF_3ppy]_2(bpy)[PF_6]$ facilitated the room temperature coupling of C_{sp}^3-hybrizied potassium trifluoroborate salts and aryl bromides at room temperature. The additive, 2,6-lutidine helped sequester the boron salts that formed in the reaction mixture (Scheme 10).[11] The authors proposed that oxidative addition of the aryl bromide to Ni(0) provides a Ni(II) species. This organometallic species intercepts the benzylic radical, afforded by the reduction of a benzyl BF_3K salt by the photoexcited Ir(III)*. The resulting Ni(III) species undergoes reductive elimination

Scheme 10. Photoredox cross-coupling of benzylic trifluoroborates and aryl bromides

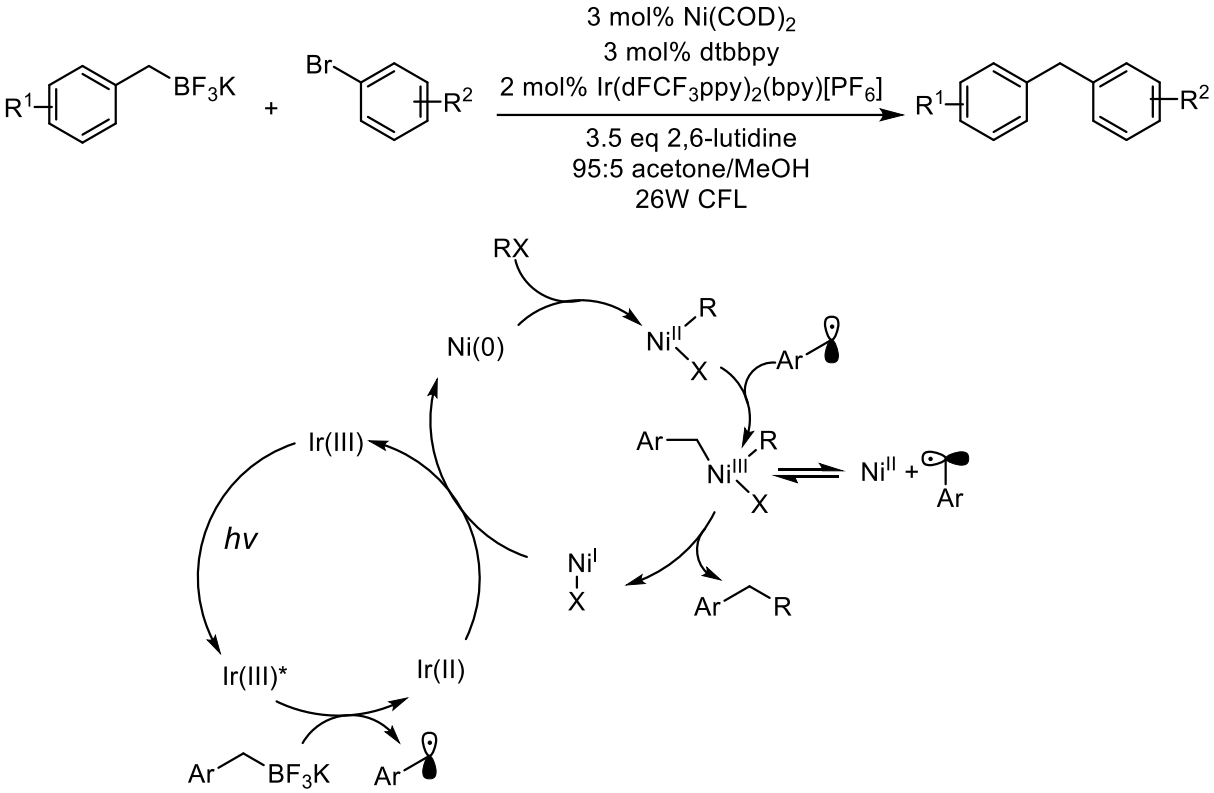

to provide the desired product and Ni(I) which is then reduced by the Ir(II) photocatalyst back to Ni(0). Preliminary mechanistic studies revealed that aryl trifluoroborates were not reduced to the corresponding radicals and that when the dtbbpy ligand was replaced with an enantiopure bidentate ligand stereoconvergent cross-coupling of racemic starting materials occurred. Subsequently, the replacement of air and moisture sensitive $Ni(COD)_2$ with $NiCl_2$dme broadened the utility of the reaction.[12] The reaction conditions tolerated a wide range of non-benzylic secondary potassium alkyltrifluoroborates. Additionally, aryl- and heteroaryl bromides bearing electron donating and electron withdrawing substituents with a variety of functional groups were also incorporated.

The dual catalytic cycle presented in Scheme 10 was also evaluated computationally.[13] The addition of a benzyl radical to a Ni(II) species to from Ni(III) proceeded via a low energy barrier and was reversible. Thus, the origin of the observed stereoselectivity should arise from dynamic kinetic resolution (DKR) of the Ni(III) complex prior to reductive elimination. With this

knowledge in hand, the Molander group has applied similar reaction conditions for the construction of benzylic ethers,[14] α-alkoxyketones,[15] 1,1-diaryl trifluoroethanes,[16] the cross-coupling of alkyltrifluoroborates with borylated aryl bromides,[17] and the α-arylation/heteroarylation of chiral α-aminomethyltrifluoroborates.[18]

1.2.8 Single Electron Transmetalation in Ammonium Alkylsilicate Cross Coupling

Although versatile, alkyltrifluoroborate salts also have several limitations for their incorporation into dual catalytic cross-coupling manifolds. First, they have high oxidation potentials, and once oxidized, they release BF_3, which must be sequestered with excess base during the reaction to prevent inhibition. These drawbacks, coupled with the limited solubility of many analogs, led the Molander group to pursue alternate radical precursors that have lower oxidation potentials.[19] Screening led them to alkylbis(catecholato)silicate derivatives bearing an alkyl-ammonium cation (E^0 =+0.75V vs SCE) which could be prepared by reluxing an alkyltrimethoxy silane in THF with an amine base (Scheme 11).

Scheme 11. Preparation of Ammonium Alkylbis(catecholato)silicates

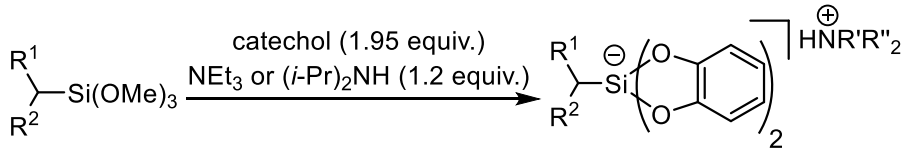

These radical precursors provide innocuous byproducts upon oxidation, and do not require the addition of base. Because of these advantages, a wide range of protic functional groups, including unprotected primary amines successfully reacted with a wide-range of heteroaryl- and arylbromides.[19] Shortly after, the Molander group also reported the successful coupling of the same alkylsilicates with a range of alkenyl halides.[20] The mechanism, based on previous DFT studies, likey begins by the addition of an alkyl radical, generated by the single electron oxidation of the silicate by Ru(II)*, to Ni(0) (Scheme 12). The resulting Ni(I) intermediate undergoes oxidative addition to an aryl or alkenylhalide to provide a Ni(III) intermediate that is in equilibrium

Scheme 12. Photoredox cross-coupling of alkyl silicates

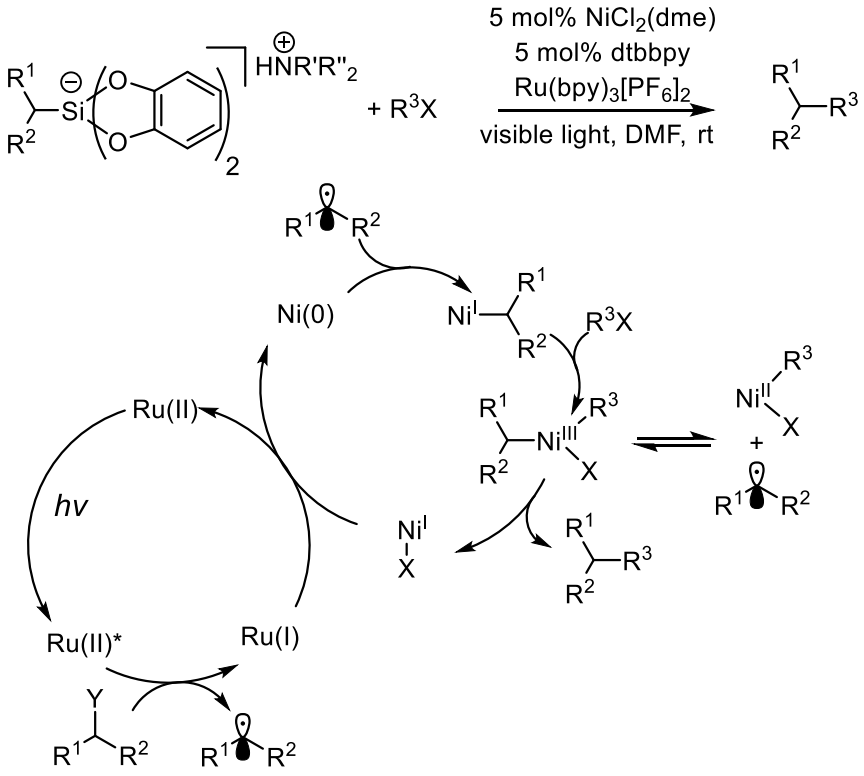

with Ni(II) and the alkyl radical. Reductive elimination from the Ni(III) species provides the product and Ni(I) which is reduced by Ru(I) to recycle both catalysts to their active species.

1.2.9 Single-electron Decarboxyative Cross-Coupling

At the same time as the Molander group, the MacMillan and Doyle labs reported a complimentary strategy to access the same reaction intermediates, an alkyl radical/Ni(II) species, using dual-catalytic conditions.[21] Instead of organoboron intermediates, they employed readily available α-heteroatomic carboxylic acids. Treatment of the carboxylic acid with base produces a carboxylate, which can be oxidized by one electron by a photoexcited catalyst. This single electron oxidation triggers radical decarboxylation resulting in the formation of an alkyl radical, which enters the nickel-catalyzed cross-coupling cycle, and the innocuous byproduct CO_2 (Scheme 13).[21] It is of note that preformed organometallics are not required for use as radical precursors. Additionally, only the volatile innocuous gas, carbon dioxide, generated from radical

Scheme 13. Photoredox cross-coupling of α-carboxyl carbons and aryl halides

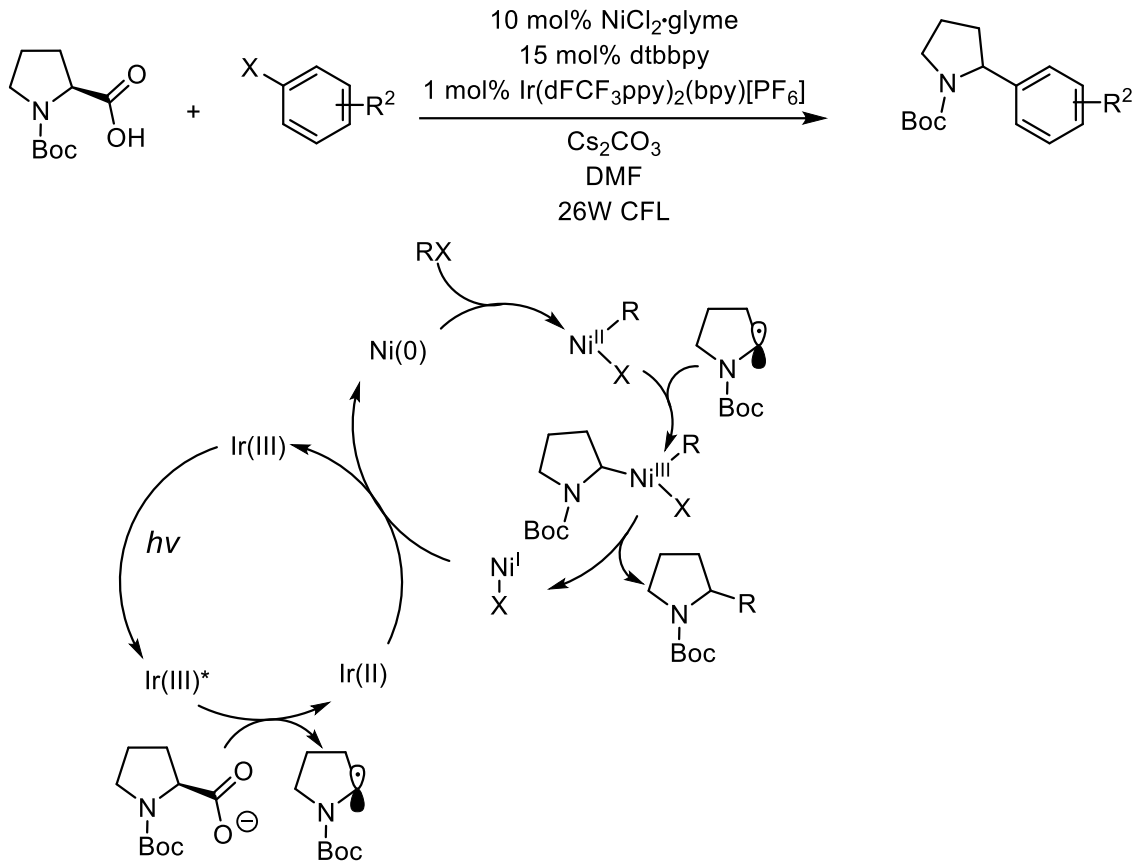

formation, and readily removed from reaction mixture. One disadvantage, however, is that the substrates are limited to α-amino and α-oxy acids.

Subsequently, the reaction scope was expanded to include vinyl iodides instead of aryl halides. Two alkyl carboxylic acids, phenylacetic acid and cyclohexane carboxylic acid, were also compatible coupling partners (Scheme 14).[22]

Scheme 14. Photoredox cross-coupling of α-carboxyl carbons and vinyl iodides

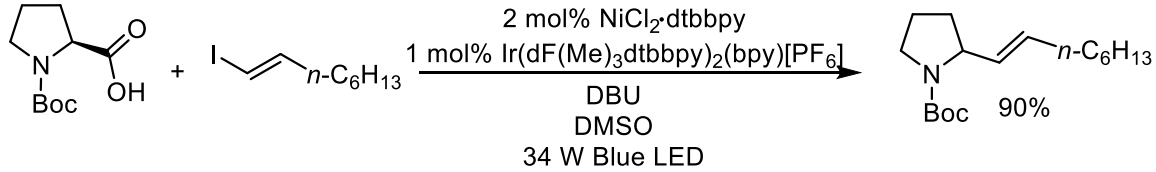

Aryl ketones were also synthesized by the MacMillan lab from aryl halides and keto acids. They proposed that corresponding carboxylate of the keto acid underwent radical decarboxylation upon oxidation by the Ir(III)* photocatalyst to provide an acyl radical that was intercepted by a Ni(II) aryl species (Scheme 15).[23]

Scheme 15. Photoredox cross-coupling of α-oxy acids and aryliodides

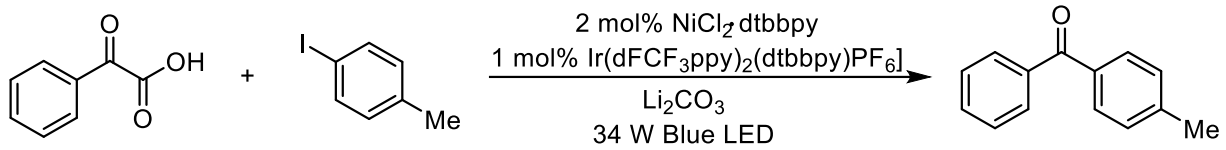

Subsequently, the MacMillan and Fu labs also developed a chiral ligand for nickel for stereoconvergent cross-coupling.[24] Although the arylbromides were limited to electron deficient species, and the %ee was modest to good (82-92%) the reaction represented significant progress towards the synthesis of chiral benzylamines from racemic α-amino radicals. Although no mechanistic rational is proposed, perhaps dynamic kinetic resolution-controlled reductive elimination as suggested computationally by Molander and Kozlowski.[13] A chiral BOX type ligand was found to be most efficient. When an electron-neutral aryl halide, iodobenzene, was employed the ee and the yields dropped to 66 and 64% respectively (Scheme 16).[24]

A similar system was also developed by the MacMillan lab for the synthesis of ketones via CO_2 extrusion-recombination of mixed anhydrides. The anhydrides, which were directly prepared from carboxylic acids and acyl chlorides *in situ*, undergo oxidative addition to Ni(0) to provide a Ni(II) intermediate.

Scheme 16. Enantioselective decarboxylative arylation

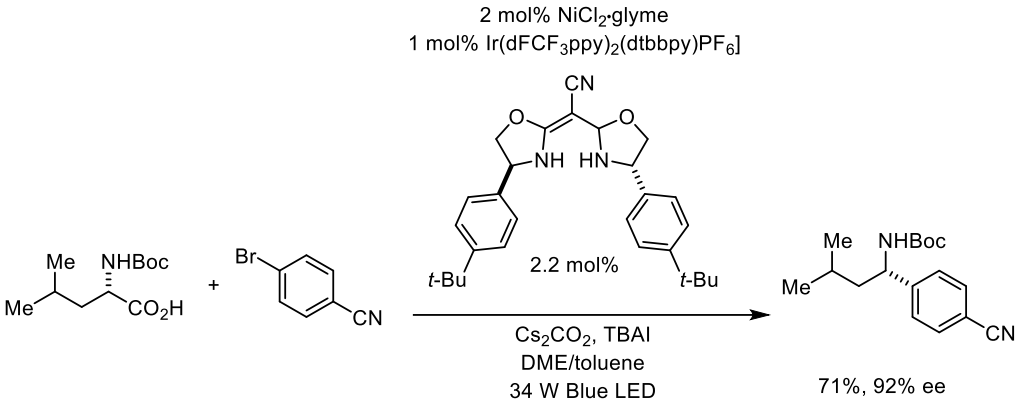

Oxidation of this intermediate by one electron triggers decarboxylation and gives a Ni(III) species, which after reductive elimination, provides the product and Ni(I). Reduction by one electron regenerates the Ni(0) catalyst (Scheme 17).[25]

Scheme 17. Decarboxylative coupling of mixed anhydrides

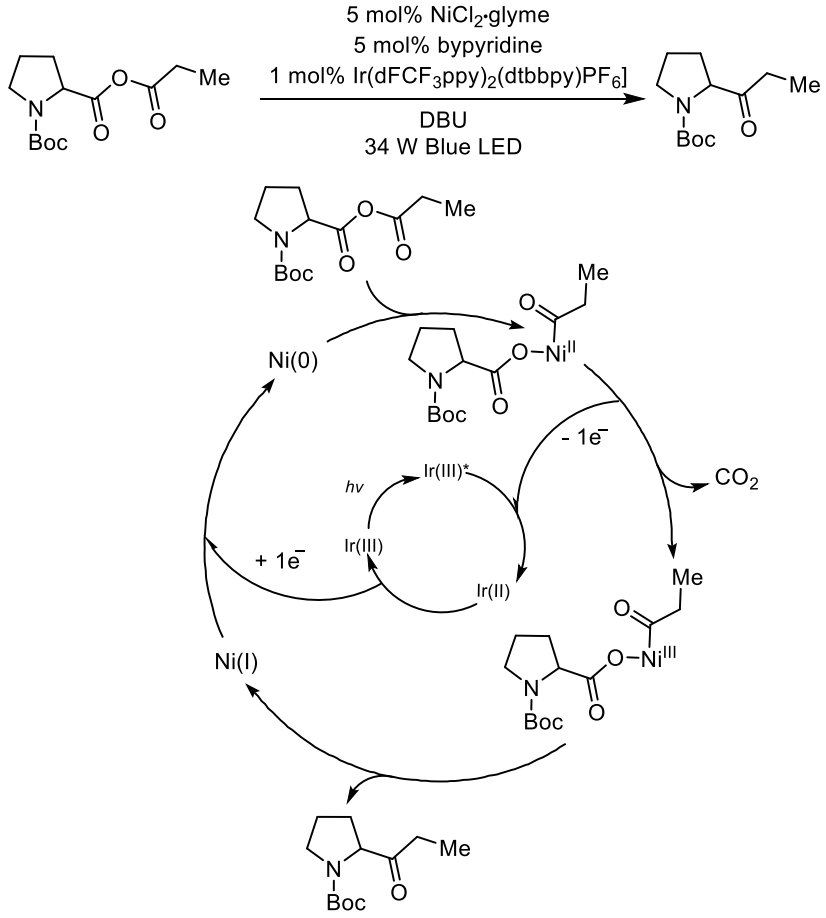

Progress has also been made in the field of dual palladium/photoredox decarboxylative coupling by our group and the Lu/Xiao groups which will be detailed in chapters 2/3.

1.2.10 Ni/Photoredox Catalyzed Etherification

The MacMillan group also used an iridium photocatalyst to modulate nickel oxidation states resulting in catalysis.26 A Ni(II) aryl alkoxide species does not undergo reductive elimination to produce an aryl ether and Ni(0), because this elimination is endothermic. However, oxidizing the Ni(II) center to Ni(III) renders this reductive elimination exothermic. As demonstrated previously, the reduced photocatalyst can then transfer an electron to Ni to regenerate the catalyst. In this cycle, the photocatalyst does not activate a radical pronucleophile, but rather directly enables the odd electron Ni(I)/Ni(III) cycle instead of the more common even electron Ni(0)/Ni(II) cycle (Scheme 18).[26]

Scheme 18. Synthesis of aryl ethers

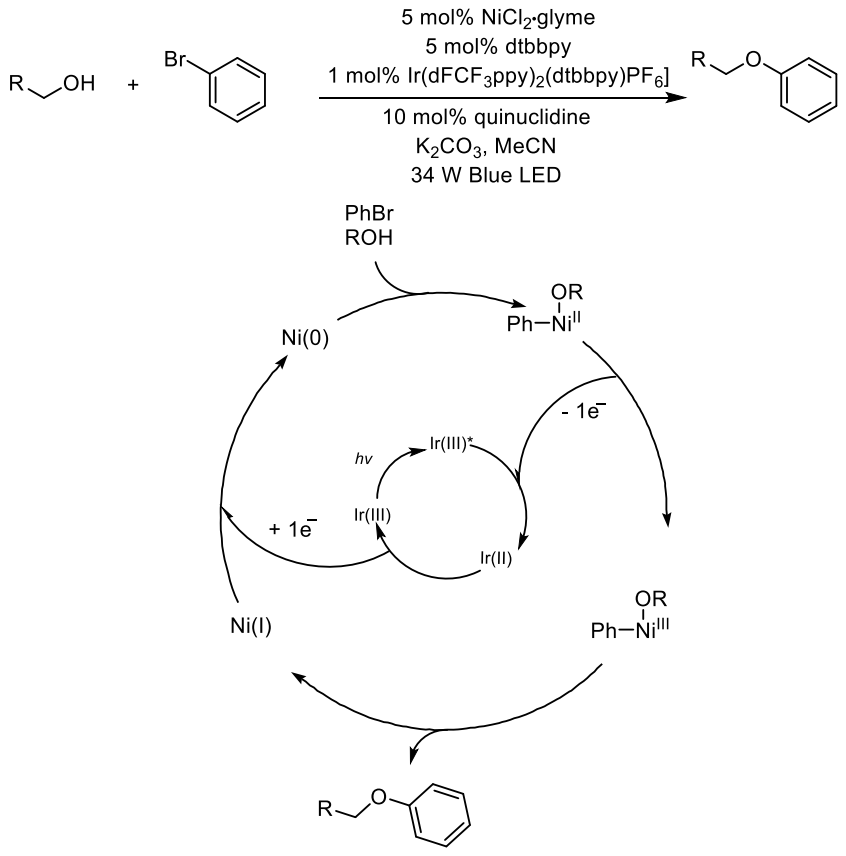

1.3 Dual catalysis involving atom transfer

In 2015, the Sorensen lab reported that the combination of tetra-*n*-butylammonium decatugstate (TBADT) and cobaloxoxime pyridine chloride (COPC) is competent for the dehydrogenation of unactivated alkanes and alcohols under near-UV irradiation. They hypothesized that sequential hydrogen atom transfer between the catalysts facilitates dehydrogenation.27 TBADT is known to abstract strong C–H bonds and the resultant product is a hydrogen atom donor. COPC is also known to abstract weak C–H bonds and produce hydrogen. Together, these catalysts may work in unison to effect dehydrogenation. The authors found that both saturated alkanes and primary and secondary alcohols could be dehydrogenated although a very limited substrate scope and variable yields resulted. (Scheme 19).[27]

Scheme 19. Cooperative hydrogen atom transfer

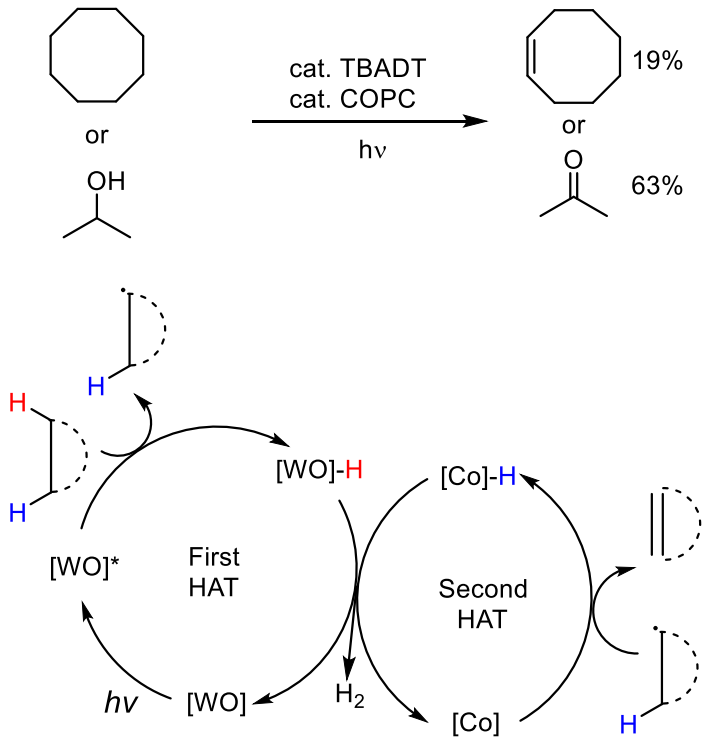

1.4 Dual catalysis involving energy transfer

The Kobayashi lab found that the combination of an iridium-based photocatalyst and a copper salt facilitated the Ullman-type C–N cross-coupling of carbazoles and aryl iodides. Given that the $Ir(ppy)_3$ complex is not a good oxidant ($E_{1/2}^{*III/II}$ = -0.3 V vs Fc/Fc^+), the authors proposed that energy transfer from the photoexcited iridium complex to a Cu(I) complex to form Cu(I)*, which can then reduce iodobenzene by one electron. Importantly, Stern-Volmer studies revealed that $Ir(ppy)_3$* is not quenched by iodobenzene, lending further support to their hypothesis. Based on these results the formation of a bis-ligated Cu(I) complex under basic conditions is proposed. Next, energy transfer from Ir(III)* generated a Cu(I)* complex, which reduced iodobenzene by one electron. The phenyl radical produced by disproportionation can then combine with the Cu(II) species to provide the product and regenerate the Cu(I) catalyst (Scheme 20).[28]

Scheme 20. Visible light-mediated Ullmann-type couplings

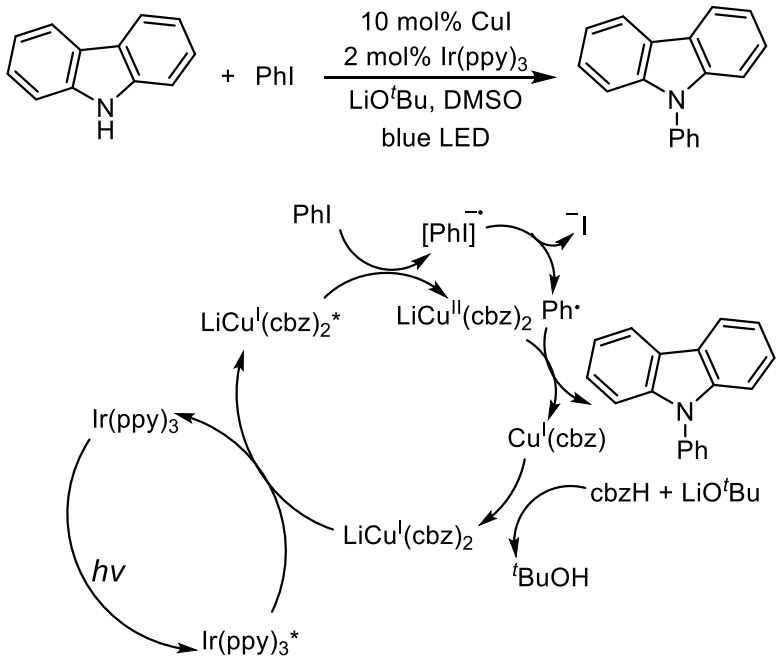

1.5 Conclusion

As shown throughout this review, the combination of transition-metal and photocatalysis can effect previously inaccessible transformations under mild conditions by making use of single-electron transmetalation pathways. One major implication of the works presented is that odd electron pathways and oxidation states in transition-metal catalyzed cycles, which have been under researched, certainly deserve the attention of organic chemists. This budding field has begun expanding rapidly and will likely enable chemists to construct new bonds with a wider substrate scope in the future.

1.6 References for Chapter 1

1) Osawa, M.; Nagai, H.; Akita, M. "Photo-activation of Pd-catalyzed Sonogashira coupling using a Ru/bipyridine complex as energy transfer agent" *Dalton Trans.* **2007**, 827-829.

2) Yu, W.-Y.; Sitm W.; Zhou, Z.; Chan, A. S. C. "Palladium-Catalyzed Decarboxylative Arylation of C-H Bonds by Aryl Acylperoxides" *Org. Lett.* **2009**, *15*, 3174-3177.

3) Kalyani, D.; McMurtrey, K. B.; Neufeldt, S. R.; Sanford, M. S. "Room-Temperature C-H Arylation: Merger of Pd-Catalyzed C-H Functionalization and Visible-Light Photocatalysis" *J. Am. Chem. Soc.* **2011,** *133*, 18566-18569.

4) Ye, Y.; Sanford, M. S. "Mering Visible-Light Photocatalysis and Transition-Metal Catalysis in the Copper-Catalyzed Trifluoromethylation of Boronic Acids with CF_3I" *J. Am. Chem. Soc.* **2012**, *134*, 9034-9037.

5) Rueping, M.; Koenigs, R. M.; Poscharny, K.; Fabry, D. C.; Leonori, D.; Vila, C. "Dual Catalysis: Combination of Photocatalytic Aerobic Oxidation and Metal Catalyzed Alkynylation Reactions- C-C Bond Formation Using Visible Light" *Chem. Eur. J.* **2012**, *18*, 5170-5174.

6) Perepichka, I.; Kundu, S.; Hearne, Z.; Li C.-J. "Efficient merger of copper and photoredox catalysis for the asymmetric cross-dehydrogenative-coupling of alkynes and tetrahydroisoquinolines" *Org. Biomol. Chem.* **2015**, *13*, 447-451.

7) Sahoo, B.; Hopkinson, M. N.; Glorius F. "Combining Gold and Photoredox Catalysis: Visible Light-Meditated Oxy- and Aminoarylation of Alkenes" *J. Am. Chem. Soc,* **2013**, *135*, 5505-5508.

8) Shu, X.; Zhang, M.; He, Y.; Frei, H.; Toste, F. F. "Dual Visible Light Photoredox and Gold-Catalyzed Arylative Ring Expansion" *J. Am. Chem. Soc.* **2014**, *136*, 5844-5847.

9) Fabry, D. C.; Zoller, J.; Raja, S.; Rueping, M. “Combining Rhodium and Photoredox Cataylsis for C-H Functionalization of Arenes: Oxidative Heck Reactions with Visible Light” *Angew. Chem. Int. Ed.* **2014**, *53*, 10228-10231.

10) Zoller, J.; Fabry, D. C.; Ronge, M. A.; Rueping, M. “Synthesis of Indoles Using Visible Light: Photoredox Catalysis for Palladium-Catalyzed C-H Activation” *Angew. Chem. Int. Ed.* **2014**, *53*, 13264-13268.

11) Tellis, J. C.; Primer, D. N.; Molander, G. A. “Single-electron transmetalation in organoboron cross-coupling by photoredox/nickel dual catalysis” *Science* **2015**, *345*, 433-436.
12) Primer, D. N.; Karakaya, I.; Tellis. J. C.; Molander, G. A. “Single-Electron Transmetalation: An Enabling Technology for Secondary Alkylboron Cross-Coupling” *J. Am. Chem. Soc.* **2015**, *137*, 215-2198.

13) Gutierrez, O.; Tellis, J. C.; Primer, D. N.; Molander, G. A.; Kozlowski, M. C. “Nickel-Catalyzed Cross-Coupling of Photoredox-Generated Radicals: Uncovering a General Manifold for Stereoconvergence in Nickel-Catalyzed Cross-Couplings” *J. Am. Chem. Soc.* **2015**, *137*, 4896-4899.

14) Karakaya, I.; Primer, D. N.; Molander, G. A. “Photoredox Cross-Coupling: Ir/Ni Dual Catalysis for the Synthesis of Benzylic Ethers” *Org. Lett.* **2015**, *17*, 3294-3297.

15) Amani, J.; Sodagar, E.; Molander, G. A. “Visible Light Photoredox Cross-Coupling of Acyl Chlorides with Potassium Alkoxymethyltrifluoroborates: Synthesis of α-Alkoxyketones” *Org. Lett.* **2016**, *18*, 732-735.

16) Ryu, D.; Primer, D. N.; Tellis, J. C.; Molander, G. A. “Single-Electron Transmetalation: Synthesis of 1,1-Diaryl-2,2,2-trifluoroethanes by Photoredox/Nickel Dual Catalytic Cross-Coupling” *Chem. Eur. J.* **2016**, *22*, 120-123.

17) Yamashita, Y.; Tellis, J. C.; Molander, G. A. “Protecting group-free, delective cross-coupling of alkyltrifluoroborates with borylated aryl bromides via photoredox/nickel dual catalysis” *Proc. Natl. Acad. Sci. U. S. A.,* **2015**, *112*, 12026.

18) El Khatib, M.; Serafim, R. A. M.; Molander, G. A. “α-Arylation/Heteroarylation of Chiral α-Aminomethyltrifluoroborates by Synergistic Iridium Photoredox/Nickel Cross-Coupling Catalysis” *Angew. Chem. Int. Ed.* **2016**, *55*, 254-258.

19) Jouffroy, M.; Primer, D. N.; Molander, G. A. “Base-Free Photoredox/Nickel Dual-Catalytic Cross-Coupling of Ammonium Alkylsilicates” *J. Am. Chem. Soc.* **2016**, *138*, 475-478.

20) Patel, N. R.; Kelly, C. B.; Jouffroy, M.; Molander, G. A. “Engaging Alkenyl Halides with Alkylsilicates via Photoredox Dual Catalysis” *Org. Lett.* **2016**, *18*, 764-767.

21) Zuo, Z.; Ahneman, D. T.; Chu, L.; Terrett, J. A.; Doyle, A. G.; MacMillan, D. W. C. “Merging photoredox with nickel catalysis: Coupling of α-carboxyl sp^3-carbons with aryl halides” *Science* **2014**, *345*, 437-440.

22) Noble, A.; McMarver, S. J.; MacMillan, D. W. C. “Merging Photoredox and Nickel Catalysis: Decarboxylative Cross-Coupling of Carboxylic Acids with Vinyl Halides” *J. Am. Chem. Soc.* **2015**, *137,* 624-627.

23) Chu, L.; Lipshultz, J. M.; MacMillan, D. W. C. “Merging Photoredox and Nickel Catalysis: The Direct Synthesis of Ketones by the Decarboxylative arylation of α-Oxo Acids” *Angew. Chem. Int. Ed.* **2015**, *54*, 7929-7933. *Nature Commun.* **2015**, *6*, 10093.

24) Zuo, Z.; Cong, H.; Li, W.; Choi, J.; Fu, G. C.; MacMillan, D. W. C. “Enantioselective Decarboxylative Arylation of α-Amino Acids via the Merger of Photoredox and Nickel Catalysis” *J. Am. Chem. Soc.* **2016**, *138*, 1832-1835.

25) Le, C.; MacMillan, D. W. C. “Fragment Couplings via CO_2 Extrusion-Recombination: Expansion of a Classic Bond-Forming Strategy via Metallaphotoredox” *J. Am. Chem. Soc.* **2015**, *137*, 11938-11941.

26) Terrett, J. A.; Cuthbertson, J. D.; Shurtleff, V. W.; MacMillan, D. W. C. “Switching on elusive organometallic mechanisms with photoredox catalysis” *Nature* **2015**, *524*, 330-334.

27) West, J. G.; Huang, D.; Sorensen, E. J. “Acceptorless dehydrogenation of small molecules through cooperative base metal catalysis” *Nat. Commun.* **2015**, *6*, 10093.

28) Yoo, W-J.; Tsukamoto, T.; Kobayashi, S. “Visible Light-Mediated Ullmann-Type C-N Coupling Reactions of Carbazole Derivatives and Aryl Alcohols” *Org. Lett.* **2015**, *17*, 3640-3642.

Chapter 2. Dual catalytic decarboxylative allylation of amino acids and esters

2.1 Introduction

This chapter details the motivation for the development of the radical decarboxylative allylation (DcA) reaction of α-amino acids and esters. Initial inspiration, subsequent reaction development, and exploration of the substrate scope is presented. Mechanistic analysis of the reaction ultimately enabled the proposal of competing mechanisms based on the relative stability of the alkyl radical that is formed by decarboxylation.

2.2 Palladium-catalyzed decarboxylative allylation

Transition metal-catalyzed cross-coupling reactions have revolutionized the way chemists make molecules as evidenced by the bestowment of the 2010 Nobel Prize in Chemistry to Richard Heck, Ei-ichi Negishi, and Akira Suzuki for palladium-catalyzed bond forming reactions. These reactions typically proceed via the oxidative addition of a aryl halide to palladium(0) followed by

Scheme 1. Standard versus decarboxylative cross coupling

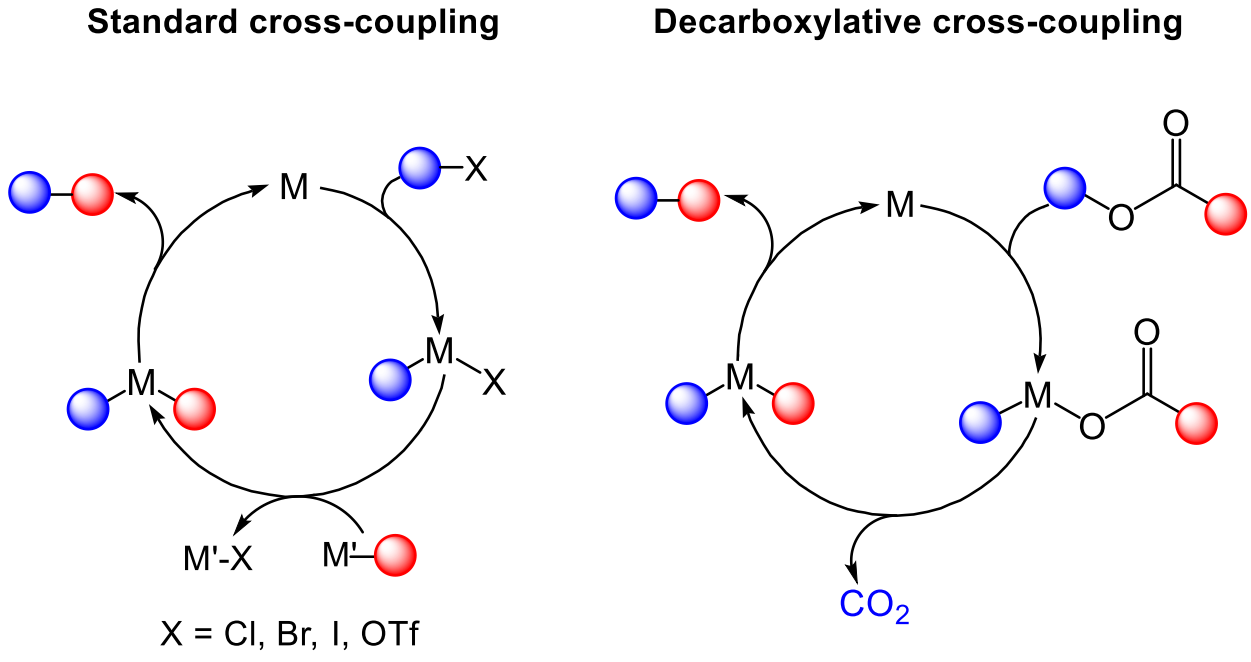

transmetalation and reductive elimination to provide the desired product. Transmetalation is generally accomplished using air sensitive, basic, or toxic pre-functionalized organometallic reagents and produces a stoichiometric amount of halogenated waste (Scheme 1).[1] Conversely, decarboxylative coupling generates reactive organometallic intermediates via decarboxylative metalation which may provide the same desired products after reductive elimination. The fact that the reagents are derived from abundant inexpensive carboxylic acids, the reactions proceed under mild conditions, and that the only stoichiometric byproduct is readily removed carbon dioxide gas make decarboxylative coupling an attractive reaction from environmental and atom economy standpoints.[2] One such example of this transformation is the Tsuji–Trost allylation reaction. Traditionally, an electrophilic palladium-π-allyl complex is formed via the displacement of an allylic acetate or allylic carbonate by palladium. This complex can then undergo attack by a nucleophile to install the valuable allyl functional group and regenerate the palladium(0) catalyst. Typically, stoichiometric base is added to generate the nucleophile *in situ*. An alternative to this approach is decarboxylative allylation (DcA) in which the allyl moiety and the pronucleophile are linked via an ester and the nucleophile in generated *in situ* via the loss of carbon dioxide.

The first DcA reaction was disclosed by Tsuji and co-workers in 1980.[3] Immediately after Saegusa and co-workers also disclosed a similar DcA reaction.[4] Both groups demonstrated that β-keto allyl esters undergo decarboxylative allylation in the presence of $Pd(PPh_3)_4$. The nucleophile and the electrophile are both generated *in situ* which eliminates the need for added base or transmetalation partner (Scheme 2).

Scheme 2. DcA

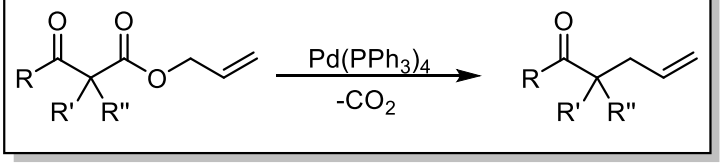

Scheme 3. DcA of allyl vinyl carbonates and related enantioselective studies

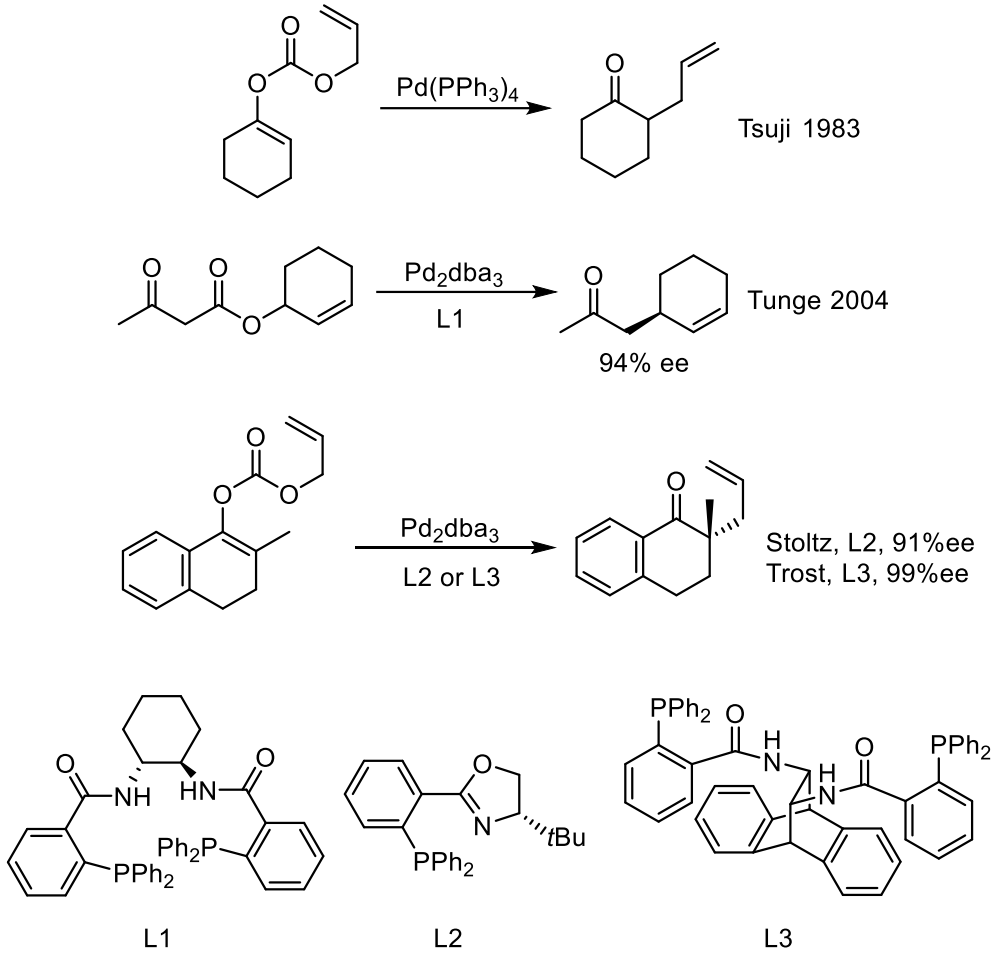

A few years later Tsuji also reported that ketones and aldehydes could also be allylated from the corresponding enol carbonate. It was not until 2004 that Tunge demonstrated that the DcA of allyl β-ketoesters could be rendered asymmetric.[5] Stoltz[6] and Trost[7] also reported the enantioselective DcA of allyl vinyl carbonates using PHOX and Trost ligands, respectively (Scheme 3).

The DcA reaction has also been extended to Csp^3 pronucleophiles other than enolates. The Tunge lab first reported that homoallylic amines were provided from the decarboxylative coupling of amino acid derivatives in 2006. The key to this reactivity is the formation of an α-ketamine, which stabilizes the resultant anion post decarboxylation.[8] Shortly after, the Churma lab also reported a complementary method for the generation of 2-azaallyl anions and their use

to form homoallylic amines (Scheme 4).[9] One disadvantage to this approach is that the transient azaallyl anion can be allylated at either the 1 or 3-position, which decreases the synthetic utility.

Scheme 4. DcA of azaallyl anions

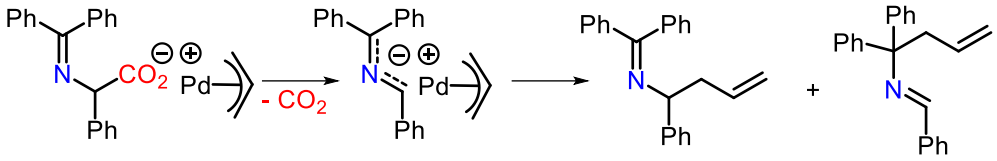

The Tunge lab also demonstrated that allyl nitroacetic esters[10] and nitroarene allyl acetic esters[11] are competent substrates for DcA. When nitroarenes were employed it was noted that the rate of the reaction increases with more stable benzylic anions, suggesting that decarboxylation is rate-limiting. Additionally, α-cyano allyl acetic esters were also shown to be effective (Scheme 5).[12]

Lastly, the Tunge group also harnessed α-sulfonyl esters as surrogates for hydrocarbon DcA. Fully substituted α-sulfonyl esters were readily prepared and subjected to DcA conditions. After allylation, net protodesulfonylation could be accomplished to provide various allylic hydrocarbons (Scheme 6).[13]

Scheme 5. DcA of nitro alkanes and arenes and α-cyano acetic esters

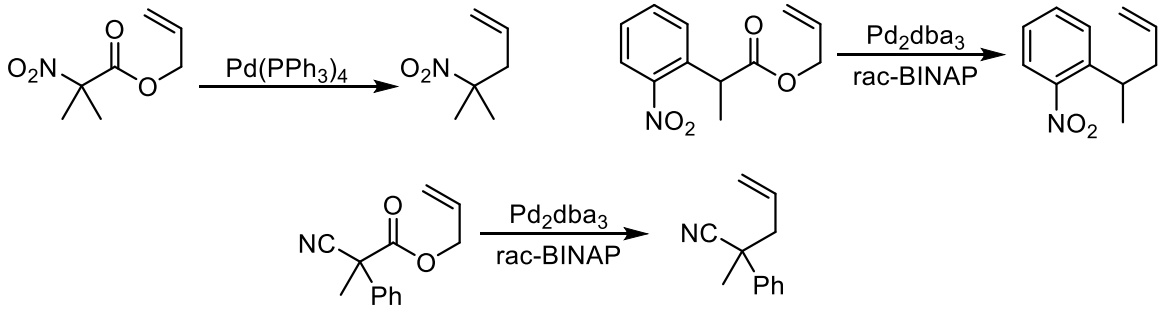

Scheme 6. DcA of sulfones

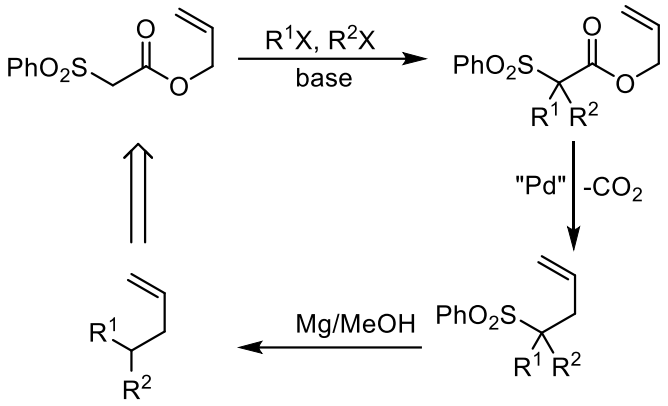

2.3 Expansion of the substrate scope of DcA

Thus far, all examples of DcA have involved anionic, two-electron decarboxylation. Decarboxylation does not occur, however, if the resulting anion is not stabilized and the pK_a of the corresponding conjugate acid is high. For example consider the product of oxidative addition of phenyl acetic acid allyl ester to palladium (Scheme 7). Decarboxylation would produce a tolyl anion whose corresponding acid (toluene) has a pK_a of ~ 43 in DMSO. Thus, the carboxylate will not decarboxylate, even under forcing conditions. One notable solution to this problem was disclosed by the Walsh lab in 2011.[14] They found that if chromium was pre-complexed to toluene it could be deprotonated with the strong base $LiN(SiMe_3)_2$ in the presence of an electrophilic Pd-π-allyl species to afford the allylated aryl product. After the reaction the chromium could be

Scheme 7. Limitation of anionic decarboxylation

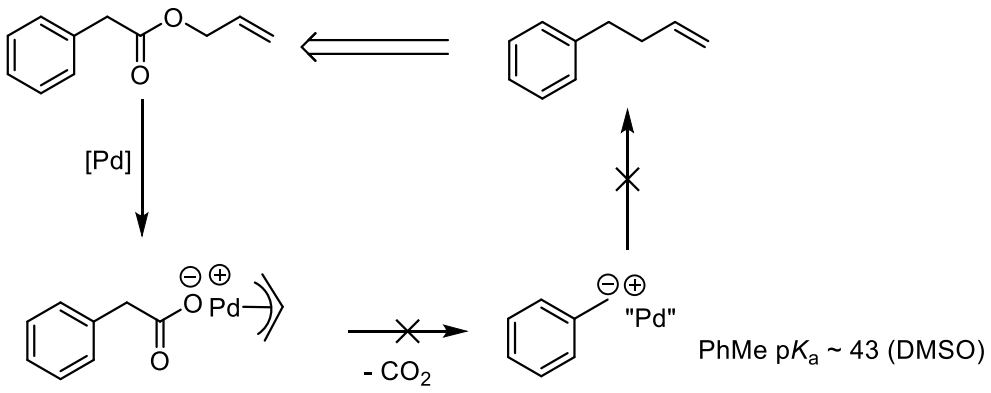

removed to provide the un-complexed product. Although this represented a valuable synthetic transformation, the pre-installation and subsequent removal of chromium combined with the use of superstoichiometric amounts of strong base is not desirable (Scheme 8).

Scheme 8. Benzyllic allylation

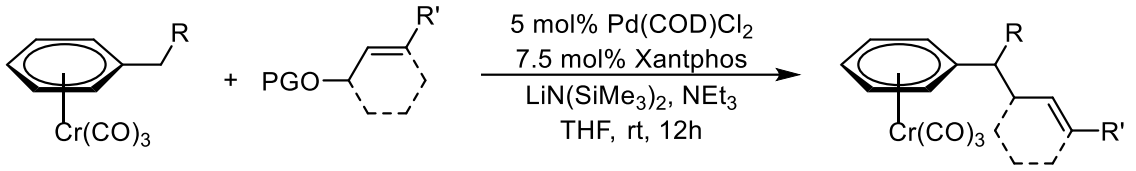

We became intrigued with the possibility of effecting radical decarboxylation instead of anionic decarboxylation. If the anionic carboxylate is oxidized by one electron it will form an electron deficient oxygen radical species, which will undergo radical decarboxylation to liberate carbon dioxide and the more stable benzylic radical (Scheme 9). This phenomena is well docume-

Scheme 9. Radical decarboxylation

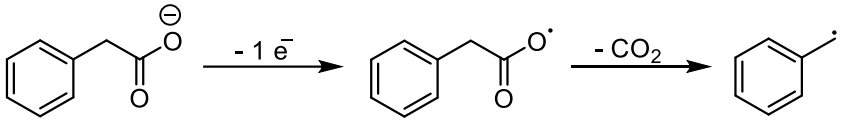

in the literature. For example, Grossweiner reported that flash-photolysis of arylacetic acid carboxylates resulted in their radical decarboxylation in 1966 (Scheme 10).[15] The single-electron oxidation of various carboxylates has also been studied by the Kochi lab and they found that once

Scheme 10. Radical decarboxylation via flash photolysis

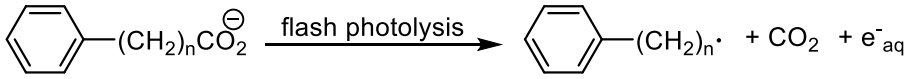

the corresponding carboxylate was oxidized by manganese(III) complexes decarboxylation occurred at rates > 10^9 sec^{-1}.[16] The radical decarboxylation of carboxylates has also been used for synthetic purposes. For example, dimeric alkanes may be prepared via the Kolbe electrolysis.[17] In 1998 the Oh group also demonstrated that amine-containing spirocycles can be

Scheme 11. Synthetic application of radical decarboxylation

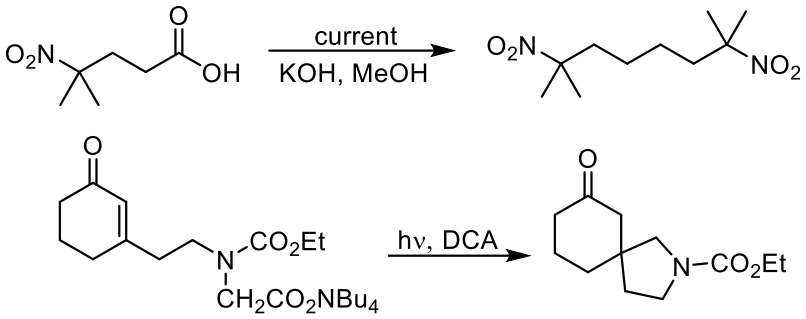

formed via intramolecular trapping of the radical, formed post decarboxylation, by an alkene (Scheme 11).[18]

While these are important advances, most methods require the use of non-selective high energy UV light or electrical current. These conditions often lend themselves to byproduct formation or intolerance of various functional groups. One significant report that inspired our approach towards extending the scope of the DcA reaction came from the Nishibayashi lab in 2013. They reported that the visible light excitation of the photocatalyst $Ir(ppy)_2(bpy)[BF_4]$ promoted radical decarboxylation of para-amino phenyl acetic acids under mild conditions. The resultant radical was then trapped by electron deficient alkenes such as benzylidenemalononitrile (Scheme 12).[19]

Scheme 12. Photoredox mediated decarboxylation of arylacetic acids

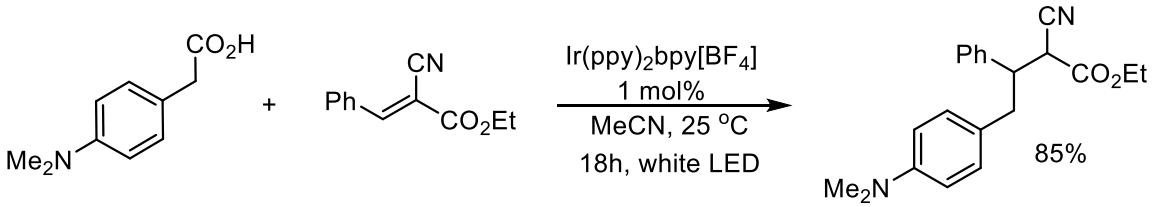

The question we posed was: What would happen when a benzylic radical was generated in the presence of an electrophilic Pd-π-allyl species? Specifically, could we study the interactions of radical and Pd-π-allyl species and use the results to effect benzylic allylation? Thus, we embarked on the synthesis of the materials that would allow us to answer this question. The

photocatalyst was prepared in a two-step procedure described by Nishibayashi.[20] The requisite carboxylic acids were prepared via a palladium-catalyzed Buchwald–Hartwig amination, followed by saponification and then esterified to the allylic esters (Scheme 13). The allylic esters were then subjected to a combination of palladium and photoredox catalysts under irradiation from a white LED. The palladium(0) species $Pd(PPh_3)_4$ was chosen since it readily forms Pd-π-allyl

Scheme 13. Synthesis of starting materials

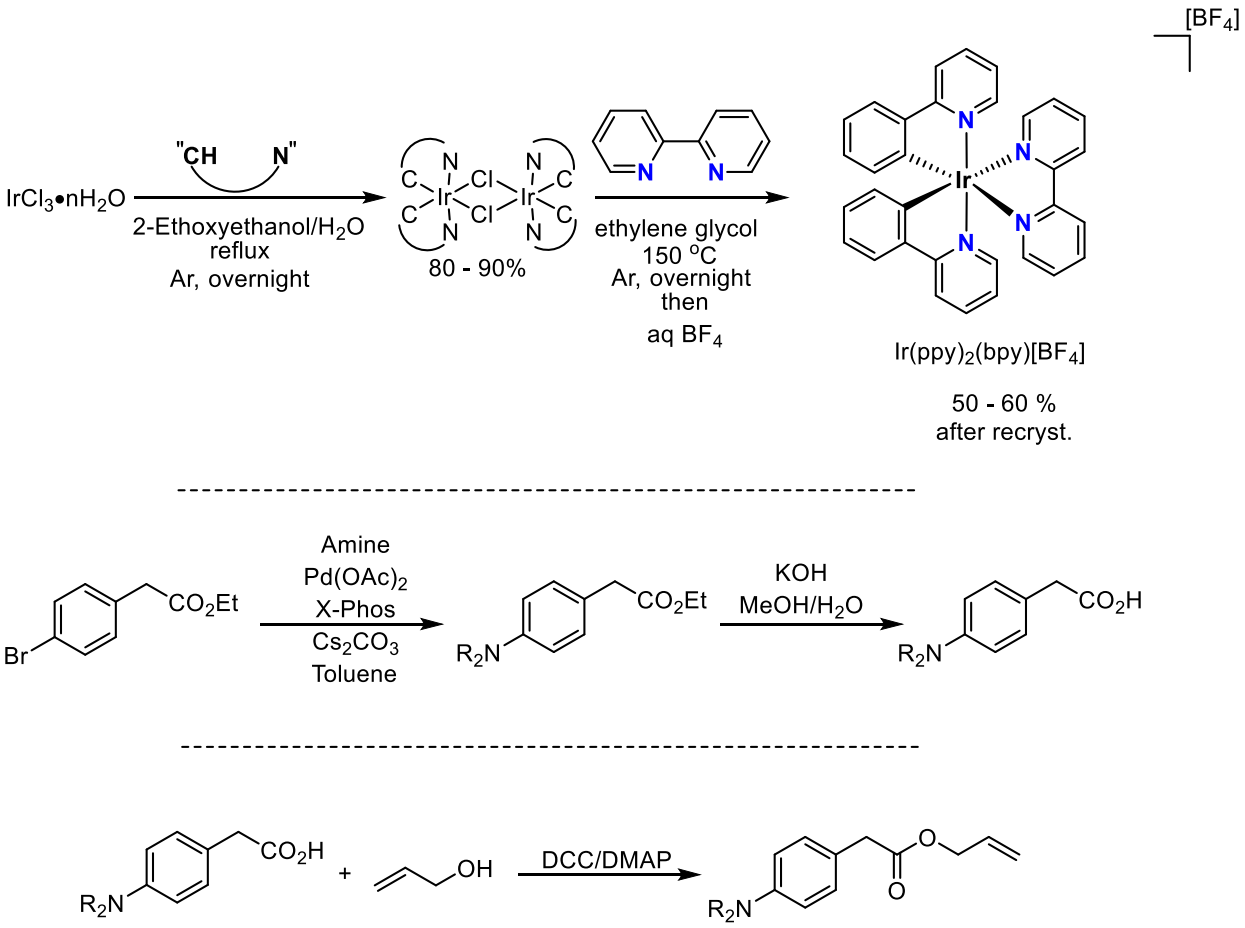

species at room temperature. The commercially available photocatalyst $Ru(bpy)_3[BF_4]_2$, whose photoexcited state is both weakly oxidizing and reducing, was a competent catalyst providing a 95% conversion of starting material after 9 hours. Analysis of the reaction mixture by GC/MS and ^{1}H NMR spectroscopy revealed that the desired allylated product and benzyl dimer were produced in approximately a 2:1 ratio (Scheme 14).

Scheme 14. Radical DcA

Next, the relationship between the photocatalyst and the rate of the reaction/ratio of the product was studied. When the very reducing homoleptic $Ir(ppy)_3$ was employed a much lower conversion was observed after 9 hours (Scheme 15, entry 2). Complete conversion was observed after 9 hours when $Ir(ppy)_2(bpy)[BF_4]$, which has intermediate redox potentials, was employed (entry 3). The more reducing, less oxidizing $Ir(dFppy)_3$ only reached 41% conversion after 9 hours (entry 4). When the photocatalyst was switched to highly oxidizing, minimally reducing Ru species only trace conversion was detected (entries 5-6). Returning to the most successful photocatalyst, $Ir(ppy)_2(bpy)[BF_4]$, the reaction reached complete conversion in 1 hour, and the palladium loading could be reduced at the cost of slightly longer reaction times (entry 8). Lastly, no conversion of starting material to product was detected by GC/MS when palladium, photocatalyst, or light were omitted.

With these results in hand, we turned our attention towards the ligated palladium species in an attempt to control the ratio of product to dimer (Scheme 16). Standard Pd(0) precursors CpPdallyl and CpPdcinnamyl and the nitrogen-containing bypyridine ligand were not effective. A variety of mono- and bidentate phosphine ligands promoted the reaction although the ratio of product:dimer did not change significantly. Additionally, many palladium/ligand combinations were not successful in changing the product ratio, which may indicate that the active species did not form at room temperature in the acetonitrile solvent. $Pd(PPh_3)_4$ was chosen as the catalyst of choice due to its commercial availability and the fact that it does not require the “activation” step of reducing Pd(II) to Pd(0) or ligand exchange.

Scheme 15. Optimization of the photocatalyst in radical DcA

Entry	$Pd(PPh_3)_4$	1 mol % Photocat.	Time	Conv.	P/D
1	5 mol%	$Ru(bpy)_3[BF_4]_2$	9h	95%	67:33
2	5 mol%	$Ir(ppy)_3$	9h	32%	nd
3	5 mol%	$Ir(ppy)_2(bpy)[BF_4]$	9h	100%	64:36
4	5 mol%	$Ir(dFppy)_3$	9h	41%	nd
5	5 mol%	$Ru(bpm)_3[PF_6]_2$	9h	trace	nd
6	5 mol%	$Ru(bpz)_3[PF_6]_2$	9h	trace	nd
7	5 mol%	$Ir(ppy)_2(bpy)[BF_4]$	1h	100%	66:34
8	2.5 mol%	$Ir(ppy)_2(bpy)[BF_4]$	2h	100%	66:34
9	5 mol%	none	1h	none	nd
10	none	$Ir(ppy)_2(bpy)[BF_4]$	1h	none	nd

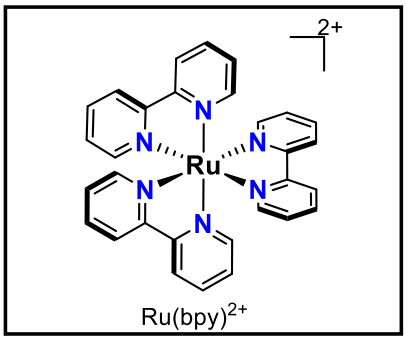

$Ru(bpy)^{2+}$

$E_{1/2}^{ox}$ = 0.77V, $E_{1/2}^{red}$ = -0.81V

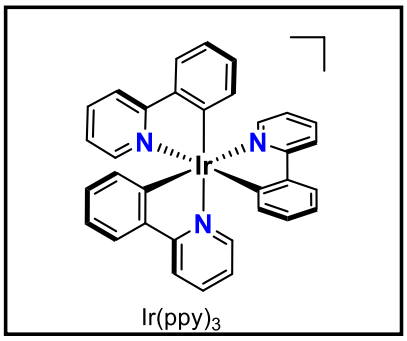

$Ir(ppy)_3$

$E_{1/2}^{ox}$ = 0.31V, $E_{1/2}^{red}$ = -1.74V

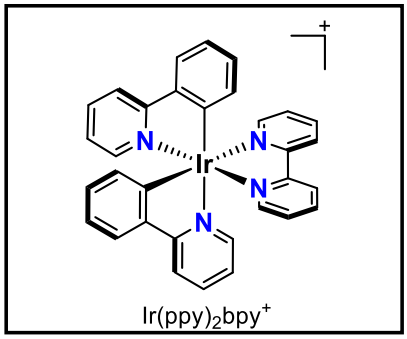

$Ir(ppy)_2bpy^{+}$

$E_{1/2}^{ox}$ = 0.95V, $E_{1/2}^{red}$ = -1.05V

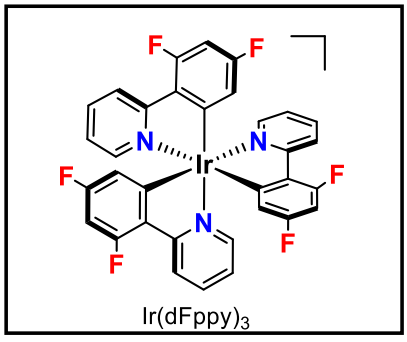

$Ir(dFppy)_3$

$E_{1/2}^{ox}$ = 0.45V, $E_{1/2}^{red}$ = -1.44V

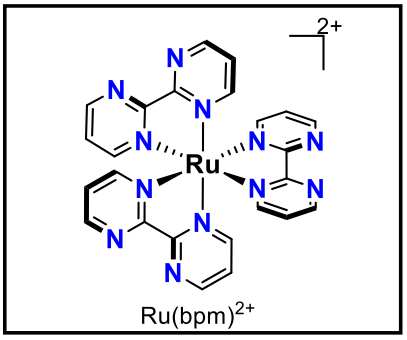

$Ru(bpm)^{2+}$

$E_{1/2}^{ox}$ = 0.99V, $E_{1/2}^{red}$ = -0.21V

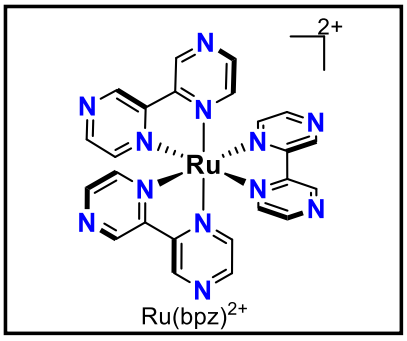

$Ru(bpz)^{2+}$

$E_{1/2}^{ox}$ = 1.45V, $E_{1/2}^{red}$ = -0.80V

Scheme 16. Evaluation of the Pd source for radical DcA

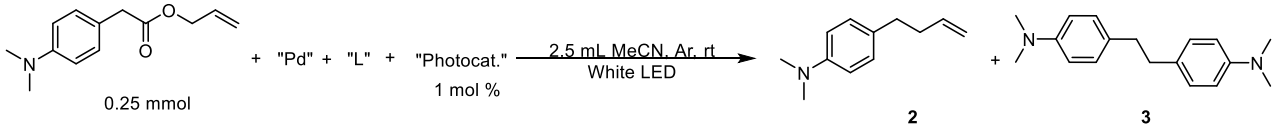

Pd Source	Ligand	photocat.	2:3
2.5 mol % $Pd(PPh_3)_4$	-	$Ru(bpy)_3[BF_4]_2$	70:30
5 mol % $Pd(PPh_3)_4$	-	$Ir(ppy)_2(bpy)[BF_4]$	63:37
5 mol % CpPdallyl	6 mol % bpy	$Ir(ppy)_2(bpy)[BF_4]$	low conv.
5 mol % CpPdCinnamyl	6 mol % bpy	$Ir(ppy)_2(bpy)[BF_4]$	low conv.
5 mol % $Pd(II)OAc_2$	11 mol % TFP	$Ir(ppy)_2(bpy)[BF_4]$	68:32
5 mol % $Pd(II)OAc_2$	11 mol % PCy_3	$Ir(ppy)_2(bpy)[BF_4]$	66:34
5 mol % $Pd(II)OAc_2$	6 mol % (S,S)-Anden Phenyl Trost	$Ir(ppy)_2(bpy)[BF_4]$	66:33
2.5 mol % Pd_2dba_3	6 mol % (S,S)-Anden Phenyl Trost	$Ir(ppy)_2(bpy)[BF_4]$	58:42
2.5 mol %$Pd(II)OAc_2$	4 mol % dppf	$Ru(bpy)_3[BF_4]_2$	62:38
2.5 mol % $Pd(II)OAc_2$	4 mol % xantphos	$Ru(bpy)_3[BF_4]_2$	71:29
2.5 mol % $Pd(II)OAc_2$	6 mol % *p*-^{t}Bu-triphenyl phosphite	$Ru(bpy)_3[BF_4]_2$	70:30

Additionally, the following Pd/L combinations produced poor to no conversion even with extended reaction times:

$Pd(II)OAc_2$ pentafluoro-PPh_3 | Pd_2dba_3 pentafluoro-PPh_3 | $Pd(II)OAc_2$ dppe | Pd_2dba_3 dppe | $Pd(II)OAc_2$ $MePPh_2$ | $Pd(II)OAc_2$ S-Phos

$Pd(II)OAc_2$ rac-BINAP | $Pd(II)OAc_2$ | $Pd(II)OAc_2$ | $Pd(II)OAc_2$ | $Pd(II)OAc_2$ X-Phos

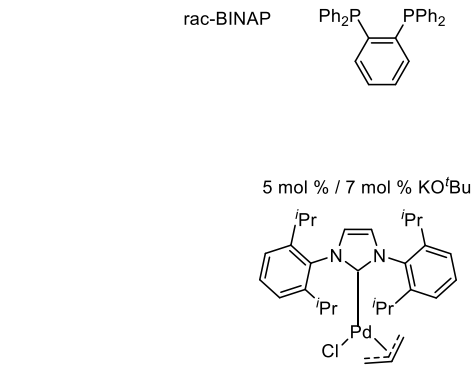

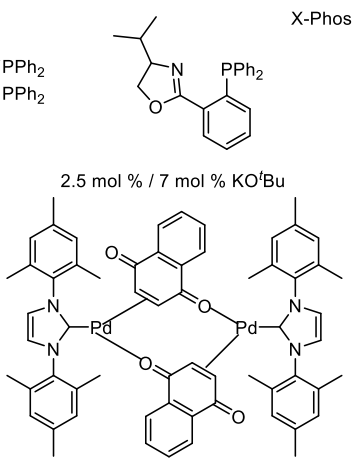

With suitable reaction conditions in hand, we evaluated the scope of acids that underwent radical DcA (Scheme 17). Allyl and β-methallyl (**1b**) were well tolerated by the reaction conditions, giving similar yields. Increasing the steric bulk about the benzylic radical that formed, post decarb-

Scheme 17. Scope of alkanoic esters

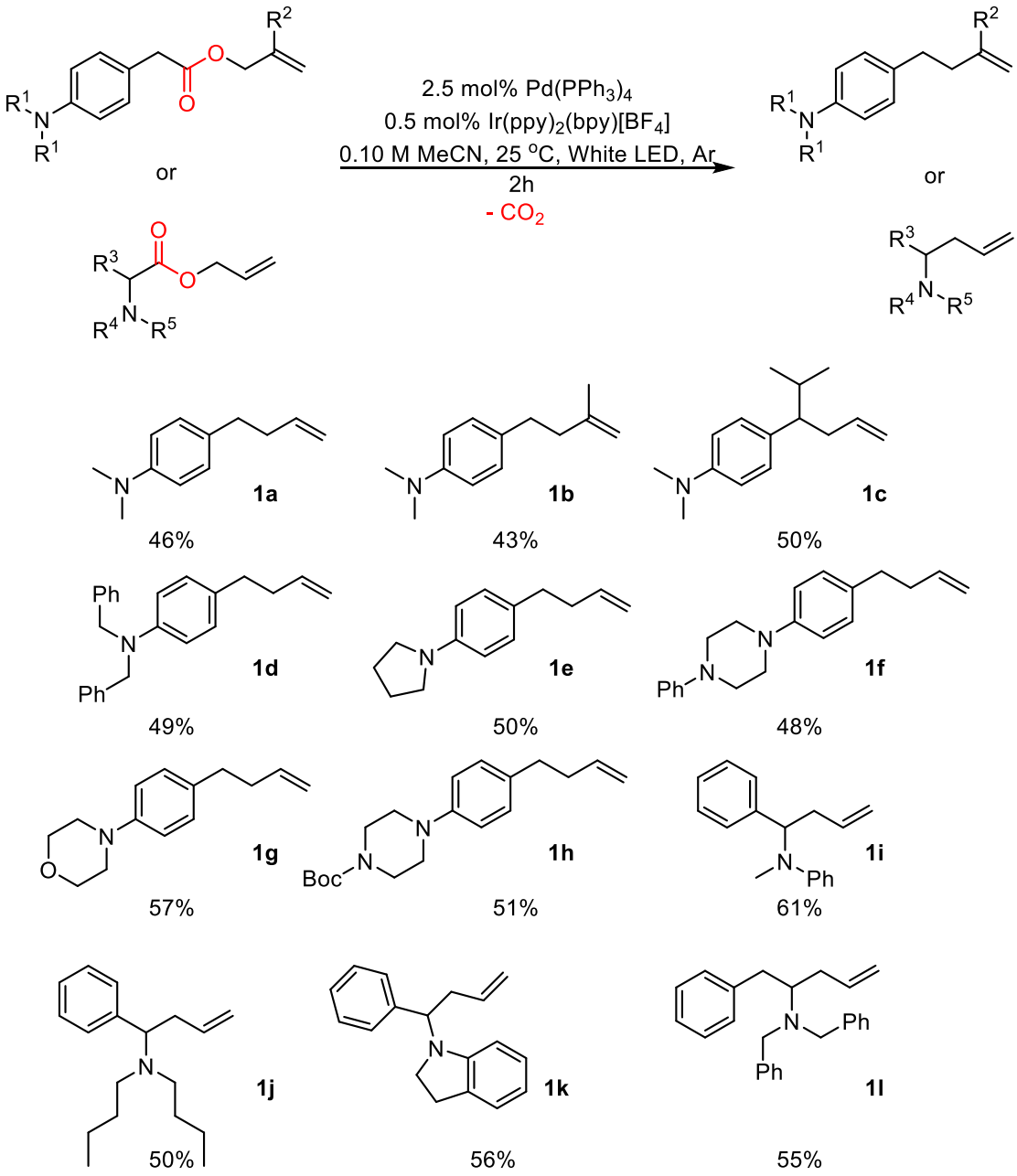

oxylation, did not improve yields of the desired product (**1c**). Dibenzyl and cyclic amine substituents on the *para* position, including rings containing nitrogen and oxygen heteroatoms, were well-tolerated (**1d-1h**). Amino acid derivatives also readily participated in the radical DcA reaction. Both aryl and alkyl substituents on the tertiary nitrogen atom were tolerated, and N,N-dibenzyl phenylalanine was also successfully allylated, which showed the reaction was not strictly limited to the allylation of benzylic positions (**1i-1l**).

We also hypothesized that the radical decarboxylation would be site-specific for the carbon bearing the carboxylate. In order to test this hypothesis substrate **1m'** was synthesized, which has two electron rich benzyl substituents on the tertiary nitrogen. Upon subjection to the standard reaction conditions, exclusive allylation at the least electron rich benzylic position was detected by ^{1}H NMR spectroscopy. This means that the radical formed site-specifically and was allylated prior to isomerization to a more thermodynamically stable species (Scheme 18).

While radical DcA of allylic esters represents a powerful new method for the construction of homoallylic amines, we also recognized that having to pre-link the electrophile and pronucleophile prior to the reaction is detrimental from a step-economic viewpoint. If the same two intermediates, an anionic carboxylate and an electrophilic Pd-π-allyl complex, could be produced via an intermolecular reaction it would obviate allylic ester pre-formation. We postulated

Scheme 18. Site-specific allylation

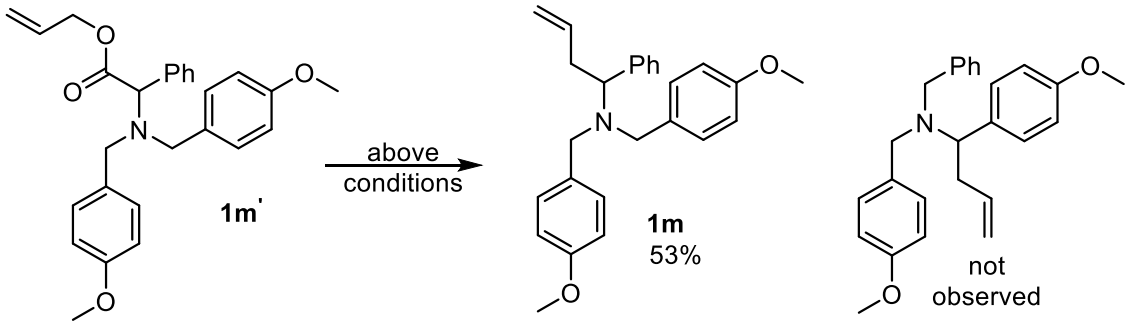

that treatment of allyl methyl carbonate with Pd(0) would produce the desired Pd-π-allyl species and a carbonate anion capable of deprotonating a phenylacetic acid. Pleasingly, the intermolecular DcA was realized under the standard reaction conditions with allyl methyl carbonate and free acids (Scheme 19).

Scheme 19. Intermolecular radical DcA

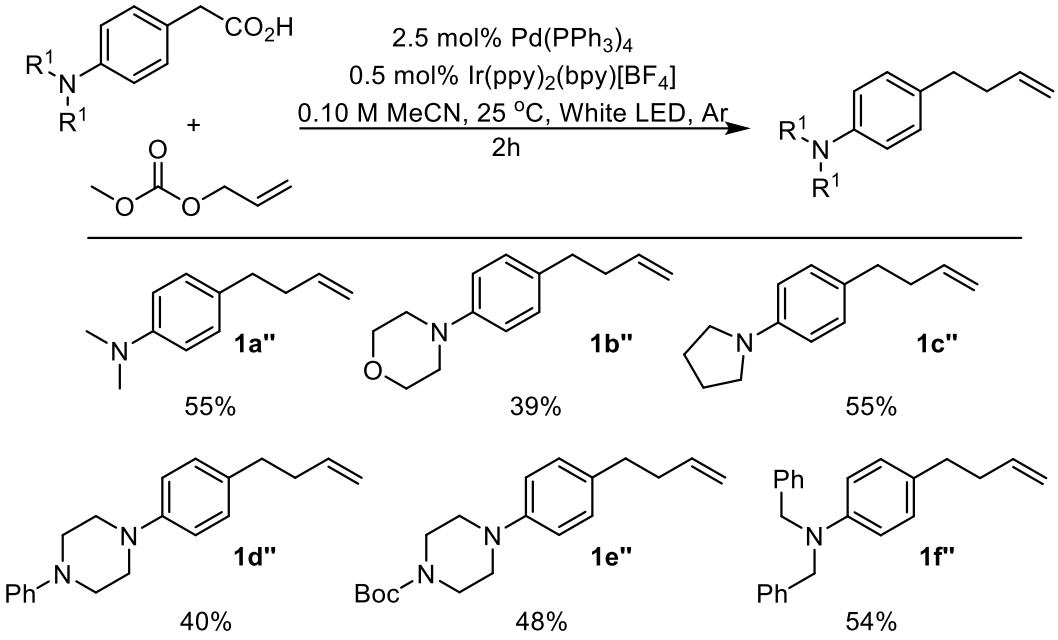

Next, we investigated the potential mechanistic courses of radical DcA. The modest yields of products and the observation of benzylic dimer suggested that free radicals may form in the reaction leading to these products. If the allylated product arose from the combination of a benzylic radical with an allylic radical then 1,5-hexadiene would form. Although 1,5-hexadiene is a volatile liquid, we endeavored to detect its formation by ^{1}H NMR spectroscopy. Thus, a reaction was performed in deuterated MeCN in an NMR tube and at the end the reaction was spiked with exogenous 1,5-hexadiene. Observation of an increased intensity in the peaks corresponding exclusively to 1,5-hexadiene confirmed that it was formed in the reaction, along with desired product and benzylic dimer (Scheme 20).

Scheme 20. Detection of hexadiene by 1H NMR spectroscopy

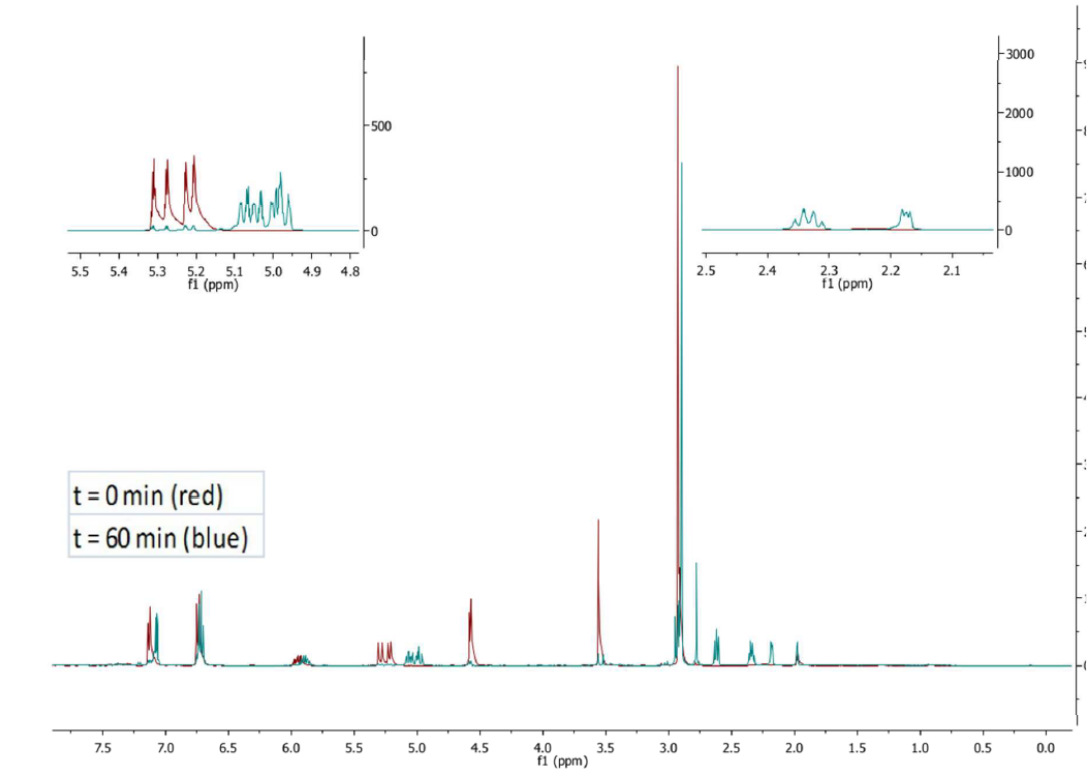

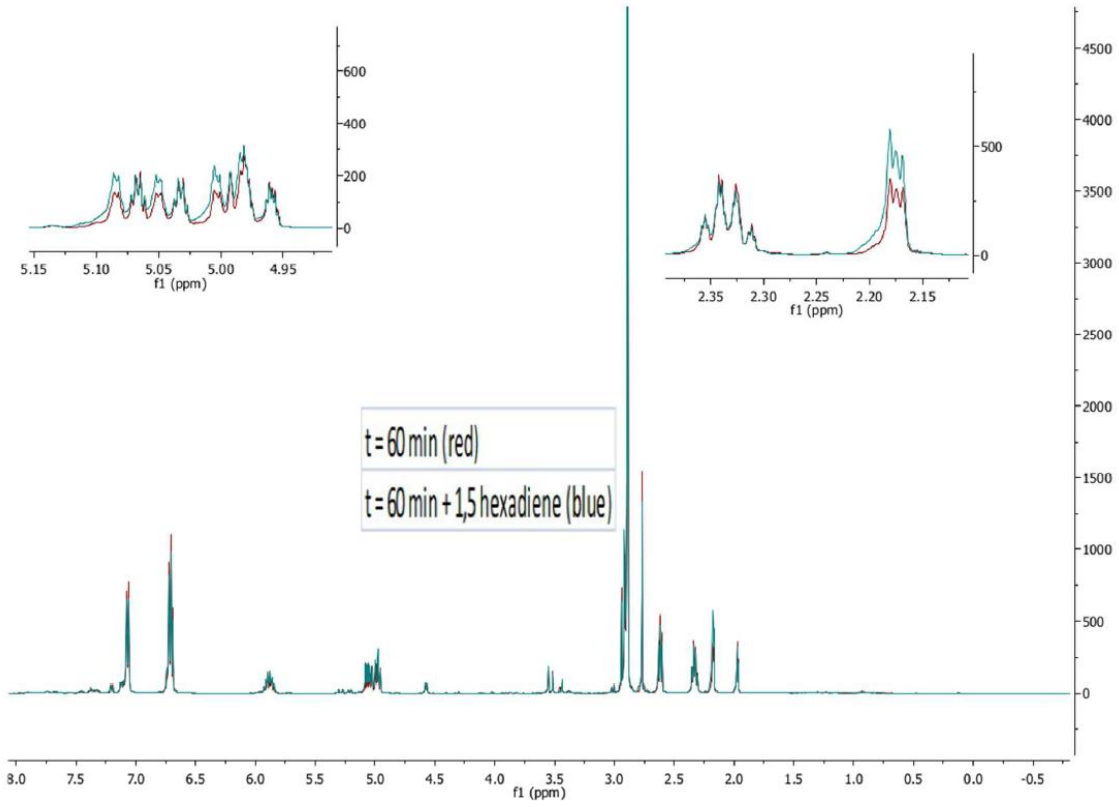

A cross-over experiment was also conducted in an attempt to gather more evidence for free radical formation. To this end, two different para amino phenyl acetic acid allyl esters were subjected to the reaction conditions (Scheme 21). When the crude reaction mixture was analyzed

Scheme 21. GC/MS analysis of crossover experiment.

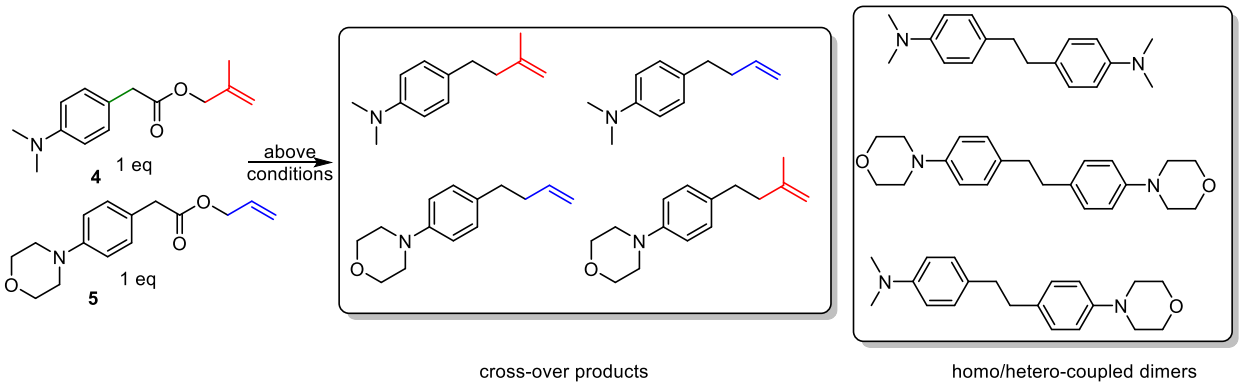

by GC/MS, the expected allylic and benzylic crossover products were detected. Unfortunately, after more careful analysis of reaction time points, it became clear that Pd(0) underwent preferential oxidative addition to the simple allylic ester over the β-methallyl ester. Only after most of the allyl ester was consumed did the β-methyallyl substituent begin to react. Additionally, it should be noted that palladium carboxylate salts may undergo metathesis *prior to decarboxylation* which further complicates conclusions from such crossover experiments (Scheme 22).

We also attempted to probe the course of a reaction where the palladium allyl species and the carboxylate were tethered together. To this end, a known lactone was prepared and subjected to the standard reaction conditions. Analysis of the crude reaction mixture by ^{1}H NMR

Scheme 22. Pd carboxylate metathesis

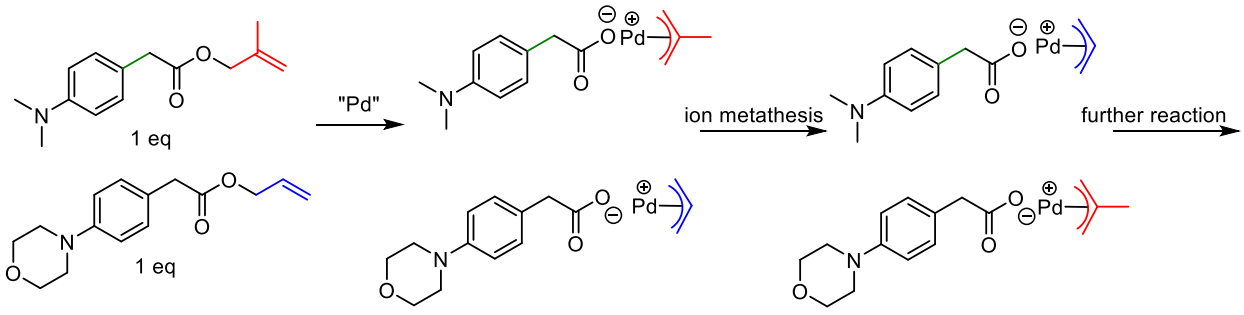

spectroscopy and GC/MS revealed that several products formed, but not the expected cyclization product. Attempts to isolate and characterize the products were not fruitful, although a small amount of the diene, which is derived from β-hydride elimination after oxidative addition, may have formed based on observed mass in the GC/MS chromatogram (Scheme 23).

Scheme 23. Reaction of an allylic lactone

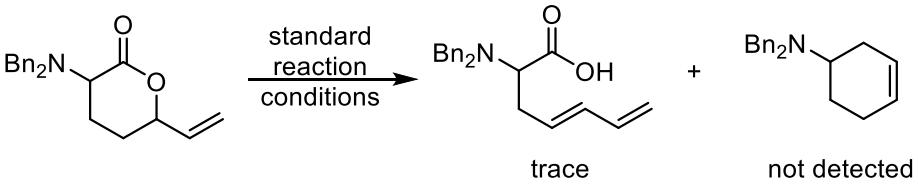

These observations suggest the dual catalytic mechanism presented in Scheme 24. Oxidative addition provides the palladium allyl complex and an anionic carboxylate. The photoexcited iridium photocatalyst then removes an electron from the aniline, generating a radical cation. Decarboxylation quenches this charge to provide a benzylic radical and carbon dioxide. Then the

Scheme 24. Proposed Dual Catalytic Mechanism

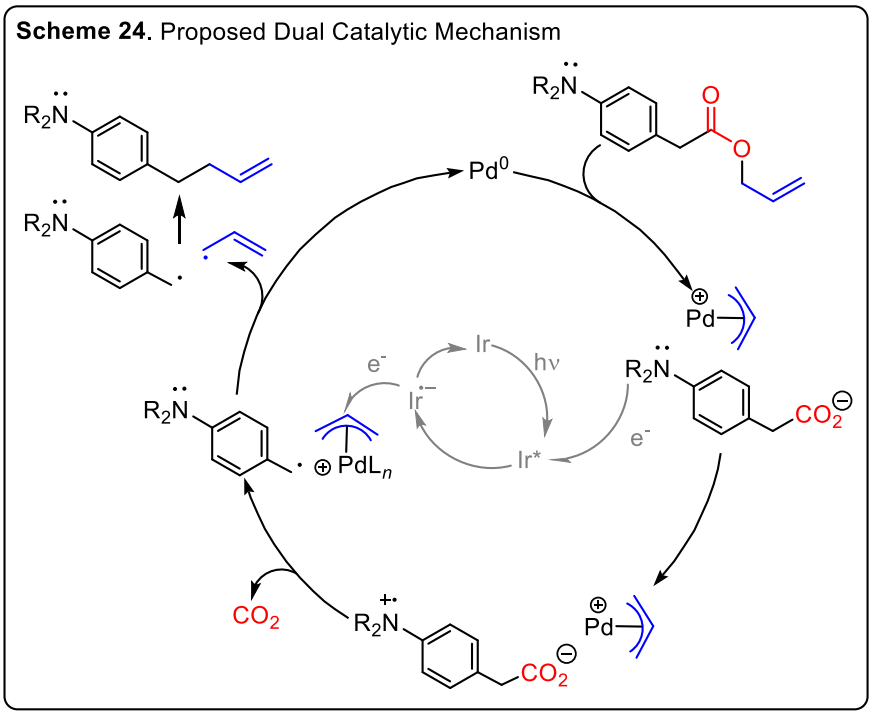

reduced photocatalyst can transfer an electron to palladium[21] to regenerate the photocatalyst and the Pd(0) catalyst following homolysis to provide an allylic radical. This radical may then form the desired products and byproducts observed in the reaction mixture.

Shortly after our report the Lu and Xiao groups reported a similar radical strategy towards homoallylic amines utilizing a photocatalyst to generate an α-*N*-phenyl amino radical in the presence of a palladium allyl species (Scheme 25).[22]

Scheme 25. Allylation of *N*-phenyl tetrahydroisoquinilines

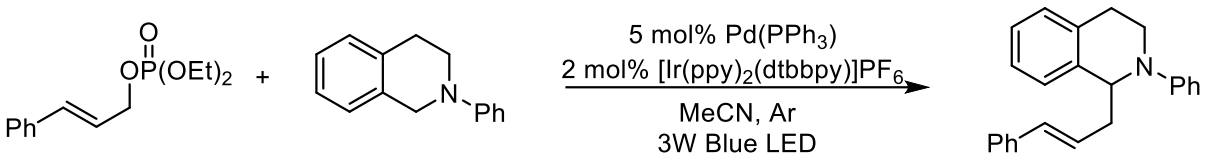

2.4 DcA of amino acids and esters

Although the radical DcA of alkylamino esters was a significant step forward, the alkyl protecting groups on the amines are not readily manipulated. We aimed to include more synthetically useful *N*-protecting groups that could be later manipulated, furthering the utility of our allylation reaction. Functionally rich *N*-protected amino acids, which do not undergo two electron decarboxylation, were selected as model substrates due to their commercial availability. During the course of our initial radical DcA the Molander and Kozlowski groups modelled the course of a related dual catalytic nickel/photoredox system by DFT calculations and found that that a free benzylic radical and the nickel bound species are nearly equienergetic (see Chapter 1 and Scheme 26). These studies suggested that less stable radicals (i.e. non-benzylic) may not readily dissociate from palladium and instead participate in reductive elimination rather than free radical formation/recombination. We postulated that we may be able to raise yields and limit byproduct formation based upon these observations.

Scheme 26. Observation by Molander and Kozlowski on a related Ni system

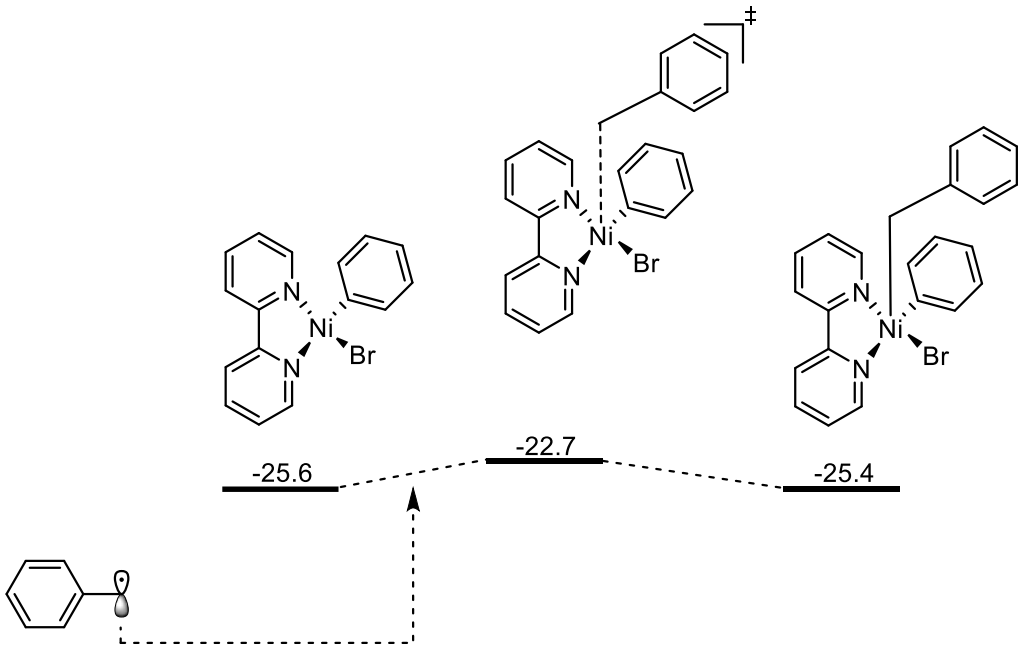

Ni(II) to Ni(III) proceeds via a low barrier and is reversible

N-Boc proline allyl ester was chosen as the model substrate for optimization. A solvent screen revealed that the combination of DMSO and the oxidizing heteroleptic Ir species Ir{dF(CF_3)ppy}$_2$(dtbbpy)[PF_6] led to rapid conversion of material to product with minimal side-product formation. The electron withdrawing ligands render iridium more electron deficient and thus a more potent oxidant in the photoexcited state (Scheme 27). This increased potential is beneficial due to the fact the carbamate moiety is more electron withdrawing than an alkyl group and thus likely raises the oxidation potential of the corresponding carboxylate anion. When light, photocatalyst, or palladium was removed from the reaction mixture, no conversion to product was detected by GC/MS analysis of the crude reaction mixture.

Scheme 27. DcA of *N*-Boc proline allyl ester

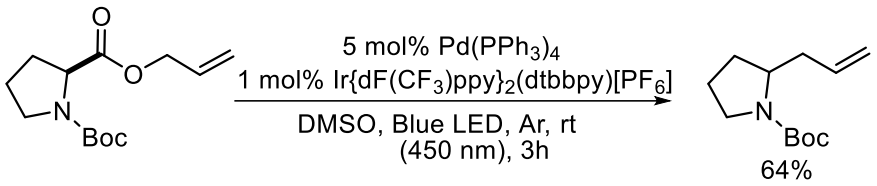

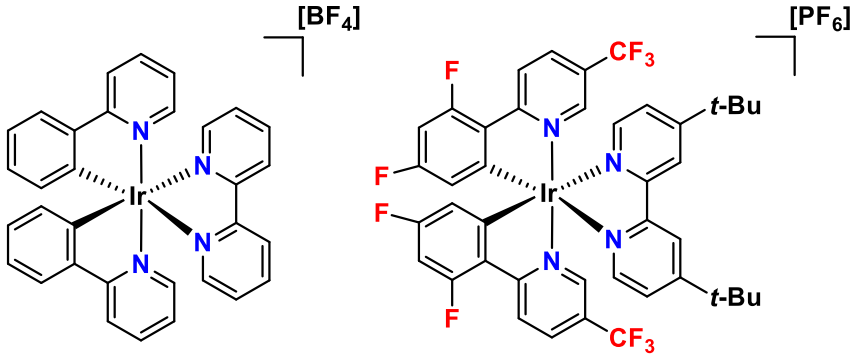

$Ir(ppy)_2(bpy)[BF_4]$

$E_{1/2}^{ox}$ = 0.95 V
$E_{1/2}^{red}$= -1.05 V

$Ir\{dF(CF_3)ppy\}_2(dtbbpy)[PF_6]$

$E_{1/2}^{ox}$ = 1.21 V
$E_{1/2}^{red}$= -0.89 V

This success prompted us to evaluate the scope of amino acid allyl ester derivatives that could undergo radical DcA. Several different phenylalanine allyl esters were evaluated, and it was found that Boc, Cbz, and acyl protecting groups were all well-tolerated (**2a-2c**). Next, the substitution about the phenyl ring of *N*-Boc phenylalanine was varied. Trifluoromethyl-, fluoro-, nitrile-, chloro-, and O-benzyl substituents all provided products in good yields (**2d-2i**). Additionally, the reaction worked well on the gram scale (**2h**). The reaction was not limited to secondary Boc-amines, as demonstrated by the successful allylation of *N-Boc, N-Me* phenylalanine allyl ester (**2j**). Phenyl glycine and various proline derivatives including hydroxyl-, thio, and homo-proline also participated in the radical DcA reaction (**2k-2o**). Other amino acids such as alanine, methionine, and aspartic acids were also rapidly allylated (**2p-2r**). The primary radical formed after decarboxylation of glycine was allylated in a lower yield. Various heterocycle-containing amino allyl esters including benzothiophene, indole, and pyridine were also competent, although lower yields were obtained (**2t-2v**), (Scheme 28).

Scheme 28. Substrate scope of the DcA of amino esters[a,b]

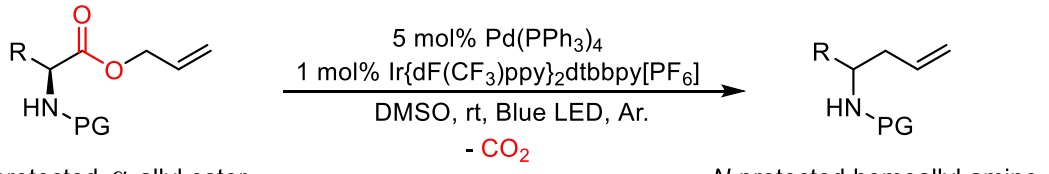

N-protected α-allyl ester

N-protected homoallyl amine

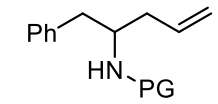

PG = Boc, 5 h, 65% (**2a**)
PG = Cbz, 5 h, 65% (**2b**)
PG = Ac, 7 h, 69% (**2c**)

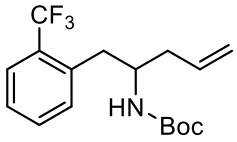

6 h, 67% (**2d**)

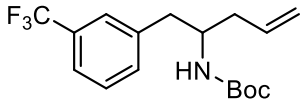

6 h, 73% (**2e**)

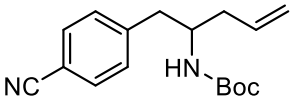

6 h, 72% (**2f**)

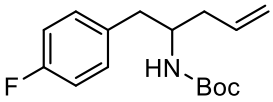

6 h, 83% (**2g**)

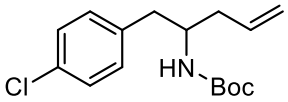

7 h, 79% (**2h**)
24 h, 71%[c]

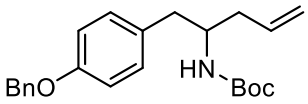

5 h, 77% (**2i**)

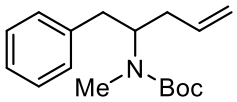

4 h, 72% (**2j**)

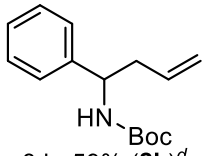

8 h, 59% (**2k**)[d]

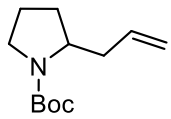

3 h, 64% (**2l**)

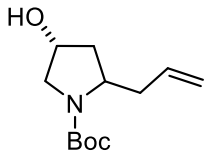

6 h, 69% (**2m**)
1:1 d.r.

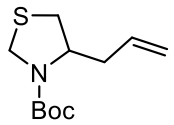

6 h, 42% (**2n**)

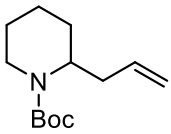

5 h, 77% (**2o**)

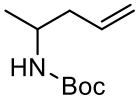

4 h, 81% (**2p**)[e]

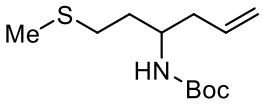

5 h, 58% (**2q**)

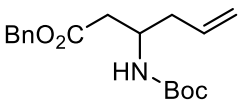

4 h, 57% (**2r**)

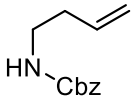

3 h, 44% (**2s**)

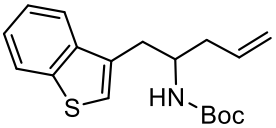

7 h, 56% (**2t**)

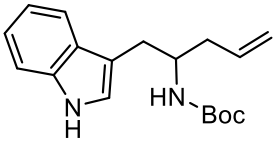

5 h, 39% (**2u**)

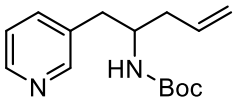

7 h, 22% (**2v**)

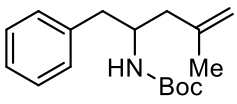

14 h, 45 °C, 52% (**2w**)

[a] Reactions performed on a 0.25 mmol scale at 0.13M. [b] Isolated yields.
[c] Gram scale, 0.37 M. [d] 95 %pure. [e]Average yield of two runs.

Lastly, a β-methallyl ester required heating to reach complete conversion which may suggest that oxidative addition of such species is not facile at room temperature (**2w**).

We also wished to demonstrate that formation of radicals was site-specific for the position bearing the carboxylate anion. Thus, the allyl ester of tetrahydro-3-isoquinoline carboxylic was compared to the *N*-phenyltetrahydro-isoquinoline employed by Xiao and Lu. Directed site-specific allylation occurred indicating that the radical did not isomerize to the more thermodynamically stable species. (Scheme 29).

Scheme 29. Site specific DcA

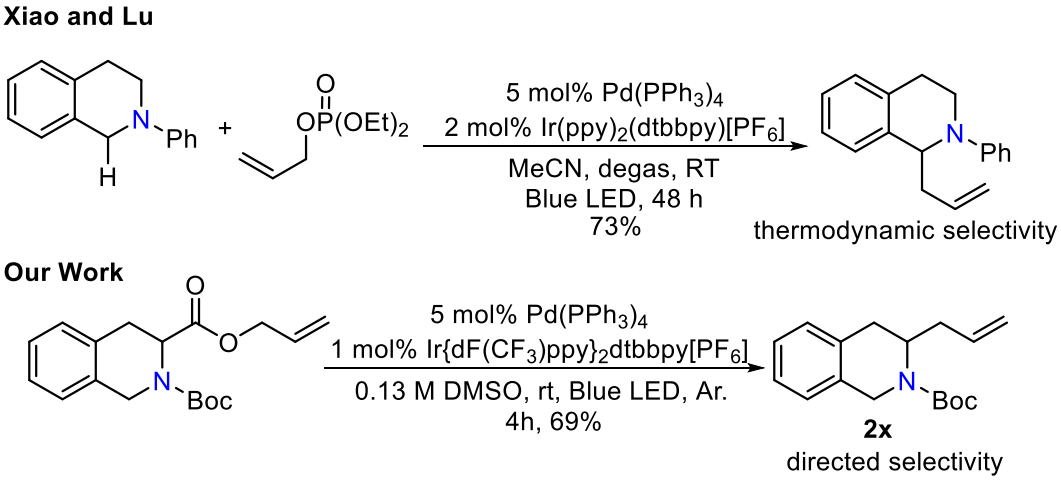

Several *N*-Boc amino acids were also allylated with allyl methyl carbonate, avoiding the need for intramolecular tethering via the corresponding allyl ester. The yields obtained were also markedly higher than those from the pre-formed esters (yields in parentheses refer to Scheme 28). Pleasingly, dipeptides could also be site-specifically decarboxlyated, although longer reaction times were required. These observations indicate that our method may serve as a way to selectively label the C-termini of various peptides (Scheme 30).

Scheme 30. DcA of acids and dipeptides[a,b,c]

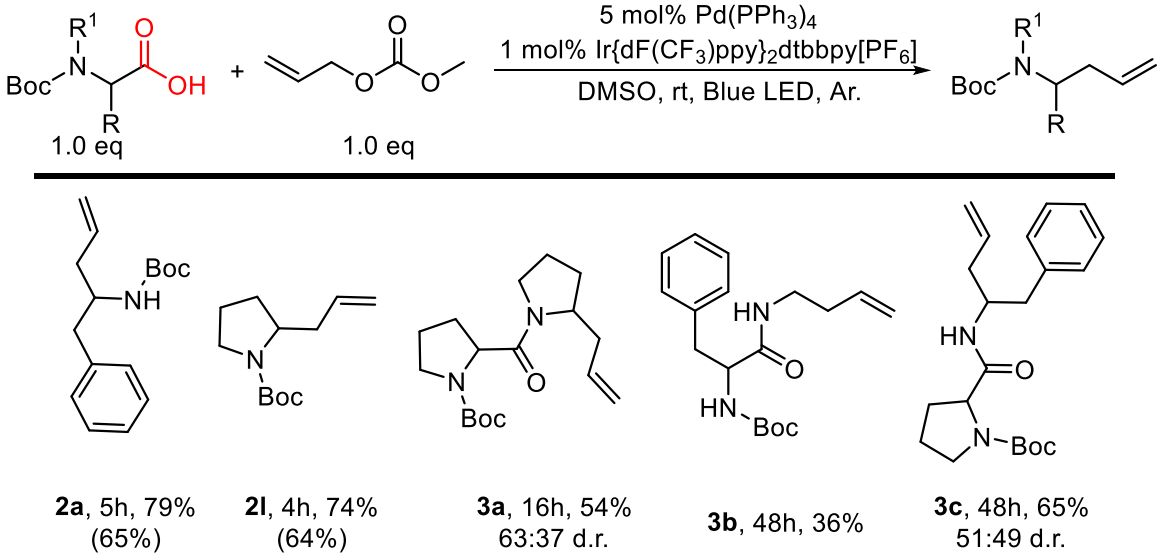

2a, 5h, 79% (65%) | **2l**, 4h, 74% (64%) | **3a**, 16h, 54% 63:37 d.r. | **3b**, 48h, 36% | **3c**, 48h, 65% 51:49 d.r.

[a] Reactions performed on a 0.25 mmol scale at 0.13M.[b] Isolated Yields.
[c]Yields in parentheses refer to entries in Scheme 28

We next turned our attention towards the mechanism of the reaction. We hoped to elucidate whether the key bond forming reaction occurred via reductive elimination from palladium or by the coupling of free radicals. Our hypothesis that if the resultant radical free radical was sufficiently unstable, it would not dissociate from palladium. To this end, three substrates that form radicals of varying stability were synthesized (Scheme 31).

Scheme 31. Substrates used for mechanstic probing

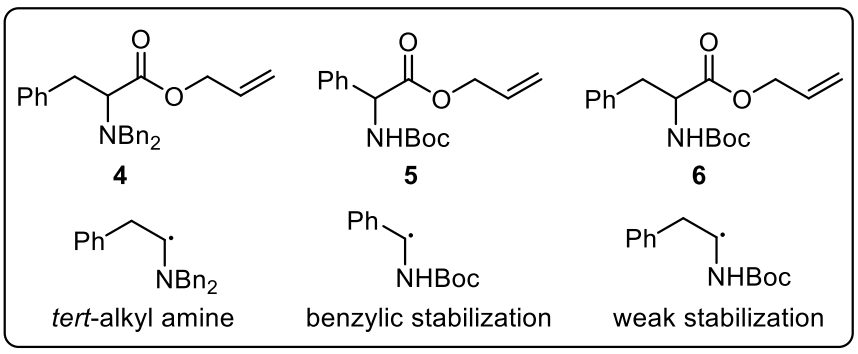

Substrate **4** contains electron rich benzyl substituents on the α-amine and we predicted that this would confer additional stability to the radical formed via decarboxylation. Substrate **5** has an electron withdrawing carbamate functionality but also an α-phenyl group which generates a benzylic radical post decarboxylation. Substrate **6** has the same electron withdrawing carbamate, but does not have benzylic stabilization. The most direct evidence for the stability of a radical changing the mechanistic course of the reaction came from accessing the transfer of chiral information from a palladium complex ligated by chiral ligands (Scheme 32).

Scheme 32. Probing radical stability versus stereochemical outcome of radical DcA

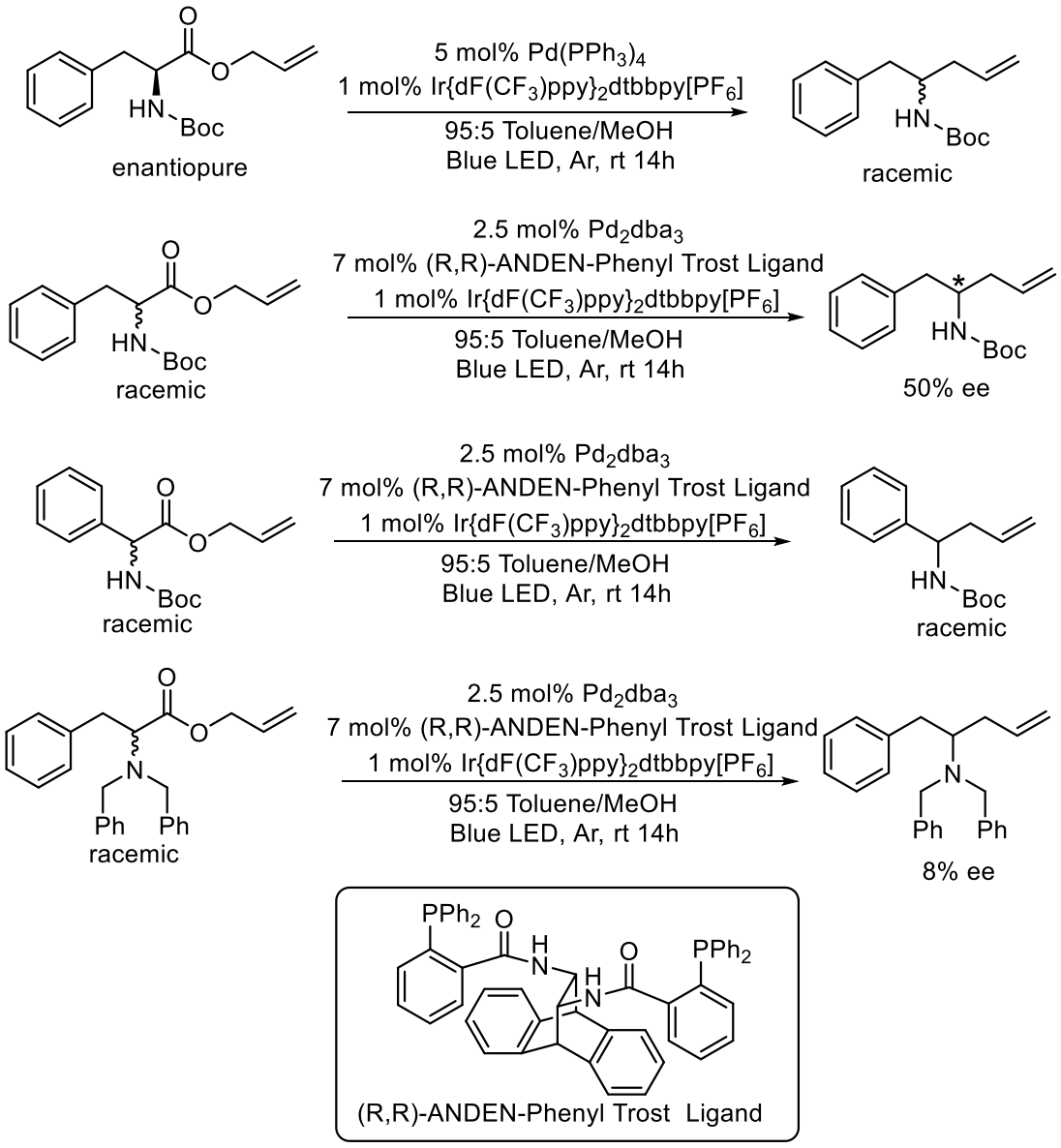

First, we verified that when enantiopure starting material was used the resulting product was racemic. These results confirmed that a radical formed via decarboxylation, destroying the chiral information of the starting material prior to allylation. Then, racemic substrates **4**, **5**, and **6** were subjected to the exact same reaction conditions with Pd_2dba_3 and a chiral Trost ligand. When substrate **6**, which forms the least stable radical was employed (the bond dissociation of this species is 5-6 kcal/mol higher than substrates **4/5**),[23] the resulting product was isolated with a 50%ee, indicating that a chiral palladium species is involved in the C–C bond forming step. Substrate **5**, which contains the electron withdrawing Boc group and an α-phenyl substituent, provided racemic product. This observation supports our hypothesis that the bond formation did not occur within the coordination sphere of palladium. Similarly, substrate **6** provided only slightly enantioenriched product, indicating that two pathways could be in directly compete with each other.

However, this experiment does not account for the fact that substrates **4** and **5** could just be less affected by the asymmetric environment about palladium. To account for this, we subjected substrates **5** and **6** to varying concentrations of palladium and monitored the reactions by ^{1}H NMR spectroscopy. If palladium was involved in the C–C bond step, then an increased concentration of palladium should lead to more desired product formation via reductive elimination, and less byproduct formation. On the other hand, if the products formed via radical coupling away from the coordination sphere, then the concentration of palladium should not change the ratio of desired product to undesired byproduct. When substrate **5** was subjected to varying concentrations of palladium the ratio of desired product to hexadiene dimer did not appreciably change. However, when substrate **6** was subjected to varying concentrations of palladium the ratio of product to hexadiene did change. As the concentration of palladium decreased the amount of undesired hexadiene increased. These observations suggest that two

Scheme 33. Palladium concentration and byproduct formation

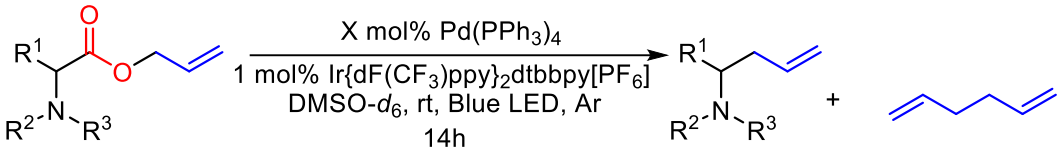

substrate	intermediate radical	mol% Pd[a]	product : hexadiene
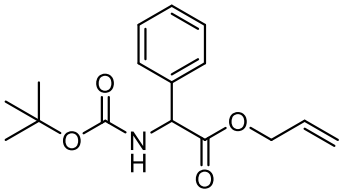 **5**	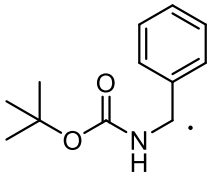	5	1.0 : **0.30**
		2.5	1.0 : **0.28**
		1	1.0 : **0.27**
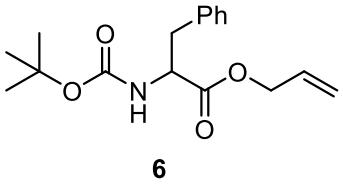 **6**	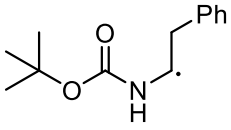	5	1.0 : **0.08**
		2	1.0 : **0.11**
		1[b]	1.0 : **0.43**

[a] At a constant substrate concentration of 0.0125M.
[b] Reaction did not reach complete conversion

mechanisms compete with each other, when less stable radicals, such as that formed with substrate **6**, are utilized (Scheme 33).

These experiments allowed us to propose a mechanism that was consistent with our observations. As before, we propose that palladium forms an electrophilic Pd-π-allyl complex and an anionic carboxylate. Oxidation of the carboxylate by one electron by the photoexcited Ir species triggers radical decarboxylation and yields an α-amino radical. From here, if the radical is unstable, it may coordinate to palladium generating a transient Pd^{III} species which provides the desired product after reductive elimination. The reduced photocatalyst then reduces palladium back to Pd(0). Alternatively, if the radical does not readily coordinate to palladium it can dissociate and the photocatalyst can reduce the palladium-allyl species to provide Pd(0) and an allylic radical, which form desired products or homodimeric byproducts (Scheme 34).

Scheme 34. Divergent mechanisms for radical DcA based on radical stability

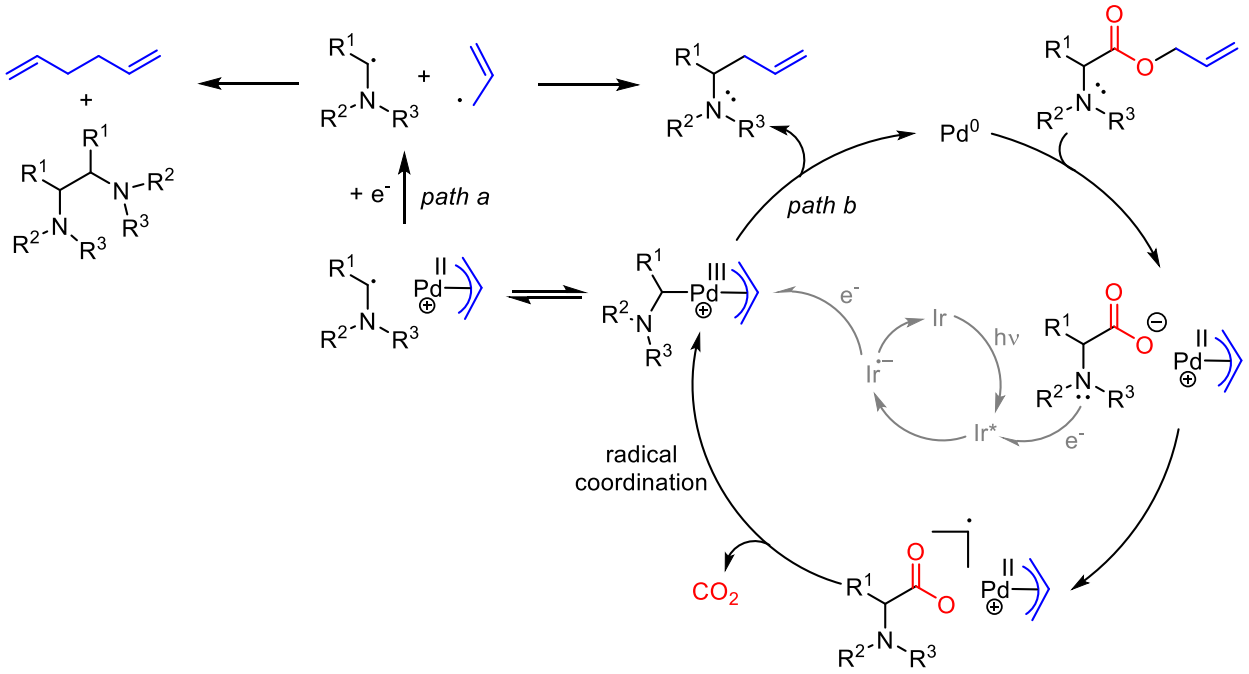

We also attempted to examine the stereochemical course of the radical DcA reaction using (Z)-5-(methoxycarbonyl)-2-cyclohexen-1-yl methyl carbonate (Scheme 35). Palladium should add to the bottom face of this molecule to form the π-allyl complex. If the radical directly attacks palladium (inner sphere attack) and reductive elimination occurs, then the new bond would be *trans* to the pendant ester. If the radical displaces palladium in an S_N2 type attack (outer sphere), then the new bond would be cis to the ester.[24] Unfortunately only the corresponding allylic ester was isolated when the methyl carbonate was subjected to the standard reaction conditions with Boc-Phe-OH, no decarboxylation occurred.

Scheme 35. Failed stereochemical test

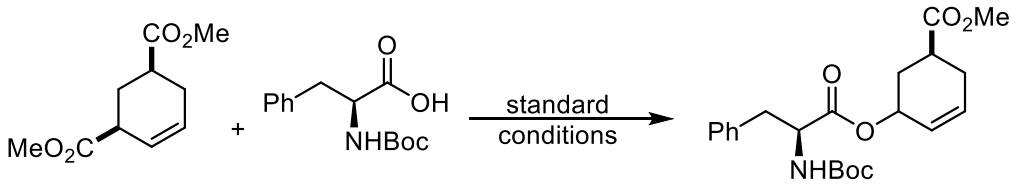

Additional attempts to improve the enantioselecitivity of the reaction by screening commercially available chiral ligands and palladium(0) precursors were not successful (Scheme 36). The results obtained in Scheme 32 represent the highest %ee achieved. Endeavors were also made to extend the reaction to α-ethereal allylic esters. Although reactivity was observed in many cases yields were low and byproducts of similar R_f values were often observed. Extensive solvent screening, variation of ligands on palladium, and catalyst selection were utilized in attempts to encourage product reactions. Unfortunately, general conditions for well-behaved reactions of these classes of molecules were not realized after over 150 experiments (Scheme 36).

Scheme 36. Studies on stereoconvergent allylation and failed substrate classes.

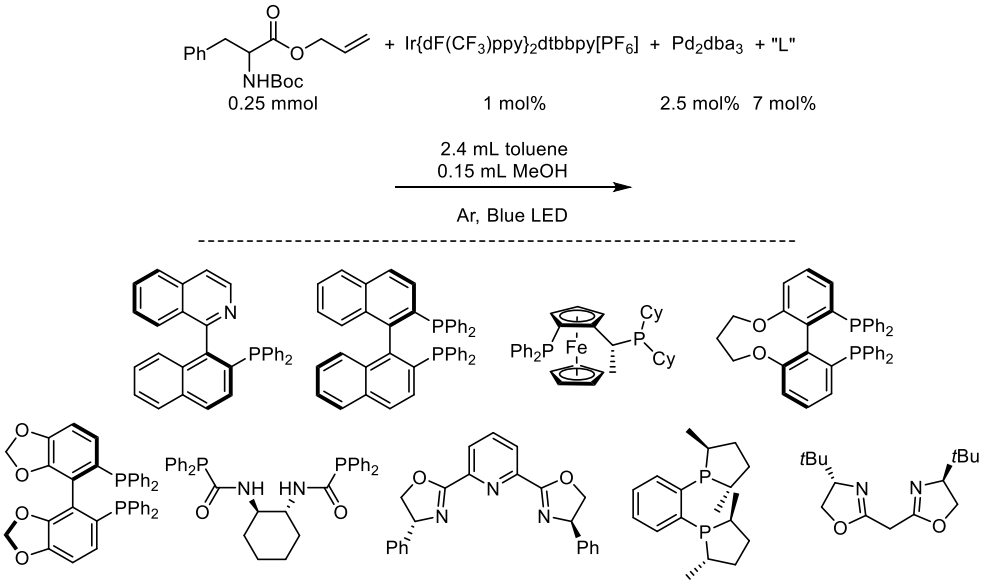

2.5 Conclusion

In conclusion, we have expanded the scope of the DcA reaction to synthetically useful amino acid derivatives that do not undergo two electron decarboxylation. Subsequent mechanistic analysis revealed that divergent mechanisms based upon radical stability are likely operative.

2.6 References for Chapter 2

[1] Weaver, J. D.; Recio III, A.; Grenning, A. J.; Tunge, J. A. "Transition Metal-Catalyzed Decarboxylative Allylation and Benzylation Reactions" *Chem. Rev.* **2011**, *111*, 1846-1913.

[2] Trost, B. M. "Atom Economy: A Search for Synthetic Efficiency" *Science* **1991**, *254*, 1471-1477.

[3] Shimizu, I.; Yamada, T.; Tsuji, J. "Palladium-Catalyzed Rearrangement of Allylic Esters of Acetoacetic Acid to Give γ,σ-unsaturated Methyl Ketones" *Tett. Lett.* **1980**, *21*, 3199-3202.

[4] Tsuda, T.; Chujo, Y.; Nishi, S.; Tawara, K.; Saegusa, T. "Facile Generation of a Reactive Palladium(II) Enolate Intermediate by the Decarboxylation of Palladium(II) β-Ketocarboxylate and Its Utilization in Allylic Acylation" *J. Am. Chem. Soc.* **1980**, *102*, 6381-6385.

[5] Burger, E. C.; Tunge, J. A. "Asymmtric Allylic Alkylation of Ketone Enolates: An Asymmetric Claisen Surrogate" *Org. Lett.* **2004**, *11*, 4113.

[6] Behenna, D. C.; Stoltz, B. M. "The Enantioselective Tsuji Allylation" *J. Am. Chem. Soc.* **2004**, *126*, 15044-15045.

[7] Trost, B. M.; Xu, J. "Regio- and Enantioselective Pd-Catalyzed Allylic Alkylations of Ketones through Allyl Enol Carbonates" *J. Am. Chem. Soc.* **2005**, *127*, 2846-2847.

[8] Burger, E. C.; Tunge, J. A. "Synthesis of Homoallylic Amines via the Palladium-Catalyzed Decarboxylative Coupling of Amino Acids Derivatives" *J. Am. Chem. Soc.* **2006**, *128*, 10002-10003.

[9] Yeagley, A. A.; Churma, J. J. "C-C Bond-Forming Reactions via Pd-Mediated Decarboxylative α-Imino Anion Generation" *Org. Lett.* **2007**, *9*, 2879-2882.

[10] Grenning, A. J.; Tunge, J. A. "Rapid Decarboylative Allylation of Nitroalaknes" *Org. Lett.* **2010**, *12*, 740-742.

[11] Waetzig, S. R.; Tunge, J. A. "Palladium-Catalyzed Decarboxylative sp^3-sp^3 Coupling of Nitrobenzene Acetic Esters" *J. Am. Chem. Soc.* **2007**, *129*, 14860-1481.

[12] Recio III, A.; Tunge, J. A. "Regiospecific Decarboxylative Allylation of Nitriles" *Org. Lett.* **2009**, *11*, 5630-5633.

[13] Weaver, J. D.; Tunge, J. A. “Decarboxylative Allylation using Sulfones as Surrogates of Alkanes” *Org. Lett.* **2008**, *10*, 4657-4660.

[14] Zang, J.; Stanciu, C.; Wang, B.; Hussain, M. M.; Da, C.; Carroll, P. J.; Dreher, S. D.; Walsh, P. J. “Palladium-Catalyzed Allylic Substitution with (η^6-Arene-CH_2Z)$Cr(CO)_3$-Based Nucleophiles” *J. Am. Chem. Soc.* **2011**, *133*, 20552-20560.

[15] Joschek, H.; Grossweiner, L. I. “Optical Generation of Hydrated Electrons from Aromatic Compounds” *J. Am. Chem. Soc.* **1966**, *88*, 3261-3268.

[16] Anderson, J. M.; Kochi, J. K. “Manganese(III) complexes in oxidative decarboxylation of acids” *J. Am. Chem. Soc.* **1970**, *92*, 2450-2460.

[17] Sharkey, W. H.; Langkammerer, C. M. “2,7-dimethyl-2,7-dinitrooctane” *Org. Synth.* **1961** *41*, 24**.**

[18] Su, Z.; Mariano, P. S.; Falvey, D. E.; Yoon, U. C.; Oh, S. W. “Dynamics of Anilinium Radical α-Heterolytic Fragmentation Processes. Electrofugal Group, Subtituent, and Medium Effects on Desylation, Decarboxylation and Retro-Aldol Cleavage Pathways” *J. Am. Chem. Soc.* **1998**, *120*, 10676-10686.

[19] Miyake, Y.; Nakajima K.; Nishibayashi, Y. “Visible light-mediated oxidative decarboxylation of arylacetic acids into benzyl radicals: addition to electron-deficient alkenes by using photoredox catalysts” *Chem. Commun.* **2013**, *49*, 7854-7856.

[20] Miyake, Y.; Nakajima, K.; Nishibayashi, Y. “Visible-Light-Mediated Utilization of α-Aminoalkyl Radicals: Addition to Electron-Deficient Alkenes Using Photoredox Catalysts” *J. Am. Chem. Soc.* **2012** *134*, 3338-3341.

[21] Kunkely, H.; Vogler, A. “Excited state properties of dimeric allylpalladium(II) chloride. Photoreduction of palladium induced by lignd-to-metal charge transfer excitation” *Inorg. Chim. Acta.* **2003**, *344*, 262-264.

[22] Xuan, J.; Zeng, T-T.; Feng, Z-J.; Deng, Q-H.; Chen, J-R.; Lu, L-Q.; Xiao, W-J.; Alper, H. “Redox-Neutral α-Allylation of Amines by Combining Palladium Catalysis and Visible-Light Photoredox Catalysis” *Angew. Chem. Int. Ed.* **2015**, *54*, 1625-1628.

[23] Lang, S. B.; O’Nele, K. M.; Douglas, J. T.; Tunge, J. A. “Dual Catalytic Decarboxylative Allylation of α-Amino Acids and Their Divergent Mechanisms” *Chem. Eur. J.* **2015**, *21*, 18589-18593.

[24] Trost, B. M.; Verhoeven, T. R. “Allylic Alkylation. Palladium-Catalyzed Substitutions of Allylic Carboxylates. Stereo- and Regiochemistry” *J. Am Chem. Soc.* **1980**, *102*, 4730-4743.

Chapter 2 Appendix

Experimental methods and spectral analysis for Ch. 2 compounds

Table of Contents

General Information:

TLC analysis was performed (fluorescence quenching of $KMnO_4$ stain) with silica gel HL TLC plates with UV254 purchased from Sorbent Technologies.

Silica gel used for column chromatography (60 Å porosity, 230 x 400 mesh, standard grade) was purchased from Sorbent Technologies.

$Pd(PPh_3)_4$, (R,R)-ANDEN-Phenyl Trost ligand and the photocatalyst $[Ir\{dF(CF_3)ppy\}_2(dtbbpy)]PF_6$ were purchased from Sigma Aldrich and stored in an Ar filled glovebox. Pd_2dba_3 was purchased from Strem and stored in a glovebox.

Allyl methyl carbonate was purchased from Sigma Aldrich.

Anhydrous DMSO, MeCN, and toluene were purchased from Sigma Aldrich and stored in a glove box.

GC/MS data was obtained on a Shimadzu GCMS-QP2010 SE. ^{1}H and ^{13}C NMR spectra were obtained on a Bruker ADVANCE 500 DRX equipped with a QNP cryoprobe. NMR spectra were referenced to their residual protio solvent systems. HRMS data was obtained on a ESI LC-TOF Micromass LCT (Waters).

GC/MS Method: Column oven temp: 110 ^{o}C. Injection temp: 290 ^{o}C. Injection mode: split. Carrier gas: He, 9.5 psi. Flow: 45.8 mL/min. Column flow: 0.88 mL/min. Linear velocity 35 cm/sec. Purge flow: 1.0 mL/min. Split rate: 50. The temperature is maintained at 110 ^{o}C for 2 mins after injection. Then, the temperature is raised 30 ^{o}C/min to 320^{o}C. This temperature is held for 8 mins.

Final DcA reactions that yielded products **1**x were run in an oven dried 2.0 – 5.0 mL microwave vial from Biotage using a TCP 14W white LED bulb (LED14E26P3027KFL). A water bath was

used to ensure the reaction remained at room temperature. See photo 1 for a representative experimental setup.

Final DcA reactions that yielded products **2x** were run in screw threaded tubes from Chemglass. Two different blue LED light baths were employed. Room temperature reactions were run in a beaker wrapped with blue LEDs which was then covered in aluminum foil. A fan was placed directly above the beaker (photo 2). Reactions performed at elevated temperatures were done in a glass crystallization dish with the outside walls wrapped in blue LED strips. The dish was covered in aluminum foil and filled wither water which was heated to a preset temperature with stirring using a stir plate. The reaction tubes were held in place by a cardboard lid (photo 3).

Photo 1:

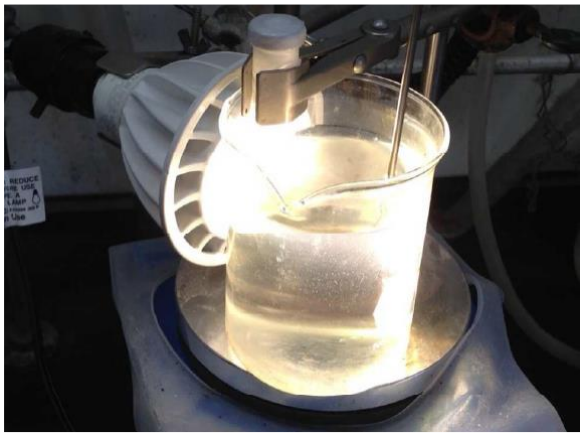

Photo 2:

Photo 3:

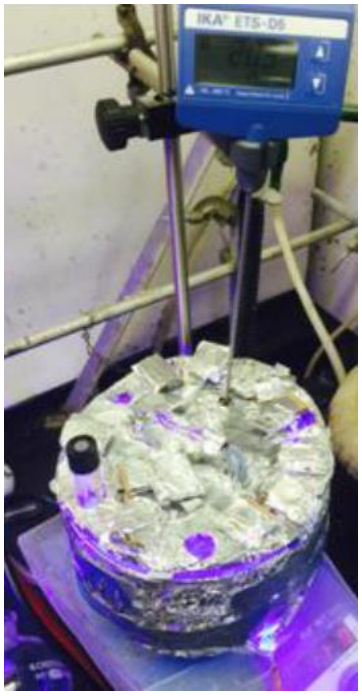

Representative Procedure for the preparation of phenylacetic acids:

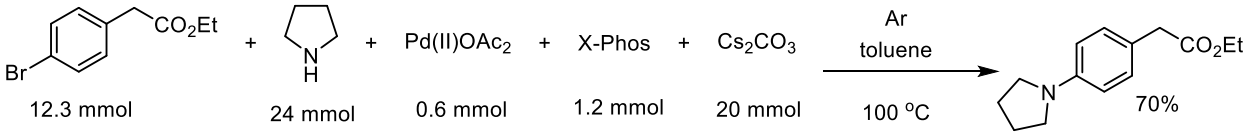

Prepared via the procedure detailed by Nishibayashi[1]: In a flame dried Schlenk flask cooled under Argon was added palladium acetate, cesium carbonate, X-Phos, and toluene (30 mL). The amine was added via syringe and the reaction mixture heated at 100 °C overnight. The reaction mixture was concentrated *in vacuo*, loaded onto silica gel and purified via flash column chromatography to yield the desired product in a 70% yield.

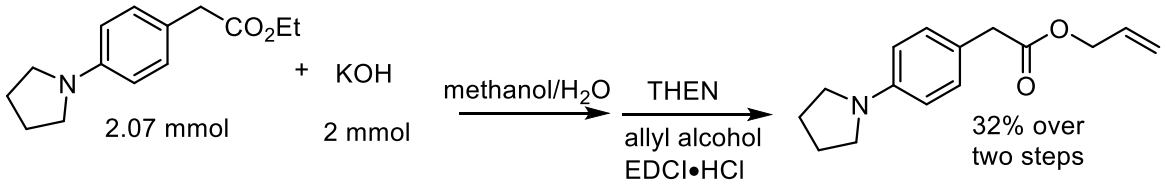

The corresponding esters were then saponified using the same procedure published by Nishibayashi [1] using KOH in MeOH/water. The following acids (4/5 known) were prepared:

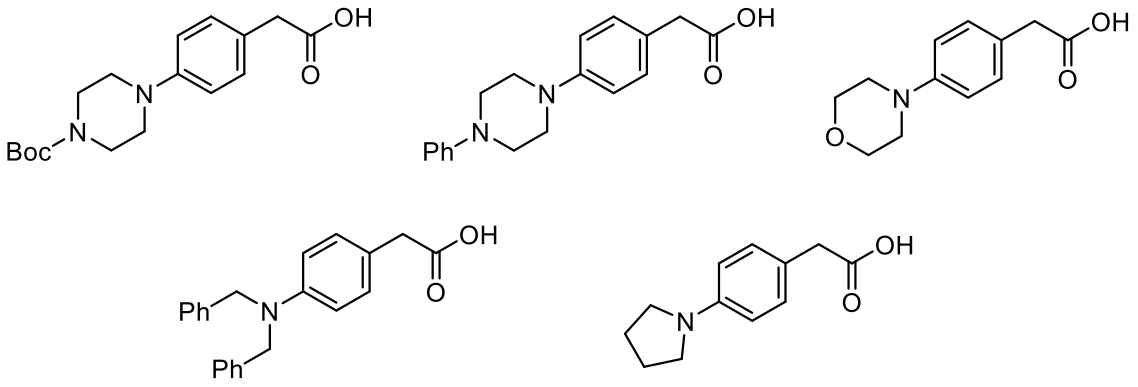

The characterization data for the novel phenylpiperazine analog:

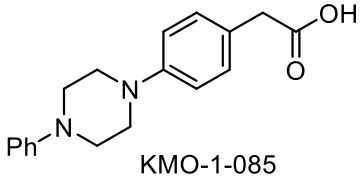

KMO-1-085

^{1}H NMR Spectra (500 MHz, $CDCl_3$): δ 7.30 (dd, *J* = 8.70, 7.25 Hz, 2H), 7.21 (d, *J* = 8.60 Hz, 2H), 6.96 (m, 5H), 3.59 (s, 2H), 3.34 (s, H).

^{13}C NMR (126 MHz, $CDCl_3$): δ 175.8, 151.2, 150.4, 130.1, 129.2, 124.7, 120.2, 116.5, 116.4, 49.4, 49.4, 39.9.

HRMS:M+H calc: 297.1603, M+H found: 297.1599.

Synthesis of para amino substituted phenyl acetic allyl esters (1a'-1h'):

Reactions were typically run on a 1 to 5 mmol scale.

General procedure: To a cooled stirred solution under argon of the para amino phenylacetic acid (1.0 equiv.) in DCM was added base (Et_3N or Hunig's base, 2.5 equiv.), followed by allyl

alcohol (1.3 equiv.), and then coupling reagent (1.3 equiv.). The solution was allowed to warm to rt and stirred overnight. The solvent was evaporated and the crude product purified by flash chromatography (eluent was typically 1:20 EtOAc:Hexanes).

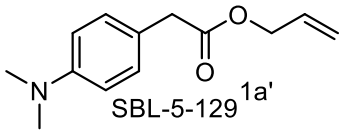

SBL-5-129 1a'

DCC and catalytic DMAP (no base) were used. 2.8 mmol scale, 0.435g, 72% yield.

^{1}H NMR Spectra (500 MHz, $CDCl_3$): δ 7.16 (d, *J* = 8.62 Hz, 2H), 6.70 (d, *J* = 8.67 Hz, 2H), 5.90 (m, 1H), 5.25 (m, 2H), 4.58 (dt, *J* = 5.64, 1.40 Hz, 2H), 3.55 (s, 2H), 2.93 (s, 6H).

^{13}C NMR (126 MHz, $CDCl_3$): δ 172.0, 149.8, 132.2, 129.9, 121.7, 118.1, 112.8, 65.3, 40.7, 40.4.

HRMS:M+H calc: 220.1338, M+H found: 220.1332.

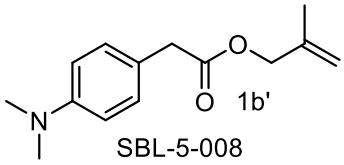

SBL-5-008

PyBOP and β-methallyl alcohol were used. 2.8 mmol scale, 0.285g, 44% yield.

^{1}H NMR Spectra (500 MHz, $CDCl_3$): δ 7.16 (d, *J* = 8.64 Hz, 2H), 6.70 (d, *J* = 8.67 Hz, 2H), 4.91 (d, *J* = 15.70 Hz, 2H), 4.50 (s, 2H), 3.56 (s, 2H), 2.93 (s, 6H), 1.72 (s, 3H).

^{13}C NMR (126 MHz, $CDCl_3$): δ 172.0, 149.8, 140.0, 129.9, 121.8, 112.8, 112.7, 67.8, 40.7, 40.4, 19.5.

HRMS:M+H calc: 234.1494, M+H found: 234.1490.

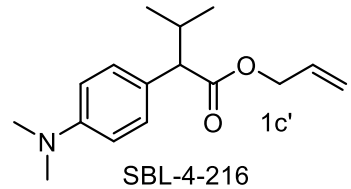

SBL-4-216

10 mL of DMF was added to 4-dimethylamino phenylacetic acid allyl ester (0.20 g, 0.91 mmol) in a Schlenk flask under argon. The solution was cooled to 0 ^{o}C and KO^{t}Bu (0.10 g, 0.91 mmol) was added followed by 2-bromopropane (0.11 g, 0.91 mmol). After

stirring overnight at room temperature, the reaction mixture was taken up in EtOAc, washed with water, dried, concentrated, and purified by flash column chromatography to give the desired product (0.166g) in a 70% yield.

^{1}H NMR Spectra (500 MHz, $CDCl_3$): δ 7.19 (d, *J* = 8.71 Hz, 2H), 6.68 (d, *J* = 8.72 Hz, 2H), 5.87 (m, 1H), 5.21 (m, 2H), 4.59 (ddt, *J* = 13.41, 5.67, 1.45 Hz, 1H), 4.49 (ddt, *J* = 13.42, 5.61, 1.46 Hz, 1H), 2.93 (s, 3H), 2.30 (m, 1H), 1.02 (d, *J* = 6.51 Hz, 3H), 0.72 (d, *J* = 6.69 Hz, 3H).

^{13}C NMR (126 MHz, $CDCl_3$): δ 174.2, 149.8, 132.3, 129.1, 126.2, 117.9, 112.5, 65.0, 59.1, 40.6, 31.8, 21.5, 20.3.

HRMS: M+H calc: 262.1807, M+H found: 262.1809.

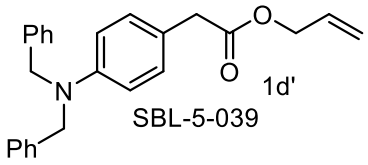

SBL-5-039

EDCI HCl was used as the coupling reagent, 3.0 mmol scale, 0.687g, 61% yield.

^{1}H NMR Spectra (500 MHz, $CDCl_3$): δ 7.32 (m, 4H), 7.25 (m, 6H), 7.08 (d, *J* = 6.86 Hz, 2H), 6.69 (d, *J* = 8.11 Hz, 2H), 5.90 (m, 1H), 5.24 (m, 2H), 4.64 (s, 4H), 4.58 (d, *J* = 4.50 Hz, 2H), 3.53 (s, 2H).

^{13}C NMR (126 MHz, $CDCl_3$): δ 172.0, 148.2, 138.5, 132.2, 130.1, 128.7, 126.9, 126.6, 121.8, 118.1, 112.5, 65.3, 54.2, 40.2.

HRMS:M+H calc: 372.1964, M+H found: 372.1976.

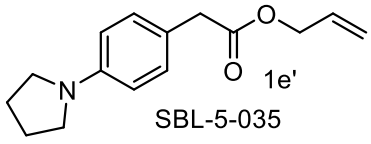

SBL-5-035

EDCI HCl was used. 7.7 mmol scale, 0.603g, 32% yield.

^{1}H NMR Spectra (500 MHz, $CDCl_3$): δ 7.14 (d, *J* = 8.56 Hz, 2H), 6.52 (d, *J* = 8.59 Hz, 2H), 5.90 (m, 1H), 5.24 (m, 2H), 4.58 (dt, *J* = 5.67, 1.42 Hz, 2H), 3.54 (s, 2H), 3.26 (m, 4H), 1.99 (m, 4H).

^{13}C NMR (126 MHz, $CDCl_3$): δ 172.1, 147.1, 132.3, 130.0, 120.4, 118.0, 111.7, 65.3, 47.6, 40.5, 25.5.

HRMS: M+H calc: 246.1494, M+H found: 246.1489.

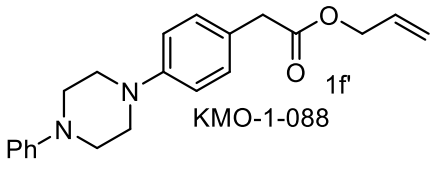

EDCI HCl was used, 1.2 mmol scale, 0.626g, 88% yield.

^{1}H NMR Spectra (500 MHz, $CDCl_3$): δ 7.31 (m, 2H), 7.24 (m, 2H), 7.01 (m, 2H), 6.97 (m, 2H), 6.92 (tt, *J* = 7.35, 1.06 Hz, 1H), 5.93 (m, 1H), 5.27 (m, 2H), 4.61 (dt, *J* = 5.66, 1.43 Hz, 2H), 3.61 (s, 2H), 3.35 (s, 8H).

^{13}C NMR (126 MHz, $CDCl_3$): δ 171.7, 151.3, 150.3, 132.2, 130.1, 129.2, 125.3, 120.1, 118.2, 116.5, 116.4, 65.4, 49.5, 49.4, 40.5.

HRMS: M+H calc: 337.1916, M+H found: 337.1913.

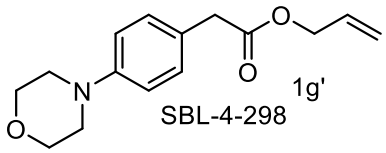

PyBOP was used, 5.1 mmol scale, 0.733g, 55% yield over two steps from the ethyl ester.

^{1}H NMR Spectra (500 MHz, $CDCl_3$): δ 7.20 (d, *J* = 8.61 Hz, 2H), 6.87 (d, *J* = 8.65 Hz, 2H), 5.90 (m, 1H), 5.24 (m, 2H), 4.58 (dt, *J* = 5.72, 1.46 Hz, 2H), 3.85 (m, 4H), 3.57 (s, 2H), 3.14 (m, 4H).

^{13}C NMR (126 MHz, $CDCl_3$): δ 171.6, 150.4, 132.1, 130.0, 125.3, 118.2, 115.8, 66.9, 65.4, 49.4, 40.4.

HRMS: M+H calc: 262.1443, M+H found: 262.1448.

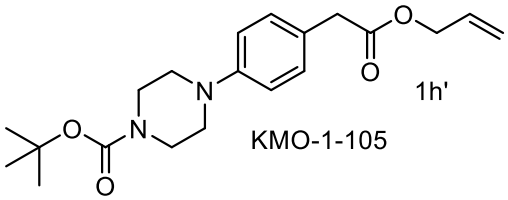

EDCI HCl was used, 3.1 mmol scale, 0.620g, 55% yield.

^{1}H NMR Spectra (500 MHz, $CDCl_3$): δ 7.19 (d, *J* = 8.59 Hz, 2H), 6.88 (d, *J* = 8.61 Hz, 2H), 5.90 (m, 1H), 5.24 (m, 2H), 4.58 (dt, *J* = 5.68, 1.42 Hz, 2H), 3.57 (m, 6H), 3.11 (t, *J* = 5.12 Hz, 4H), 1.48 (s, 9H).

^{13}C NMR (126 MHz, $CDCl_3$): δ 171.6, 154.7, 150.4, 132.1, 130.0, 125.5, 118.2, 116.7, 79.9, 65.4, 49.4, 40.4, 28.4.

HRMS: M+H calc: 361.2127, M+H found: 361.2133.

General procedure for the synthesis of α-amino allyl esters (1'-1m'):

α-bromo phenylacetic acid allyl ester (1.0 equiv.) in DMF was cooled to 0 ^{o}C under argon. The secondary amine (1.0 equiv.), K_2CO_3 (1.0 equiv.), and tetrabutyl ammonium iodide (0.25 equiv.) were added and the reaction stirred at room temperature overnight. The solution was taken up in EtOAc, washed with water, dried, concentrated, and purified by flash column chromatography (typical eluent1:30 EtOAc:Hexanes).

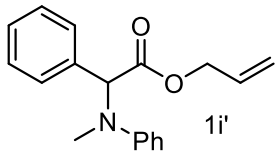

1i'

SBL-5-063

4.2 mmol scale, 1.03g, 87% yield.

^{1}H NMR Spectra (500 MHz, $CDCl_3$): δ 7.34 (m, 7H), 6.89 (m, 2H), 6.82 (m, 1H), 5.90 (m, 1H), 5.70 (s, 1H), 5.26 (m, 2H), 4.71 (m, 2H), 2.81 (s, 3H).

^{13}C NMR (126 MHz, $CDCl_3$): δ 171.6, 149.9, 135.8, 131.7, 129.3, 128.7, 128.5, 128.1, 118.9, 118.1, 113.5, 65.7, 65.6, 34.6.

HRMS: M+H calc: 282.1494, M+H found: 282.1498.

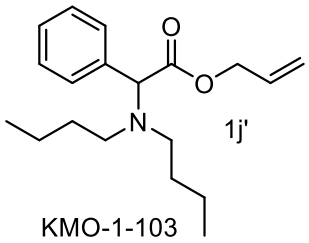

KMO-1-103 4.0 mmol scale, 0.798g, 66% yield.

^{1}H NMR Spectra (500 MHz, $CDCl_3$): δ 7.38 (m, 2H), 7.31 (m, 3H), 5.90 (m, 1H), 5.24 (m, 2H), 4.64 (m, 2H), 4.59 (s, 1H), 2.54 (t, *J* = 7.44 Hz, 4H), 1.39 (m, 4H), 1.21 (m, 4H), 0.83 (t, *J* = 7.35 Hz, 6H).

^{13}C NMR (126 MHz, $CDCl_3$): δ 172.2, 137.4, 132.1, 128.8, 128.2, 127.7, 118.4, 68.9, 65.0, 50.4, 29.7, 20.4, 14.0.

HRMS: M+H calc: 304.2277, M+H found: 304.2269.

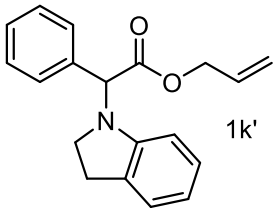

KMO-1-096 4.0 mmol scale, 0.620g, 53% yield.

^{1}H NMR Spectra (500 MHz, $CDCl_3$): δ 7.38 (m, 5H), 7.06 (m, 2H), 6.69 (td, *J* = 7.41, 0.93 Hz, 1H), 6.46 (d, *J* = 7.98 Hz, 1H), 5.86 (m, 1H), 5.31 (s, 1H), 4.67 (m, 2H), 3.65 (q, *J* = 9.42, 8.60 Hz, 1H), 3.14 (m, 1H), 3.14 (ddd, *J* = 9.71, 8.52, 5.63, 1H), 2.93 (m, 2H).

^{13}C NMR (126 MHz, $CDCl_3$): δ 170.9, 150.9, 135.1, 131.7, 130.3, 128.7, 128.7, 128.4, 127.2, 124.7, 118.8, 118.4, 106.8, 65.6, 63.8, 49.8, 28.2.

HRMS:M+H calc: 294.1494, M+H found: 294.1487.

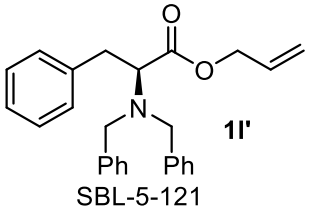

SBL-5-121 Boc-Phe-OH (2.0 g, 7.54 mmol) was dissolved in 20 mL and cooled to 0 ^{o}C under argon. K_2CO_3 (1.38 g, 10 mmol) and tetrabutyl ammonium bromide (0.34 g, 1 mmol)

were added followed by allyl bromide (0.75 mL, 8.5 mmol). The reaction was stirred at room temperature overnight. The mixture was taken up in EtOAc and washed with water, dried, and concentrated. The residue was purified by column chromatography and then treated with 30% TFA/DCM until TLC indicated complete conversion to the free amine. The mixture was washed with aq K_2CO_3 to provide the phenyl alanine allyl ester in a 81% yield over two steps.

The ester (6.09 mmol) was dissolved in MeCN under argon and benzyl bromide (1.60 mL, 13.4 mmol) was added followed by Hunig's base (2.60 mL, 15 mmol). The mixture was refluxed overnight, concentrated, and purified by column chromatography to provide the desired dibenzyl allyl ester (1.45g) in a 62% yield.

^{1}H NMR Spectra (500 MHz, $CDCl_3$):

δ 7.26 (m, 9H), 7.19 (m, 4H) 7.03 (m, 2H), 5.95 (m, 1H), 5.30 (m, 2H), 4.65 (m, 2H), 3.97 (d, *J* = 13.99 Hz, 2H), 3.71 (t, *J* = 7.73 Hz, 1H), 3.58 (d, *J* = 13.91 Hz, 2H), 3.14 (dd, *J* = 13.96, 7.20 Hz, 1H), 3.02 (dd, *J* = 13.98, 8.31 Hz, 1H).

^{13}C NMR (126 MHz, $CDCl_3$):

δ 172.0, 139.3, 138.1, 132.2, 129.5, 128.7, 128.2, 126.9, 126.3, 118.5, 65.0, 62.3, 54.4, 35.8.

HRMS: M+H calc: 386.2120, M+H found: 386.2121.

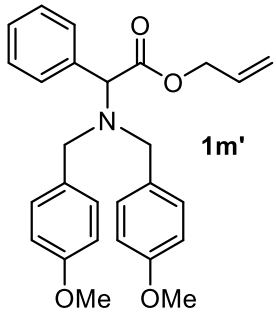

1m'

SBL-5-088

4.0 mmol scale, 0.70 g, 40% yield.

^{1}H NMR Spectra (500 MHz, $CDCl_3$):

δ 7.34 (d, *J* = 4.35 Hz, 4H), 7.29 (m, 1H), 7.24 (d, *J* = 8.62 Hz, 4H), 6.85 (m, 4H), 5.95 (m, 1H), 5.29 (m, 2H), 4.71 (m, 2H), 4.62 (m, 1H), 3.79 (s, 6H), 3.66 (q, *J* = 13.75, 10.5 Hz, 4H).

^{13}C NMR (126 MHz, $CDCl_3$):

δ 171.9, 158.6, 136.8, 132.0, 131.6, 129.9, 128.8, 128.3, 127.8, 118.7, 113.6, 65.6, 65.0, 55.3, 53.3.

HRMS:

M+H calc: 432.2175, M+H found: 432.2165.

Representative procedure for the synthesis of allylic esters (2a'-2x'): The N-protected amino acid (5.0 mmol) was added to DMF (15 mL) and the solution cooled to 0 °C (ice bath). Hunig's base (6.5 mmol) was added followed by allyl bromide (6.5 mmol) and the solution was allowed to warm to room temperature and stir overnight. The solution was diluted with EtOAc (40 mL) and then washed with water (2 x 30 mL) and brine (30 mL). The organic phase was dried with $MgSO_4$, concentrated *in vacuo*, and purified via flash column chromatography (1:10 EtOAc:Hexanes was the typical eluent).

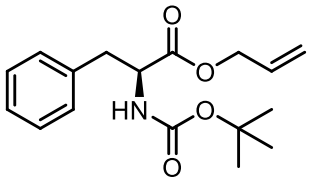

KMO-1-170 2a'

Prepared according to the representative procedure (7.5 mmol scale, 2.25g, 98% yield). The spectroscopic data matched that already reported in the literature.

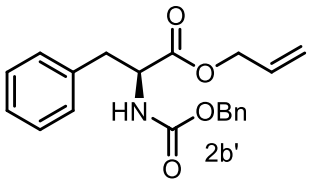

2b'

SBL-6-072

Prepared according to the representative procedure (6.7 mmol scale, 2.35g, 99% yield). The spectroscopic data matched that already reported in the literature.

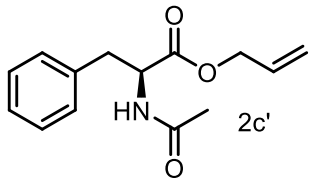

SBL-6-070

Prepared according to the representative procedure (9.7 mmol scale, 1.93g, 81% yield). The spectroscopic data matched that already reported in the literature.

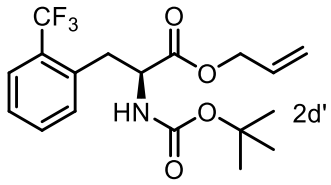

SBL-6-200

Prepared according to the representative procedure (3 mmol scale, 0.76g, 69% yield). A mixture of rotamers. Major resonances reported.

^{1}H NMR (500 MHz, $CDCl_3$) δ 7.64 (d, *J* = 7.95 Hz, 1H), 7.48 (t, *J* = 7.52 Hz, 1H), 7.36 (m, 2H), 5.81 (ddt, *J* = 16.5, 10.9, 5.70, 1H), 5.23 (m, 2H), 5.07 (d, *J* = 8.75 Hz, 1H), 4.61 (m, 3H), 3.34 (dd, *J* = 14.5, 5.95 Hz, 1H), 3.09 (dd, *J* = 14.4, 9.01 Hz, 1H), 1.36 (s, 9H).

^{13}C NMR (126 MHz, $CDCl_3$) δ 171.7, 155.1, 135.4, 131.9, 131.7, 131.4, 129.2 (q, *J* = 29.6 Hz), 127.1, 126.2 (q, *J* = 5.59 Hz), 124.6 (q, *J* = 273.7 Hz), 118.8, 80.1, 66.1, 54.6, 35.6, 28.3.

IR (film) 3367, 2980, 2935, 1745, 1715, 1504, 1454, 1367, 1315, 1251, 1171, 1120, 1060, 1039, 989, 935, 767 cm^{-1}.

HRMS: Calc'd $C_{18}H_{22}F_3NO_4Na$ (M+Na) = 396.1399, found 396.1389.

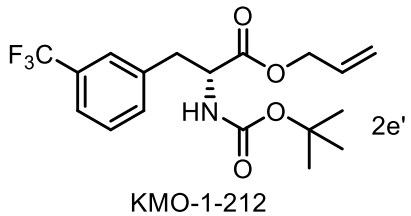

KMO-1-212

Prepared according to the representative procedure (3 mmol scale, 0.68g, 61% yield).

^{1}H NMR (500 MHz, $CDCl_3$) δ 7.50 (d, *J* = 7.77 Hz, 1H), 7.38 (m, 3H), 5.85 (ddt, *J* = 16.5, 10.4, 5.95 Hz, 1H), 5.28 (m, 2H), 5.04 (d, *J* = 7.90 Hz, 1H), 4.60 (m, 3H), 3.22 (dd, *J* = 13.8, 5.95 Hz, 1H), 3.12 (dd, *J* = 13.9, 6.07 Hz, 1H), 1.42 (s, 9H).

^{13}C NMR (126 MHz, $CDCl_3$) δ 171.2, 155.1, 137.2, 132.9, 131.3, 130.9 (q, *J* = 32.3 Hz), 129.1, 126.3 (q, *J* = 3.36 Hz), 124.1 (q, *J* = 273 Hz), 124.0 (q, *J* = 3.61 Hz), 119.6, 80.3, 66.3, 54.4, 38.3, 28.4.

IR (film) 3365, 2979, 2935, 1745, 1714, 1504, 1454, 1367, 1328, 1251, 1164, 1126, 1074, 991, 937, 794, 703, 659
cm^{-1}.

HRMS: Calc'd $C_{18}H_{22}F_3NO_4Na$ $(M+Na)^+$ = 396.1399, found = 396.1397.

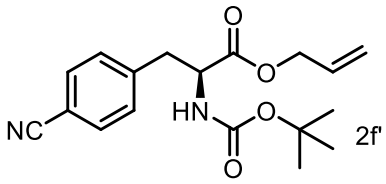

KMO-1-211

Prepared according to the representative procedure (3.4 mmol scale, 0.67g, 59% yield).

^{1}H NMR (500 MHz, $CDCl_3$) δ 7.58 (d, *J* = 7.91 Hz, 2H), 7.26 (d, *J* = 7.99 Hz, 2H), 5.85 (ddt, *J* = 16.6, 11.1, 5.91 Hz, 1H), 5.28 (m, 2H), 5.04 (d, *J* = 8.05 Hz, 1H), 4.61 (m, 3H), 3.22 (dd, *J* = 13.8, 5.86 Hz, 1H), 3.08 (dd, *J* = 13.8, 6.51 Hz, 1H), 1.40 (s, 9H).

^{13}C NMR (126 MHz, $CDCl_3$) δ 171.1, 155.0, 142.0, 132.3, 131.3, 130.4, 119.5, 118.9, 111.1, 80.4, 66.4, 54.2, 38.8, 28.4.

IR (film) 3367, 2977, 2933, 2227, 1743, 1714, 1650, 1608, 1504, 1454, 1367, 1274, 1251, 1166, 1054, 1022, 991, 937, 825, 748, 557 cm^{-1}.

HRMS: Calc'd $C_{18}H_{22}N_2O_4Na$ $(M+Na)^+$ = 353.1477, found = 353.1474.

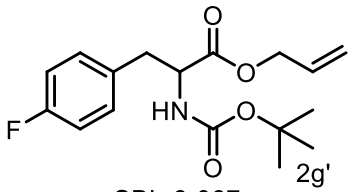

SBL-6-067

The free amino acid (1.0 g, 5.5 mmol) was added to a 1:1 mixture of THF/H_2O (15 mL each) and the mixture was cooled to 0 °C (ice bath). Triethylamine (0.91 g, 9.0 mmol) was added to the reaction mixture followed by Boc_2O (1.53 g, 7.0 mmol). The reaction was allowed to warm to room temperature and stirred overnight. Next the volatiles were removed *in vaccuo*, the pH was

adjusted to 3 with 1M HCl and the reaction mixture extracted with EtOAc (40 mL). The organic phase was washed with brine (20 mL), dried with $MgSO_4$ and concentrated *in vacuo*. The crude product was subjected to the representative procedure to yield the desired allyl ester after flash column chromatography (1.16g, 66% yield over two steps).

^{1}H NMR (500 MHz, $CDCl_3$) δ 7.10 (m, 2H), 6.97 (t, *J* = 8.67 Hz, 2H), 5.86 (ddt, *J* = 17.2, 10.3, 5.85 Hz, 1H), 5.29 (m, 2H), 4.98 (d, *J* = 8.31 Hz, 1H), 4.60 (m, 3H), 3.11 (dd, *J* = 14.0, 5.86 Hz, 1H), 3.03 (dd, *J* = 14.0, 6.19 Hz, 1H), 1.42 (s, 9H).

^{13}C NMR (126 MHz, $CDCl_3$) δ 171.6, 162.1 (d, *J* = 245 Hz), 155.1, 131.8 (d, *J* = 3.12 Hz), 131.5, 131.0 (d, *J* = 7.95 Hz), 119.2, 115.5 (d, *J* = 21.3 Hz), 80.2, 66.2, 55.6, 37.8, 28.4.

IR (film) 3434, 3365, 2977, 2933, 1745, 1714, 1602, 1510, 1446, 1367, 1222, 1168, 1097, 1056, 1016, 991, 935, 825, 748 cm^{-1}.

HRMS: Calc'd $C_{17}H_{22}FNO_4Na$ $(M+Na)^+$ = 346.1431, found = 346.1412.

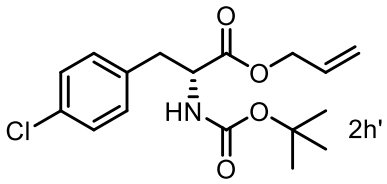

SBL-6-146

Prepared according to the representative procedure (2.2 mmol scale, 0.70g, 95% yield).

^{1}H NMR (500 MHz, $CDCl_3$) δ 7.26 (m, 2H), 7.07 (d, *J* = 8.38 Hz, 2H), 5.86 (ddt, *J* = 17.2, 10.4, 5.90 Hz, 1H), 5.29 (m, 2H), 4.97 (d, *J* = 8.27 Hz, 1H), 4.60 (m, 3H), 3.11 (dd, *J* = 13.9, 5.80 Hz, 1H), 3.03 (dd, *J* = 13.9, 6.10 Hz, 1H), 1.42 (s, 9H).

^{13}C NMR (126 MHz, $CDCl_3$) δ 171.4, 155.1, 134.6, 133.1, 131.5, 130.9, 128.8, 119.3, 80.2, 66.2, 54.5, 37.9, 28.4.

IR (film) 3355, 2977, 2933, 1741, 1714, 1492, 1454, 1367, 1253, 1166, 1091, 1056, 1016, 989, 933, 748 cm^{-1}.

HRMS: Calc'd $C_{17}H_{22}ClNO_4Na$ $(M+Na)^+$ = 362.1135, found = 362.1128.

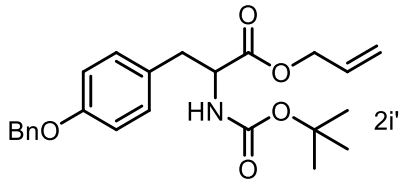

SBL-8-077

Prepared according to the representative procedure (6.5 mmol scale, 0.874g, 32% yield).

^{1}H NMR (500 MHz, $CDCl_3$) δ 7.40 (m, 4H), 7.33 (m, 1H), 7.05 (d, *J* = 8.59 Hz, 2H), 6.90 (m, 2H), 5.87 (ddt, *J* = 17.2, 10.4, 5.84 Hz, 1H), 5.31 (dq, *J* = 17.2, 1.49 Hz, 1H), 5.24 (dd, *J* = 10.4, 1.31 Hz, 1H), 5.04 (s, 2H), 4.96 (d, *J* = 8.35 Hz, 1H), 4.58 (m, 3H), 3.04 (m, 2H), 1.42 (s, 9H).

^{13}C NMR (126 MHz, $CDCl_3$) δ 171.8, 158.0, 155.2, 137.1, 131.7, 130.5, 128.7, 128.3, 128.1, 127.6, 119.1, 115.0, 80.0, 70.1, 66.1, 54.7, 37.6, 28.5.

IR (film) 3367, 3031, 2977, 2931, 1741, 1714, 1610, 1583, 1512, 1454, 1367, 1244, 1174, 1056, 1018, 991, 931, 862, 821, 738, 696 cm^{-1}.

HRMS: Calc'd $C_{24}H_{29}NO_5Na$ $(M+Na)^+$ = 434.1943, found = 434.1940.

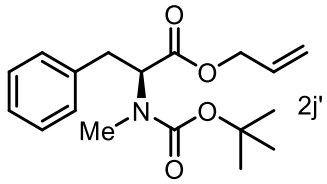

KMO-1-213

Prepared according to the representative procedure (3.6 mmol scale, 0.58g, 51% yield). A

mixture of rotamers.

^{1}H NMR (500 MHz, $CDCl_3$) δ 7.27 (m, 2H), 7.19 (m, 3H), 5.91 (dtt, *J* = 16.4, 10.8, 5.65 Hz, 1H), 5.29 (m, 2H), 4.92 (dd, *J* = 10.7, 5.33 Hz, 0.5H), 4.63 (m, 2.5H), 3.31 (m, 1H), 3.03 (m, 1H), 2.74 (s, 1.6 H), 2.71 (s, 1.4H), 1.37 (s, 3.8H), 1.33 (s, 5.2H).

^{13}C NMR (126 MHz, $CDCl_3$) δ 171.1 (br s), 155.5 (br s), 137.7 (br s), 131.9 (br s), 129.1 (br s), 128.6 (br s), 126.7 (br s), 118.6 (br s), 80.3 (br s), 65.9 (br s), 60.8 (br s), 35.4 (br s), 32.4 (br s), 28.3 (br s).

IR (film) 3064, 3028, 2975, 2931, 1745, 1697, 1479, 1454, 1392, 1367, 1326, 1274, 1257, 1218, 1170, 1143, 1080, 1029, 987, 933, 869, 750, 700 cm^{-1}.

HRMS: Calc'd $C_{18}H_{25}NO_4Na$ $(M+Na)^+$ = 342.1681, found = 342.1678.

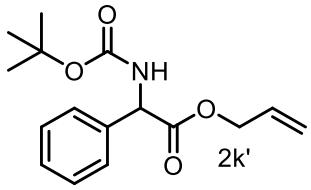

SBL-6-222

The free amino acid (3.83 g, 25.3 mmol) was added to 1M NaOH (35.0 mL). To this solution was added Boc_2O (6.14 g, 28.1 mmol) in ^{t}BuOH (20.0 mL) and the mixture was stirred for 1 h. After removing volatiles *in vaccuo* the pH was adjusted to 3 with 1M HCl and the solution was extracted with DCM (3 x 50 mL) which was dried with $MgSO_4$, and concentrated *in vaccuo*. The crude material was subjected to the representative reaction conditions to furnish the desired allyl ester after flash column chromatography (76% yield over two steps). The spectroscopic data matched that already reported in the literature.

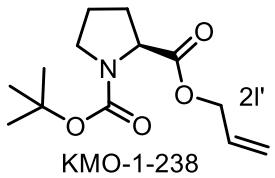

KMO-1-238

Prepared according to the representative procedure (3 mmol scale, 0.73g, 95% yield). The spectroscopic data matched that already reported in the literature.

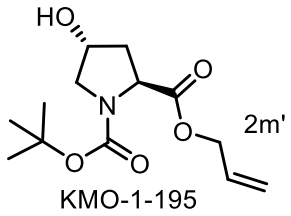

KMO-1-195

Prepared according to a literature procedure with matching spectroscopic data.[2]

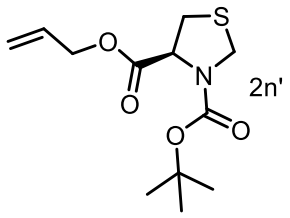

SBL-6-136

Prepared according to the representative procedure (2 mmol scale, 0.447g, 82% yield). A mixture of rotamers.

^{1}H NMR (500 MHz, $CDCl_3$) δ 5.91 (m, 1H), 5.31 (m, 2H), 4.91 (m, 0.5H), 4.63 (m, 3H), 4.50 (m, 1.5H), 3.32 (m, 1H), 3.20 (m, 1H), 1.47 (s, 4.5H), 1.43 (s, 4.5H).

^{13}C NMR (126 MHz, $CDCl_3$) δ 170.5 (br s), 153.3 (br s), 131.6 (br s), 118.8 (br s), 81.4, 66.2, 61.7 (br s), 48.7 (br s), 34.2 (br s), 28.4 (br s).

IR (film) 3429, 2977, 2935, 1749, 1697, 1650, 1456, 1384, 1367, 1336, 1274, 1257, 1163, 1108, 985, 914, 889, 864, 763, 748 cm^{-1}.

HRMS: Calc'd $C_{12}H_{19}NO_4SNa$ $(M+Na)^+$ = 296.0933, found = 296.0919.

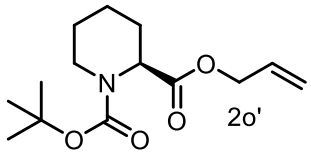

SBL-6-141

Prepared according to the representative procedure (2.2 mmol scale, 0.56g, 96% yield). A mixture of rotamers.

^{1}H NMR (500 MHz, $CDCl_3$) δ 5.90 (ddt, *J* = 16.6, 10.8, 5.54 Hz, 1H), 5.32 (d, *J* = 17.0 Hz, 1H), 5.23 (d, *J* = 10.5 Hz, 1H), 4.91 (s, 0.5H), 4.73 (s, 0.5H), 4.63 (m, 2H), 4.02 (d, *J* = 11.9 Hz, 0.5H), 3.91 (d, *J* = 11.9 Hz, 0.5H), 2.98 (t, *J* = 13.2 Hz, 0.5H), 2.87 (t, *J* = 13.3 Hz, 0.5H), 2.22 (t, *J* = 13.8 Hz, 1H), 1.67 (m, 3H), 1.44 (m, 10H), 1.22 (q, *J* = 14.0 Hz, 1H).

^{13}C NMR (126 MHz, $CDCl_3$) δ 171.8 (br s), 155.8 (br s), 132.0 (br s), 118.4 (br s), 80.1, 65.6, 54.5 (br s), 41.7 (br s), 28.5, 26.9, 24.8 (br s), 20.8 (br s).

IR (film) 2974, 2941, 2862, 1743, 1693, 1650, 1475, 1448, 1392, 1365, 1338, 1323, 1269, 1247, 1186, 1157, 1124, 1091, 1043, 1000, 977, 931, 871, 771, 559 cm^{-1}.

HRMS: Calc'd $C_{14}H_{23}NO_4Na$ $(M+Na)^+$ = 292.1525, found = 292.1523.

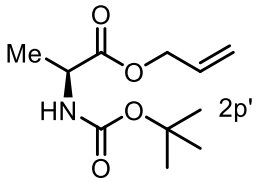

SBL-6-118

Prepared according to the representative procedure (5 mmol scale, 1.21g, 99% yield). The spectroscopic data matched that already reported in the literature.

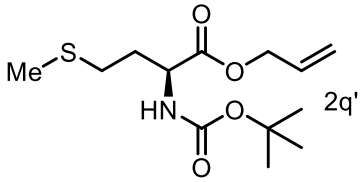

SBL-6-131

The free amino acid (2.50 g, 16.8 mmol) was added to a solution of 1M NaOH (16.0 mL) and dioxane (20.0 mL). The solution was cooled to 0 ^{o}C (ice bath) and Boc_2O (3.84 g, 17.6 mmol) was added and allowed to stir at room temperature overnight. Next, the volatiles were removed *in vaccuo*, the pH was adjusted to 3 with 1M HCl, and the solution was extracted with EtOAc (2 x 20 mL). The organic phase was washed with brine (15 mL), dried with $MgSO_4$, and concentrated *in vaccuo*. The crude product was subjected to the representative reaction conditions to provide the desired product after flash column chromatography (3.04 g, 63% yield over two steps). The spectroscopic data matched that already reported in the literature.

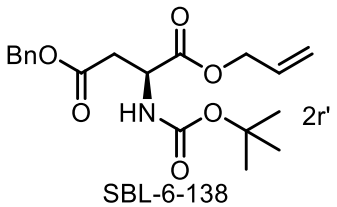

SBL-6-138

Prepared according to the representative procedure (6.2 mmol scale, 2.25g, 99% yield). The spectroscopic data matched that already reported in the literature.

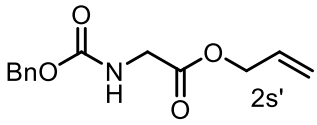

SBL-6-129

Prepared according to the representative procedure (5 mmol scale, 1.07g, 86% yield). The spectroscopic data matched that already reported in the literature.

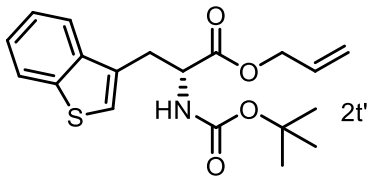

KMO-1-226

Prepared according to the representative procedure (3.1 mmol scale, 0.47g, 41% yield).

^{1}H NMR (500 MHz, $CDCl_3$) δ 7.85 (d, *J* = 7.52 Hz, 1H), 7.76 (m, 1H), 7.36 (m, 2H), 7.17 (s, 1H), 5.80 (ddt, *J* = 16.4, 11.1, 5.82 Hz, 1H), 5.24 (m, 2H), 5.10 (d, *J* = 8.20 Hz, 1H), 4.73 (q, *J* = 6.13 Hz, 1H), 4.56 (m, 2H), 3.41 (dd, *J* = 14.7, 5.89 Hz, 1H), 3.34 (dd, *J* = 14.7, 6.12 Hz, 1H), 1.43 (s, 7.5H, Boc), 1.25 (s, 1.5H, Boc).

^{13}C NMR (126 MHz, $CDCl_3$) δ 171.7, 155.2, 140.4, 139.1, 131.5, 131.0, 124.5, 124.2, 124.0, 123.0, 121.8, 119.2, 80.2, 66.3, 53.8, 31.4, 28.3 (br s).

IR (film) 3357, 2977, 2931, 1739, 1712, 1504, 1458, 1365, 1274, 1251, 1166, 1058, 1020, 989, 933, 854, 761, 732
cm^{-1}.

HRMS: Calc'd $C_{19}H_{23}NO_4SNa$ $(M+Na)^+$ = 384.1246, found = 384.1241.

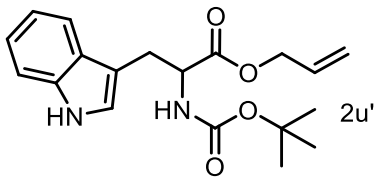

KMO-1-235

The free amino acid (1.50 g, 7.3 mmol) was added to a solution of H_2O (15 mL) and THF (15 mL). NaOH (0.32 g, 8.0 mmol) was added followed by Boc_2O (1.75 g, 8.0 mmol). After stirring overnight the THF was removed *in vaccuo* and the pH adjusted to 4 using 1M HCl. The aqueous phase was extracted with DCM (2 x 20 mL) which was dried with $MgSO_4$ and concentrated *in vaccuo*. The crude material was subjected to the representative reaction conditions to furnish the desired

allyl ester (0.41g) after flash column chromatography in a 16% yield. The spectroscopic data matched that already reported in the literature.

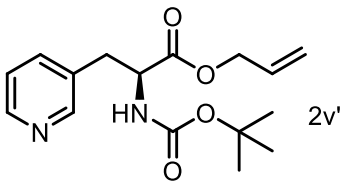

KMO-1-225

Prepared according to the representative procedure (3.8 mmol scale, 0.39g, 34% yield).

^{1}H NMR (500 MHz, $CDCl_3$) δ 8.49 (d, *J* = 4.64 Hz, 1H), 8.39 (br s, 1H), 7.48 (dt, *J* = 7.78, 1.99 Hz, 1H), 7.22 (dd, *J* = 7.84, 4.81 Hz, 1H), 5.86 (m, 1H), 5.30 (m, 2H), 5.06 (br s, 1H), 4.62 (m, 3H), 3.17 (dd, *J* = 14.0, 5.72 Hz, 1H), 3.05 (dd, *J* = 14.0, 6.17 Hz, 1H), 1.41 (s, 9H).

^{13}C NMR (126 MHz, $CDCl_3$) δ 171.2, 155.1, 150.8, 148.6, 137.0, 131.8, 131.4, 123.5, 119.6, 80.3, 66.4, 54.3, 35.8, 28.4.

IR (film) 3350, 3217, 2977, 2933, 1743, 1712, 1649, 1577, 1519, 1481, 1446, 1425, 1367, 1276, 1253, 1168, 1054, 1027, 991, 935, 750, 713 cm^{-1}.

HRMS: Calc'd $C_{16}H_{23}N_2O_4$ $(M+H)^+$ = 307.1658, found = 307.1664.

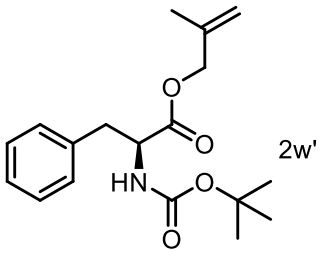

SBL-6-171

Boc-Phe-OH (1.51 g, 5.7 mmol) was added to 20 mL DCM under Ar. The solution was cooled to 0 ^{o}C (ice bath) and β-Methallyl alcohol (0.53 g, 7.3 mmol) and triethylamine (1.41 g, 14 mmol) were added. After stirring for 5 mins, PyBOP (3.82 g, 7.3 mmol) was added and the solution was allowed to warm to room temperature and stir overnight. Next, the reaction mixture was washed with water (1 x 10 mL), brine (1 x 10 mL), concentrated *in vaccuo*, and purified via flash column chromatography to provide the desired allyl ester in a 96% yield.

^{1}H NMR (500 MHz, $CDCl_3$) δ 7.29 (m, 2H), 7.25 (m, 1H), 7.14 (d, *J* = 7.03 Hz, 2H), 4.95 (m, 3H), 4.63 (q, *J* = 6.18 Hz, 1H), 4.52 (s, 2H), 3.14 (dd, *J* = 13.8, 5.88 Hz, 1H), 3.07 (dd, *J* = 13.9, 6.28 Hz, 1H), 1.71 (s, 3H), 1.41 (s, 9H).

^{13}C NMR (126 MHz, $CDCl_3$) δ 171.8, 155.2, 139.4, 136.1, 129.5, 128.7, 127.2, 113.9, 80.0, 68.7, 54.6, 38.5, 28.4, 19.7.

IR (film) 3369, 3064, 3029, 2977, 2931, 1745, 1693, 1604, 1487, 1454, 1367, 1251, 1164, 1054, 1022, 960, 912, 860, 744, 700, 568 cm^{-1}.

HRMS: Calc'd $C_{18}H_{25}NO_4Na$ (M+Na)+ = 342.1681, found = 342.1670.

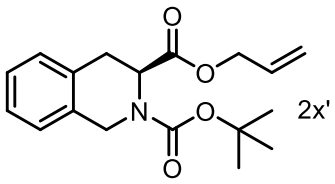

SBL-6-073

The free amino acid (2.50 g, 14.1 mmol) was added to a solution of 1,4 dioxane (30 mL) and 1M NaOH (18 mL). The solution was cooled to 0°C (ice bath), and Boc_2O (3.93 g, 18.0 mmol) was added. The solution was allowed to warm to room temperature and stirred overnight. Next, the dioxane was removed *in vacuo*, the pH was adjusted to 3 with 1 M HCl and the reaction mixture extracted with EtOAc (50 mL). The organic phase was washed with brine (30 mL), dried with $MgSO_4$, and concentrated *in vacuo*. The crude product was subjected to the representative procedure to yield the desired allyl ester after flash column chromatography (58% yield over two steps) as a mixture of rotamers.

^{1}H NMR (500 MHz, $CDCl_3$) δ 7.15 (m, 4H), 5.76 (dddd, *J* = 18.0, 12.9, 6.31, 3.70 Hz, 1H), 5.14 (m, 2.5H), 4.81 (t, *J* = 5.40 Hz, 0.5H), 4.70 (dd, *J* = 16.3, 9.82 Hz, 1H), 4.51 (m, 3H), 3.27 (dd, *J* = 15.8, 3.11 Hz, 0.5H), 3.18 (m, 1.5H), 1.53 (s, 4.5H), 1.45 (s, 4.5H).

^{13}C NMR (126 MHz, $CDCl_3$) δ 171.5 (br s), 155.3 (br s), 134.1, 133.0, 132.1(br s), 131.8 (br s), 128.3 (br s), 127.0 (br s), 126.8 (br s), 126.4 (br s), 118.2 (br s), 80.7, 65.7 (br s), 53.6 (br s), 44.5 (br s), 31.6 (br s), 28.5 (br s).

IR (film) 3336, 2975, 2931, 1737, 1697, 1456, 1392, 1367, 1357, 1332, 1251, 1220, 1164, 1122, 997, 923, 757 cm^{-1}.

HRMS: Calc'd $C_{18}H_{23}NO_4Na$ $(M+Na)^+$ = 340.1525, found = 340.1517.

Example experimental procedure for allyl esters (Products 1a-1m):

An oven dried 2.0 – 5.0 mL Biotage microwave vial charged with a stirbar was taken into the glovebox. $Pd(PPh_3)_4$ and $Ir(ppy)_2(bpy)[BF_4]$ (.007 g, 2.5 mol% and 0.001 g, 0.5 mol%, respectively) were added to the vial followed by 2.5 mL MeCN. The vial was capped with a Biotage cap using a crimper and removed from the glovebox. Allyl ester (0.25 mmol) was added via syringe and the vial was placed into a 25 ^oC water bath directly in front of a white LED. After stirring for 2 hours the reaction mixture was analyzed by GC/MS and loaded directly onto a flash column.

Example experimental procedure for carboxylic acids (Products 1n-1s):

An oven dried 2.0 – 5.0 mL Biotage microwave vial charged with a stirbar was taken into the glovebox. $Pd(PPh_3)_4$ and $Ir(ppy)_2(bpy)[BF_4]$ (.007 g, 2.5 mol% and .001 g, 0.5 mol%, respectively) were added to the vial followed by the carboxylic acid (0.25 mmol), and 2.5 mL MeCN. The vial was capped with a Biotage cap using a crimper and removed from the glovebox. Allyl methyl carbonate (0.029 g, 0.25 mmol) was added via syringe and the vial was placed into a 25 ^oC water bath directly in front of a white LED. After stirring for 2 hours the reaction mixture was analyzed by GC/MS and loaded directly onto a flash column.

SBL-5-013 0.020g, 46 %, 1:20 EtOAc:Hexanes

^{1}H NMR Spectra (500 MHz, $CDCl_3$): δ 7.08 (d, *J* = 8.23 Hz, 2H), 6.71 (d, *J* = 8.63 Hz, 2H), 5.88 (m, 1H), 5.01 (m, 2H), 2.92 (s, 6H), 2.63 (m, 2H), 2.34 (m, 2H).

^{13}C NMR (126 MHz, $CDCl_3$): δ 149.0, 138.6, 130.1, 129.0, 114.6, 113.0, 40.9, 35.9, 34.4.

HRMS: M+H calc: 176.1439, M+H found: 176.1433.

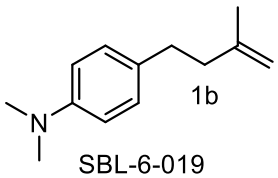

SBL-6-019 0.020g, 43%, 1:20 EtOAc:Hexanes

^{1}H NMR Spectra (500 MHz, $CDCl_3$): δ 7.09 (d, *J* = 8.51 Hz, 2H), 6.71 (d, *J* = 8.53 Hz, 2H), 4.73 (d, *J* = 5.83 Hz, 2H), 2.92 (s, 6H), 2.67 (m, 2H), 2.29 (dd, *J* = 9.82, 6.53 Hz, 2H), 1.77 (s, 3H).

^{13}C NMR (126 MHz, $CDCl_3$): δ 149.0, 145.9, 130.5, 128.9, 113.0, 109.9, 41.0, 40.0, 33.2, 22.7.

HRMS: M+H calc: 190.1596, M+H found: 190.1522.

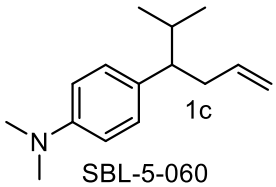

SBL-5-060 0.027g, 50%, 1:40 EtOAc:Hexanes

^{1}H NMR Spectra (500 MHz, $CDCl_3$): δ 7.00 (d, *J* = 8.67 Hz, 2H), 6.70 (d, *J* = 8.68 Hz, 2H), 5.64 (m, 1H), 4.92 (m, 2H), 2.93 (s, 6H), 2.49 (m, 1H), 2.36 (m, 2H), 1.83 (m, 1H), 0.94 (d, *J* = 6.68 Hz, 3H), 0.76 (d, *J* = 6.77 Hz, 3H).

^{13}C NMR (126 MHz, $CDCl_3$): δ 147.8, 137.1, 130.6, 128.2, 114.0, 111.3, 50.6, 39.8, 36.4, 31.8, 19.9, 19.0.

HRMS: M+H calc: 218.1909, M+H found: 218.1892.

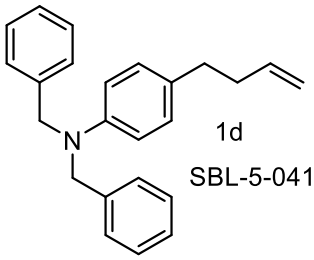

0.040g, 49%, 100:1 Hexanes:Diethyl Ether

^{1}H NMR Spectra (500 MHz, $CDCl_3$): δ 7.33 (m, 4H), 7.25 (m, 6H), 7.00 (d, *J* = 8.46 Hz, 2H), 6.68 (d, *J* = 8.53 Hz, 2H), 5.88 (m, 1H), 5.01 (m, 2H), 4.63 (s, 4H), 2.60 (dd, *J* = 9.29, 6.57 Hz, 2H), 2.32 (q, *J* = 7.13, 6.94 Hz, 2H).

^{13}C NMR (126 MHz, $CDCl_3$): δ 146.4, 137.8, 137.5, 129.0, 128.0, 127.5, 125.8, 125.6, 113.5, 111.5, 53.3, 34.7, 33.3.

HRMS: M+H calc: 328.2065, M+H found: 328.2055.

SBL-5-038 0.025g, 50%, 100:1 Hexanes:Diethyl Ether

^{1}H NMR Spectra (500 MHz, $CDCl_3$):

δ 7.07 (d, *J* = 8.10 Hz, 2H), 6.54 (s, 2H), 5.88 (m, 1H), 5.01 (m, 2H), 3.27 (s, 4H), 2.62 (dd, *J* = 9.07, 6.68 Hz, 2H), 2.34 (m, 2H), 2.00 (s, 4H).

^{13}C NMR (126 MHz, $CDCl_3$):

δ 146.3, 138.6, 129.1, 114.6, 111.6, 47.8, 36.1, 34.5, 25.4.

HRMS:

M+H calc: 202.1596, M+H found: 202.1586.

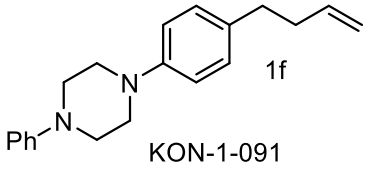

KON-1-091 0.041g, 48%, 1:50 EtOAc:Hexanes

^{1}H NMR Spectra (500 MHz, $CDCl_3$): δ 7.30 (dd, *J* = 8.76, 7.27 Hz, 2H), 7.12 (d, *J* = 8.56 Hz, 2H), 7.00 (m, 2H), 6.92 (m, 3H), 5.87 (m, 1H), 5.01 (m, 2H), 3.32 (m, 8H), 2.65 (dd, *J* = 8.97, 6.70 Hz, 2H), 2.36 (m, 2H).

^{13}C NMR (126 MHz, $CDCl_3$): δ 151.3, 149.4, 138.3, 133.6, 129.2, 129.1, 120.0, 116.5, 116.3, 114.8, 49.8, 49.5 35.7, 34.5.

HRMS: M+H calc: 293.2018, M+H found: 293.2012.

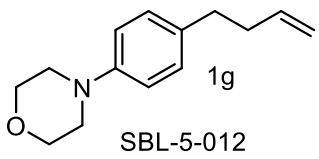

SBL-5-012 0.031g, 57%, 1:12 EtOAc:Hexanes

^{1}H NMR Spectra (500 MHz, $CDCl_3$): δ 7.11 (d, *J* = 8.55 Hz, 2H), 6.86 (d, *J* = 8.52 Hz, 2H), 5.86 (m, 1H), 5.00 (m, 2H), 3.86 (m, 4H), 3.13 (m, 4H), 2.64 (m, 2H), 2.34 (m, 2H).

^{13}C NMR (126 MHz, $CDCl_3$): δ 149.4, 138.3 133.6, 129.1, 115.9, 114.8, 67.0, 49.7, 35.7, 34.4.

HRMS: M+H calc: 218.1545, M+H found: 218.1541.

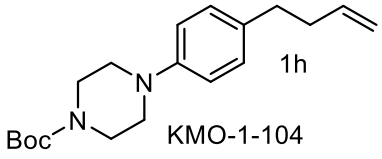

KMO-1-104 0.038g, 48%, 1:10 EtOAc:Hexanes

^{1}H NMR Spectra (500 MHz, $CDCl_3$): δ 7.10 (d, *J* = 8.68 Hz, 2H), 6.87 (d, *J* = 8.58 Hz, 2H), 5.85 (m, 1H), 4.99 (m, 2H), 3.57 (t, *J* = 6.25 Hz, 4H), 3.09 (t, *J* = 5.47 Hz, 4H), 2.64 (dd, *J* = 8.95, 6.70 Hz, 2H), 2.34 (m, 2H), 1.48 (s, 9H).

^{13}C NMR (126 MHz, $CDCl_3$): δ 154.8, 149.4, 138.3, 133.9, 129.1, 116.8, 114.8, 79.9, 49.8, 35.7, 34.5, 28.6.

HRMS: M+H calc: 317.2229, M+H found: 317.2223.

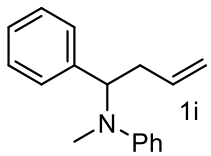

SBL-5-069 0.036g, 61%, 1:150 Diethyl Ether:Pentanes

^{1}H NMR Spectra (500 MHz, $CDCl_3$): δ 7.30 (m, 4H), 7.24 (m, 3H), 6.83 (d, *J* = 8.13 Hz, 2H), 6.73 (t, *J* = 7.24 Hz, 1H), 5.84 (m, 1H), 5.16 (dq, *J* = 17.06, 1.63 Hz, 1H), 5.05 (m, 2H), 2.81 (m, 2H), 2.72 (s, 3H).

^{13}C NMR (126 MHz, $CDCl_3$): δ 150.5, 141.1, 135.8, 129.2, 128.4, 127.2, 127.0, 116.8, 116.6, 113.0, 61.4, 36.1, 31.9.

HRMS: M+H calc: 238.1596, M+H found: 238.1591.

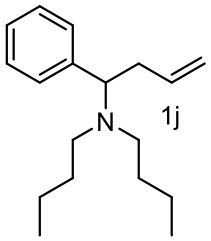

KMO-1-106 0.034g, 50%

^{1}H NMR Spectra (500 MHz, $CDCl_3$): δ 7.29 (m, 2H), 7.24 (m, 3H), 5.71 (m, 1H), 4.96 (m, 2H), 3.72 (dd, *J* = 8.80, 5.79 Hz, 1H), 2.64 (dt, *J* = 13.85, 6.78 Hz, 1H), 2.50 (dt, *J* = 12.30, 7.60 Hz, 3H), 2.23 (m, 2H), 1.39 (m, 4H), 1.26 (m, 4H), 0.87 (t, *J* = 7.32 Hz, 6H).

^{13}C NMR (126 MHz, $CDCl_3$): δ 140.7, 136.7, 128.6, 127.6, 126.5, 115.6, 64.1, 49.5, 36.1 30.0, 20.4, 13.9.

HRMS:

M+H calc: 260.2378, M+H found: 260.2377.

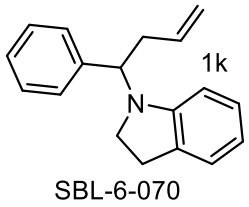

SBL-6-070 0.035g, 56%

This material is ~95% pure by 1H NMR spectroscopy. The suspected contaminant is thought to be *N*-benzylindoline (singlet at 4.26 ppm).

^{1}H NMR Spectra (500 MHz, $CDCl_3$): δ 7.33 (m, 4H), 7.26 (m, 1H), 7.02 (m, 2H), 6.58 (t, *J* = 7.32 Hz, 1H), 6.47 (d, *J* = 7.75 Hz, 1H), 5.83 (m, 1H), 5.08 (m, 2H), 4.69 (t, *J* = 7.60 Hz, 1H), 3.49 (m, 1H), 3.30 (m, 1H), 2.93 (m, 2H), 2.77 (ddt, *J* = 8.00, 6.76, 1.41 Hz, 2H).

^{13}C NMR (126 MHz, $CDCl_3$): δ 151.3, 140.1, 135.7, 129.6, 128.3, 127.9, 127.2, 127.2, 124.5, 116.8, 116.7, 106.6, 58.9, 47.2, 35.6, 28.1.

HRMS: M+H calc: 250.1596, M+H found: 250.1596.

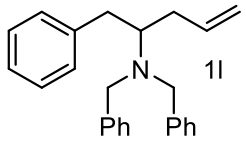

1l

SBL-5-123 0.047g, 55%, 1:50 EtOAc:Hexanes

^{1}H NMR Spectra (500 MHz, $CDCl_3$): δ 7.25 (m, 10H), 7.20 (m, 3H), 7.03 (m, 2H), 5.75 (m, 1H), 5.01 (m, 2H), 3.71 (d, *J* = 13.83 Hz, 2H), 3.63 (d, *J* = 13.78 Hz, 2H), 2.96 (m, 2H), 2.57 (m, 1H), 2.45 (m, 1H), 2.08 (m, 1H).

^{13}C NMR (126 MHz, $CDCl_3$): δ 139.6, 139.1, 136.4, 128.4 127.7, 127.1, 127.0, 125.7, 124.7, 114.8, 58.4, 52.2, 34.8, 33.4.

HRMS: M+H calc: 342.2222, M+H found: 342.2215.

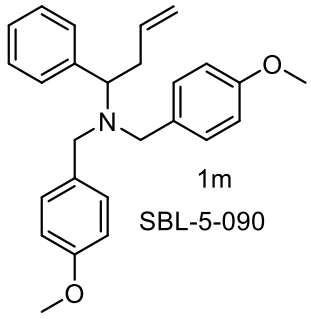

1m

SBL-5-090 0.051g, 53%, 1:50 Ether:Pentanes

^{1}H NMR Spectra (500 MHz, $CDCl_3$): δ 7.38 (t, *J* = 7.62 Hz, 2H), 7.30 (d, *J* = 8.44 Hz, 5H), 7.24 (d, *J* = 7.72 Hz, 2H), 6.87 (d, *J* = 8.24 Hz, 4H), 5.80 (m, 1H), 5.04 (m, 2H), 3.81 (m, 7H), 3.74 (d, *J* = 13.59 Hz, 2H), 3.13 (d, *J* = 13.54 Hz, 2H), 2.85 (m, 1H), 2.57 (m, 1H).

^{13}C NMR (126 MHz, $CDCl_3$): δ 158.5, 138.8, 136.9, 132.3, 129.8, 129.0, 128.0, 127.0, 116.0, 113.6, 61.2, 55.3, 52.6, 35.2.

HRMS: M+H calc: 388.2277, M+H found: 388.2262.

For conversion of allylic esters to homoallylic amines (Products 2a-2x): An oven dried 16 x 125 mm threaded glass tube charged with a stirbar was taken into the glovebox. $Pd(PPh_3)_4$ and $[Ir\{dF(CF_3)ppy\}_2(dtbpy)]PF_6$ (0.014 g, 5.0 mol % and 0.003g, 1.0 mol %, respectively) were added to the vial. If the starting material was a solid, 0.25 mmol was added at this time. 2.0 mL DMSO was added to the vial which was then capped and removed from the glovebox. If the starting

material was a liquid, it was added via syringe at this time. The reaction was placed in a room temperature blue LED light bath (photo 1, S-2) and analyzed by GC/MS. The crude reaction mixture was directly loaded onto a silica gel column and purified using EtOAc/Hexanes as the eluent.

For conversion of carboxylic acids to homoallylic amines (Products 2a, 2l, 3a-3c): An oven dried 16 x 125 mm threaded glass tube charged with a stirbar was taken into the glovebox. $Pd(PPh_3)_4$ and $[Ir\{dF(CF_3)ppy\}_2(dtbpy)]PF_6$ (0.014 g, 5.0 mol % and 0.003 g, 1.0 mol%, respectively) were added to the vial followed by the carboxylic acid (0.25 mmol), and 2.0 mL DMSO. The vial was capped, removed from the glovebox, and 0.25 mmol (0.029 g) of allyl methyl carbonate was added via syringe. The reaction was placed in a room temperature blue LED light bath (photo 1, S-2) and analyzed by GC/MS. The crude reaction mixture was directly loaded onto a silica gel column and purified using EtOAc/Hexanes as the eluent.

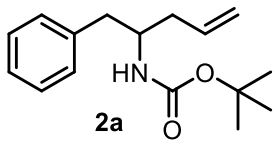

2a

SBL-6-105

0.043g, 65%, 1:10 EtOAc:Hexanes.

^{1}H NMR (500 MHz, $CDCl_3$) δ 7.29 (m, 2H), 7.21 (m, 3H), 5.80 (ddt, *J* = 17.3, 10.5, 7.04 Hz, 1H), 5.10 (m, 2H), 4.40 (s, 1H), 3.91 (s, 1H), 2.78 (m, 2H), 2.26 (m, 1H), 2.11 (m, 1H), 1.41 (s, 9H).

^{13}C NMR (126 MHz, $CDCl_3$) δ 155.5, 138.3, 134.6, 129.6, 128.5, 126.5, 118.1, 79.3, 51.2, 40.6, 38.2, 28.5.

IR (film) 3348, 3076, 2977, 2927, 1697, 1641, 1523, 1496, 1454, 1438, 1388, 1363, 1272, 1251, 1230, 1172, 1045, 1024, 910, 856, 742, 698 cm^{-1}.

HRMS: Calc'd $C_{16}H_{23}NO_2Na$ $(M+Na)^+$ = 284.1626, found = 284.1616.

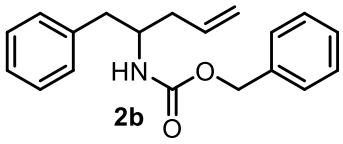

2b

SBL-6-104

0.048g, 65%, 1:5 EtOAc:Hexanes.

^{1}H NMR (500 MHz, $CDCl_3$) δ 7.33 (m, 7H), 7.19 (m, 3H), 5.79 (ddt, *J* = 17.3, 10.4, 7.04 Hz, 1H), 5.09 (m, 4H), 4.63 (d, *J* = 8.34 Hz, 1H), 3.99 (m, 1H), 2.81 (m, 2H), 2.29 (dt, *J* = 12.7, 6.09 Hz, 1H), 2.14 (dt, *J* = 14.2, 7.13 Hz, 1H).

^{13}C NMR (126 MHz, $CDCl_3$) δ 155.9, 137.9, 136.7, 134.3, 129.6, 128.6, 128.5, 128.2, 128.1, 126.6, 118.4, 66.7, 51.7, 40.5, 38.2.

IR (film) 3325, 3062, 3029, 2943, 1697, 1531, 1514, 1454, 1440, 1342, 1257, 1222, 1041, 1027, 993, 914, 746, 698 cm^{-1}.

HRMS: Calc'd $C_{19}H_{21}NO_2Na$ $(M+Na)^+$ = 318.1470, found = 318.1469.

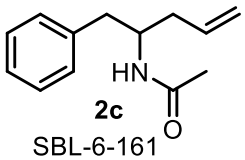

2c

SBL-6-161

0.035g, 69%, 1:1 EtOAc:Hexanes

^{1}H NMR (500 MHz, $CDCl_3$) δ 7.29 (m, 2H), 7.20 (m, 3H), 5.79 (ddt, *J* = 17.3, 10.3, 7.07 Hz, 1H), 5.30 (d, *J* = 7.47 Hz, 1H), 5.10 (m, 2H), 4.26 (m, 1H), 2.79 (dd, *J* = 14.0, 6.27 Hz, 2H), 2.28 (m, 1H), 2.13 (m, 1H), 1.92 (s, 3H).

^{13}C NMR (126 MHz, $CDCl_3$) δ 169.6, 137.9, 134.5, 129.5, 128.6, 126.6, 118.2, 49.6, 40.1, 37.9, 23.6.

IR (film) 3274, 3076, 2927, 1645, 1556, 1496, 1438, 1373, 1298, 991, 748, 700 cm^{-1}.

HRMS: Calc'd $C_{13}H_{17}NONa$ $(M+Na)^+$ = 226.1208, found = 226.1187.

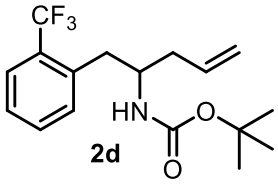

2d

SBL-6-204

0.055g, 67%, 1:8 EtOAc:Hexanes.

^{1}H NMR (500 MHz, $CDCl_3$) δ 7.62 (d, *J* = 7.83 Hz, 1H), 7.46 (m, 2H), 7.30 (m, 1H), 5.81 (ddt, *J* = 17.7, 9.66, 7.10 Hz, 1H), 5.12 (m, 2H), 4.42 (d, *J* = 9.23 Hz, 1H), 4.00 (m, 1H), 2.96 (m, 2H), 2.28 (m, 2H), 1.33 (s, 9H).

^{13}C NMR (126 MHz, $CDCl_3$) δ 155.4, 137.5, 134.3, 131.8, 131.6, 129.0 (q, *J* = 29.7 Hz), 126.5, 126.0 (q, *J* = 6.32 Hz), 124.8 (q, *J* = 274 Hz), 118.3, 79.3, 51.3, 39.6, 37.4, 28.4.

IR (film) 3363, 2981, 2931, 1681, 1606, 1523, 1454, 1367, 1307, 1271, 1251, 1163, 1107, 1049, 914, 767 cm^{-1}.

HRMS: Calc'd $C_{17}H_{22}F_3NO_2Na$ $(M+Na)^+$ = 352.1500, found = 352.1505.

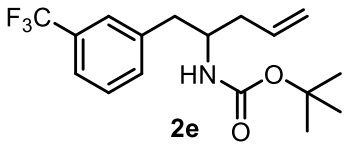

2e

SBL-6-196

0.060g, 73%, 1:10 EtOAc:Hexanes.

^{1}H NMR (500 MHz, $CDCl_3$) δ 7.48 (m, 1H), 7.41 (m, 3H), 5.79 (ddt, *J* = 17.3, 10.3, 7.05 Hz, 1H), 5.11 (m, 2H), 4.39 (m, 1H), 3.91 (m, 1H), 2.85 (d, *J* = 6.65 Hz, 2H), 2.26 (m, 1H), 2.13 (m, 1H), 1.39 (s, 9H).

^{13}C NMR (126 MHz, $CDCl_3$) δ 155.4, 139.3, 134.2, 133.0, 130.7 (q, *J* = 30.9 Hz), 128.9, 126.3, 124.4 (q, *J* = 272 Hz), 123.4 (q, *J* = 3.65 Hz), 118.5, 79.5, 51.1, 40.4, 38.3, 28.4.

IR (film) 3363, 2979, 2935, 1681, 1523, 1446, 1392, 1367, 1332, 1159, 1116, 1074, 918, 800, 750, 703 cm^{-1}.

HRMS: Calc'd $C_{17}H_{22}F_3NO_2Na$ $(M+Na)^+$ = 352.1500, found = 352.1470.

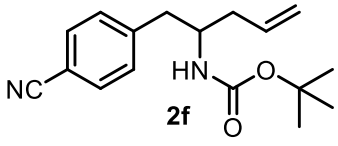

2f

SBL-6-201

0.052g, 72%, 1:6 EtOAc:Hexanes.

^{1}H NMR (500 MHz, $CDCl_3$) δ 7.58 (m, 2H), 7.31 (d, *J* = 8.07 Hz, 2H), 5.77 (ddt, *J* = 17.2, 10.3, 7.04 Hz, 1H), 5.13 (m, 2H), 4.38 (d, *J* = 8.68 Hz, 1H), 3.91 (m, 1H), 2.84 (d, *J* = 6.74 Hz, 2H), 2.25 (m, 1H), 2.14 (m, 1H), 1.38 (s, 9H).

^{13}C NMR (126 MHz, $CDCl_3$) δ 155.3, 144.2, 133.9, 132.3, 130.3, 119.1, 118.7, 110.4, 79.6, 51.0, 41.0, 38.5, 28.5.

IR (film) 3363, 2979, 2962, 2929, 2225, 1681, 1645, 1608, 1523, 1461, 1442, 1390, 1367, 1350, 1272, 1251, 1174, 1049, 1029, 919, 842, 823, 750, 655, 567 cm^{-1}.

HRMS: Calc'd $C_{17}H_{22}N_2O_2Na$ $(M+Na)^+$ = 309.1579, found = 309.1585.

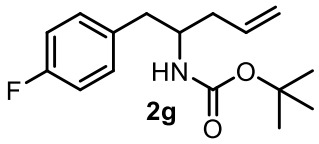

2g

SBL-6-117

0.058g, 83%, 1:10 EtOAc:Hexanes.

^{1}H NMR (500 MHz, $CDCl_3$) δ 7.14 (m, 2H), 6.97 (m, 2H), 5.78 (ddt, *J* = 17.3, 10.4, 7.07 Hz, 1H), 5.10 (m, 2H), 4.37 (s, 1H), 3.86 (s, 1H), 2.73 (m, 2H), 2.24 (m, 1H), 2.10 (m, 1H), 1.40 (s, 9H).

^{13}C NMR (126 MHz, $CDCl_3$) δ 161.6 (d, *J* = 244 Hz), 155.4, 134.4, 134.0 (d, *J* = 3.03 Hz), 130.9 (d, *J* = 7.65 Hz), 118.2, 115.3 (d, *J* = 21.1 Hz), 79.4, 51.2, 39.9, 38.2, 28.5.

IR (film) 3342, 2979, 2929, 1687, 1600, 1504, 1454, 1365, 1271, 1253, 1218, 1172, 1045, 914, 831, 750 cm^{-1}.

HRMS: Calc'd $C_{16}H_{22}FNO_2Na$ $(M+Na)^+$ = 302.1532, found = 302.1546.

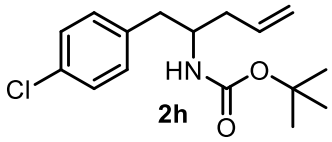

2h

SBL-6-126

0.059g, 79%, 1:10 EtOAc:Hexanes.

^{1}H NMR (500 MHz, $CDCl_3$) δ 7.27 (m, 2H), 7.13 (d, *J* =8.26 Hz, 2H), 5.79 (ddt, *J* = 17.2, 10.3, 7.06 Hz, 1H), 5.11 (m, 2H), 4.38 (s, 1H), 3.88 (s, 1H), 2.76 (m, 2H), 2.25 (m, 1H), 2.11 (m, 1H), 1.41 (s, 9H).

^{13}C NMR (126 MHz, $CDCl_3$) δ 155.4, 136.8, 134.3, 132.3, 130.9, 128.6, 118.3, 79.4, 51.1, 40.0, 38.2, 28.5.

IR (film) 3344, 2977, 2929, 1687, 1643, 1519, 1492, 1444, 1390, 1365, 1269, 1251, 1170, 1091, 1043, 1016, 667 cm^{-1}.

HRMS: Calc'd $C_{16}H_{22}ClNO_2Na$ $(M+Na)^+$ = 318.1237, found = 318.1220.

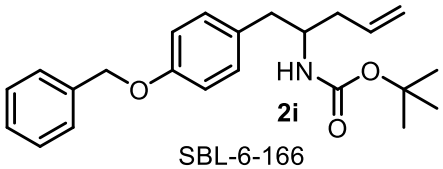

SBL-6-166 .071g, 77%, 1:8 EtOAc:Hexanes.

^{1}H NMR (500 MHz, $CDCl_3$) δ 7.43 (m, 2H), 7.39 (ddd, *J* = 7.65, 6.80, 1.29 Hz, 2H), 7.33 (m, 1H), 7.11 (d, *J* = 8.35 Hz, 2H), 6.91 (m, 2H), 5.79 (ddt, *J* = 17.5, 10.5, 7.02 Hz, 1H), 5.09 (m, 2H), 5.04 (s, 2H), 4.39 (s, 1H), 3.87 (s, 1H), 2.72 (m, 2H), 2.45 (m, 1H), 2.10 (m, 1H), 1.41 (s, 9H).

^{13}C NMR (126 MHz, $CDCl_3$) δ 157.6, 155.5, 137.2, 134.6, 130.6, 128.7, 128.1, 127.6, 118.0, 114.9, 79.2, 70.2, 51.3, 39.7, 38.1, 28.5.

IR (film) 3365, 2977, 2929, 1687, 1610, 1510, 1454, 1390, 1365, 1242, 1170, 1024, 914, 742, 696, 667 cm^{-1}.

HRMS: Calc'd $C_{23}H_{29}NO_3Na$ $(M+Na)^+$ = 390.2045, found = 390.2039.

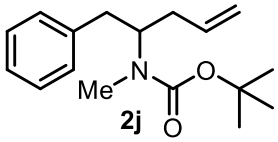

SBL-6-192

A mixture of rotamers. 0.049g, 72%, 1:8 EtOAc:Hexanes.
^{1}H NMR (500 MHz, $CDCl_3$) δ 7.26 (m, 2H), 7.17 (m, 3H), 5.73 (br m, 1H), 5.06 (br m, 2H), 4.47 (br m, 0.4H), 4.29 (br m, 0.6H) 2.77 (d, *J* = 7.76 Hz, 1H), 2.71 (t, *J* = 3.39 Hz, 3H), 2.62 (s, 1H), 2.27 (br m, 2H), 1.36 (s, 4H), 1.28 (s, 5H).

^{13}C NMR (126 MHz, $CDCl_3$) δ 156.0, 139.0 (br s), 135.2 (br s), 129.1 (br s), 128.4 (br s), 126.3 (br s), 116.9 (br s), 79.2 (br s), 56.5 (br s), 38.9 (br s), 36.9 (br s), 29.5 (br s), 28.4 (br s).

IR (film) 3028, 2975, 2927, 1693, 1643, 1479, 1454, 1392, 1365, 1298, 1253, 1224, 1172, 1143, 991, 914, 873, 769, 746, 700 cm^{-1}.

HRMS: Calc'd $C_{17}H_{25}NO_2Na$ $(M+Na)^+$ = 298.1783, found = 298.1772.

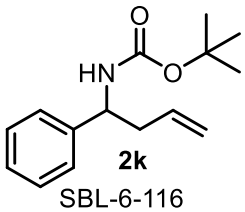

SBL-6-116 0.036g, 59%.

^{1}H NMR (500 MHz, $CDCl_3$) δ 7.32 (m, 2H), 7.26 (m, 3H), 5.68 (ddt, *J* = 17.2, 10.2, 7.05 Hz, 1H), 5.09 (m, 2H), 4.87 (s, 1H), 4.74 (s, 1H), 2.52 (m, 2H), 1.42 (s, 9H).

^{13}C NMR (126 MHz, $CDCl_3$) δ 155.3, 142.5, 134.1, 128.6, 127.3, 126.4, 118.3, 79.6, 54.1, 41.4, 28.5.

IR (film) 3338, 3064, 2977, 2931, 1693, 1519, 1494, 1454, 1367, 1251, 1170, 1018, 916, 756, 700 cm^{-1}.

HRMS: Calc'd $C_{15}H_{21}NO_2Na$ $(M+Na)^+$ = 270.1470, found = 270.1468.

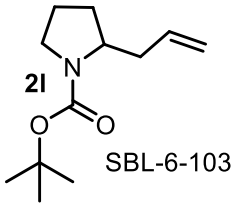

A mixture of rotamers. 0.034g, 64%, 1:10 EtOAc:Hexanes.
^{1}H NMR (500 MHz, $CDCl_3$) δ 5.73 (br m, 1H), 5.04 (m, 2H), 3.80 (br m, 1H), 3.35 (br m, 2H), 2.45 (br m, 1H), 2.11 (br m, 1H), 1.80 (br m, 4H), 1.46 (s, 9H).

^{13}C NMR (126 MHz, $CDCl_3$) δ 154.7, 135.4, 117.1, 79.1 (br s), 56.9, 46.6 (br s), 38.8 (br s), 29.8 (br s), 28.70, 23.4(br s).

IR (film) 3076, 2974, 2875, 1693, 1641, 1479, 1454, 1392, 1365, 1253, 1172, 1108, 995, 914, 771 cm^{-1}.

HRMS: Calc'd $C_{12}H_{21}NO_2Na$ $(M+Na)^+$ = 234.1470, found = 234.1452.

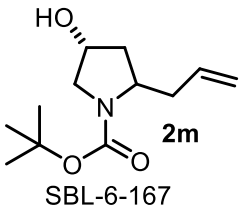

0.039g, 69%, 1:1 EtOAc:Hexanes.

A mixture of diastereomers and rotamers.
^{1}H NMR (500 MHz, $CDCl_3$) δ 5.73 (br m, 1H), 5.07 (br m, 2H), 4.38 (br m, 1H), 3.43 (br m, 3H), 2.34 (br m, 2H), 2.09 (br m, 2H), 1.84 (br m, 1H), 1.46 (s, 9H).

^{13}C NMR (126 MHz, $CDCl_3$, major resonances reported) δ 154.6, 135.4, 117.6, 79.6, 70.1 (br s), 56.6, 55.4 (br s), 39.4 (br s), 38.2 (br s), 28.6.

IR (film) 3419, 2975, 2931, 1693, 1668, 1407, 1365, 1255, 1166, 1118, 1080, 914, 765 cm^{-1}.

HRMS: Calc'd $C_{12}H_{21}NO_3Na$ $(M+Na)^+$ = 250.1419, found = 250.1411.

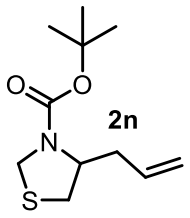

SBL-6-143

A mixture of rotamers. 0.024g, 42%, 1:10 EtOAc:Hexanes.
^{1}H NMR (500 MHz, $CDCl_3$) δ 5.76 (ddt, *J* = 17.1, 10.1, 7.01 Hz, 1H), 5.09 (m, 2H), 4.62 (br s, 1H), 4.22 (br m, 2H), 3.07 (m, 1H), 2.80 (dd, *J* = 11.2, 2.53 Hz, 1H), 2.46 (br s, 1H), 2.33 (m, 1H), 1.47 (s, 9H).

^{13}C NMR (126 MHz, $CDCl_3$) δ 153.4, 134.7, 118.0, 80.6, 59.2, 48.0 (br s), 37.7 (br s), 34.6 (br s), 28.5.

IR (film) 3367, 2977, 2931, 1735, 1693, 1384, 1369, 1330, 1255, 1151, 1041, 918, 852, 767, 667 cm^{-1}.

HRMS: $[M - \text{isobutylene} + H]^+$ = 174.0589, found = 174.0581. GC/MS: $[M]^+$ = 229.1, found = 229.2.

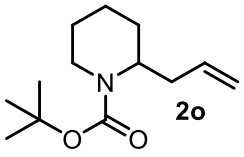

SBL-6-169 0.044g, 77%, 1:10 EtOAc:Hexanes.

^{1}H NMR (500 MHz, $CDCl_3$) δ 5.74 (ddt, *J* = 17.2, 10.1, 7.15 Hz, 1H), 5.01 (m, 2H), 4.27 (s, 1H), 3.96 (d, *J* = 12.3 Hz, 1H), 2.75 (m, 1H), 2.39 (m, 1H), 2.22 (dt, *J* = 14.1, 7.19 Hz, 1H), 1.57 (m, 5H), 1.44 (s, 9H), 1.39 (m, 1H).

^{13}C NMR (126 MHz, $CDCl_3$) δ 115.2, 135.8, 116.7, 79.2, 50.2, 39.0, 34.6, 28.6, 27.8, 25.6, 19.0.

IR (film) 3076, 2975, 2933, 2858, 1693, 1643, 1446, 1409, 1365, 1319, 1267, 1170, 1147, 1068, 1033, 995, 912, 869, 806, 767 cm^{-1}.

HRMS: Calc'd $C_{13}H_{23}NO_2Na$ $(M+Na)^+$ = 248.1626, found = 248.1615.

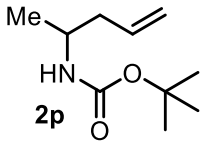

SBL-6-130 0.039g, 83%, 1:10 EtOAc:Hexanes.

^{1}H NMR (500 MHz, $CDCl_3$) δ 5.77 (m, 1H), 5.08 (m, 2H), 4.38 (s, 1H), 3.73 (m, 1H), 2.19 (m, 2H), 1.43 (s, 9H), 1.12 (d, *J* = 6.63 Hz, 3H).

^{13}C NMR (126 MHz, $CDCl_3$) δ 155.4, 134.6, 117.8, 79.2, 46.0, 41.4, 28.6, 20.7.

IR (film) 3338, 3078, 2977, 2931, 1693, 1643, 1519, 1454, 1390, 1365, 1251, 1174, 1056, 993, 914, 781, 634 cm^{-1}.

HRMS: Calc'd $C_{10}H_{19}NO_2Na$ $(M+Na)^+$ = 208.1313, found = 208.1293.

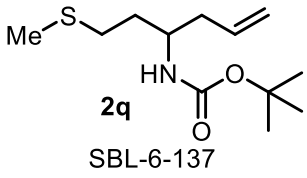

SBL-6-137 0.036g, 58%, 1:8 EtOAc:Hexanes.

^{1}H NMR (500 MHz, $CDCl_3$) δ 5.76 (ddt, *J* = 17.6, 9.55, 7.13 Hz, 1H), 5.09 (m, 2H), 4.39 (d, *J* = 9.23 Hz, 1H), 3.74 (m, 1H), 2.52 (m, 2H), 2.23 (m, 2H), 2.10 (s, 3H), 1.79 (m, 1H), 1.63 (m, 1H), 1.43 (s, 9H).

^{13}C NMR (126 MHz, $CDCl_3$) δ 155.7, 134.2, 118.2, 79.3, 49.7, 39.7, 34.6, 30.9, 28.5, 15.8.

IR (film) 3336, 3076, 2977, 2918, 1693, 1641, 1519, 1442, 1390, 1365, 1290, 1251, 1170, 1049, 1020, 993, 914, 856, 779, 748, 649 cm^{-1}.

HRMS: Calc'd $C_{12}H_{23}NO_2SNa$ $(M+Na)^+$ = 268.1347, found = 268.1338.

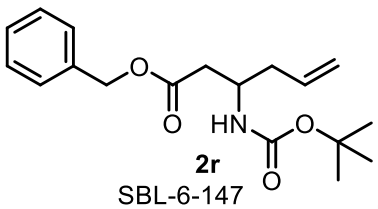

SBL-6-147 0.046g, 57%, 1:7 EtOAc:Hexanes.

^{1}H NMR (500 MHz, $CDCl_3$) δ 7.36 (m, 5H), 5.74 (ddt, *J* = 17.4, 10.5, 7.15 Hz, 1H), 5.08 (m, 4H), 4.95 (m, 1H), 4.01 (m, 1H), 2.58 (d, *J* = 5.73 Hz, 2H), 2.29 (m, 2H), 1.42 (s, 9H).

^{13}C NMR (126 MHz, $CDCl_3$) δ 171.6, 155.3, 135.8, 134.1, 128.8, 128.5, 128.4, 118.4, 79.5, 66.6, 47.3, 38.9, 38.5, 28.5.

IR (film) 3359, 3066, 2977, 1714, 1697, 1643, 1504, 1456, 1390, 1365, 1249, 1170, 1047, 1026, 993, 918, 750, 698 cm^{-1}.

HRMS: Calc'd $C_{18}H_{25}NO_4Na$ $(M+Na)^+$ = 342.1681, found = 342.1674.

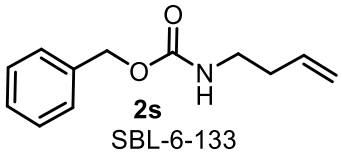

2s
SBL-6-133

0.023g, 44%, 1:8 EtOAc:Hexanes.

^{1}H NMR (500 MHz, $CDCl_3$) δ 7.35 (m, 5H), 5.75 (ddt, *J* = 17.2, 10.4, 6.82 Hz, 1H), 5.09 (m, 4H), 4.79 (s, 1H), 3.28 (q, *J* = 6.48 Hz, 2H), 2.27 (q, *J* = 6.92 Hz, 2H).

^{13}C NMR (126 MHz, $CDCl_3$) δ 156.4, 136.7, 135.2, 128.6, 128.3, 128.2, 117.5, 66.8, 40.2, 34.2.

IR (film) 3330, 3074, 3031, 2935, 1697, 1641, 1523, 1454, 1253, 1217, 1134, 1026, 914, 748, 695 cm^{-1}.

HRMS: Calc'd $C_{12}H_{15}NO_2Na$ $(M+Na)^+$ = 228.1000, found = 228.0989.

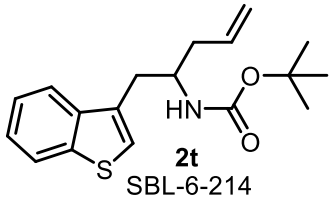

2t
SBL-6-214

0.067g, 56%, 1:12 EtOAc:Hexanes.

^{1}H NMR (500 MHz, $CDCl_3$) δ 7.86 (m, 2H), 7.38 (m, 2H), 7.17 (s, 1H), 5.82 (ddt, *J* = 17.3, 10.4, 7.02 Hz, 1H), 5.12 (m, 2H), 4.48 (d, *J* = 8.89 Hz, 1H), 4.08 (m, 1H), 3.10 (m, 1H), 3.00 (dd, *J* = 14.3, 6.99 Hz, 1H), 2.32 (m, 1H), 2.18 (m, 1H), 1.43 (s, 9H).

^{13}C NMR (126 MHz, $CDCl_3$) δ 155.5, 140.4, 139.3, 134.4, 132.9, 124.4, 124.2, 123.3, 122.9, 122.2, 118.3, 79.4, 49.8, 38.5, 33.6, 28.5.

IR (film) 3425, 3340, 3074, 2975, 2929, 1697, 1641, 1502, 1458, 1429, 1390, 1365, 1251, 1168, 1047, 1020, 914, 852, 759, 732 cm^{-1}.

HRMS: Calc'd $C_{18}H_{23}NO_2SNa$ (M+Na) = 340.1347, found 340.1330.

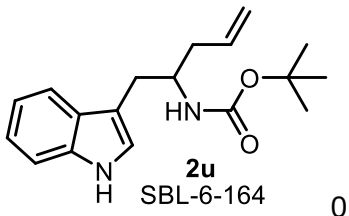

2u
SBL-6-164

0.029g, 39%, 1:3 EtOAc:Hexanes.

^{1}H NMR (500 MHz, $CDCl_3$) δ 8.10 (s, 1H), 7.65 (d, *J* = 7.92 Hz, 1H), 7.36 (dt, *J* = 8.16, 0.96 Hz, 1H), 7.20 (ddd, *J* = 8.14, 6.97, 1.20 Hz, 1H), 7.13 (ddd, *J* = 8.04, 7.03, 1.06 Hz, 1H), 7.03 (s, 1H),

5.83 (m, 1H), 5.09 (m, 2H), 4.48 (s, 1H), 4.02 (m, 1H), 2.95 (m, 2H), 2.32 (m, 1H), 2.15 (m, 1H), 1.43 (s, 9H).

^{13}C NMR (126 MHz, $CDCl_3$) δ 155.7, 136.3, 134.9, 128.1, 122.8, 122.1, 119.6, 119.3, 117.8, 112.3, 111.1, 79.2, 50.5, 38.6, 30.1, 28.6.

IR (film) 3411, 3325, 3056, 2975, 2929, 1693, 1641, 1504, 1438, 1392, 1365, 1249, 1168, 1099, 1060, 1010, 914, 742 cm^{-1}.

HRMS: Calc'd $C_{18}H_{24}N_2O_2Na$ $(M+Na)^+$ = 323.1735, found = 323.1725.

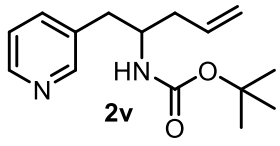

SBL-6-213

0.014g, 22%, 4:1 EtOAc:Hexanes.

^{1}H NMR (500 MHz, $CDCl_3$) δ 8.47 (dd, *J* = 4.89, 1.67 Hz, 1H), 8.43 (s, 1H), 7.54 (m, 1H), 7.22 (dd, *J* = 7.63, 4.92 Hz, 1H), 5.78 (ddt, *J* = 17.2, 10.3, 7.05 Hz, 1H), 5.12 (m, 2H), 4.42 (m, 1H), 3.90 (m, 1H), 2.80 (m, 2H), 2.25 (m, 1H), 2.13 (m, 1H), 1.38 (s, 9H).

^{13}C NMR (126 MHz, $CDCl_3$) δ 155.4, 150.8, 148.0, 137.0, 134.0, 133.8, 123.4, 118.5, 79.5, 50.9, 38.4, 37.8, 28.5.

IR (film) 3336, 3240, 2977, 2929, 1693, 1519, 1440, 1425, 1390, 1365, 1249, 1170, 1045, 1027, 914, 844, 715 cm^{-1}.

HRMS: Calc'd $C_{15}H_{23}N_2O_2$ $(M+H)^+$ = 263.1760, found = 263.1764.

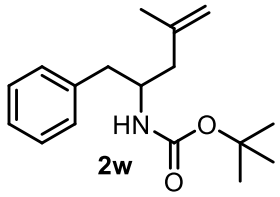

SBL-6-188

0.036g, 52%, 1:12 EtOAc:Hexanes.

^{1}H NMR (500 MHz, $CDCl_3$) δ 7.29 (m, 2H), 7.21 (m, 3H), 4.81 (s, 1H), 4.73 (s, 1H), 4.32 (s, 1H), 3.99 (s, 1H), 2.79 (m, 2H), 2.18 (dd, *J* = 14.3, 5.57 Hz, 1H), 2.06 (dd, *J* = 14.2, 8.97 Hz, 1H), 1.72 (s, 3H), 1.40 (s, 9H).

^{13}C NMR (126 MHz, $CDCl_3$) δ 155.5, 142.6, 138.3, 129.7, 128.4, 126.4, 113.3, 79.2, 49.6, 42.8, 41.1, 28.5, 22.2.

IR (film) 3350, 3072, 3028, 2975, 2929, 1701, 1496, 1454, 1390, 1365, 1247, 1170, 1049, 1016, 889, 746, 700, 667 cm^{-1}.

HRMS: Calc'd $C_{17}H_{25}NO_2Na$ $(M+Na)^+$ = 298.1783, found = 298.1786.

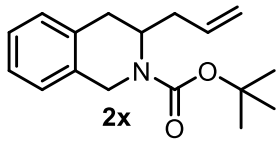

SBL-6-240

A mixture of rotamers. 0.047g, 69%, 1:15 EtOAc:Hexanes.
^{1}H NMR (500 MHz, $CDCl_3$) δ 7.18 (m, 2H), 7.11 (m, 2H), 5.78 (m, 1H), 5.00 (m, 2H), 4.48 (br m, 1H), 4.54 (br m, 1H), 4.26 (s, 0.5H), 4.23 (s, 0.5H), 3.03 (dd, *J* = 15.9, 5.93 Hz, 1H), 2.69 (d, *J* = 15.3 Hz, 1H), 2.24 (m, 1H), 2.06 (m, 1H), 1.49 (s, 9H).

^{13}C NMR (126 MHz, $CDCl_3$) δ 155.1, 135.2 (br s), 133.2 (br s), 132.9 (br s), 129.4 (br s), 126.7, 126.3 (br s), 117.3 (br s), 79.9, 49.2 (br s), 42.9 (br s), 36.7 (br s), 32.6 (br s), 28.6.

IR (film) 3350, 2975, 2931, 1697, 1456, 1392, 1367, 1245, 1168, 1124, 1010, 993, 914, 862, 753, 648 cm^{-1}.

HRMS: Calc'd $C_{17}H_{23}NO_2Na$ $(M+Na)^+$ = 296.1626, found = 296.1620.

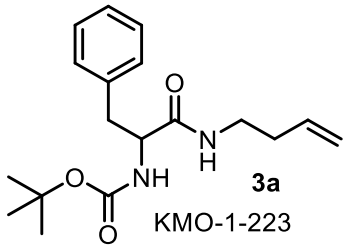

KMO-1-223

0.029g, 36%, 2:3 EtOAc:Hexanes.

^{1}H NMR (500 MHz, $CDCl_3$) δ 7.29 (tt, *J* = 6.98, 1.11 Hz, 2H), 7.24 (m, 1H), 7.20 (m, 2H), 5.72 (br s, 1H), 5.61 (ddt, *J* = 17.1, 10.6, 6.89 Hz, 1H), 5.08 (br s, 1H), 4.97 (m, 2H), 4.26 (q, *J* = 7.51 Hz, 1H), 3.22 (m, 2H), 3.04 (m, 2H), 2.09 (m, 2H), 1.41 (s, 9H).

^{13}C NMR (126 MHz, $CDCl_3$) δ 171.1, 155.5, 137.0, 135.0, 129.4, 128.8, 127.0, 117.4, 80.2, 56.2, 38.9, 38.4, 33.5, 28.4.

IR (film) 3415, 2256, 2129, 1650, 1519, 1496, 1454, 1365, 1249, 1170, 1049, 1026, 1000, 825, 763, 700, 632 cm^{-1}.

HRMS: Calc'd $C_{18}H_{26}N_2O_3Na$ $(M+Na)^+$ = 341.1841, found = 341.1835.

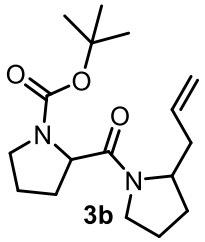

3b

KMO-1-218

A mixture of diastereomers and rotamers. 0.042g, 54%, 2:1 EtOAc:Hexanes.

^{1}H NMR (500 MHz, DMSO-d_6) δ 5.86 – 5.68 (m, 1H), 5.18 – 4.98 (m, 2H), 4.43 – 4.29 (m, 1H), 4.09 – 3.79 (m, 1H), 3.60 – 3.22 (m, 4H), 2.47 – 2.29 (m, 1H), 2.29 – 1.95 (m, 2H), 1.94 – 1.61 (m, 7H), 1.48 – 1.22 (m, 9H).

In the 1D 13C spectrum of **3b**, there are 8 peaks for each carbon, corresponding to 2 diastereomers and 4 rotomers for each diastereomer (see below).

^{13}C NMR (126 MHz, DMSO-d_6) δ 171.4, 170.5, 170.4, 169.9, 153.3, 153.0, 153.0, 135.5, 135.5, 135.2, 135.1, 134.7, 117.9, 117.6, 117.5, 117.1, 117.0, 117.0, 78.5, 78.3, 78.3, 78.1, 64.9, 57.8, 57.7, 57.7, 57.6, 57.5, 57.5, 56.6, 56.5, 56.2, 55.9, 55.7, 55.7, 55.6, 46.7, 46.6, 46.5, 46.4, 46.4, 46.2, 46.1, 46.1, 46.0, 45.9, 45.2, 45.1, 40.1, 40.0, 39.9, 39.8, 39.7, 39.6, 39.6, 39.5, 39.4, 39.3, 39.1, 39.0, 38.6, 38.4, 37.0, 36.7, 36.6, 31.5, 30.3, 29.9, 29.5, 29.4, 29.1, 29.0, 28.7, 28.6, 28.2, 28.2, 28.1, 28.0, 27.9, 27.9, 27.9, 27.8, 23.8, 23.7, 23.7, 23.6, 23.6, 23.4, 23.3, 23.2, 23.1, 22.9, 22.7, 21.2, 20.7, 20.6, 15.1.

IR (film) 3456, 2974, 2875, 1693, 1645, 1427, 1398, 1259, 1163, 1120, 1085, 997, 912, 748 cm^{-1}.

HRMS: Calc'd $C_{17}H_{29}N_2O_3$ $(M+H)^+$ = 309.2178, found = 309.2163.

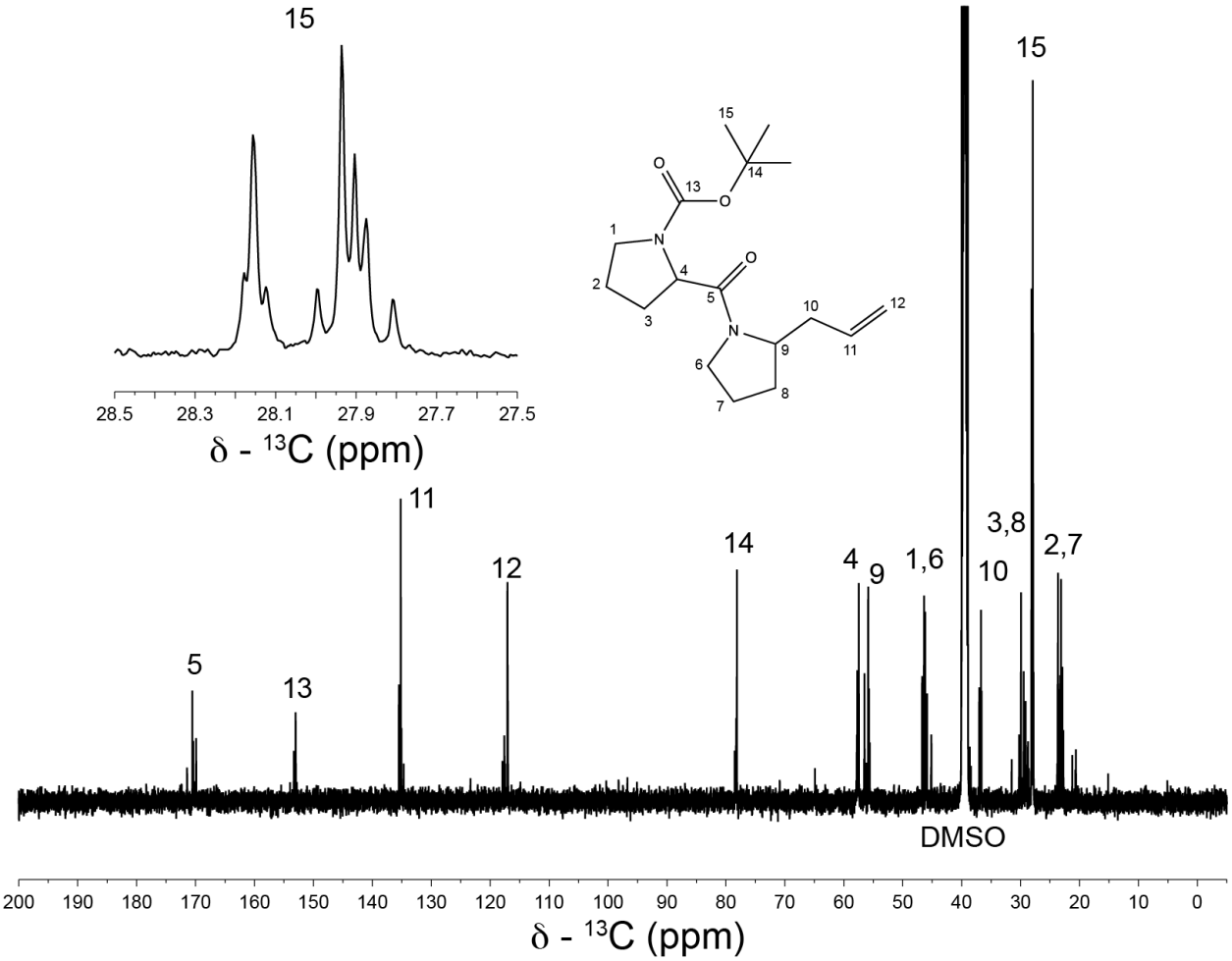
15
28.5
28.3
28.1
27.9
27.7
27.5
δ - 13C (ppm)
15
O
13
O
14
1
N
2
3
4
5
O
N
6
7
8
9
10
11
12
11
12
14
4
9
1,6
10
3,8
2,7
5
13
DMSO
200
190
180
170
160
150
140
130
120
110
100
90
80
70
60
50
40
30
20
10
0
δ - 13C (ppm)

To assign this spectrum, we used a combination of 1D and 2D homo- and heteronuclear NMR (see 2D ^{1}H-^{13}C HSQC spectrum below).

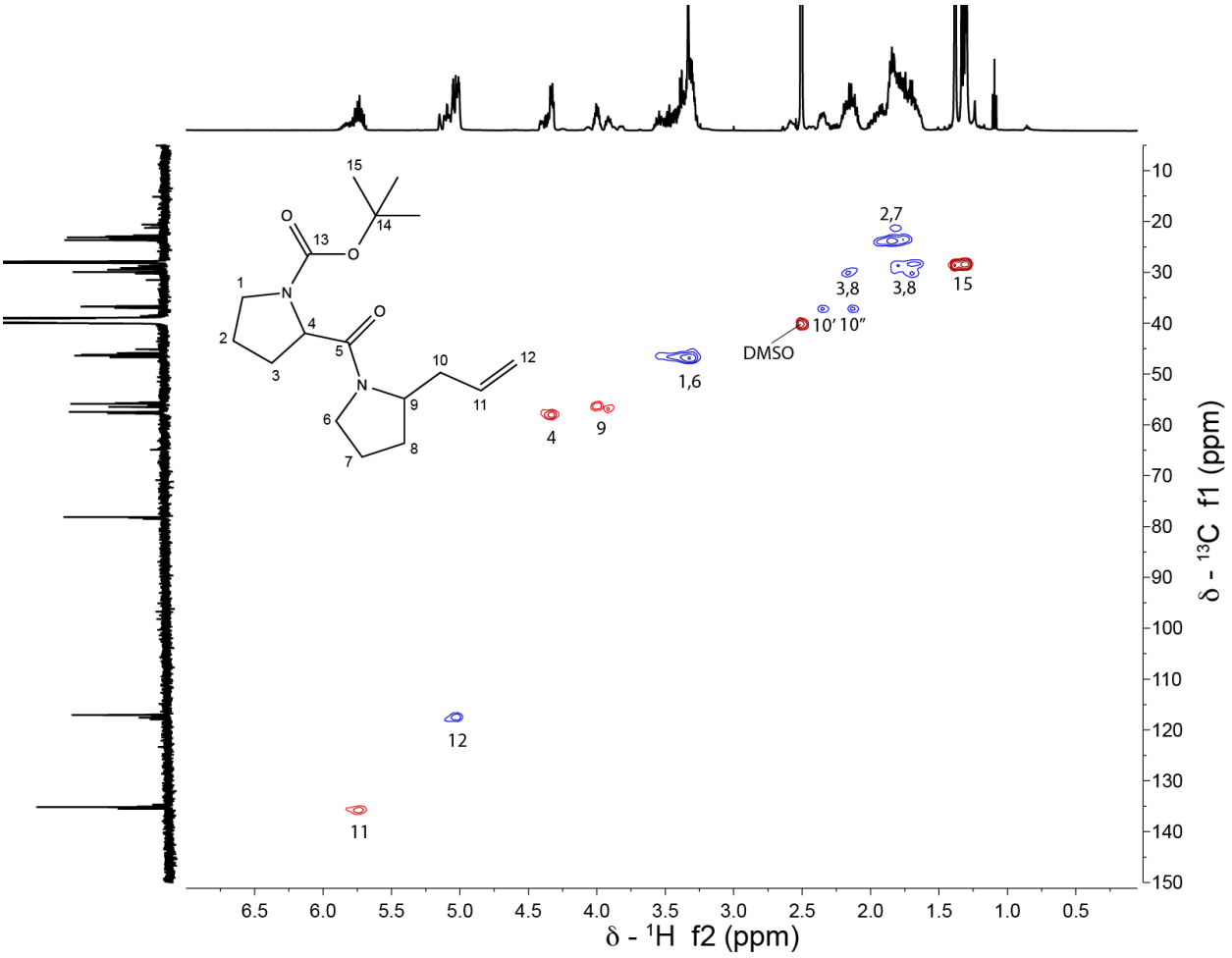

To confirm the presence of rotamers, variable temperature NMR was performed. At 145 °C the rotamers coalesce and only two peaks are present in 1D ^{1}H and 1D ^{13}C spectra.

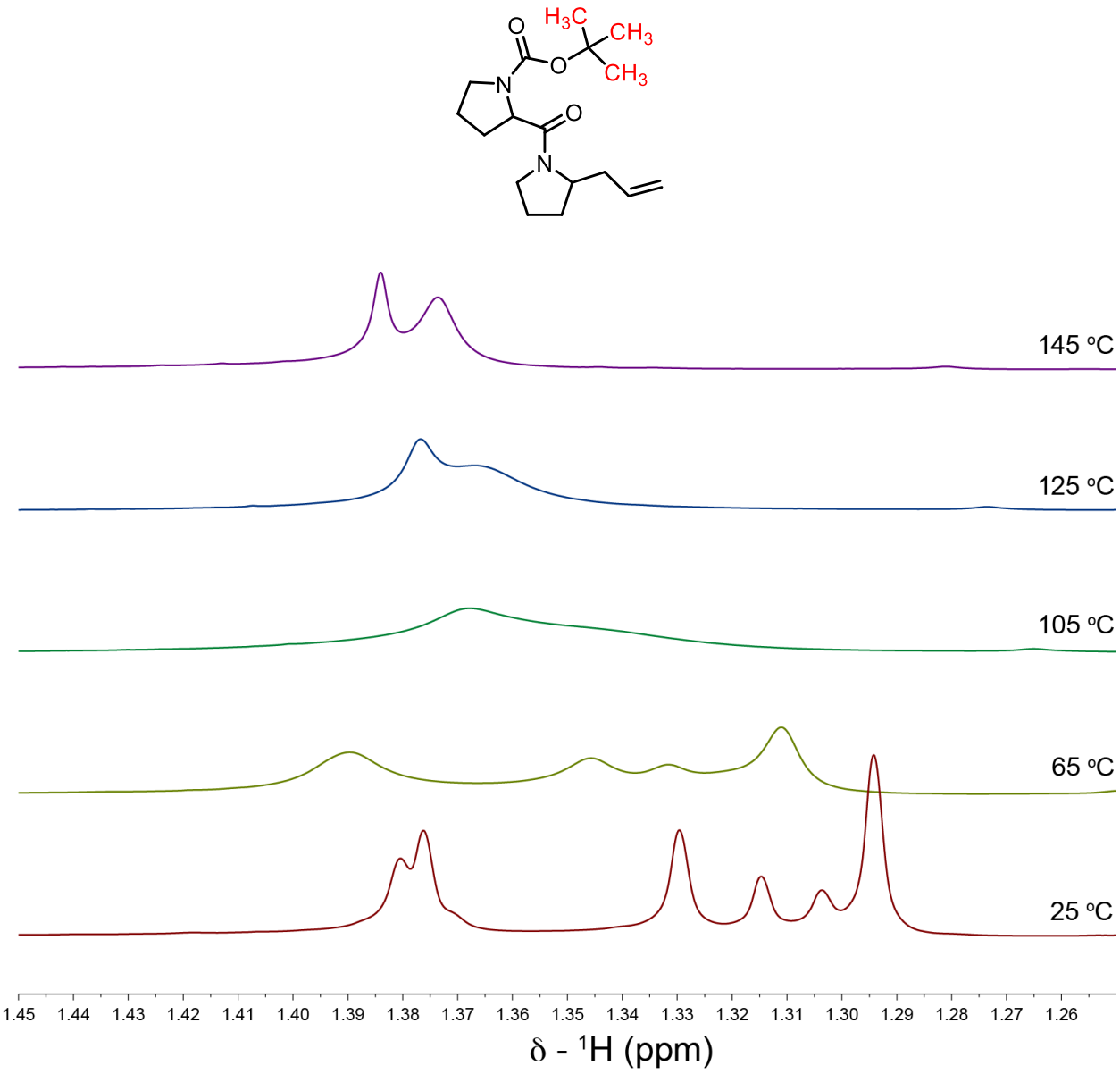

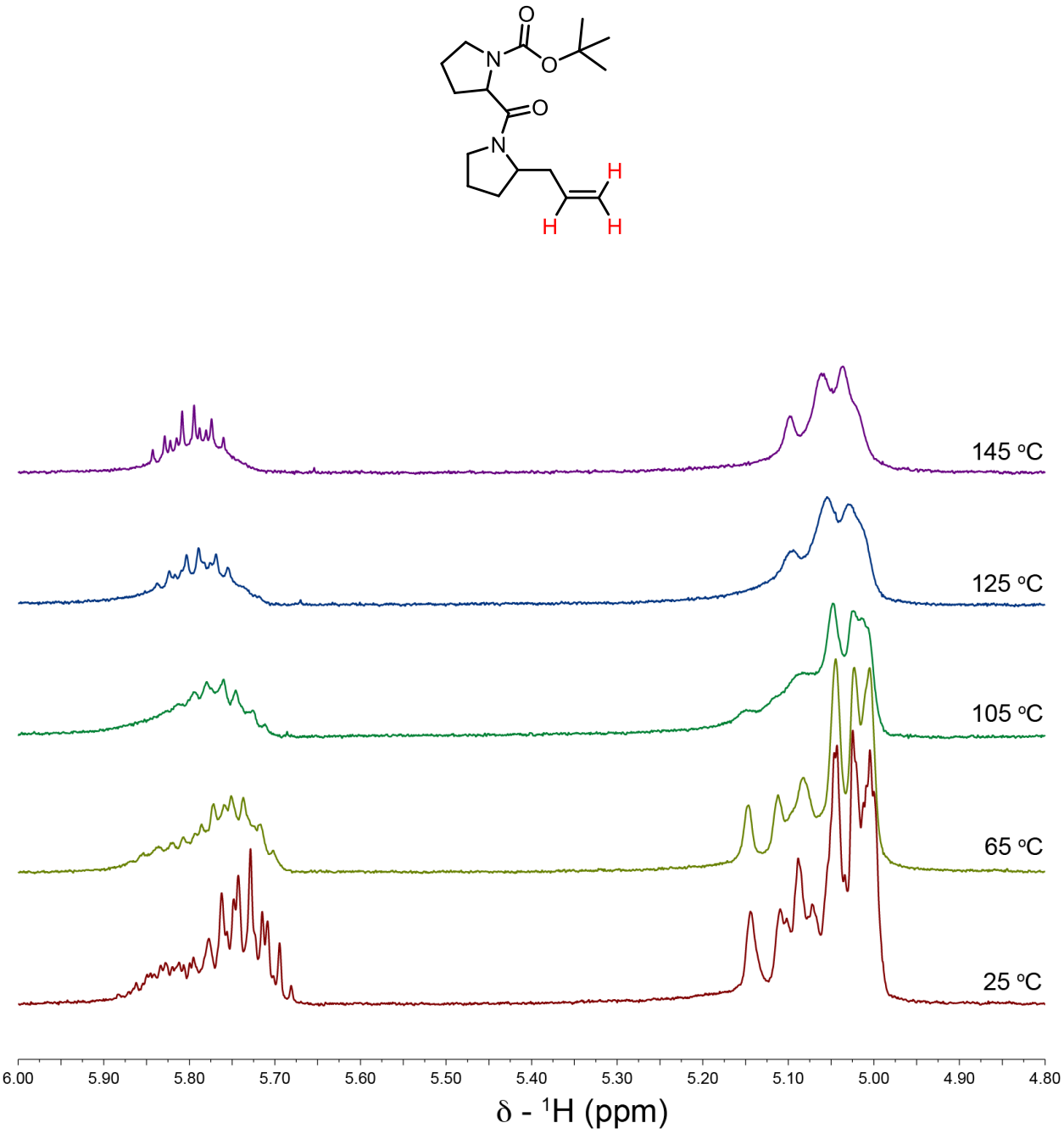
145 °C
125 °C
105 °C
65 °C
25 °C
6.00
5.90
5.80
5.70
5.60
5.50
5.40
5.30
5.20
5.10
5.00
4.90
4.80
δ - ¹H (ppm)

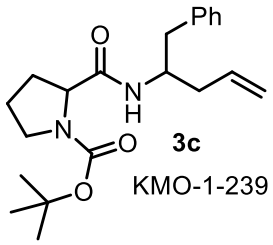

3c

KMO-1-239

Mixture of diastereomers and rotamers. 0.056g, 65%, 1:2 EtOAc:Hexanes.

^{1}H NMR (500 MHz, DMSO-*d*$_6$) δ 7.78 – 7.49 (m, 1H), 7.36 – 7.11 (m, 5H), 5.90 – 5.69 (m, 1H), 5.13 – 4.92 (m, 2H), 4.12 – 3.88 (m, 2H), 3.41 – 3.16 (m, 2H), 2.82 – 2.58 (m, 2H), 2.30 – 2.08 (m, 2H), 2.05 – 1.84 (m, 1H), 1.78 – 1.47 (m, 3H), 1.45 – 1.24 (m, 9H).

^{13}C NMR at 105 ºC (126 MHz, DMSO-*d*$_6$) δ 172.0, 154.2, 139.4, 139.4, 135.9, 135.8, 129.5, 129.5, 128.5, 128.4, 126.4, 126.3, 117.0, 117.0, 79.6, 79.0, 78.9, 60.5, 60.3, 50.1, 50.0, 47.0, 47.0, 40.4, 40.3, 38.9, 38.6, 31.0, 28.6, 28.6, 23.6.

IR (film) 3303, 3074, 2975, 2877, 1697, 1660, 1552, 1454, 1392, 1365, 1257, 1163, 1122, 912, 748 cm^{-1}.

HRMS: Calc'd $C_{21}H_{30}N_2O_3Na$ $(M+Na)^+$ = 381.2154, found = 381.2149.

At room temperature the 1D 1H of **3c** includes a mixture of diastereomers and rotamers. Upon raising the temperature to 105 ºC, these peaks coalesce into discernable signals in the 1D 1H and 1D 13C spectra (see below

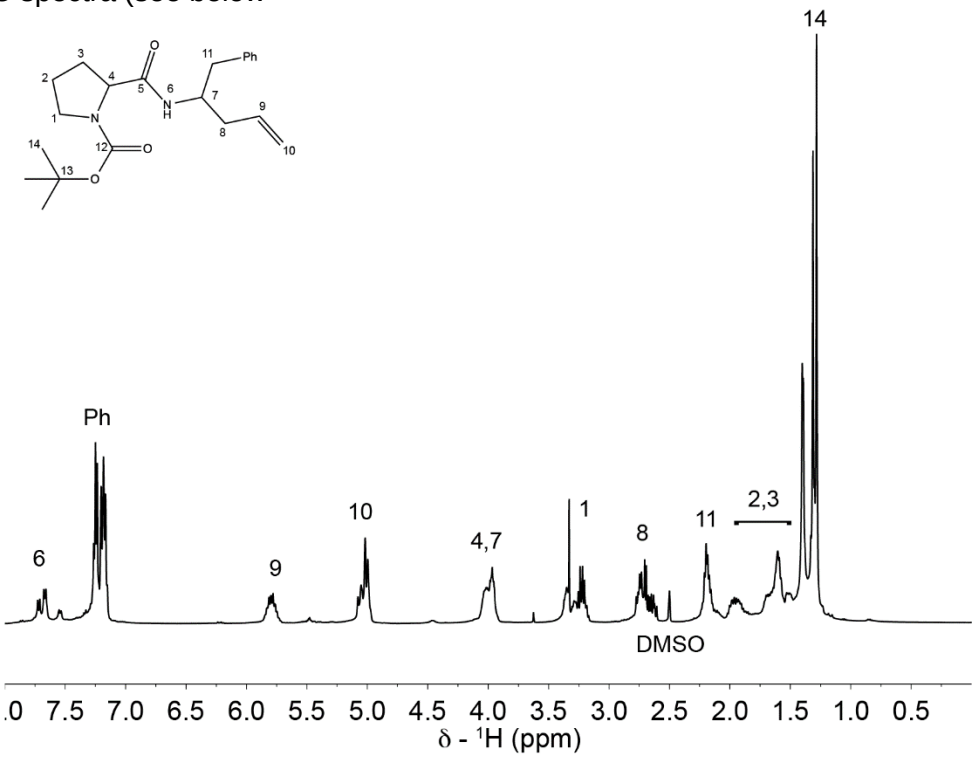

Room Temperature 1D 1H

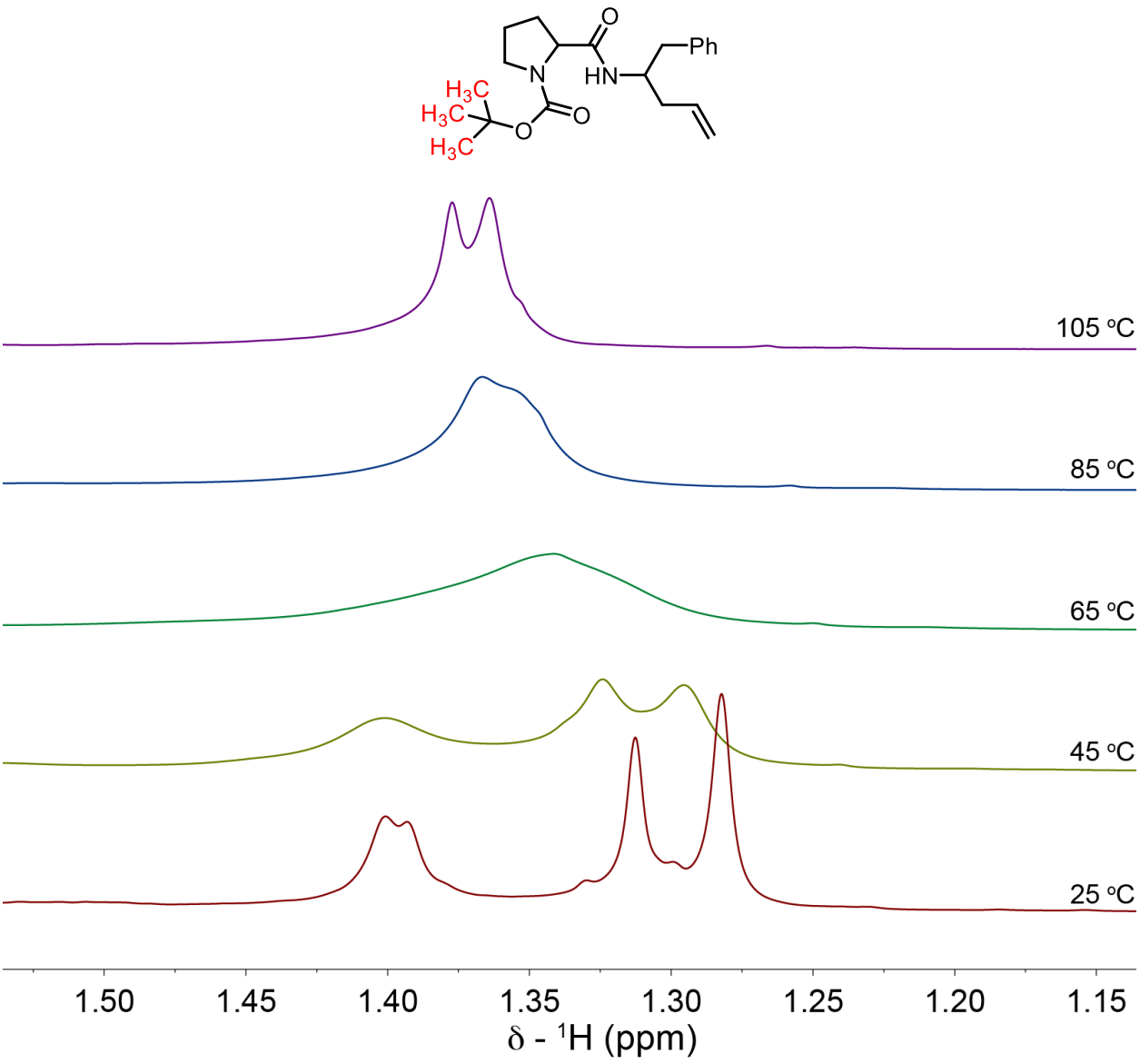

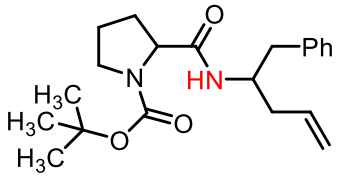
O
Ph
N
HN
H3C
H3C
O
O
H3C

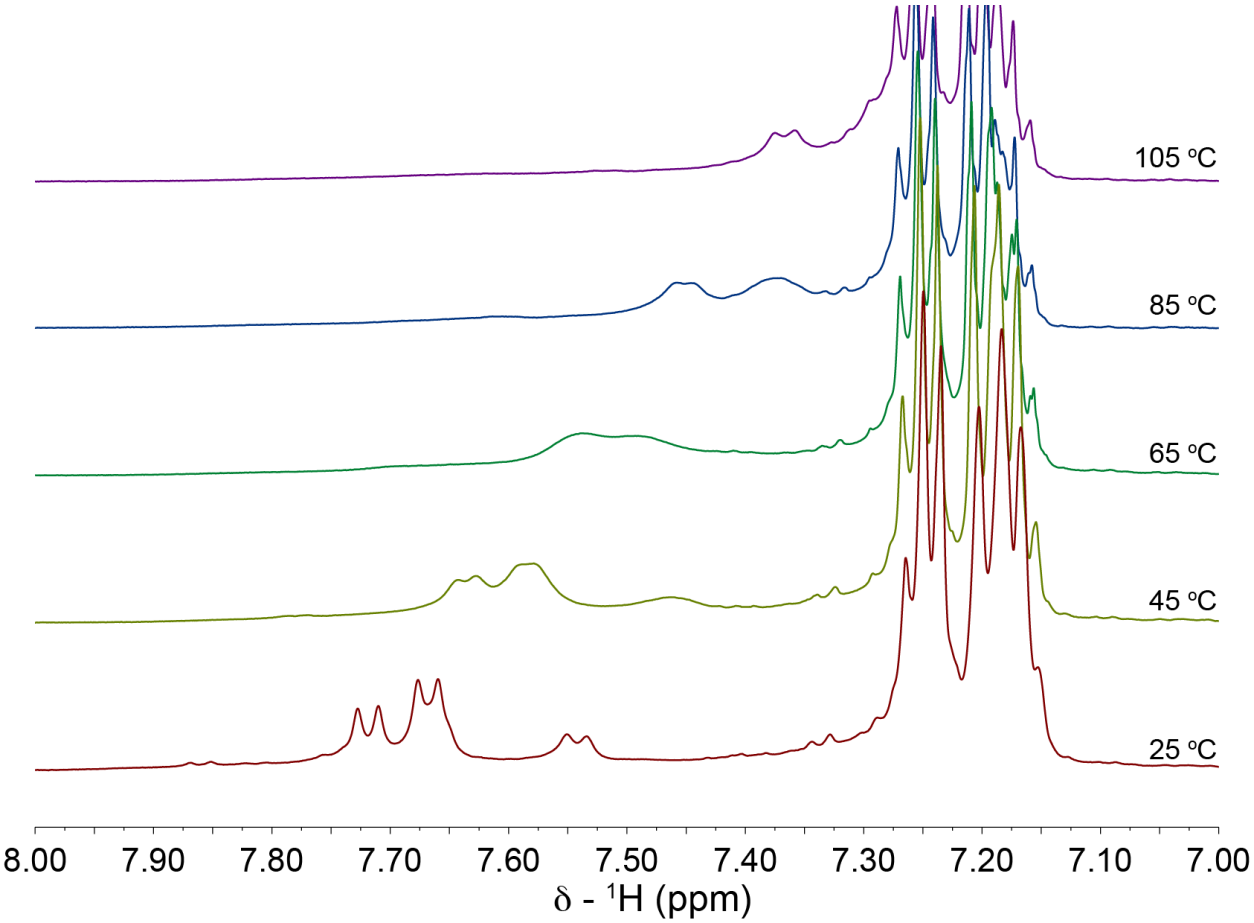
105 °C
85 °C
65 °C
45 °C
25 °C
8.00
7.90
7.80
7.70
7.60
7.50
7.40
7.30
7.20
7.10
7.00
δ - ¹H (ppm)

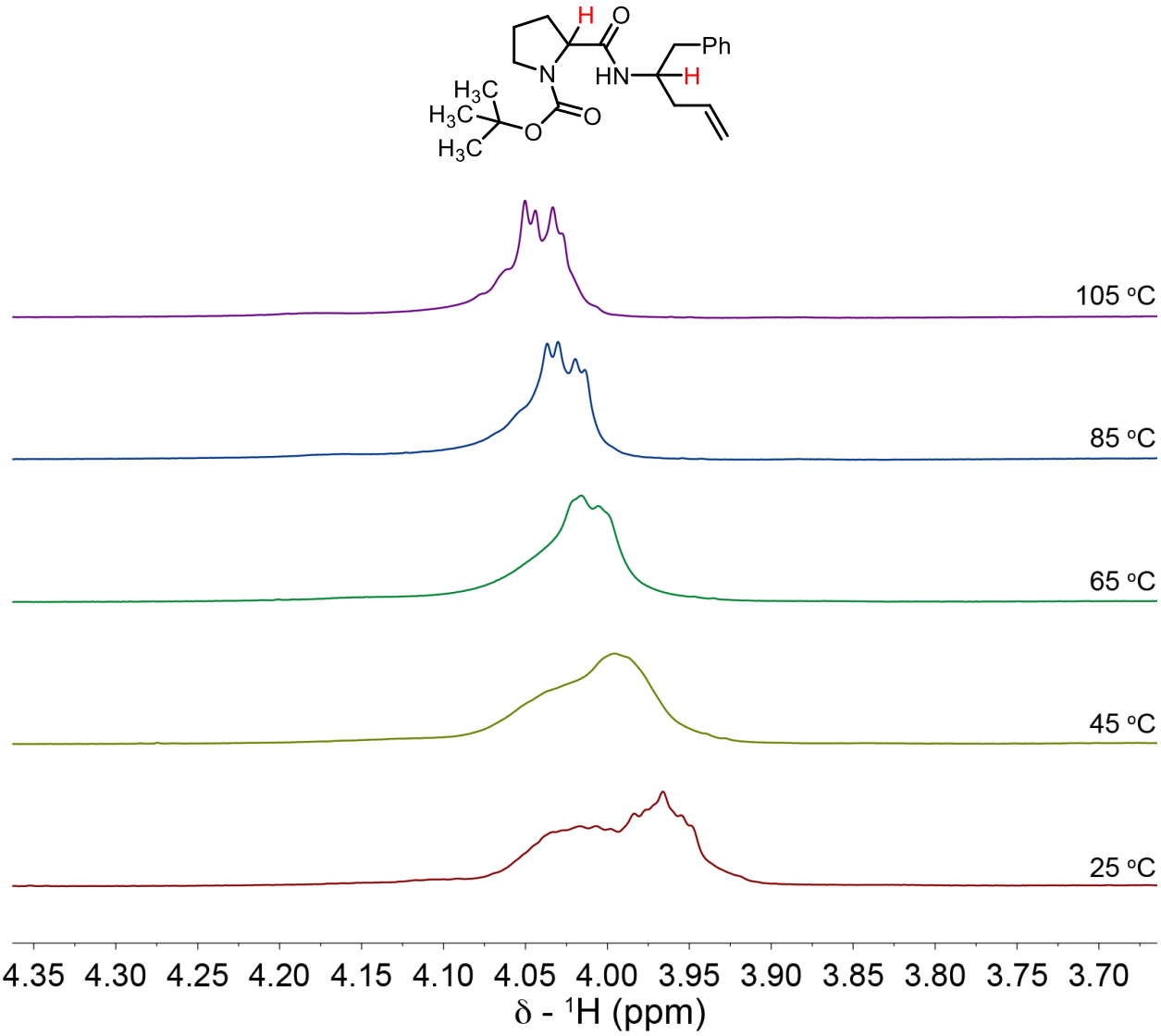
H
O
Ph
N
HN
H
H3C
H3C
H3C
O
O
105 °C
85 °C
65 °C
45 °C
25 °C
4.35 4.30 4.25 4.20 4.15 4.10 4.05 4.00 3.95 3.90 3.85 3.80 3.75 3.70
δ - 1H (ppm)

1D 13C at 105 °C

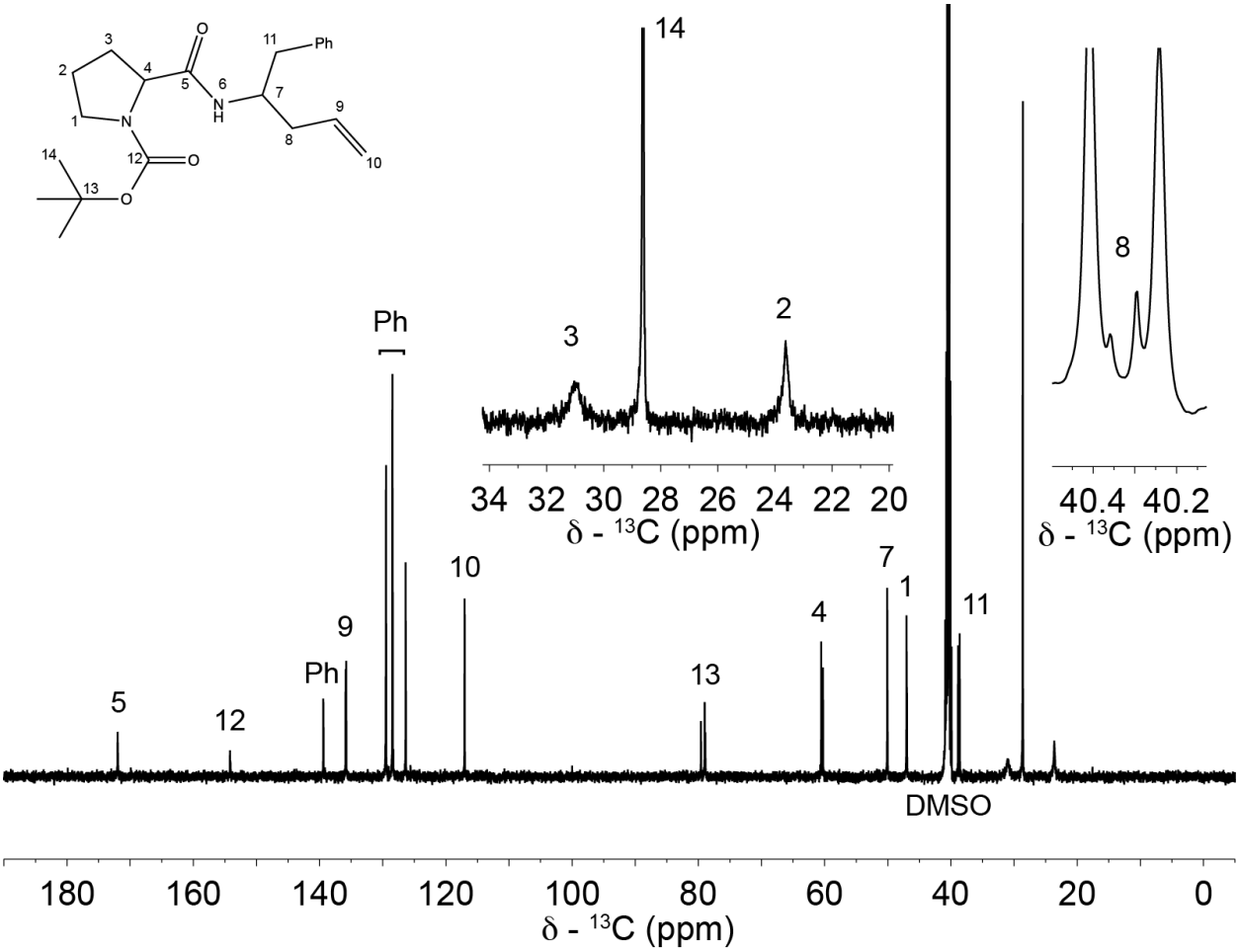

^{1}H NMR Spectroscopy Experiments

General Procedure: An oven dried 16 x 125 mm threaded glass tube and an oven dried NMR tube were taken into a glovebox. Allyl ester (0.25 mmol), was added to the threaded glass tube followed by $Pd(PPh_3)_4$ and $[Ir\{dF(CF_3)ppy\}_2(dtbpy)]PF_6$ (5.0 and 1.0 mol %, respectively). DMSO-d6 (2.0 mL) was added to the glass tube and the reaction mixture was gently shaken for 5 mins.

After this time, approximately 0.8 mL of the reaction mixture was transferred via syringe to the NMR tube, which was then capped and removed from the glovebox. A t = 0 h ^{1}H NMR spectrum was recorded and the tube was placed in a blue LED light bath at rt for 14 h. A t = 14 h ^{1}H NMR spectrum was then recorded.

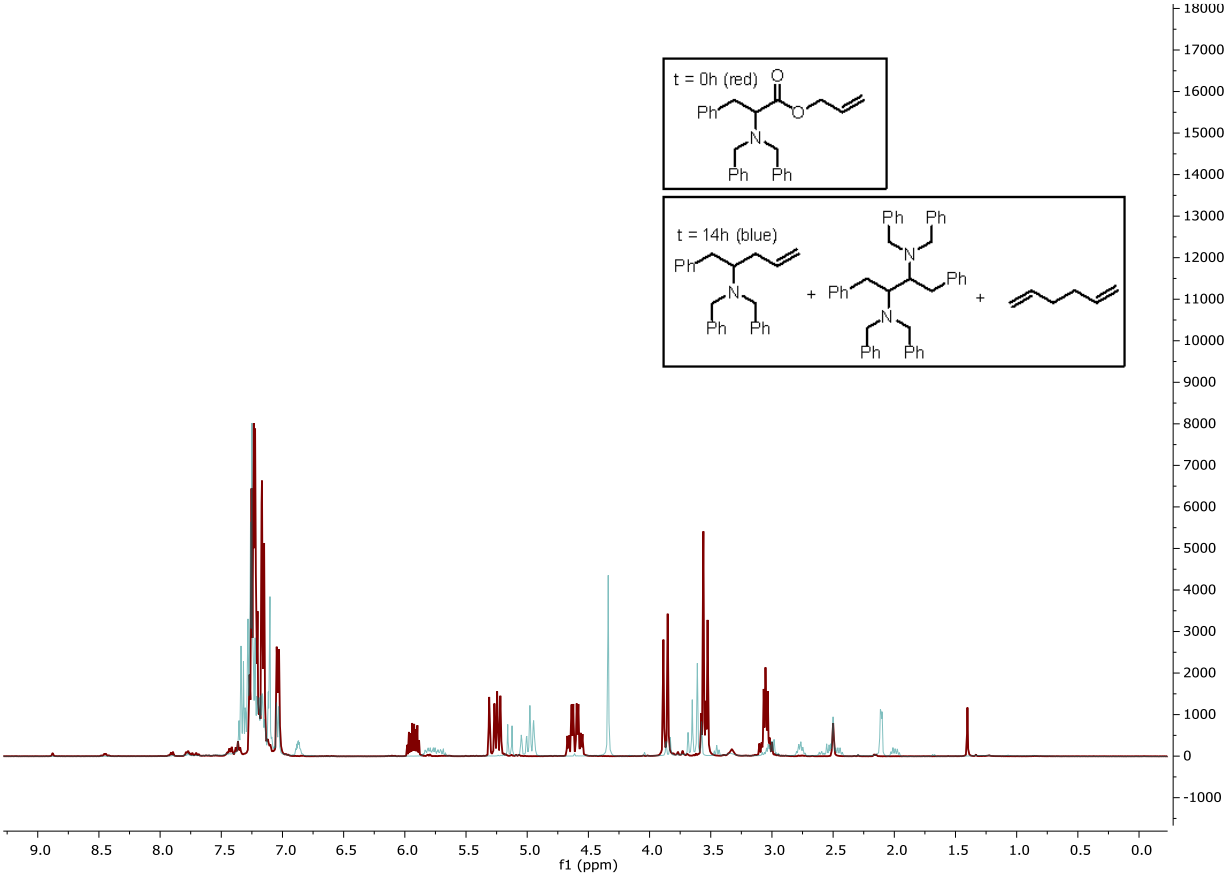

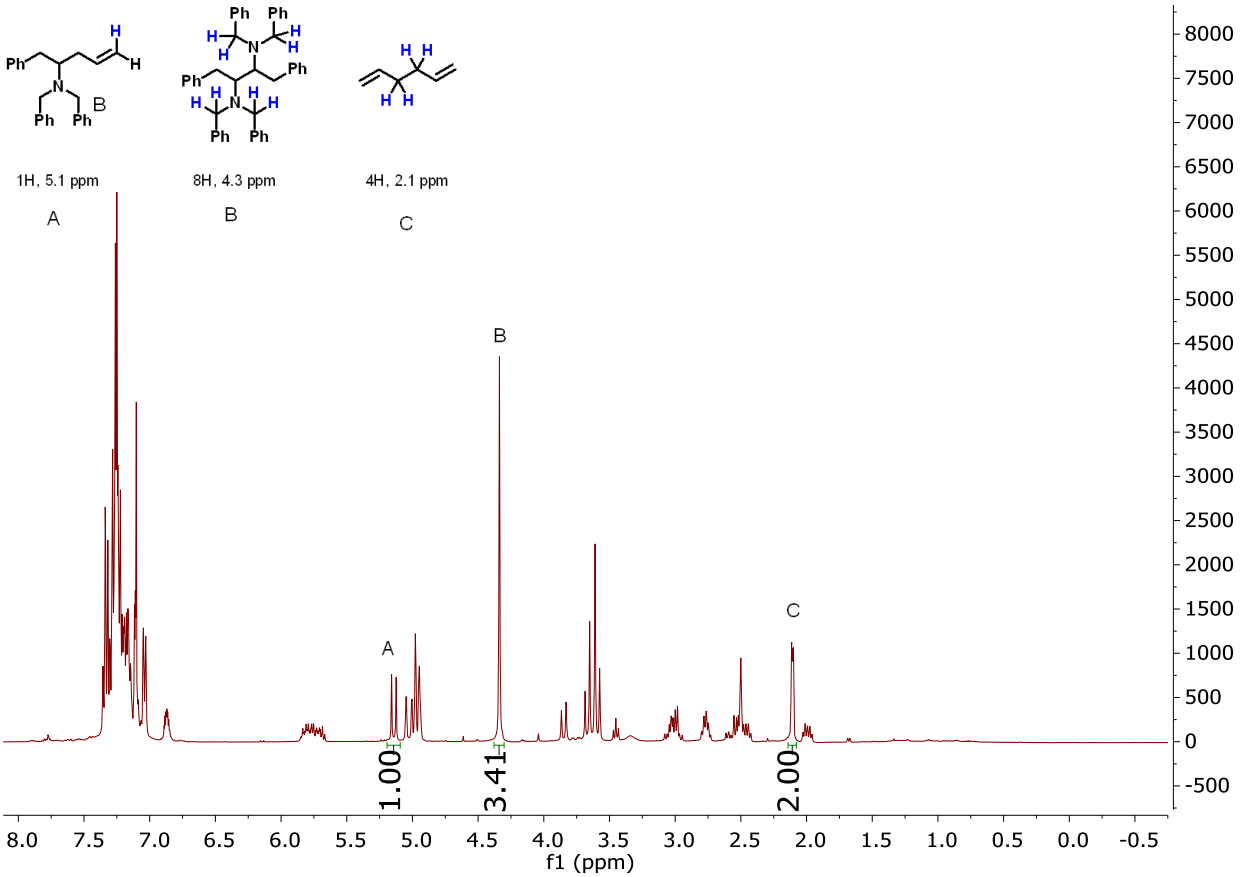

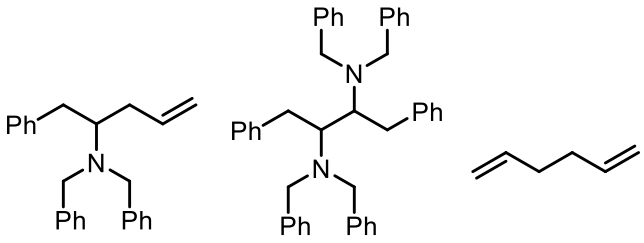

A:B:C = 1.0 : 0.43 : 0.50

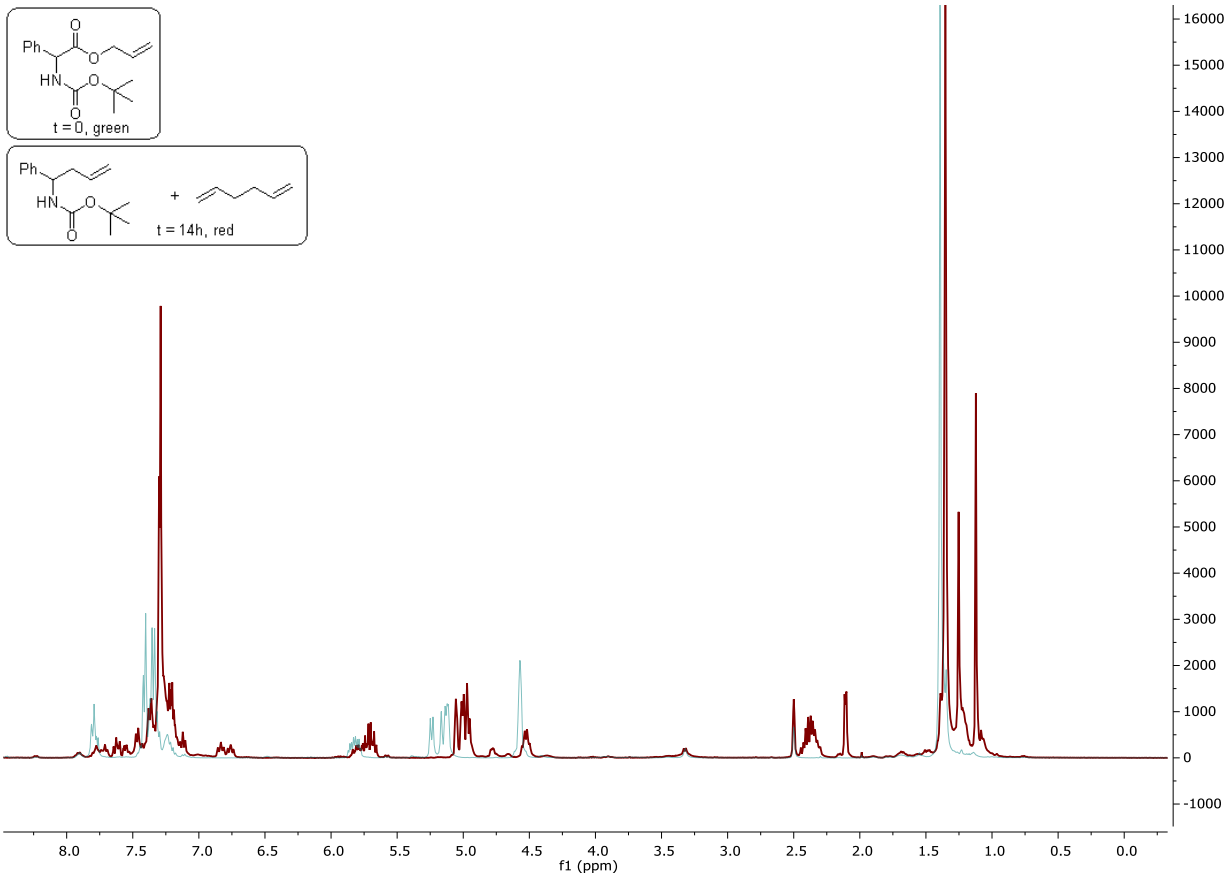
Ph
HN
O
O
O
t = 0, green
Ph
HN
O
O
+
t = 14h, red
16000
15000
14000
13000
12000
11000
10000
9000
8000
7000
6000
5000
4000
3000
2000
1000
0
-1000
8.0
7.5
7.0
6.5
6.0
5.5
5.0
4.5
4.0
3.5
3.0
2.5
2.0
1.5
1.0
0.5
0.0
f1 (ppm)

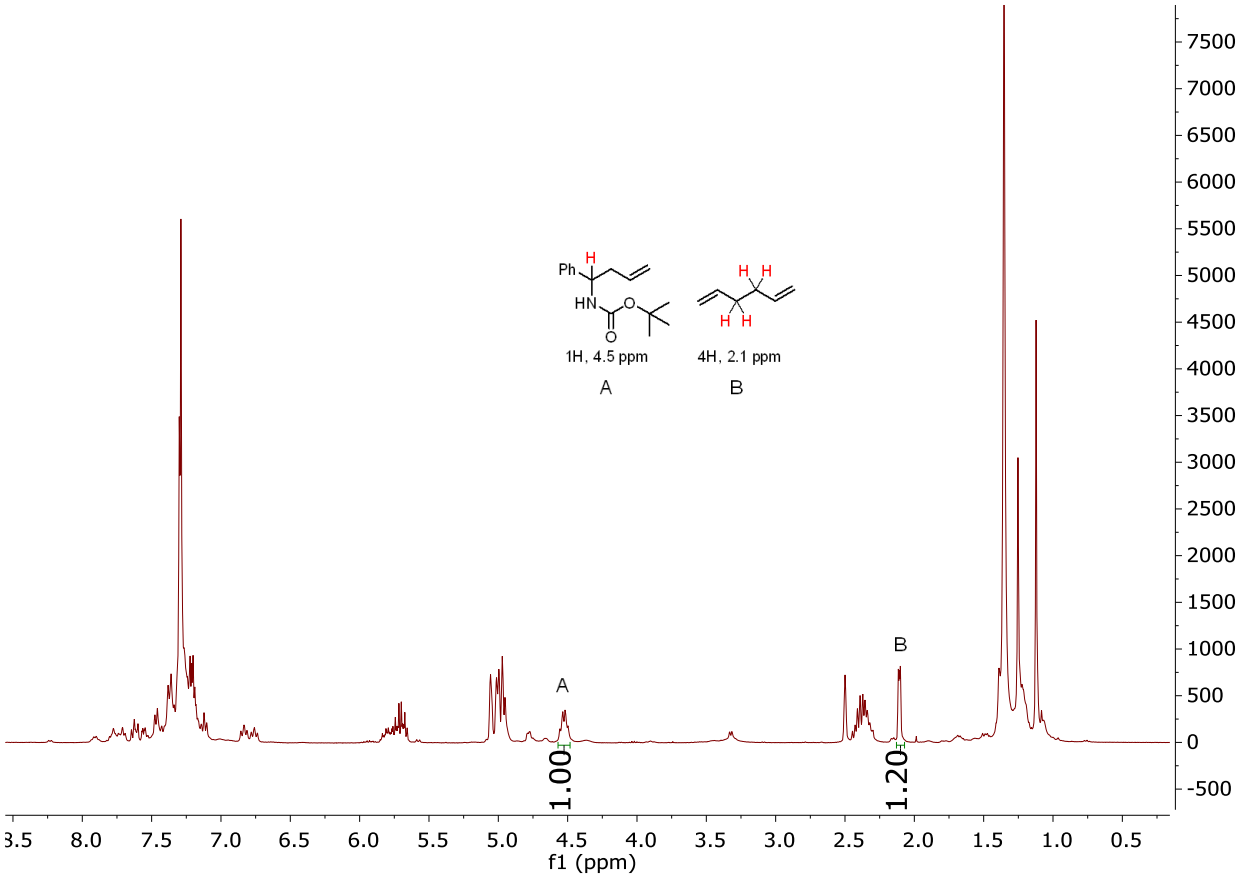
Ph
H
HN
O
O
1H, 4.5 ppm
A
H H
H H
4H, 2.1 ppm
B
A
B
1.00
1.20
7500
7000
6500
6000
5500
5000
4500
4000
3500
3000
2500
2000
1500
1000
500
0
-500
8.0
7.5
7.0
6.5
6.0
5.5
5.0
4.5
4.0
3.5
3.0
2.5
2.0
1.5
1.0
0.5
f1 (ppm)

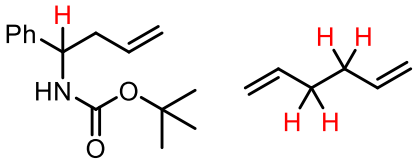
Ph
H
HN
O
O
H H
H H

A **B**

A:B = 1 : 0.30

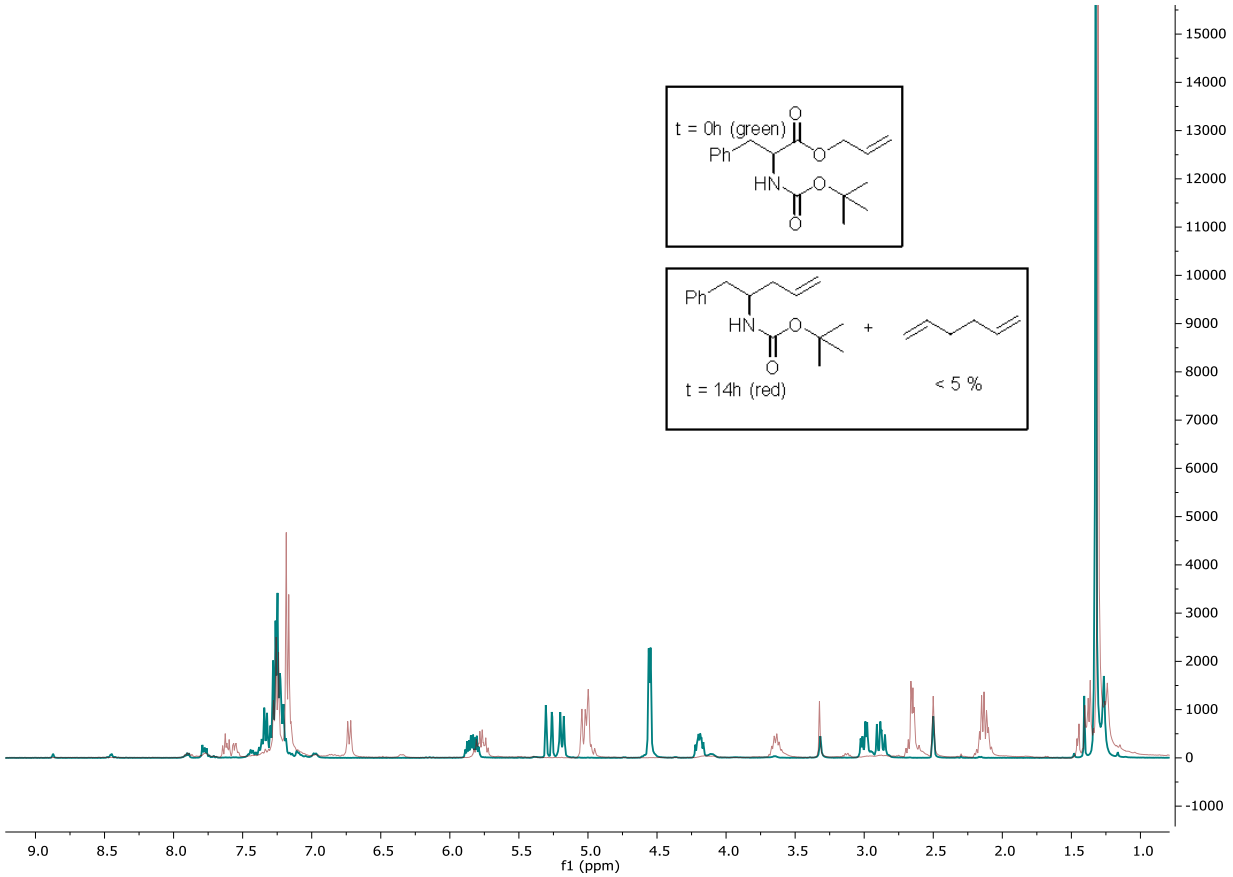
t = 0h (green)
Ph
HN
O
O
O
O
Ph
HN
O
O
+
t = 14h (red)
< 5 %
15000
14000
13000
12000
11000
10000
9000
8000
7000
6000
5000
4000
3000
2000
1000
0
-1000
9.0
8.5
8.0
7.5
7.0
6.5
6.0
5.5
5.0
4.5
4.0
3.5
3.0
2.5
2.0
1.5
1.0
f1 (ppm)

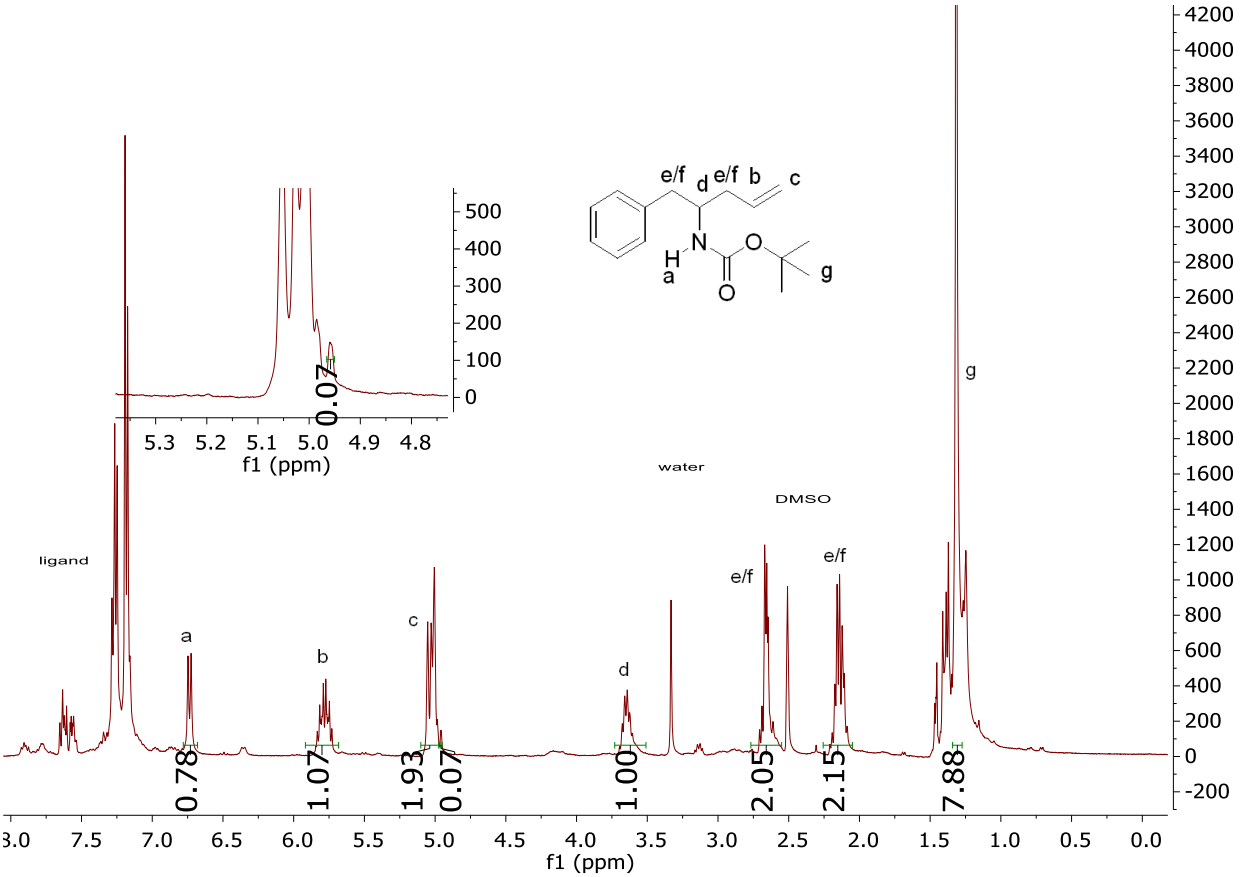

No significant amount of dibenzyl dicarbamate dimer was detected. ~ 7% 1,5 hexadiene was detected.

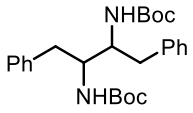

not detected

Chiral HPLC Analysis

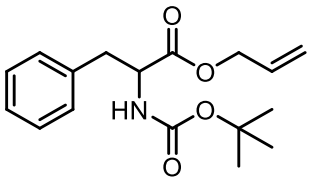

Racemic, ADH column, 30:70 ^{i}PrOH:hexanes, 0.38 mL/min

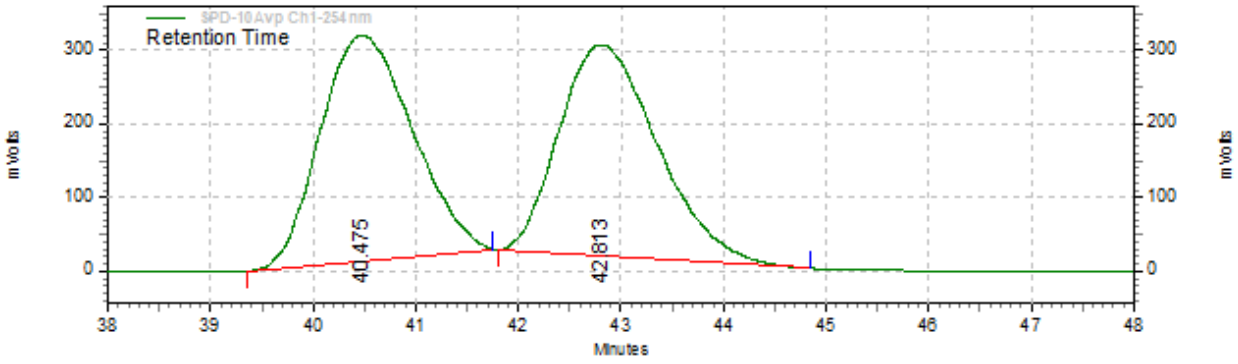

SPD-10Avp Ch1-254nm Results				
Retention Time	Area	Area %	Height	Height %
40.475	19100552	50.01	306410	51.65
42.813	19095979	49.99	286811	48.35
Totals				
	38196531	100.00	593221	100.00

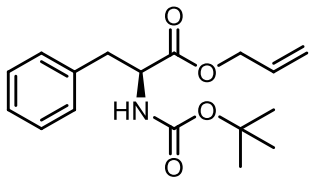

Enantioenriched, ADH column, 30:70 ^{i}PrOH:hexanes, 0.38 mL/min

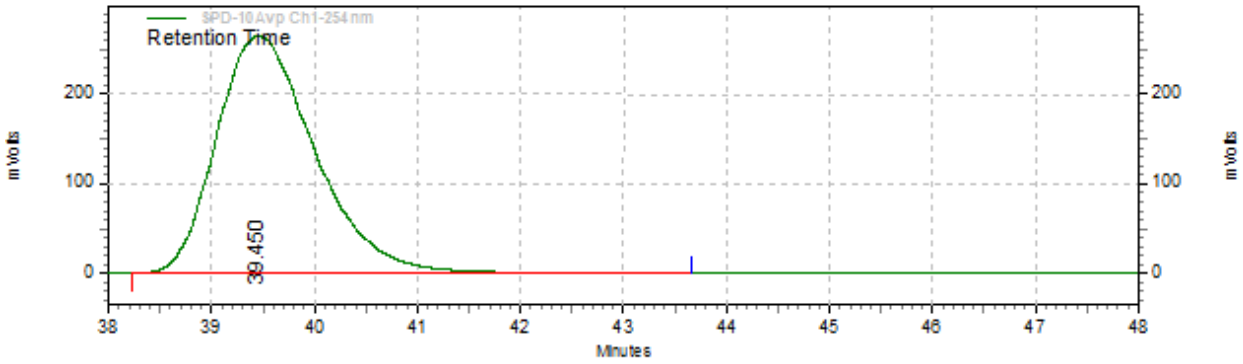

SPD-10Avp Ch1-254nm Results				
Retention Time	Area	Area %	Height	Height %
39.450	17593284	100.00	265087	100.00
Totals				
	17593284	100.00	265087	100.00

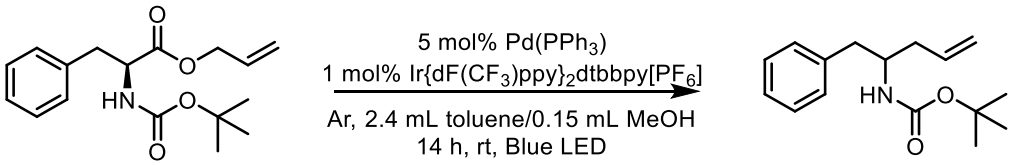

Racemic, OD column, 1:99 ^{i}PrOH:hexanes, 0.25 mL/min

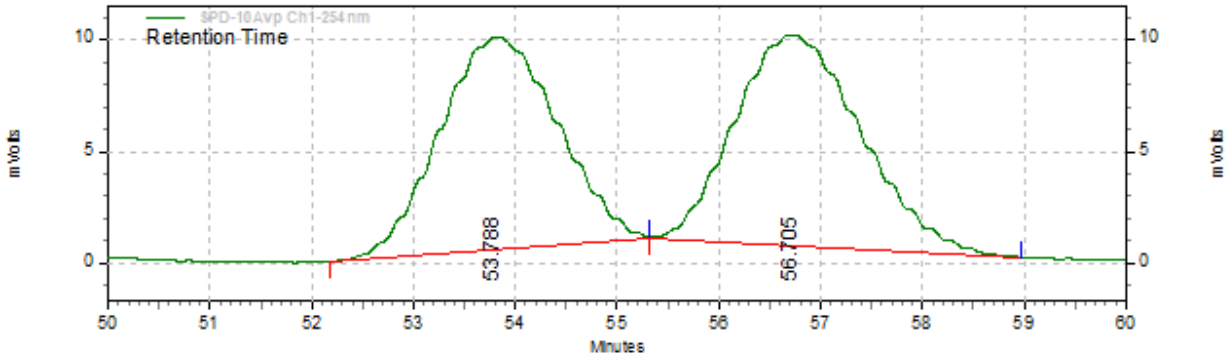

SPD-10Avp Ch1-254nm Results				
Retention Time	Area	Area %	Height	Height %
53.788	760590	48.35	9481	50.18
56.705	812548	51.65	9414	49.82
Totals				
	1573138	100.00	18895	100.00

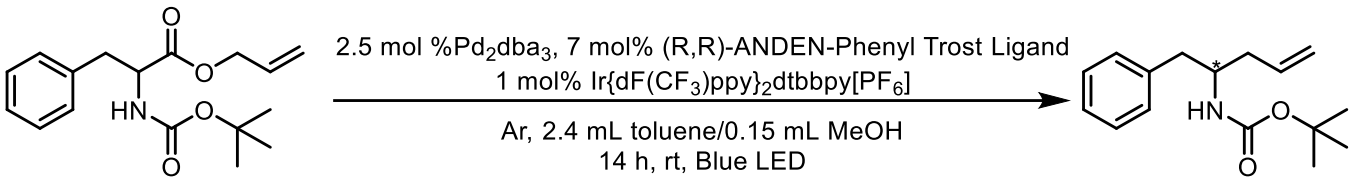

Enantioenriched, OD column, 1:99 ^{i}PrOH:hexanes, 0.25 mL/min

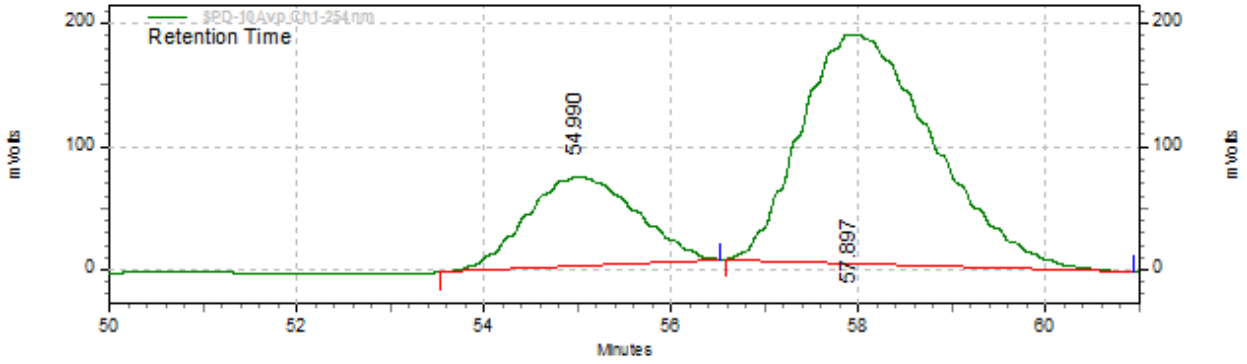

SPD-10Avp Ch1-254nm Results				
Retention Time	Area	Area %	Height	Height %
54.990	5916249	24.54	72540	28.10
57.897	18195938	75.46	185612	71.90
Totals				
	24112187	100.00	258152	100.00

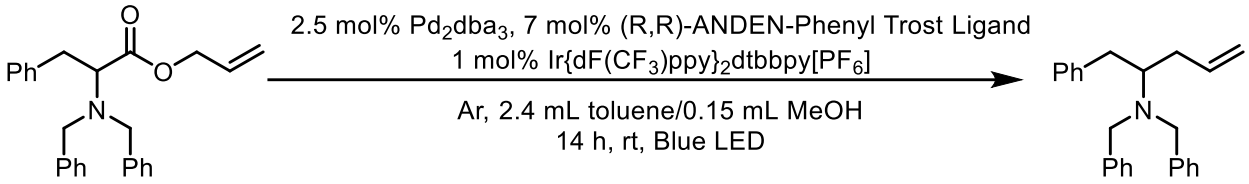

ADH column, 0.1:99.9 ^{i}PrOH:hexanes, 0.30 mL/min

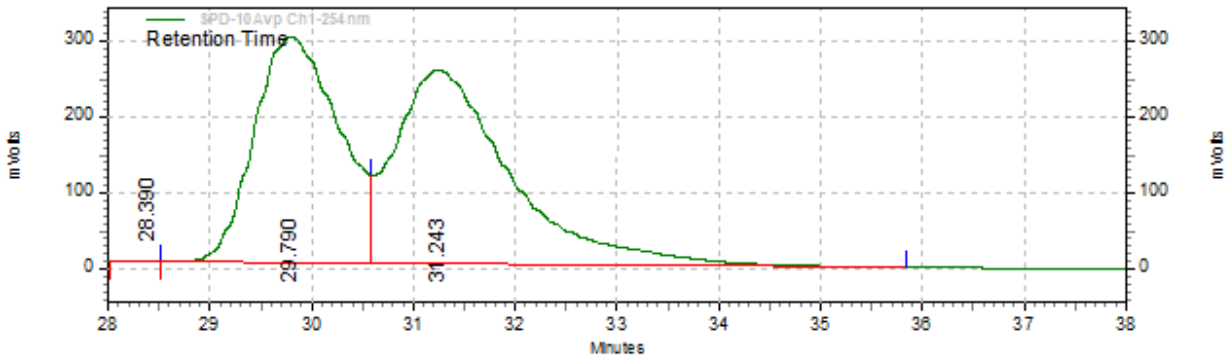

SPD-10Avp Ch1-254nm Results				
Retention Time	Area	Area %	Height	Height %
28.390	13335	0.04	656	0.12
29.790	17275395	46.03	298344	53.78
31.243	20238562	53.93	255717	46.10
Totals				
	37527292	100.00	554717	100.00

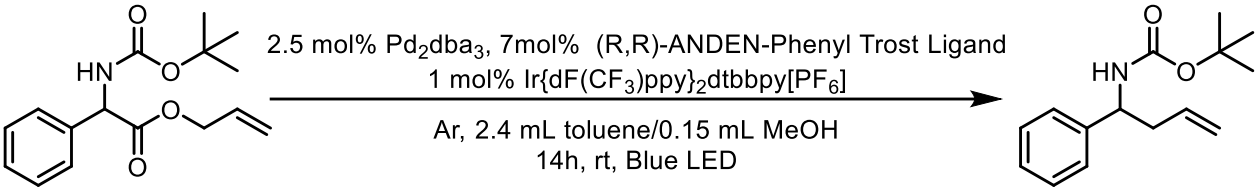

ADH column, 0.1:99.9 ^{i}PrOH:hexanes, 0.30 mL/min

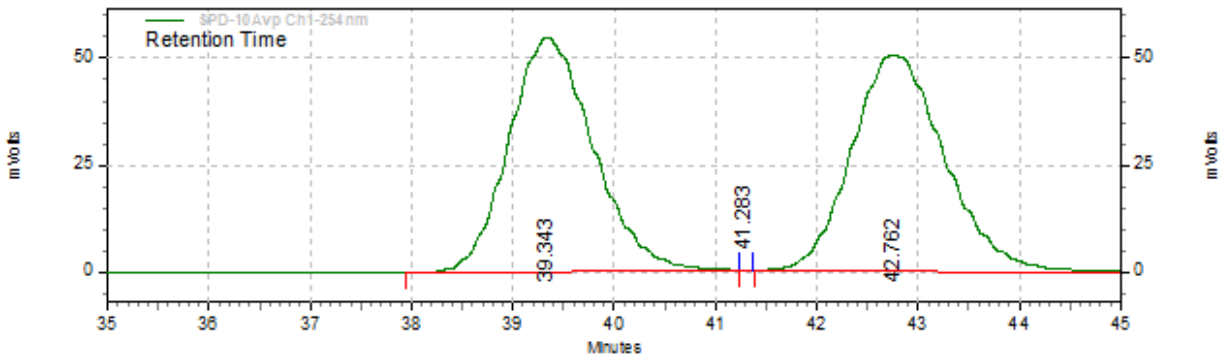

SPD-10Avp Ch1-254nm Results				
Retention Time	Area	Area %	Height	Height %
39.343	3146874	49.67	54437	52.09
41.283	380	0.01	70	0.07
42.762	3187722	50.32	49991	47.84
Totals				
	6334976	100.00	104498	100.00

[1] Miyake, Y.; Nakajima K.; Nishibayashi, Y. "Visible light-mediated oxidative decarboxylation of arylacetic acids into benzyl radicals: addition to electron-deficient alkenes by using photoredox catalysts" *Chem. Commun.* **2013**, *49*, 7854-7856.

[2] Xie, N.; Taylor, C. M. "Synthesis of a Domer of β-(1,4)-L-Arabinosyl-(2S,4R)-4-hydroxyproline Inspired by Art v 1, the Major Allergen of Mugwort" *Org. Lett.* **2010**, *12*, 4968-4971.

Chapter 3. Photocatalytic Aminodecarboxylation of Carboxylic Acids

3.1 Introduction

This chapter explores the radical decarboxylation of carboxylates by excited-state photocatalysts and the reactions of the radicals in the absence of a transition metal. A brief synopsis of the state-of-the-art is presented along with our efforts to use carboxylic acids to site-specifically effect C–N bond formation.

3.2 Photocatalytic decarboxylation of carboxylic acids

Although the radical decarboxylation of carboxylic acids has been studied for several decades (see chapter 2), the methods employed have not lent themselves to adoption by organic chemists for the construction of molecules. For example, the radiation of the quaternary ammonium salt of an α-anilinocarboxylate in acetonitrile with dicyano benzene and Pyrex filtered light (λ > 290 mM) was shown by the Oh group to afford a mixture of products (Scheme 37).[1] Besides the initial report by Nishabayashi, (see chapter 2) which inspired our studies, the general incorporation of photoredox catalysis induced radical decarboxylation into synthetic manifolds has notbeenwidely disclosed in the literature.

Scheme 37. Photoinduced radical decarboxylation

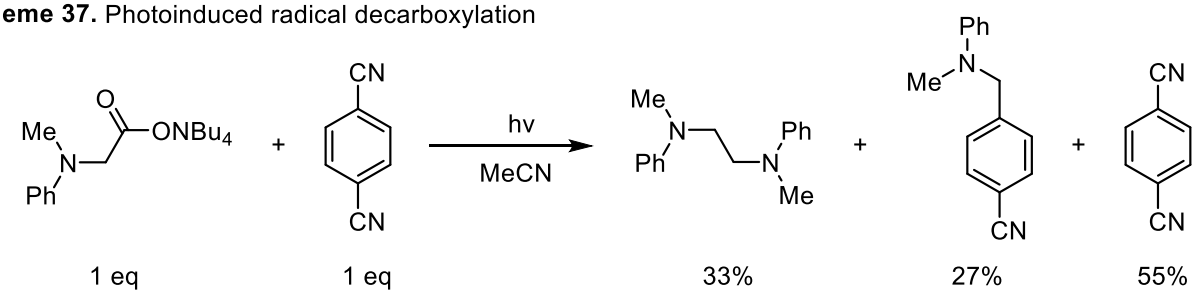

Shortly after our studies on radical dual catalytic DcA began, the MacMillan group published the photoredox-catalyzed version of the reaction described by Oh in 1998. They found that the excited state of the reducing homoleptic iridium photocatalyst Ir[*p*-F(*t*-Bu)-ppy]$_3$ readily transferred an electron to dicyanobenzene. This produced a long-lived radical which could readily intercept a transient α-amino radical after the oxidation of the carboxylate by the Ir(IV) photocatalyst and the loss of CO_2. The combination of the two radicals produced the desired product after loss of cyanide, and the ground state photocatalyst could re-enter a productive catalytic cycle (Scheme 38).[2]

Scheme 38. Decarboxylative arylation

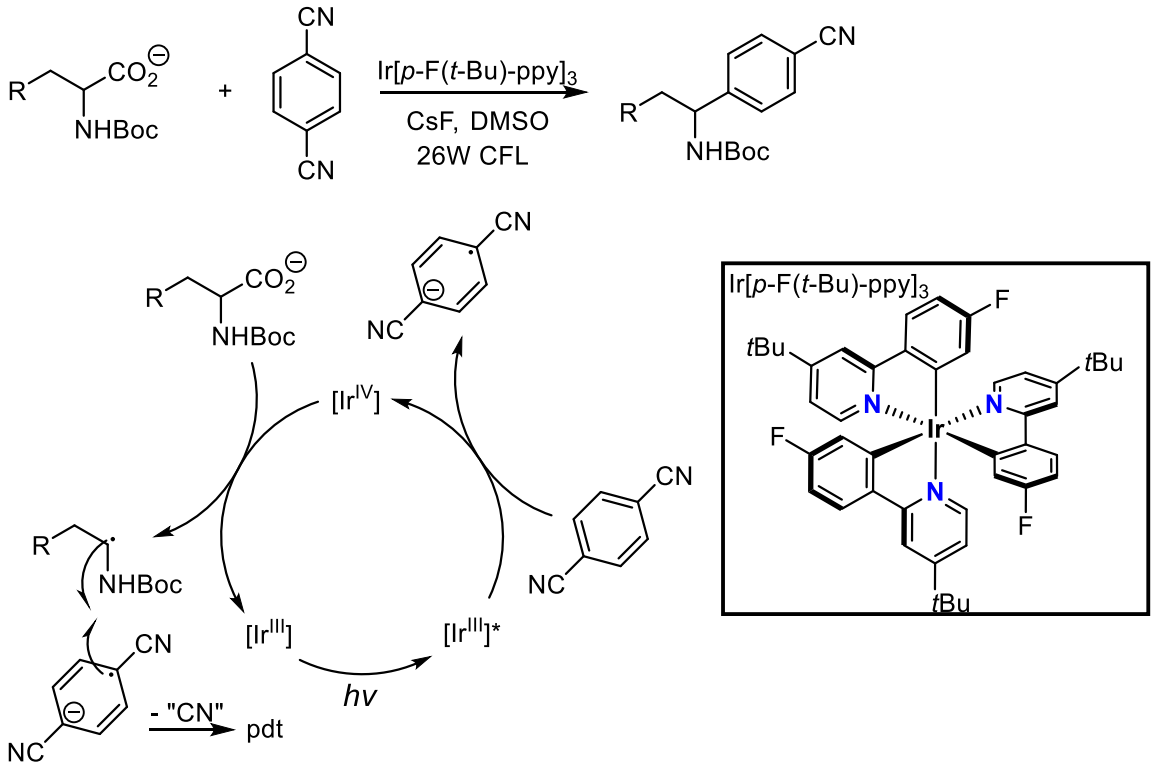

The MacMillan lab also demonstrated that Michael acceptors were competent traps for the alkyl radical generated after radical decarboxylation of carboxylic acids. After decarboxylation, the radical forms site-specifically on the carbon that bore the carboxylate. This unique reactivity imitates traditional traceless activation groups like Grignard reagents or boronic acids. Carboxylic acids are superior to such groups, however, as they are readily available, and the waste readily

leaves as a benign volatile gas. Alkenes bearing various electron-withdrawing groups, such as ketones, aldehydes, amides, sulfones, and esters participated in the reaction. Further, a more oxidizing photocatalyst Ir[dF(CF_3)ppy]$_2$dtbbpy$^+$ photocatalyst gave the best yields, prompting the authors to propose reductive quenching of the photoexcited catalyst. After oxidizing the carboxylate and triggering the decarboxylation, the photocatalyst reduces the resultant radical to close the catalytic cycle (Scheme 39).[3]

The MacMillan lab also designed a tandem radical decarboxylation, Michael addition, desulfinylation for the decarboxylative vinylation of α-amino acids using vinyl sulfones. Optimization revealed that the combination of the oxidizing photocatalyst Ir[dF(CF_3)ppy]$_2$dtbbpy$^+$, the base CsOAc, and the solvent 1,2-dichloroethane (DCE), led to high yields and >95:5 *E:Z* selectivity. The proposed mechanism involves reductive quenching of the excited photocatalyst followed by Michael addition of the α-amino radical to the vinyl sulfone. Collapse of the Michael addition adduct generates an alkene and extrudes a sulfinyl radical which is reduced by the

Scheme 39. Radical decarboxylation followed by Michael addition

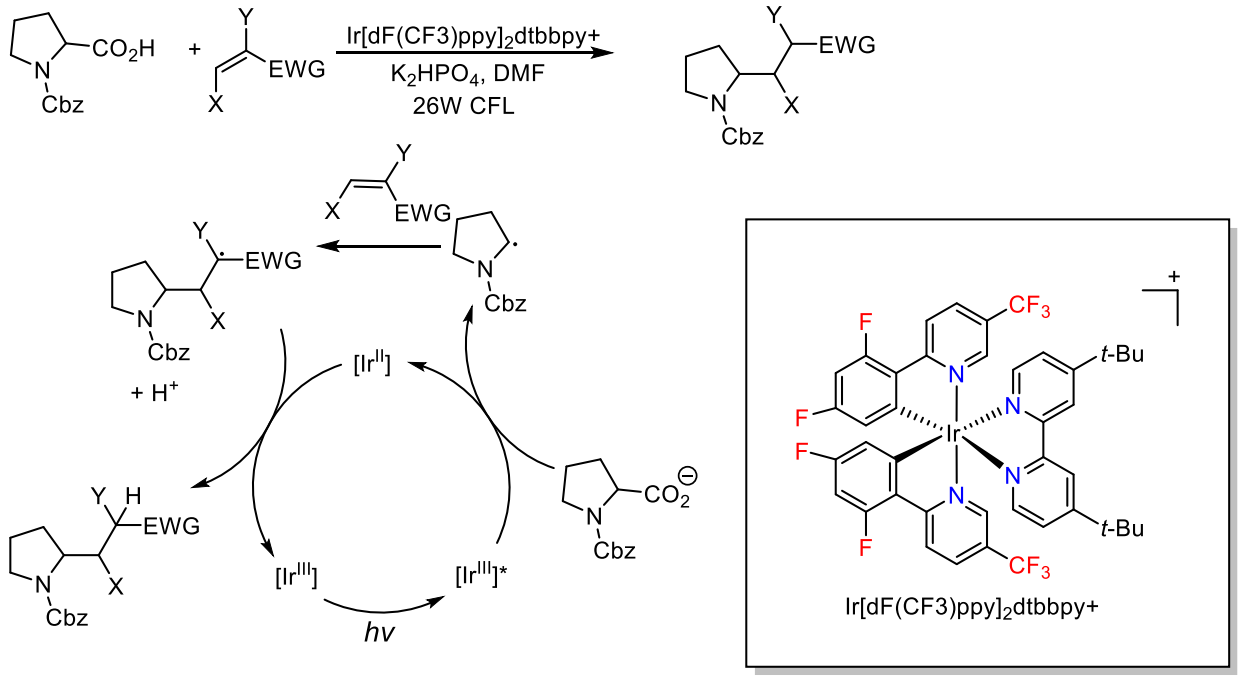

photocatalyst, returning it to the ground state (Scheme 40).[4] Tertiary *N*-aryl amines were also successfully oxidized by the photocatalyst and could be used instead of carboxylic acids.

The use of carboxylic acids as traceless activating groups (TAG) strategy was also employed for site-specific decarboxylative fluorination. MacMillan and coworkers found that alkyl radicals generated via radical decarboxylation could abstract a fluorine atom from Selectfluor®. Quenching experiments revealed that the alkyl carboxylate did not quench the photoexcited catalyst, but Selectfluor® did. The already highly oxidizing catalyst likely reduces a molecule of Selectfluor® post fluorine atom abstraction and enters an extremely oxidizing Ir^{IV} oxidation state which is sufficient to effect radical decarboxylation of unactivated alkyl species. Optimization studies revealed $Ir[dF(CF_3)ppy]_2dtbbpy^+$ to be a competent photocatalyst and Na_2HPO_4 a suitable base. A mixture of acetonitrile and water was employed to aid in solubilizing the reactants and photocatalyst. The mechanism proposed invokes the reduction of the amine radical cation post

Scheme 40 Radical decarboxylative vinylation

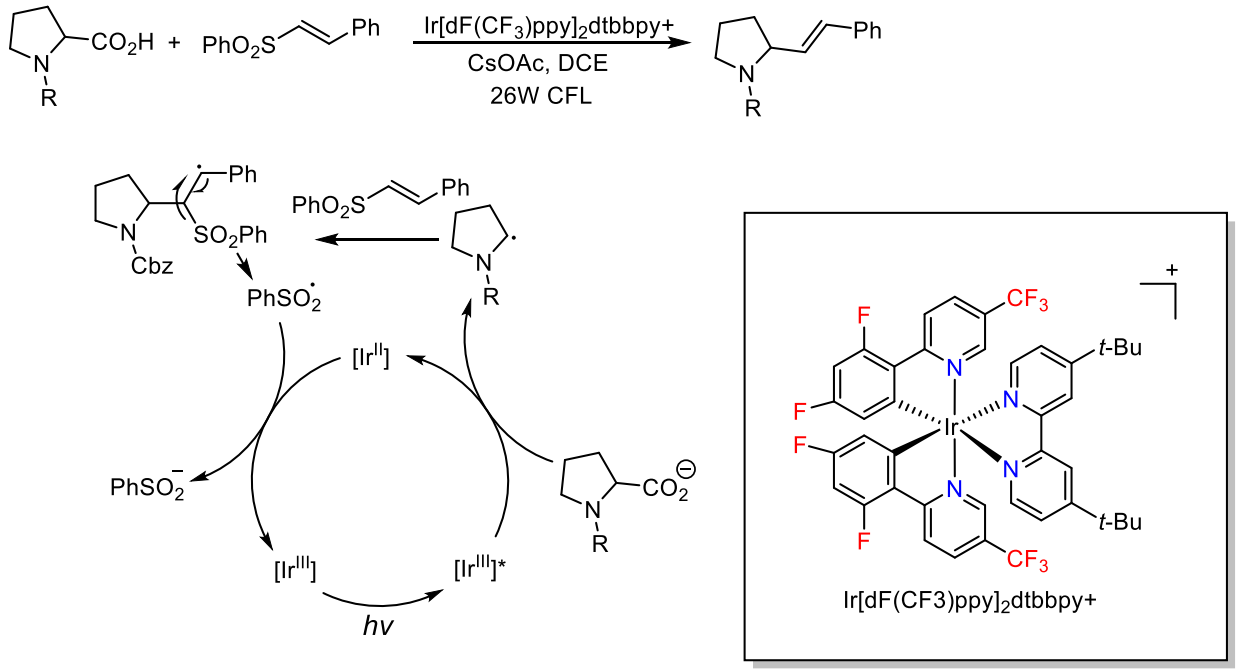

fluorine atom abstraction. This generates the oxidizing Ir^{IV} species which takes an electron from

the alkyl carboxylate triggering decarboxylation. The alky radical then abstracts a fluorine atom from the abundant Selectfluor® (3 equiv.) in the reaction mixture (Scheme 41).[5]

Scheme 41. Radical decarboxylative fluorination

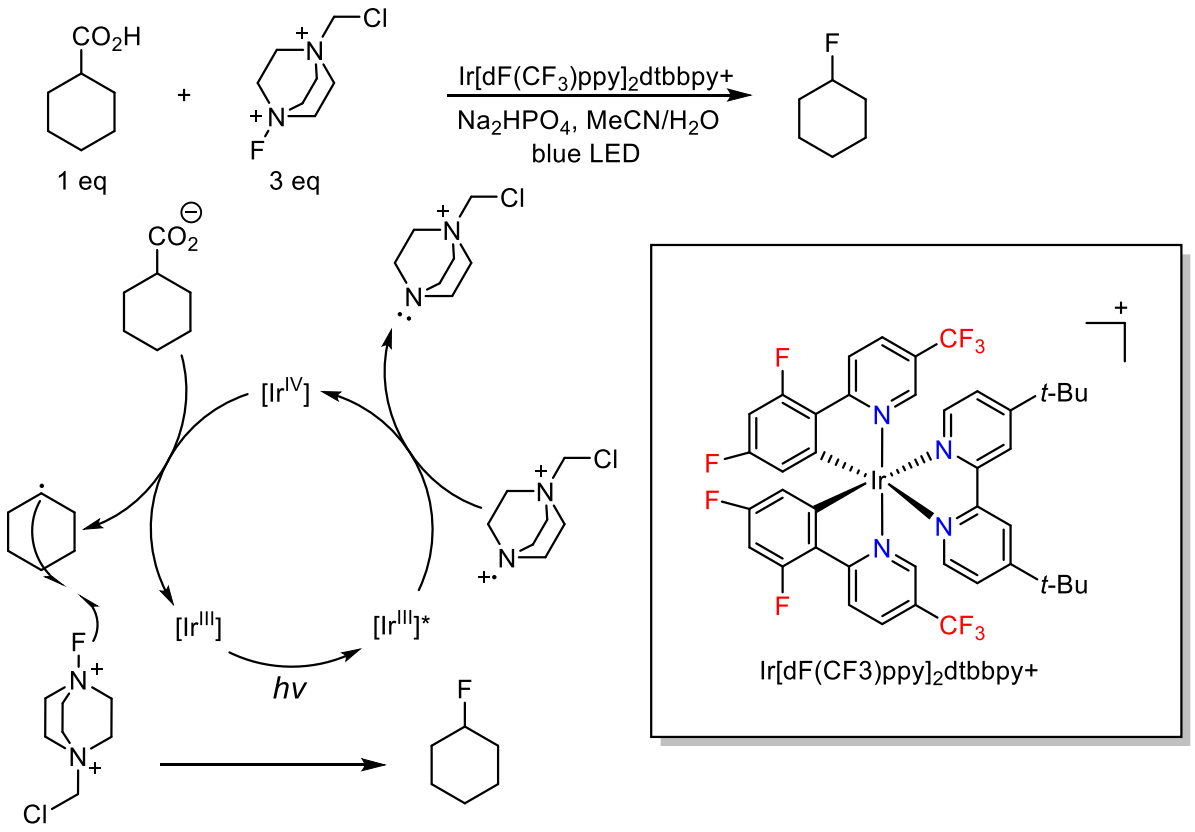

The above work was built upon the first report of photocatalytic C–F bond formation by the Sammis group in 2014. The authors found that carboxylic acids that were stabilized by an α-phenolic ether underwent decarboxylation when treated with $Ru(bpy)_3Cl_2$ and NaOH.[6] Quenching studies revealed that the catalyst is first oxidized by Selectfluor®, similar to the mechanism presented in Scheme 41. The reaction was limited to phenolic ethers, which was circumvented by the MacMillan laboratory using an iridium photocatalyst that is more oxidizing than $Ru(bpy)_3Cl_2$ after oxidative quenching.

The radical decarboxylation of amino acids was also effected in 2009 by the Hantanaka group using phenantherene, dicyanobenzene and a 100-W high-pressure mercury lamp. Upon

Scheme 42. Radical decarboxylative macrocyclization

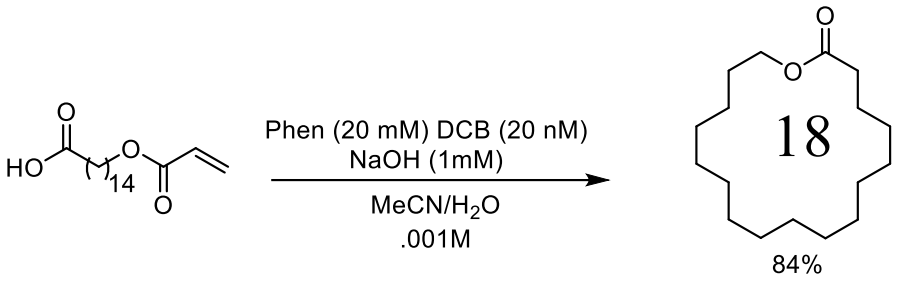

decarboxylation, the authors found that the radicals could be trapped by Michael acceptors and that intramolecular variants of the reaction could also be used to construct macrocycles under very dilute conditions (Scheme 42).[7]

Decarboxylative alkynylation of carboxylic acids was also disclosed in 2015. Specifically, ethynylbenziodoxolone (EBX) reagents efficiently intercepted alkyl radicals, post decarboxylation, to effect the desired reaction. Optimization studies reveled that CsOBz was the optimal base and the photocatayst $Ir[dF(CF_3)ppy]_2dtbbpy^+$ provided high yields. α-Amino, α-oxy, and alkyl carboxylic acids were all effectively alkynylated. The EBX reagents were limited to silicon and aryl groups at the terminal position. A tentative mechanism is proposed in Scheme 44. The photoexcited iridium species oxidizes the carboxylate, triggering decarboxylation. The resultant radical adds to the EBX reagent α to iodine followed by radical fragmentation to provide an iodine radical. This radical is reduced by the photocatalyst, completing the photocatalytic cycle.[8]

Photocatalytic decarboxylation can also reduce carboxylic acids. The Fukuzumi acridinium photocatalysts, which are highly oxidizing ($E_{1/2}^{red}$ = +2.06V vs SCE), and hydrogen donors were screened in an attempt to effect hydrodecarboxylation. Screening of donors revealed that phenyl disulfide, which can act as redox-coupled hydrogen shuttle, performed better than the hydrogen atom donor thiophenol. Base was required to initiate the reaction, consistent with previous observations that the anionic carboxylate undergoes oxidation followed by radical

decarboxylation. The authors found a range of amino acids and phenylacetic acids were compatible with the reaction conditions.

Scheme 43. Radical decarboxylative alkynylation

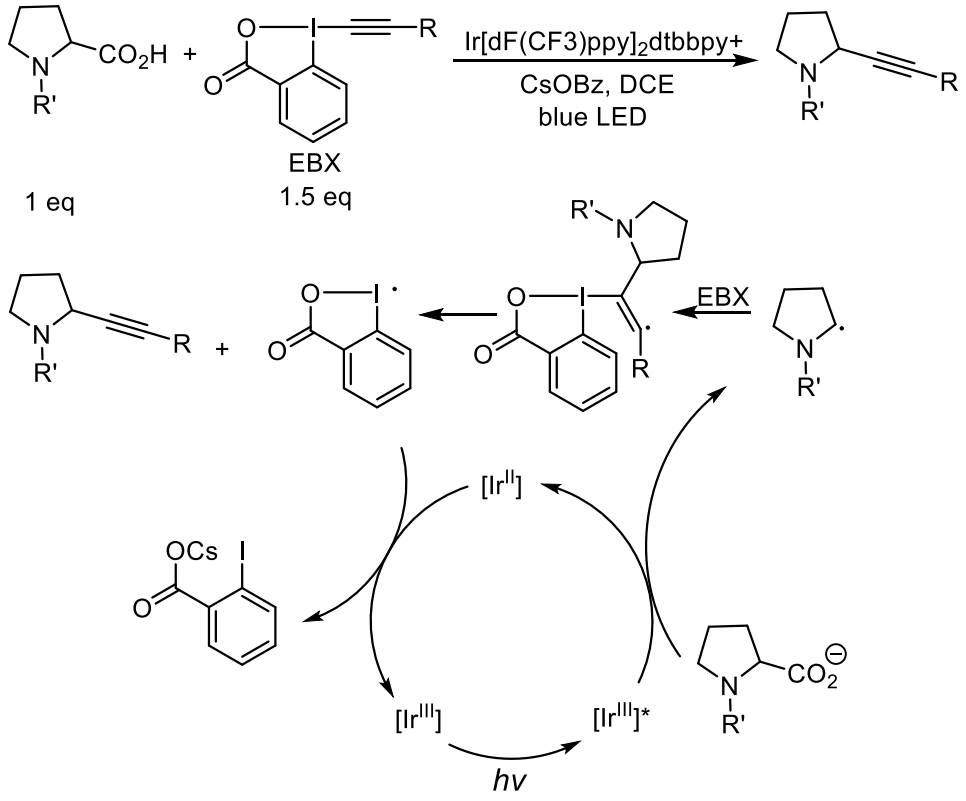

The proposed mechanism invokes oxidation of the carboxylate followed by decarboxylation. Reduction of an aryl thiyl radical to the anion by the photocatalyst closes the photocatalytic cycle. The protonated anion then serves as a hydrogen atom donor to generate the desired protonated alkane (Scheme 44).[9]

Similar conditions were used by the Nicewicz laboratory for the hydrodecarboxylation of primary, secondary, and tertiary carboxylic acids. Photocatalyst screening revealed Mes-Acr-Ph, another oxidizing Fukuzumi acridinium photocatalyst, readily effected decarboxylation. Solvent screening revealed mixtures of water and polar aprotic solvents worked well, hinting that the

Scheme 44. Radical hydrodecarboxylation

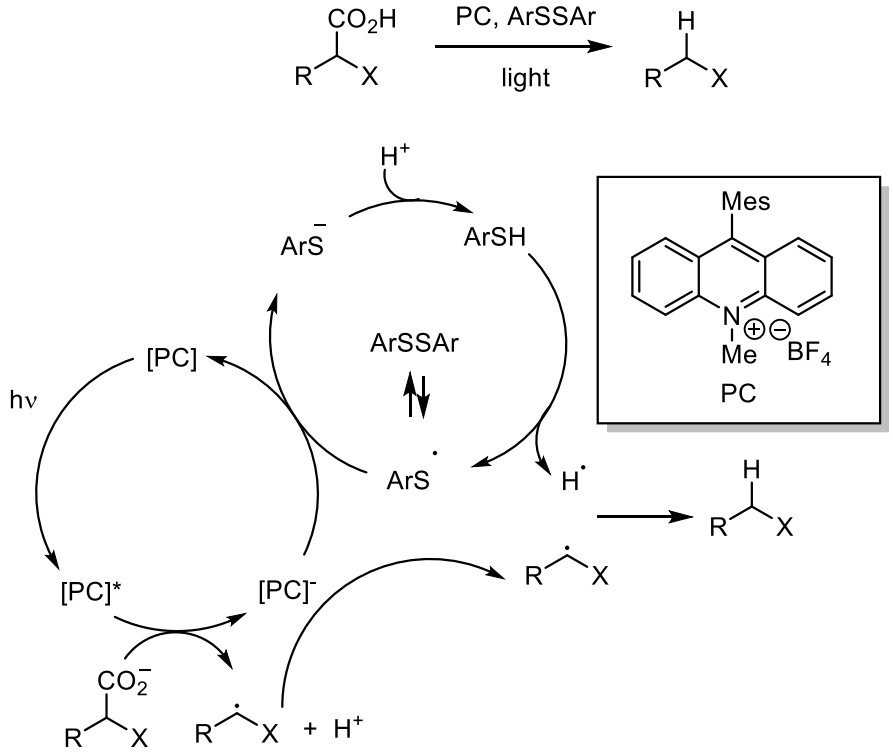

equilibrium between carboxylate anion and protonated acid was important. Eventually trifluoroethanol facilitated the desired hydrodecarboxylation most efficiently. Sub-stoichiometric amounts of amine base could also be employed which is consistent with the work previously published by the Wallentin group.[9] A variety of alkyl carboxylic acids were reduced under the optimized reaction conditions. Additionally, the authors demonstrated that the double decarboxylation of malonic acids could be achieved with increased photocatalyst loading and KO*t*Bu as the base (Scheme 45).[10] Kinetic studies found that the reaction was zero order in photocatalyst and first order in carboxylate, indicating that the reaction may be light-limited. Additional ^{1}H NMR spectroscopy experiments revealed that a pre-coordination complex likely forms between the photocatalyst and the carboxylate prior to oxidation.

Scheme 45. Radical hydrodecarboxylation of alkyl acids

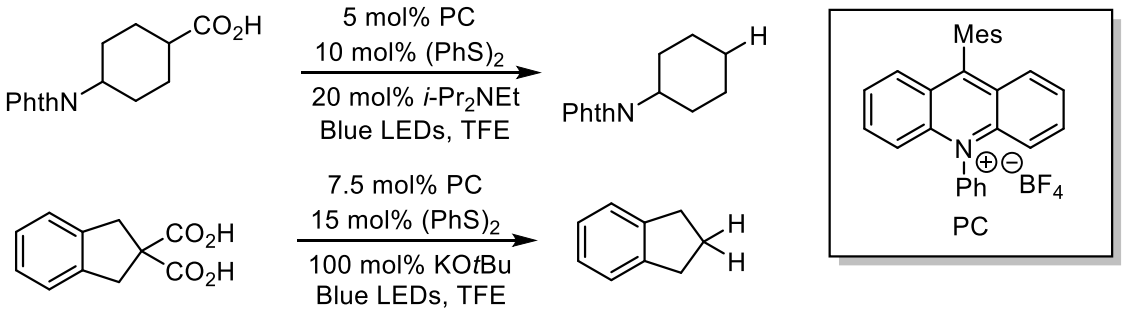

3.3 Aminodecarboxylation reactions

Although hydrodecarboxylation serves as a mild route to reduce carboxylic acids, we questioned if other transformation of the radical alkane were possible. One functional group transformation that we surveyed was aminodecarboxylation. Historically, the Schmidt reaction has been utilized to directly convert an acid to an amine by trapping out an isocyanate with water. Unfortunately, explosive hydrazoic acid and harsh reaction conditions are required, which often lead to low yields and formation of byproducts (Scheme 46).[11]

Scheme 46. The Schmidt reaction

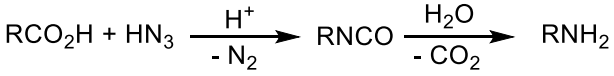

More recently, treatment of activated Barton esters with light in the prescense of electrophilic diazirines and nitroso compounds has been used for regioselective C–N bond formation. A limited substrate scope, formation of byproducts, and the need to pre-form the activated ester prior to decarboxylation are all significant drawbacks to this approach (Scheme 47).[12]

Scheme 47. Radical aminodecarboxylation of Barton esters

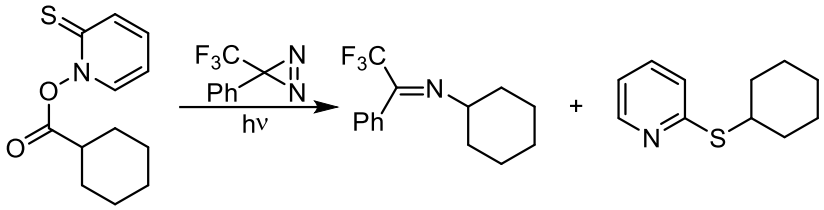

We imagined that an alkyl radical could be readily generated from the corresponding carboxylate instead of the Barton ester. Once formed, the radical could be trapped by an electrophilic amine source to provide the desired product and carbon dioxide gas. A survey of electrophilic nitrogen sources revealed that dialkyl azidocarboxylates had been used to trap similar alkyl radicals by several groups (Scheme 48).[13] The formation of a transient alkyl radical

Scheme 48. Radical trapping with azidocarboxylates

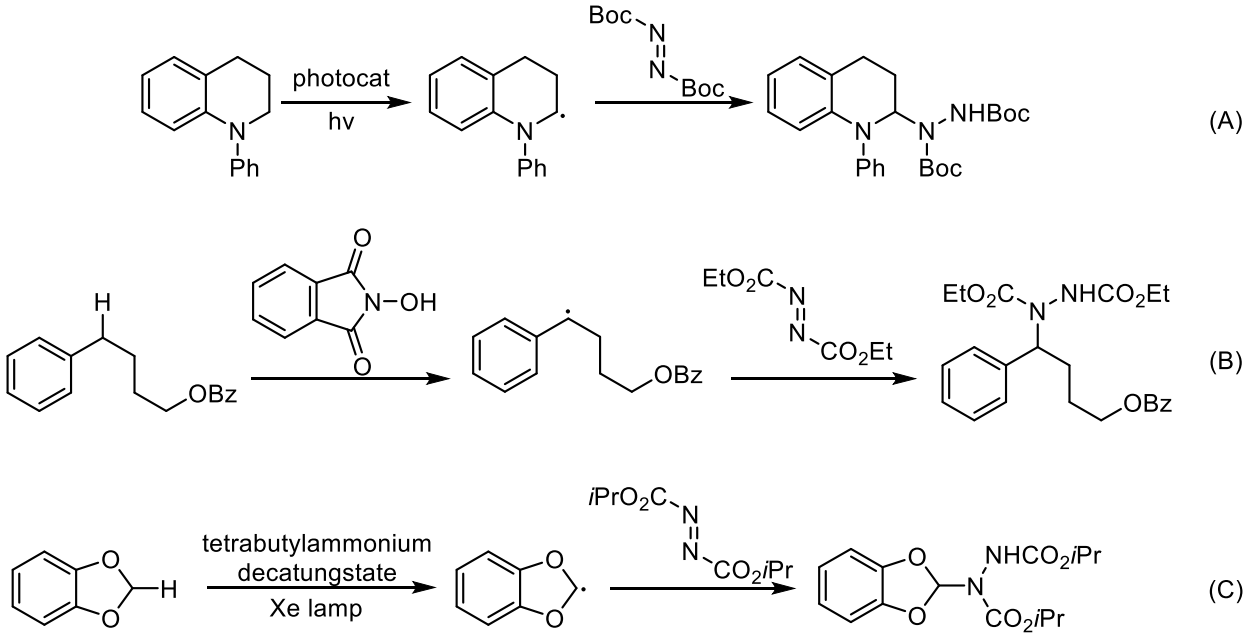

in the presence of a large excess on electrophilic nitrogen source may lead to smooth product formation without forming homodimerization adducts. With this hypothesis in hand, we started to screen reaction conditions of the aminodecarboxylation of unstabilized alkyl carboxylates.

3.4 Photocatalytic aminodecarboxylation

In order to make inroads towards our goal of using carboxylic acids as alkylating agents, we began evaluating the decarboxylation of aliphatic acids. Optimization studies began with 4-*tert*-butylcyclohexanecarboxylic acid, primarily because we wanted to be able to detect the hydrodecarboxylated product by GC/MS if it arose. Different combinations of photocatalyst, base, and azidocarboxylate were screened in an attempt to find conditions to promote aminodecarboxylation. As previously reported, the oxidizing ($E_{1/2}^{red}$ > = +2.06V vs SCE) family of Fukuzumi acridinium photocatalysts were much more competent than highly oxidizing Ru- and Ir-based systems (Scheme 49). The Mes-Acr-Ph photocatalyst was chosen (R_1=Ph, R_2=H) due to its commercial availability and reports that a methyl R_1 substituent is more prone to catalyst deactivation via dealkylation. To begin, 1.3 equiv. of the carboxylic acid, 1.6 equiv. of the base K_2HPO_4, 1 equiv. diisopropyl azodicarboxylate (DIAD) and .01 equiv. Mes-Acr-Phe were dissolved in Ar-sparged MeCN then irradiated with a blue LED. When the crude reaction mixture was analyzed by GC/MS, peaks corresponding to the DIAD starting material, the reduced hydrazine, and the desired product were observed in a 5:23:72 ratio (Scheme 50).

Scheme 49. Photocatalyst screening

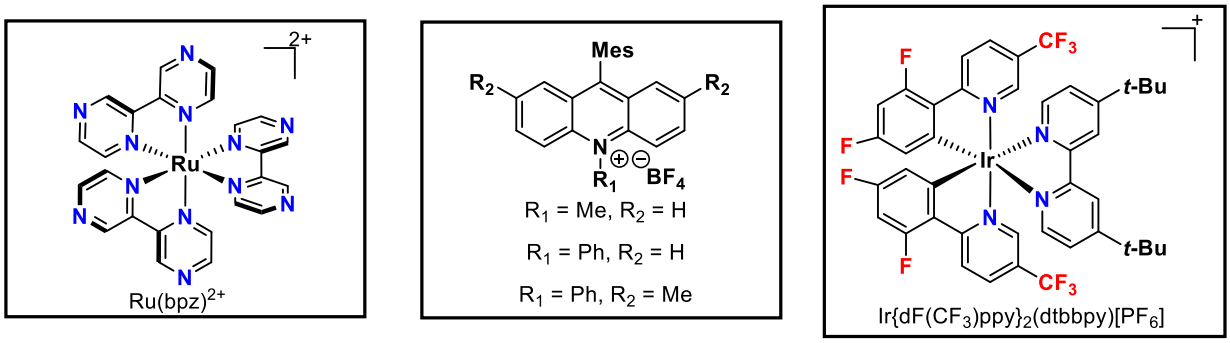

unsuccessful successful unsuccessful

Scheme 50. Reaction optimization

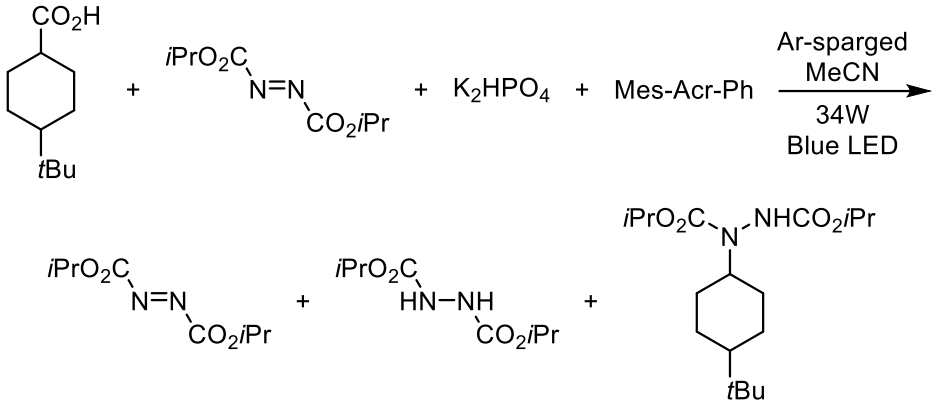

Less product formed when the base was changed to Na_2CO_3, NaOH, 2,6 lutidine, or Hunig's base. An improvement in the product distribution (~ 80% conversion to desired product occurred when 1,1,3,3-tetramethylguanidine was employed as the base. This observation led us to explore other strong, non-nucleophilic bases. 1,8-Diazabicyclo[5.4.0]undec-7-ene (DBU) proved optimal, and a solvent screen revealed that acetonitrile was the best solvent compared to other polar protic- and aprotic solvents. Routine optimization of the stoichiometry of each reagent led to the optimized reaction conditions depicted in Scheme 51. Substoichiometric amounts of DBU performed best. The lone pair on nitrogen is most likely readily protonated and not available for oxidation by the excited-state photocatalyst.

Scheme 51. Optimized reaction conditions

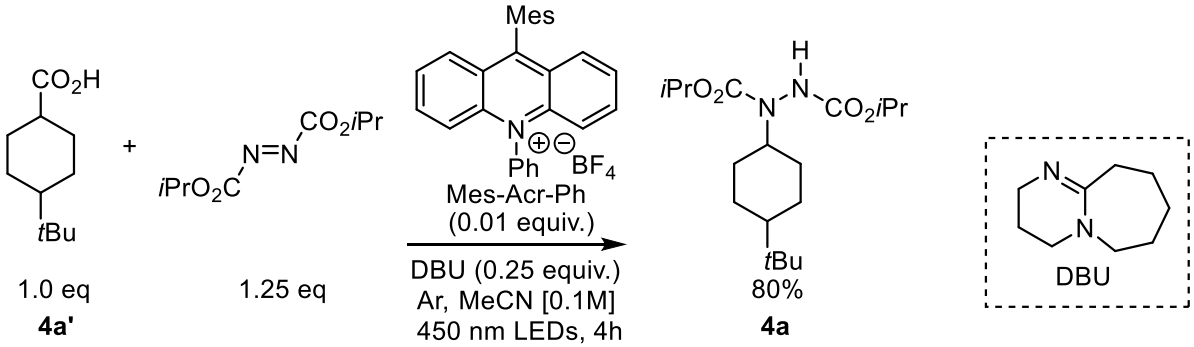

Replacing DIAD with di-*t*-butyl azidodicarboxylate or di(2,2,2-trichloroethyl) azidodicarboxylate decreased the rates of reactions, and did not reach full conversion, even after extended reaction times. Control experiments revealed that no product formed, via GC/MS analysis, when light or photocatalyst were omitted from the reaction mixture. The scope of the metal-free aminodecarboxylation was then explored (Scheme 52).

Scheme 52. Aminodecarboxylation substrate scope

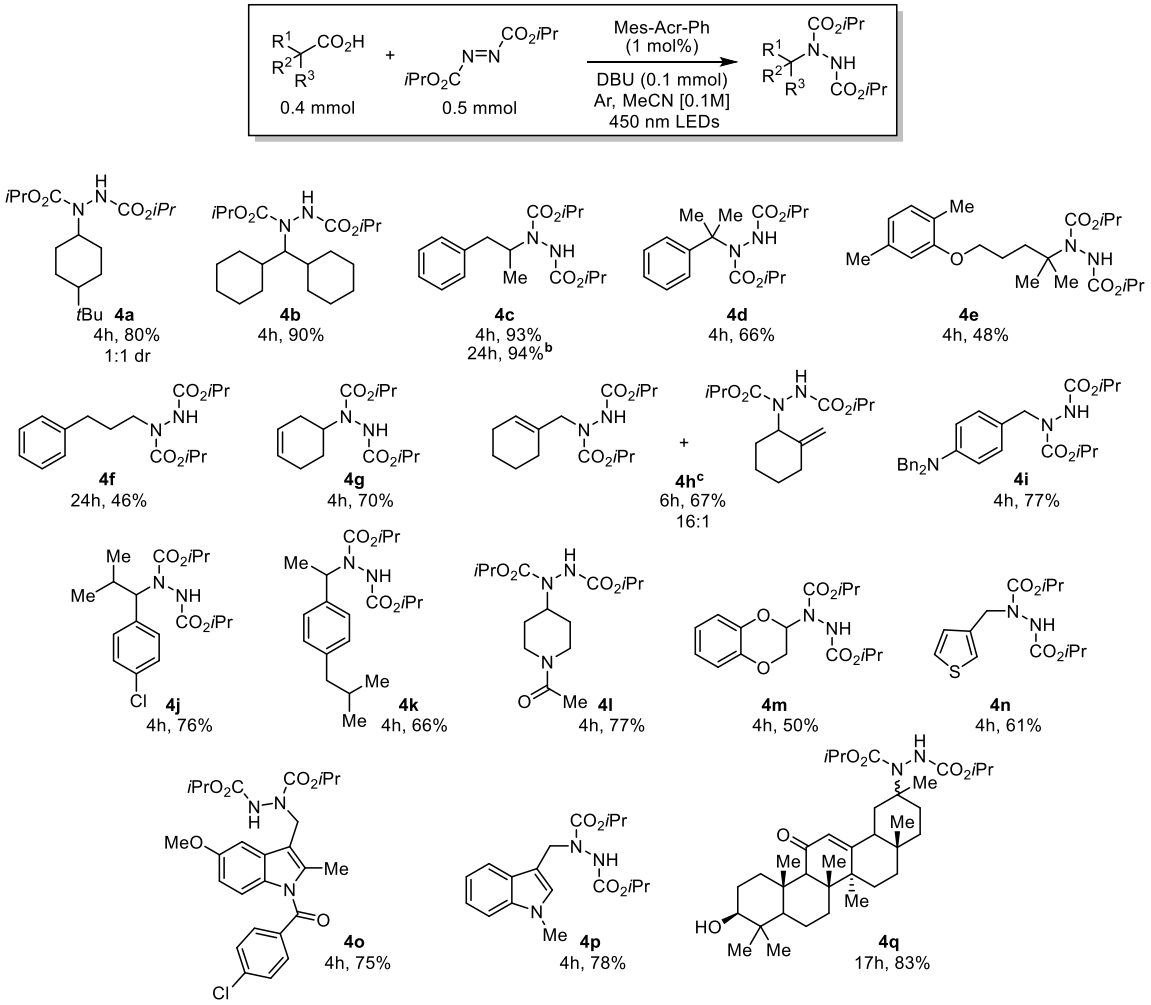

a) isolated yields b) 5 mmol scale, 2 blue LEDs [0.38M] c) from 1-cyclohexene-1-acetic acid

Secondary alkyl carboxylic acids including cyclic (**4a**) and acyclic (**4b,4c**) acids were aminated in good yields when subjected to the standard reaction conditions. The reaction could also be performed on a 5 mmol scale, but required 2 blue LEDs and 24 hour reaction times when

it was ran under more convenient concentrated conditions (**4c**). The desired aminodecarboxlyation also occurred at the sterically congested, benzylic center of substrate **4d** although a lower yield was observed. Similarly, the remote tertiary center of the phenolic ether-containing hypolipidemic agent Gemfibrozil was also aminated in a 48% yield after four hours (**4e**). A primary carboxylic acid also participated in the aminodecarboxylation reaction, although 24 hours of reaction time were required. This could be associated with the formation of the very unstable primary radical post decarboxylation (**4f**). A cyclic alkene that was not in conjugation with the acid was well-tolerated (**4g**). When 1-cyclohexene-1-acetic acid was employed, a 16:1 mixture of primary:secondary amine products was isolated which suggests that steric hindrance plays a large factor in product formation (**4h**). Various para-substituted phenylacetic acids also underwent aminodecarboxylation. Substrates bearing a tertiary amine and a chlorine in the para position were aminated in good yields (**4i**, **4j**). Ibuprofen was also a competent substrate (**4k**). Functional groups, such as an acylated amine (**4l**) and a catechol derivative (**4m**) were well-tolerated. A variety of heteroaromatics as thiophene (**4n**), indole (**4p**), and the anti-inflamatory agent Indomethacin (**4o**) were all aminated. Lastly, enoxolone, which contains a secondary alcohol and an α,β-unsaturated ketone on a rigid steroid-like scaffold, was isolated in high yield (**4q**).

One very important point to emphasize is the availability of the reagents and the operational simplicity of the reaction. All but one of the carboxylic acids employed are commercially available. Conversely, only four of the corresponding alkyl bromides were available to purchase and do not contain the diverse functionality found on the carboxylic acids we used. The DIAD, photocatalyst, and base were also commercially available. All reagents are handled in the air and added to a vial with MeCN, then simply sparged with inert gas for a period of time. Additional advantages to using carboxylic acids as traceless activating groups is that the only stoichiometric byproduct from the reaction is carbon dioxide, which is readily removed.

Next, several experiments were performed to verify that the reaction proceeded via radical intermediates. The corresponding ring-opened aminated product was obtained in a 35% yield when cyclopropaneacetic acid was subjected to the standard reaction conditions (Scheme 53).

Scheme 52. Ring-opening post radical decarboxylation

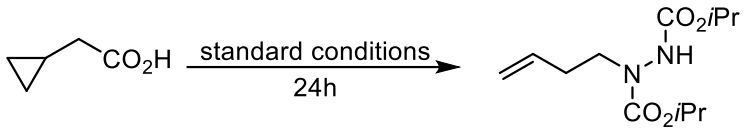

4r, 35%

The transient radical was also more readily intercepted by TEMPO than by DIAD. When two equivalents of TEMPO were added to the standard reaction conditions, an 86% yield of the TEMPO adduct 2s were obtained and only a trace amount of the aminated product was formed (Scheme 54).

Scheme 54. TEMPO interception of the alkyl radical

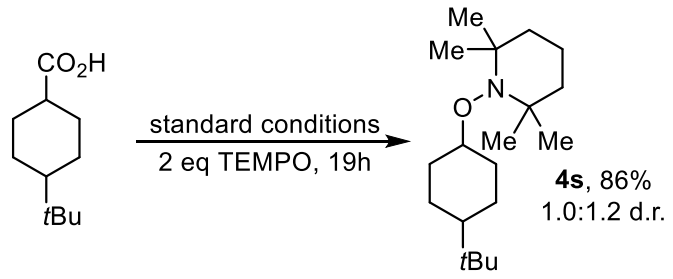

4s, 86%
1.0:1.2 d.r.

The hydrazine functional group is found in bioactive molecules[14] including drugs and insecticides.[15] They also are intermediates in the synthesis of azapeptides and heterocycles with commercial utility such as pyrazoles and triazoles.[16] Amines, however, are even more prevalent than hydrazines and thus we investigated the transformation of our products to their protected carbamate analogs. Pleasingly, the N–N bond could be readily cleaved using an E1cB reaction developed by the Magnus laboratory (Scheme 55).[17] Alkylation of the secondary nitrogen followed by treatment with base in refluxing MeCN produced the desired product in a 93% yield.

Scheme 55. Carbamate formation

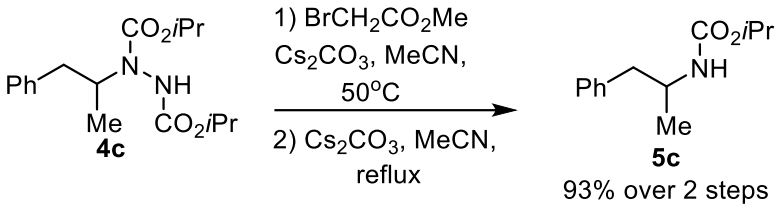

Lastly, we proposed an idealized mechanism based upon these observations and related literature examples. Photoexcitation of Mes-Acr-Ph by blue LEDs provides the highly oxidizing species Mes-Acr-Ph*, which removes an electron from the alkyl carboxylate, triggering radical decarboxylation. Once the radical forms it readily adds to DIAD to form the *N*-centered radical A. This radical can then be reduced by the photocatalyst to close the catalytic cycle. The resulting anion can then deprotonate either the protonated amine base or another carboxylic acid to provide the desired product and generate another carboxylate ready for oxidation by the Mes-Acr-Ph* photocatalyst (Scheme 56).

Scheme 56. An idealized mechanism

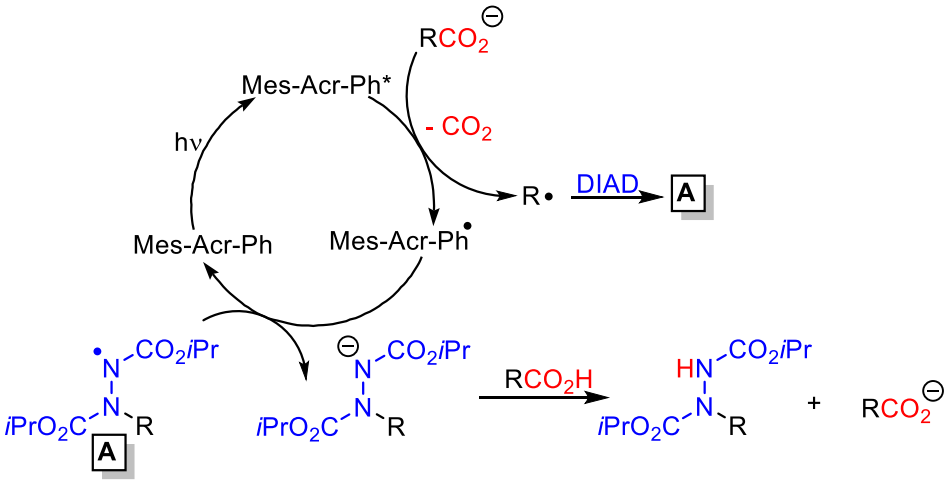

3.5 Conclusion

This chapter detailed the use of excited-state photocatalysts to facilitate the radical decarboxylation of carboxylic acids. Initial efforts by our laboratory to use carboxylic acids as

alkylating agents for site-specific C–N bond formation identified DIAD and the Mes-Acr-Ph photocatalyst as enabling reagents. The transformations of the alkyl radical, post decarboxylation, are currently limited to reactions with good radical acceptors or hydrogen atom transfer reagents. Although dual catalysis is beginning to emerge as a solution to this problem (see Chapter 2), the identification of new reaction manifolds that effectively harness the alkyl radicals generated via decarboxylation is extremely important.

3.6 References for Chapter 3

1) Su, Z.; Mariano, P. S.; Falvey, D. E.; Yoon, U. C.; Oh, S. W. "Dynamics of Anilinium Radical α-Heterolytic Fragmentation Processes. Electrofugal Group, Substituent, and Medium Effects on Desilyation, Decarboxylation, and Retro-Aldol Cleavage Pathways" *J. Am. Chem. Soc.* **1998**, *120*, 10676-10686.

2) Zuo, Z.; MacMillan, D. W. C. "Decarboxylative Arylation of α-Amino Acids via Photoredox Catalysis: A One-Step Conversion of Biomass to Drug Pharmacophore" *J. Am. Chem. Soc.* **2014**, *136*, 5257-5260.

3) Chu, L.; Ohta, C.; Zuo, Z.; MacMillan, D. W. C. "Carboxylic Acids as A Traceless Activation Group for Conjugate Additions: A Three-Step Synthesis of (rac)-Pregabalin" *J. Am. Chem. Soc.* **2014**, *136*, 10886-10889.

4) Noble, A.; MacMillan, D. W. C. "Photoredox α-Vinylation of α-Amino Acids and *N*-Aryl Amines" *J. Am. Chem. Soc.* **2014**, *136*, 11602-11605.

5) Ventre, S.; Petronijevic, F. R.; MacMillan, D. W. C. "Decarboxylative Fluorination of Aliphatic Carboxylic Acids via Photoredox Catalysis" *J. Am. Chem. Soc.* **2015**, *137*, 5654-5657.

6) Rueda-Becerril, M.; Mahé, O.; Drouin, M.; Majewski, M. B.; West, J. G.; Wolf, M. O.; Sammis, G. M.; Paquin, J-F. "Direct C−F Bond Formation Using Photoredox Catalysis" *J. Am. Chem. Soc.* **2014**, *136*, 2637-2641.

7) Yoshimi, Y.; Masuda, M.; Mizunashi, T.; Nishikawa, K.; Maeda, K.; Koshida, N.; Itou, T.; Morita, T.; Hatanaka, M. "Inter- and Intramolecular Addition Reactions of Electron-Deficient Alkenes with Alkyl Radicals, Generated by SET-Photochemical Decarboxylation of Carboxylic Acids, Serve as a Mild and Efficient Method for the Preparation of γ-Amino Acids and Macrocyclic Lactones" *Org. Lett.* **2009**, *11*, 4652-4655.

8) Vaillant, F. L.; Courant, T.; Waser, J. "Room-Temperature Decarboxylative Alkynylation of Carboxylic Acids Using Photoredox Catalysis and EBX Reagents" *Angew. Chem. Int. Ed.* **2015**, *54*, 11200-11204.

9) Cassani, C.; Bergonzini, G.; Wallentin, C.-J. “Photocatalytic Decarboxylative Reduction of Carboxylic Acids and Its Application in Asymmetric Synthesis” *Org. Lett.* **2014**, *16*, 4228-4231.

10) Griffin, J. D.; Zeller, M. A.; Nicewicz, D. A. “Hydrodecarboxylation of Carboxylic and Malonic Acid Derivatives via Organic Photoredox Catalysis: Substrate Scope and Mechanistic Insight” *J. Am. Chem. Soc.* **2015**, *137*, 11340-11348.

11) Wolff, H. “The Schmidt Reaction” *Org. React.* **1946**, 307-336 (b) Shioiri, T. *Comp. Org. Synth. 6*, 795-828; Pergamom, Oxford, 1991.

12) (a) Barton, D. H. R.; Jaszberenyi, J. C.; Throforakis, E.”Nitrogen transfer to carbon radicals” A. *J. Am. Chem. Soc.* **1992**, *114*, 5904-5905 (b) Girard, P.; Guillot, N.; Motherwell, W. B.; Potier, P. “Observation on the reaction of *O*-acylthiohydroximates with thionitrate esters: a novel free radical chain reaction for decarboxylative amination” *J. Chem. Soc. Chem. Commun.* **1995**, 2385-2386.

13) (a) Myake, Y.; Nakajima, K.; Nishibayashi. Y. “Direct sp^3 C-H Amination of Nitrogen – Containing Benzoheterocycles Mediated by Visible-Light-Photoredox Catalysts” *Chem. Eur. J. 18*, 16473-16477 (b) Amaoka, Y.; Kamijo, S.; Hoshikawa, T.; Inoue, M. “Radical Amination of C(sp^3)-H Bonds Using *N*-Hydroxyphthalimide and Dialkyl Azodicarboxylate” *J. Org. Chem.* **2012**, *77*, 9959-9969 (c) Ryu, I.; Tani, A.; Fukuyama, T.; Ravelli, D.; Montanaro, S.; Fagnoni, M. “Efficient C-H/C-N and C-H/C-CO-N Conversion via Decatungstate-Photoinduced Alkylation of Diisopropyl Azodicarboxylate” *Org. Lett.* **2013**, *15*, 2554-2557.

14) Blair, L. M.; Sperry, J. “Natural Products Containing a Nitrogen-Nitrogen Bond” *J. Nat. Prod.* **2013**, *76*, 794-812.

15) Narang, R.; Narasimhan, B.; Sharma, S. “A Review on Biological Activities and Chemical Synthesis of Hydrazine Derivatives” *Curr. Med. Chem.* **2012**, *19*, 569-612.

16) Ragnarsson, U. “Synthetic methodology for alkyl substituted hydrazines” *Chem. Soc. Rev.* **2001**, *30*, 205-213

17) Magnus, P.; Garizi, N.; Seibert, K. A.; Ornholt, A. “Synthesis of Carbamates from Diethoxycarbonyl Hydrazine Derivatives by E1cB Eliminative Cleavage of the N-N′-Bond Rather than Reduction” *Org. Lett.* **2009**, *11*, 5646-5648.

Chapter 3 Appendix

Experimental methods and spectral analysis for Ch. 3 compounds

Table of Contents

General Information:

TLC analysis was performed (fluorescence quenching or phosphomolybdic acid stain) with silica gel HL TLC plates with UV254 purchased from Sorbent Technologies.

Silica gel used for column chromatography (60 Å porosity, 230 x 400 mesh, standard grade) was purchased from Sorbent Technologies (catalog # 30930M-25).

Aluminum oxide for column chromatography (58 Å porosity, activated, neutral, Brockman I was purchased from Sigma Aldrich (CAS: 1344-28-1).

The photocatalyst, Mes-Acr-Ph, and the diisopropyl azidocarboxylate (DIAD) were purchased from Sigma Aldrich.

Anhydrous MeCN was purchased from Sigma Aldrich.

All carboxylic acid starting materials, except for 2-(4-(dibenzylamino)phenyl)acetic acid which was previously made in our lab,[1] are commercially available.

GC/MS data was obtained on a Shimadzu GCMS-QP2010 SE. ^{1}H and ^{13}C NMR spectra were obtained on a Bruker ADVANCE 500 DRX equipped with a QNP cryoprobe. These spectra were referenced to residual protio solvent signals. HRMS data was obtained on an ESI LC-TOF Micromass LCT (Waters).

Final aminodecarboxylation reactions were run in a screw threaded tube from Chemglass (CLS-4208). Kessil H150 Blue LED grow lights provided 450 nm light. A 4.0 mL solution of MeCN had an internal temperature of 33°C after 1 hour under standard reaction conditions.

GC/MS Method: Column oven temp: 110 ^{o}C. Injection temp: 290 ^{o}C. Injection mode: split. Carrier gas: He, 9.5 psi. Flow: 45.8 mL/min. Column flow: 0.88 mL/min. Linear velocity 35 cm/sec. Purge flow: 1.0 mL/min. Split rate: 50. The temperature is maintained at 110 ^{o}C for 2 mins after injection. Then, the temperature is raised 30 ^{o}C/min to 320 ^{o}C. This temperature is held for 8 mins.

For the reaction of *t-butyl cyclohexane carboxylic acid and DIAD:* *t*-Bu cyclohexane rt = 2.75 mins. DIAD rt = 4.25 mins. Hydrazine byproduct = 5.33 mins. Desired aminated product = 8.10 and 8.26 mins.

Photo of Experimental Setup:

General Experimental Procedures:

Aminodecarboxylation: A 16 x 125 mm threaded glass tube was charged with a stir bar, 0.4 mmol carboxylic acid starting material, and 0.002 g (1 mol%) of Mes-Acr-Ph photocatalyst. 4.0 mL of MeCN was added to the vial which was then capped and sparged with Ar for 5 minutes. After sparging, DBU (0.015 g, 0.1 mmol) and DIAD (0.101 g, 0.5 mmol) were added sequentially via syringe. The reaction was placed in front of 450 nm blue LEDs and analyzed by GC/MS. When the reaction was complete the solvent was removed *in vacuo* and the residue was purified by flash column chromatography on silica gel with 1% Et_3N in the eluent. If decomposition of the product was observed by GC/MS post chromatography, then neutral aluminum oxide was used as the stationary phase.

Product Manipulation[2]: A 10 mL oven dried Schlenk flask was cooled under an atmosphere of argon. A stir bar, Cs_2CO_3 (0.196g, 0.6 mmol) and 3 mL MeCN were added. Next, product **2c** (0.068g, 0.22 mmol) was added followed by methyl bromoacetate (0.069g, 0.4 mmol) and the reaction mixture was capped and heated at 50 ^oC overnight. Lastly, the reaction was quenched with 5 mL of aq NH_4Cl and extracted with EtOAc (3x10 mL). The combined organics were washed with brine, dried with $MgSO_4$, and concentrated *in vacuo*.

The crude material was dissolved in 1.0 mL MeCN and transferred to a 16 x 125 mm threaded glass tube that was charged with a stir bar and Cs_2CO_3 (0.130g, 0.4 mmol). The tube was capped and heated overnight (bath temperature 115 ^oC). The crude reaction was loaded directly onto a silica gel column and purified (1:15 to 1:10 EtOAc to hexanes) to provide 0.0455g (93%) of the desired carbamate **3c**.

Product Characterization:

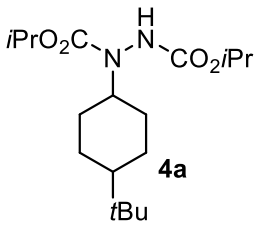

RW-1-112 0.108g, 80%, 1:10 to 1:5 EtOAc:Hexanes with 1% TEA as eluent.

A mixture of rotamers and diastereomers (1:1 d.r.).

^{1}H NMR (500 MHz, $CDCl_3$) δ 6.22 (m, 1H), 4.94 (m, 2H), 4.05 (m, 1H), 2.03 (m, 1H), 1.81 (m, 2H), 1.54 (m, 2H), 1.37 (m, 1H), 1.24 (m, 12 H), 1.01 (m, 3H), 0.83 (s, 9H).

^{13}C NMR (126 MHz, $CDCl_3$) δ 156.8, 156.0, 69.9, 69.7, 52.4, 46.9, 32.6, 30.1, 27.7, 26.3, 22.9, 22.2.

IR (film) 3298, 2943, 2867, 1731, 1467, 1373, 1307, 1226, 1180, 1110, 1033, 914, 763 cm^{-1}.

HRMS: Calc'd $C_{18}H_{34}N_2O_4Na$ $(M+Na)^+$ = 365.2416, found = 365.2410.

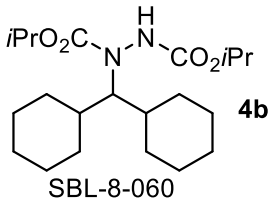

SBL-8-060 0.138g, 90%, 1:10 EtOAc:Hexanes with 1% TEA as eluent.

A mixture of rotamers.

^{1}H NMR (500 MHz, $CDCl_3$) δ 6.02 (m, 1H), 4.91 (m, 2H), 3.72 (m, 1H), 1.65 (m, 13H), 1.19 (m, 22H).

^{13}C NMR (126 MHz, $CDCl_3$) δ 157.3, 156.4, 70.2, 69.6, 66.4, 38.4, 36.6, 30.3, 29.9, 26.6, 22.8, 22.1.

IR (film) 3257, 2979, 2925, 2852, 1755, 1712, 1448, 1384, 1294, 1110, 1031, 912, 734 cm^{-1}.

HRMS: Calc'd $C_{21}H_{39}N_2O_4Na$ $(M+Na)^+$ = 383.2910, found = 383.2916.

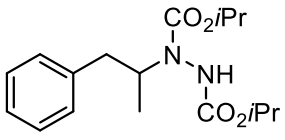

4c

SBL-8-071

A mixture of rotamers. 0.120g, 93%, 1:10 to 1:5 EtOAc:Hexanes with TEA was eluent.

^{1}H NMR (500 MHz, $CDCl_3$) δ 7.28 (m, 2H), 7.30 (m, 3H), 6.00 (m, 1H), 4.98 (p, *J* = 6.23 Hz, 1H), 4.86 (m, 1H), 4.61 (m, 1H), 2.83 (m, 2H), 1.21 (m, 15H).

^{13}C NMR (126 MHz, $CDCl_3$) δ 156.9, 155.5, 138.9, 129.1, 128.6, 126.5, 70.1, 69.8, 54.8, 40.7, 22.2, 22.1, 17.6.

IR (film) 3298, 2979, 2935, 1708, 1467, 1407, 1375, 1292, 1234, 1108, 1047, 746 cm^{-1}.

HRMS: Calc'd $C_{17}H_{26}N_2O_4Na$ $(M+Na)^+$ = 345.1790, found = 345.1777.

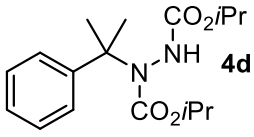

4d

RW-1-147

Purified on alumina instead of silica gel. A mixture of rotamers. 0.085g, 66%, 1:20 to 1:10 EtOAc:Hexanes with 1% TEA as eluent.

^{1}H NMR (500 MHz, $CDCl_3$) δ 7.47 (m, 2H), 7.30 (t, *J* = 7.73 Hz, 2H), 7.20 (t, *J* = 7.25 Hz, 1H), 6.50 (m, 1H), 5.03 (m, 1H), 4.71 (m, 1H), 1.72 (br s, 3H), 1.60 (s, 3H), 1.33 (m, 6H), 0.95 (m, 6H).

^{13}C NMR (126 MHz, $CDCl_3$) δ 157.3, 155.3, 148.6, 128.2, 126.3, 124.8, 70.3, 69.9, 64.1, 28.8, 27.9, 22.2, 21.7.

IR (film) 3299, 2981, 2937, 2358, 2331, 1712, 1521, 1496, 1467, 1384, 1321, 1261, 1180, 1108, 1029, 912, 763, 742, 700.

HRMS: Calc'd $C_{17}H_{26}N_2O_4Na$ $(M+Na)^+$ = 345.1790, found = 345.1797.

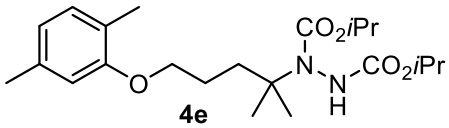

4e
RW-1-145

A mixture of rotamers. 0.078g, 48%, 1:9 EtOAc:Hexanes to 1:5 EtOAc:Hexanes with 1% TEA as eluent.

^{1}H NMR (500 MHz, $CDCl_3$) δ 7.01 (d, *J* = 7.42 Hz, 1H), 6.66 (d, *J* = 7.50 Hz, 1H), 6.63 (s, 1H), 6.30 (m, 1H), 4.94 (m, 2H), 3.94 (t, *J* = 6.27 Hz, 2H), 2.31 (s, 3H), 2.19 (s, 3H), 2.08 (m, 1H), 1.89 (m, 2H), 1.77 (m, 1H), 1.49 (m, 3H), 1.34 (m, 3H), 1.26 (m, 12H).

^{13}C NMR (126 MHz, $CDCl_3$) δ 157.1, 156.9, 155.1, 136.6, 130.4, 123.6, 120.7, 112.1, 70.0, 69.6, 68.2, 62.4, 36.9, 27.0, 26.5, 24.9, 22.3, 21.6, 16.0.

IR (film) 3315, 2979, 2935, 1712, 1614, 1585, 1510, 1467, 1373, 1315, 1265, 1130, 1112, 1047, 912, 802 cm^{-1}.

HRMS: Calc'd $C_{22}H_{36}N_2O_5Na$ $(M+Na)^+$ = 431.2522, found = 431.2506.

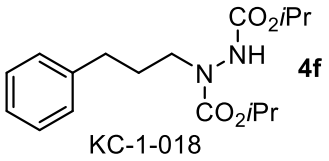

4f

KC-1-018

A mixture of rotamers. 0.059g, 46%, 1:20 EtOAc:Hexanes with 1% TEA as eluent.

^{1}H NMR (500 MHz, $CDCl_3$) δ 7.28 (m, 2H), 7.20 (d, *J* = 7.35 Hz, 3H), 6.30 (m, 1H), 4.96 (m, 2H), 3.55 (br s, 2H), 2.65 (t, *J* = 7.72 Hz, 2H), 1.92 (p, *J* = 7.33 Hz, 2H), 1.25 (m, 12H).

^{13}C NMR (126 MHz, $CDCl_3$) δ 156.3, 156.0, 141.8, 128.5, 126.1, 70.2, 69.9, 49.8, 33.1, 29.9, 22.3, 22.2.

IR (film) 3299, 2981, 2933, 1712, 1467, 1413, 1375, 1274, 1180, 1108, 1029, 912, 742 cm^{-1}.

HRMS: Calc'd $C_{17}H_{26}N_2O_4Na$ $(M+Na)^+$ = 345.1790, found = 345.1783.

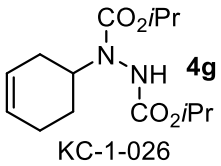

4g

KC-1-026

A mixture of rotamers. 0.080g, 70%, 1:10 to 1:5 EtOAc:Hexanes with 1% TEA as eluent.

^{1}H NMR (500 MHz, $CDCl_3$) δ 6.18 (m, 1H), 5.61 (br s, 2H), 4.95 (br s, 2H), 4.30 (br s 1H), 2.18 (m, 4H), 1.77 (m, 2H), 1.25 (m, 12H).

^{13}C NMR (126 MHz, $CDCl_3$) δ 157.0, 155.3, 126.5, 125.4, 70.1, 69.8, 53.4, 28.8, 26.5, 25.6, 22.3, 22.1.

IR (film) 3298, 2979, 2933, 1708, 1514, 1467, 1409, 1375, 1301, 1238, 1180, 1108, 1039, 914, 763 cm^{-1}.

HRMS: Calc'd $C_{14}H_{24}N_2O_4Na$ $(M+Na)^+$ = 307.1634, found = 307.1639.

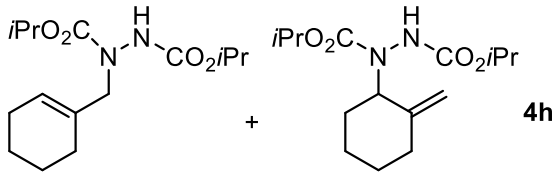

16:1, major resonances reported

KC-1-025

A mixture of rotamers. 0.080g, 67%, 1:10 to 1:5 EtOAc:Hexanes with 1% TEA as eluent.

^{1}H NMR (500 MHz, $CDCl_3$) δ 6.32 (m, 1H), 5.54 (s, 1H), 4.93 (m, 2H), 3.97 (s, 2H), 2.00 (br s, 2H), 1.92 (br s, 2H), 1.59 (m, 4H), 1.25 (m, 12H).

^{13}C NMR (126 MHz, $CDCl_3$) δ 156.3, 155.6, 133.0, 125.5, 70.2, 69.7, 56.3, 26.4, 25.2, 22.7, 22.4, 22.2, 22.1.

IR (film) 3301, 2979, 2931, 1708, 1411, 1373, 1263, 1217, 1178, 1108, 1035, 912, 742 cm^{-1}.

HRMS: Calc'd $C_{15}H_{26}N_2O_4Na$ $(M+Na)^+$ = 321.1790, found = 321.1796.

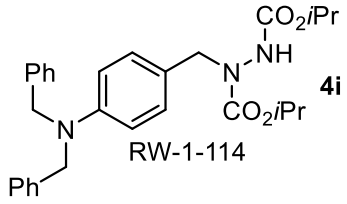

RW-1-114

A mixture of rotamers. 0.151g, 77%, 1:5 EtOAc:Hexanes with 1% TEA as eluent.

^{1}H NMR (500 MHz, $CDCl_3$) δ 7.33 (t, *J* = 7.44 Hz, 4H), 7.25 (m, 6H), 7.08 (d, *J* = 8.11 Hz, 2H), 6.68 (d, *J* = 8.27 Hz, 2H), 6.26 (m, 1H), 4.96 (m, 2H), 4.60 (m, 6H), 1.25 (m, 12H).

^{13}C NMR (126 MHz, $CDCl_3$) δ 156.0, 155.8, 148.8, 138.5, 128.8, 127.0, 126.7, 112.3, 70.1, 69.6, 54.4, 52.9, 22.2, 22.1.

IR (film) 3299, 2979, 2935, 2250, 1712, 1614, 1585, 1452, 1384, 1261, 1218, 1108, 1029, 956, 912, 804, 732 cm^{-1}.

HRMS: Calc'd $C_{29}H_{35}N_3O_4Na$ $(M+Na)^+$ = 512.2525, found = 512.2527.

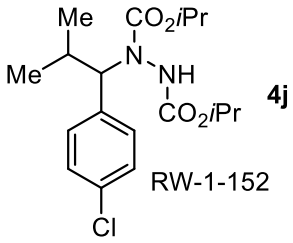

4j

Purified on alumina. A mixture of rotamers. 0.113g, 76%, 1:6 EtOAc:Hexanes with 1% TEA as eluent.

^{1}H NMR (500 MHz, $CDCl_3$) δ 7.28 (m, 4H), 5.83 (m, 1H), 4.73 (m, 3H), 2.33 (br s, 1H), 1.22 (m, 12H), 0.94 (m, 2H), 0.69 (m, 4H).

^{13}C NMR (126 MHz, $CDCl_3$) δ 156.6, 155.9, 136.9, 133.7, 130.5, 130.4, 128.7, 128.6, 70.3, 69.8, 66.9, 28.6, 22.2, 22.1, 21.0, 20.5, 20.2, 20.0.

IR (film) 3286, 2979, 1712, 1492, 1469, 1404, 1384, 1317, 1282, 1226, 1180, 1145, 1108, 1033, 966, 912, 746 cm^{-1}.

HRMS: Calc'd $C_{18}H_{27}ClN_2O_4Na$ $(M+Na)^+$ = 393.1557, found = 393.1561.

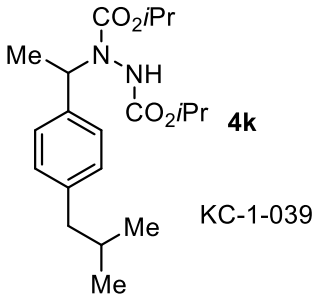

Purified on alumina. A mixture of rotamers. 0.097g, 66%, 1:5 EtOAc:Hexanes with 1% TEA as eluent.

^{1}H NMR (500 MHz, $CDCl_3$) δ 7.23 (m, 2H), 7.10 (d, *J* = 7.82 Hz, 2H), 5.86 (m, 1H), 5.48 (m, 1H), 4.96 (m, 2H), 2.45 (d, *J* = 7.16 Hz, 2H), 1.85 (dh, *J* = 13.5, 6.79 Hz, 1H), 1.54 (m, 3H), 1.25 (m, 12H), 0.90 (d, *J* = 6.62 Hz, 6H).

^{13}C NMR (126 MHz, $CDCl_3$) δ 156.5, 155.6, 141.2, 138.2, 129.3, 127.1, 70.2, 69.7, 55.1, 45.2, 30.4, 22.5, 22.3, 22.2, 22.1, 22.0, 16.7.

IR (film) 3294, 2979, 1714, 1514, 1469, 1384, 1303, 1230, 1108 cm^{-1}.

HRMS: Calc'd $C_{20}H_{32}N_2O_4Na$ $(M+Na)^+$ = 387.2260, found = 387.2252.

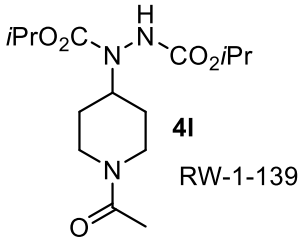

A mixture of rotamers. 0.098g. 74%, 1:70 EtOAc:Hexanes with 1% TEA as eluent.

^{1}H NMR (500 MHz, $CDCl_3$) δ 6.34 (m, 1H), 4.93 (m, 2H), 4.70 (m, 1H), 4.19 (m, 1H), 3.84 (m, 1H), 3.10 (t, *J* = 12.6 Hz, 1H), 2.55 (t, *J* = 13.1 Hz, 1H), 2.08 (s, 3H), 1.70 (m, 4H), 1.25 (m, 12H).

^{13}C NMR (126 MHz, $CDCl_3$) δ 169.0, 156.7, 155.1, 70.4, 70.0, 54.7, 45.7, 40.9, 30.0, 29.0, 22.2, 22.1, 21.6.

IR (film) 3284, 2935, 2869, 1731, 1631, 1454, 1411, 1373, 1303, 1249, 1108, 103, 912, 732 cm^{-1}.

HRMS: Calc'd $C_{15}H_{27}N_3O_5Na$ $(M+Na)^+$ = 352.1848, found = 352.1849.

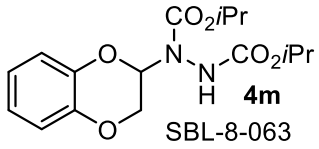

SBL-8-063

A mixture of rotamers. 0.067g, 50%, 1:9 to 1:5 EtOAc:Hexanes with 1% TEA as eluent.

^{1}H NMR (500 MHz, $CDCl_3$) δ 6.88 (m, 4H), 6.49 (m, 1H), 6.06 (m, 1H), 5.00 (m, 2H), 4.42 (m, 1H), 4.03 (t, *J* = 9.64 Hz, 1H), 1.28 (m, 12H).

^{13}C NMR (126 MHz, $CDCl_3$) δ 154.5, 142.9, 142.5, 122.1, 121.9, 117.4, 117.2, 79.2, 72.0, 70.4, 64.6, 22.1.

IR (film) 3307, 2981, 2937, 1731, 1595, 1494, 1409, 1377, 1303, 1267, 1244, 1182, 1108, 1076, 962, 912, 869, 748 cm^{-1}.

HRMS: Calc'd $C_{16}H_{22}N_2O_6Na$ $(M+Na)^+$ = 361.1376, found = 361.1383.

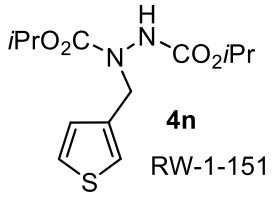

4n

RW-1-151

Purified on alumina. A mixture of rotamers. 0.073g, 61%, 1:5 to 1:1 EtOAc:Hexanes with 1% TEA as eluent.

^{1}H NMR (500 MHz, $CDCl_3$) δ 7.28 (dd, *J* = 4.96, 2.92 Hz, 1H), 7.18 (br s, 1H), 7.04 (br s, 1H), 6.29 (m, 1H), 4.95 (m, 2H), 4.67 (br s, 2H), 1.25 (m, 12H).

^{13}C NMR (126 MHz, $CDCl_3$) δ 155.9, 137.5, 128.1, 126.3, 123.7, 70.5, 69.9, 49.3, 48.4, 22.2, 22.1.

IR (film) 3298, 2979, 1712, 1502, 1407, 1384, 1269, 1238, 1207, 1180, 1107, 1039, 912, 742 cm^{-1}.

HRMS: Calc'd $C_{13}H_{20}N_2O_4SNa$ $(M+Na)^+$ = 323.1042, found = 323.1038.

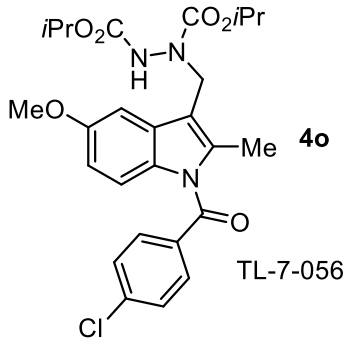

4o

TL-7-056

0.150g, 75%, 10% to 20% to 30% EtOAc in Hexanes with 1% TEA as eluent.

Purified on alumina. A mixture of rotamers.

^{1}H NMR (500 MHz, $CDCl_3$) δ 7.63 (d, *J* = 8.46 Hz, 2H), 7.46 (d, *J* = 8.33 H, 2H), 7.06 (br m, 1H), 6.84 (m, 1H), 6.66 (dd, *J* = 9.09, 2.51 Hz, 1H), 6.25 (br m, 1H), 4.95 (m, 4H), 3.81 (s, 3H), 2.38 (s, 3H), 1.23 (m, 12H).

^{13}C NMR (126 MHz, $CDCl_3$) δ 168.5, 156.2, 156.0, 155.8, 139.5, 137.7, 133.8, 131.3, 130.9, 130.6, 129.3, 115.0, 114.7, 114.4, 112.3, 111.8, 101.6, 101.4, 70.4, 69.9, 55.8, 43.1, 42.7, 42.3, 22.3, 22.1, 13.2.

IR (film) 3305, 2981, 2935, 2252, 1731, 1712, 1693, 1591, 1479, 1373, 1323, 1238, 1180, 1108, 1043, 912 cm^{-1}.

HRMS: Calc'd $C_{26}H_{30}ClN_3O_6Na$ $(M+Na)^+$ = 538.1721, found = 538.1725.

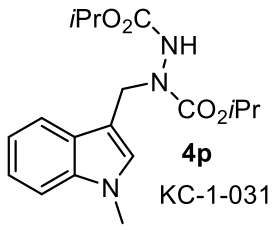

4p

KC-1-031

Purified on alumina instead of silica gel. A mixture of rotamers. 0.102g, 77%, 1:5 to 1:3 EtOAc:Hexanes with 1% TEA as eluent.

^{1}H NMR (500 MHz, $CDCl_3$) δ 7.69 (br s, 1H), 7.32 (d, *J* = 8.21 Hz, 1H), 7.26 (m, 1H), 7.14 (m, 1H), 7.05 (br s, 1H), 6.23 (m, 1H), 4.94 (m, 4H), 3.78 (s, 3H), 1.26 (m, 12H).

^{13}C NMR (126 MHz, $CDCl_3$) δ 156.0, 155.7, 137.2, 129.3, 127.6, 122.1, 119.6, 109.7, 109.4, 70.1, 69.7, 44.5, 32.9, 22.3, 22.1.

IR (film) 3299, 2981, 2935, 1731, 1714, 1693, 1469, 1328, 1269, 1220, 1108, 912, 742 cm^{-1}.

HRMS: Calc'd $C_{18}H_{25}O_4N_3Na$ $(M+Na)^+$ = 370.1743, found = 370.1730.

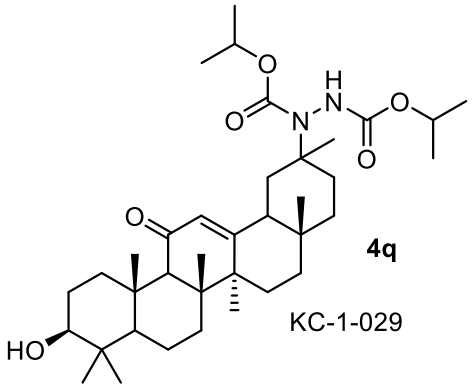

A mixture of rotamers and diastereomers. 0.2238g, 87%, 1:2 to 1:1 EtOAc:Hexanes with 1% TEA as eluent.

^{1}H NMR (500 MHz, $CDCl_3$) δ 6.37 (m, 1H), 5.57 (m, 1H), 4.90 (m, 2H), 3.20 (d, *J* = 6.46 Hz, 1H), 2.75 (d, *J* = 12.8 z, 1H), 2.32 (m, 2H), 2.11 (m, 3H), 1.67 (m, 7H), 1.37 (m, 9H), 1.23 (m, 14H), 1.11 (s, 6H), 0.98 (m, 5H), 0.84 (s, 3H), 0.78 (s, 3H), 0.67 (d, *J* = 11.6 Hz, 1H).

^{13}C NMR (126 MHz, $CDCl_3$) δ 200.45, 200.34, 200.31, 200.25, 200.21, 169.53, 169.43, 169.24, 169.04, 168.77, 168.66, 157.18, 157.05, 157.03, 156.94, 155.64, 155.03, 154.70, 154.58, 128.61, 128.57, 128.53, 128.41, 78.83, 70.07, 69.99, 69.92, 69.82, 69.76, 69.69, 69.63, 69.46, 69.37, 63.14, 63.03, 62.30, 61.93, 61.90, 61.86, 55.02, 55.00, 48.56, 48.46, 48.37, 47.56, 46.41, 45.53, 45.46, 45.43, 43.45, 43.41, 43.35, 42.85, 42.08, 40.27, 40.02, 39.92, 39.25, 39.23, 37.41, 37.25, 37.19, 37.16, 37.13, 36.66, 36.03, 32.95, 32.91, 32.84, 32.55, 32.32, 32.29, 31.83, 31.80, 31.33, 30.35, 30.11, 29.83, 28.72, 28.53, 28.36, 28.24, 27.40, 26.80, 26.74, 26.62, 26.59, 26.54, 26.48, 26.45, 26.18, 23.53, 23.35, 23.29, 23.18, 22.34, 22.31, 22.29, 22.23, 22.19, 22.12, 22.11, 22.09, 22.06, 20.82, 20.75, 20.63, 20.51, 18.85, 18.83, 18.80, 18.79, 17.61, 16.50, 16.49, 16.47, 15.75.

IR (film) 3498, 3303, 2979, 2993, 2252, 1730, 1697, 1650, 1508, 1467, 1454, 1384, 1373, 1319, 1261, 1180, 1110, 1037, 995, 912, 732, 646.

HRMS: Calc'd $C_{37}H_{60}N_2O_6Na$ $(M+Na)^+$ = 651.4349, found = 651.4343.

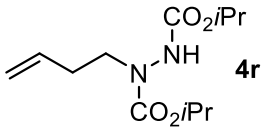

4r

KC-1-016

A mixture of rotamers. 0.037g, 35%, 1:10 EtOAc:Hexanes with 1% TEA as eluent.

^{1}H NMR (500 MHz, $CDCl_3$) δ 6.32 (m, 1H), 5.79 (dq, *J* = 16.9, 7.80 Hz, 1H), 5.07 (m, 2H), 4.96 (m, 2H), 3.59 (br s, 2H), 2.35 (q, *J* = 7.08 Hz, 2H), 1.27 (d, *J* = 6.34 Hz, 12H).

^{13}C NMR (126 MHz, $CDCl_3$) δ 156.5, 135.5, 117.0, 70.2, 69.9, 49.1, 32.0, 22.3, 22.2.

IR (film) 3301, 2981, 2935, 1714, 1415, 1386, 1265, 1211, 1108, 742 cm^{-1}.

HRMS: Calc'd $C_{12}H_{22}N_2O_4Na$ $(M+Na)^+$ = 281.1477, found = 281.1472.

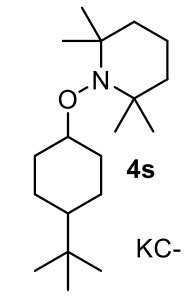

4s

KC-1-035

1.0:1.2 d.r.

0.102g, 86%, 1:25 EtOAc:Hexanes with 1% TEA as eluent.

^{1}H NMR (500 MHz, $CDCl_3$) δ 3.85 (p, *J* = 2.99 Hz, 0.45 H), 3.53 (tt, *J* = 11.2, 4.11 Hz, 0.55 H), 2.17 (m, 2H), 1.78 (m, 1H), 1.49 (m, 6H), 1.32 (m, 3H), 1.13 (m, 13H), 0.98 (m, 2H), 0.87 (s, 4H), 0.83 (s, 5H).

^{13}C NMR (126 MHz, $CDCl_3$) δ 82.6, 77.7, 59.9, 59.8, 48.0, 47.7, 40.5, 40.4, 34.7, 34.4, 33.2, 32.7, 32.4, 31.4, 27.9, 27.8, 26.4, 22.2, 20.5, 17.5, 17.3.

IR (film) 2939, 1458, 1365, 1242, 1132, 1049, 958, 914.

HRMS: Calc'd $C_{19}H_{38}NO$ $(M+H)^+$ = 296.2953, found = 296.2961.

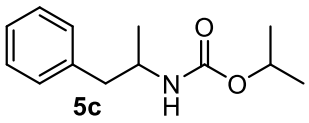

5c
SBL-8-098

0.046g, 93%, 1:15 to 1:10 EtOAc:Hexanes.

^{1}H NMR (500 MHz, $CDCl_3$) δ 7.30 (m, 2H), 7.23 (m, 1H), 7.19 (m, 2H), 4.90 (hept, *J* = 6.28 Hz, 1H), 4.48 (br s, 1H), 3.97 (br s, 1H), 2.86 (dd, *J* = 14.0, 5.25 Hz, 1H), 2.68 (dd, *J* = 13.4, 7.31 Hz, 1H), 1.22 (d, *J* = 6.28 Hz, 6H), 1.11 (d, *J* = 6.63 Hz, 3H).

^{13}C NMR (126 MHz, $CDCl_3$) δ 155.7, 138.2, 129.6, 128.5, 126.5, 67.9, 47.9, 43.1, 22.4, 20.3.

IR (film) 3328, 2977, 2931, 1693, 1531, 1454, 1373, 1251, 1180, 1114, 1045, 700 cm^{-1}.

HRMS: Calc'd $C_{13}H_{19}NO_2Na$ $(M+Na)^+$ = 244.1313, found = 244.1312.

References:

[1] Lang, S. B.; O'Nele, K. M.; Tunge, J. A. "Decarboxylative allylation of amino alkanoic acids and esters via dual catalysis" *J. Am. Chem. Soc.* **2014**, 13606.

[2] Chen, X.; Liu, X.; Mohr, J. T. "Direct Regioselective γ-Amination of Enones" *Org. Lett.* **2016**, *18*, 716-719.

Chapter 4. Activation of alcohols with carbon dioxide: intermolecular allylation of nitroalkanes, nitriles, and aldehydes[1]

4.1 Introduction to palladium-catalyzed alkylation

The three carbon allyl unit (C=C–C) is an immutable building block in synthetic organic chemistry. The double bond of this species can undergo a multitude of reactions that facilitate the construction of various organic and organometallic molecules. Additionally, the olefin is often inert to a variety of reaction conditions, and thus, can be chemoselectively transformed at a desired stage of a multi-step synthesis.[2] The allyl moiety can be appended to a molecule as a nucleophile[3,4] (allylic anion) or as an electrophile[5,6] (allylic cation). Electrophilic allylation can be accomplished from allylic halides, however these reactions are racemic, feature toxic reagents, and may suffer from regioselectivity issues. Conversely, transition metal-catalyzed allylic alkylation reactions have emerged as an environmentally friendly alternative, especially when asymmetric induction is desired. Specifically, the Pd-catalyzed alkylation of nucleophiles with electrophilic π-allylpalladium complexes (the Tsuji–Trost reaction) has been widely employed.[7]

In 1965 Tsuji demonstrated that subjecting π-allyl palladium chloride to malonate anions and enamines furnished the allylated nucleophiles and metallic palladium (Scheme 57).[8] Five years later, the catalytic variant employing $Pd(acac)_2$ and PPh_3 was reported (Scheme 58).[9]

Scheme 57. Allylation of malonates by Tsuji in 1965

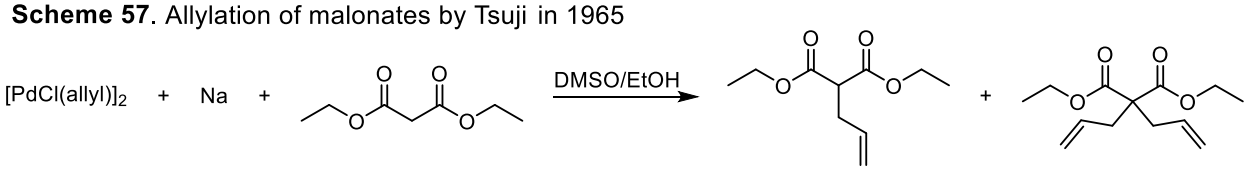

Scheme 58. Catalytic allylation of amines

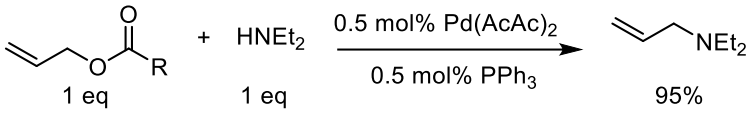

In 1973 Trost postulated that a cationic bis-ligated π-allylpalladium complex (4.1) formed *in situ* which was alkylated with soft nucleophiles regio- and stereoselectively. Hard anionic nucleophiles such as methyllithium and methylmagnesium iodide were not compatible with the reaction conditions.[10] Later in the year, Trost also demonstrated that the addition of a chiral phosphine ligand and sodium malonate to a pre-formed palladium-π-allyl complex could generate enantioenriched product (Scheme 59).[11]

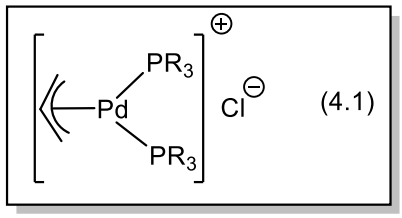

Scheme 59. Enantioselective allylation

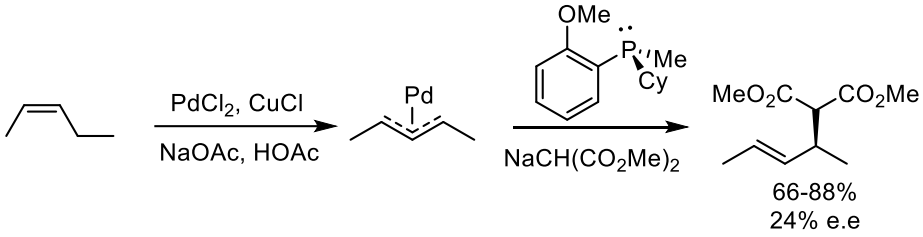

Several years later, the Trost lab disclosed a catalytic variant of the reaction utilizing $Pd(PPh_3)_4$ and the (+)-DIOP ligand. The alkylated product was obtained in an 84% yield and 46% e.e. Desulfonylation with 6% sodium amalgam gave the corresponding disubstituted alkane (Scheme 60).[12]

Scheme 60. Catalytic enantioselective allylation

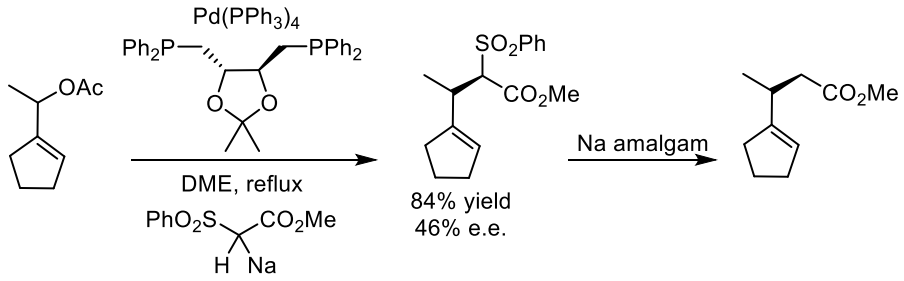

Enantioselective variants of the Tsuji–Trost reaction have since been vigorously developed and are the subject of numerous reviews.[13] The generic mechanism associated with the Tsuji–Trost reaction is presented in Scheme 61.

Scheme 61. Mechanism associated with the Tsuji-Trost reaction

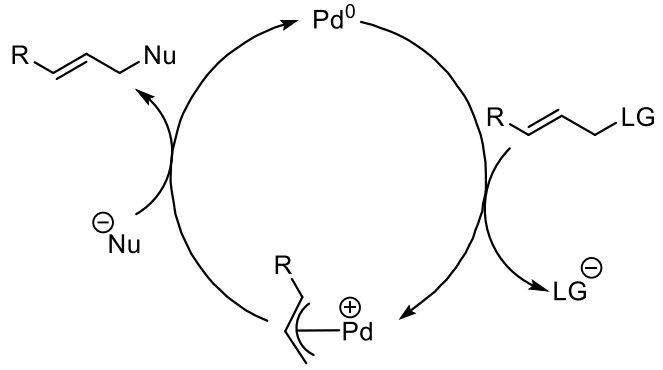

One important feature of this reaction is the interaction between the palladium-π-allyl complex and hard/soft nucleophiles.[14] Oxidative addition to palladium occurs with inversion. When hard nucleophiles are employed, binding of the nucleophile to the palladium complex occurs, followed by reductive elimination to give inversion of configuration. Soft nucleophiles displace the palladium via substitution, which leads to an overall retention of configuration (Scheme 62).[14]

Scheme 62. Interaction with hard/soft nucleophiles

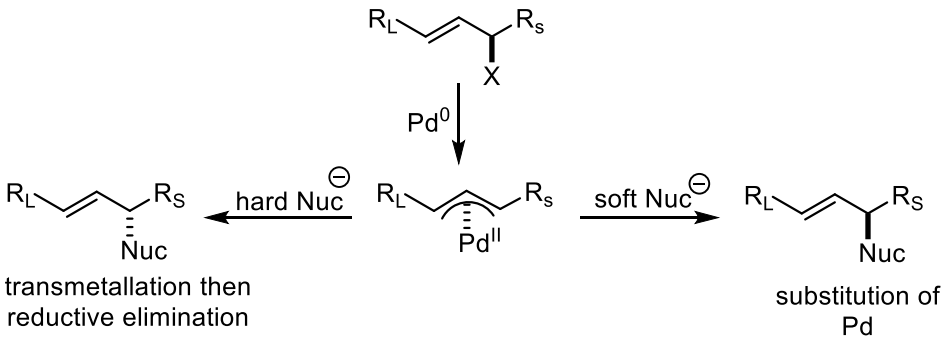

4.2 Allylic alcohols in the Tsuji–Trost reaction

The allylic leaving group has also been extensively studied, and a general reactivity scale established. Typically, halogens are the best leaving groups, followed by carbonates, acetates, and finally alcohols.[15] The inclusion of allylic alcohols directly into Tsuji–Trost type coupling manifolds would be beneficial, because they are readily available, are not as toxic as their halogenated counterparts and are often trivial to synthesize. Furthermore, the formation of a new C–C bond via the condensation of an alcohol with a C–H bond is topologically obvious. Additionally the generation of water as the only byproduct renders this reaction step and atom economic (Scheme 63).[16]

The oxidative addition of allylic alcohols to palladium is difficult, because the C–O bond is strong and hydroxide is a poor leaving group.[17] As a result, a variety of strategies have been developed to activate alcohols towards cross-coupling reactions. For examples, Lewis acids have been extensively employed (Scheme 64).[18] One drawback is that these activators are used in stoichiometric amounts, and thus generate large amounts of waste from which the product must be separated.

Brønsted acids and bases have also been utilized the activate alcohols or stabilize π-allylpalladium intermediates (Scheme 65).[19] Although some of the acids employed are readily available, the scope of the pro-nucleophiles is limited to weakly basic nucleophiles, and the additives have to be either recycled or removed from the resulting products. Others are not commercially available, and require rather specific reaction conditions.[19] We endeavored to find a general way to activate allylic alcohols towards the allylation of a variety of weakly acidic pro-nucleophiles using benign reagents.

Scheme 63. Topologically obvious assembly

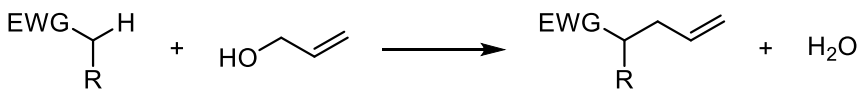

Scheme 64. Activation of allylic alcohols with Lewis acids

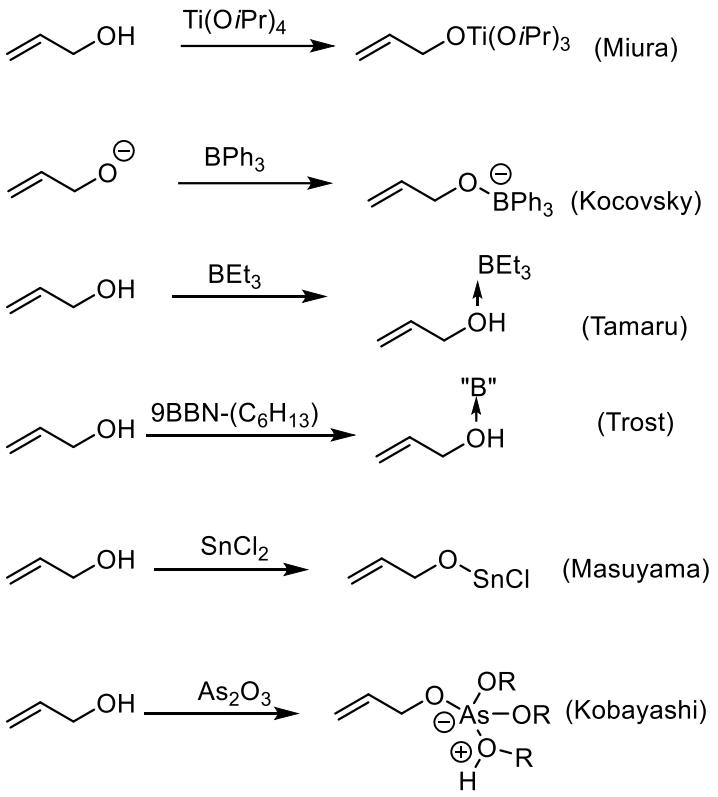

Additionally, we hoped to avoid the need for exogenous base to generate the nucleophile. Given that alcohols react reversibly with carbon dioxide,[20] we explored the generation of carbonates *in situ*.

An initial review of the literature revealed that CO_2 did indeed activate allylic alcohols towards oxidative addition to palladium.[21] The report, however, was limited to stabilized malonate-like nucleophiles and often employed high pressures of CO_2 (Scheme 66).[21] We endeavored to expand this reaction to include a wider range of pro-nucleophiles.

Scheme 65. Activation of allylic alcohols with Brønsted acids and bases

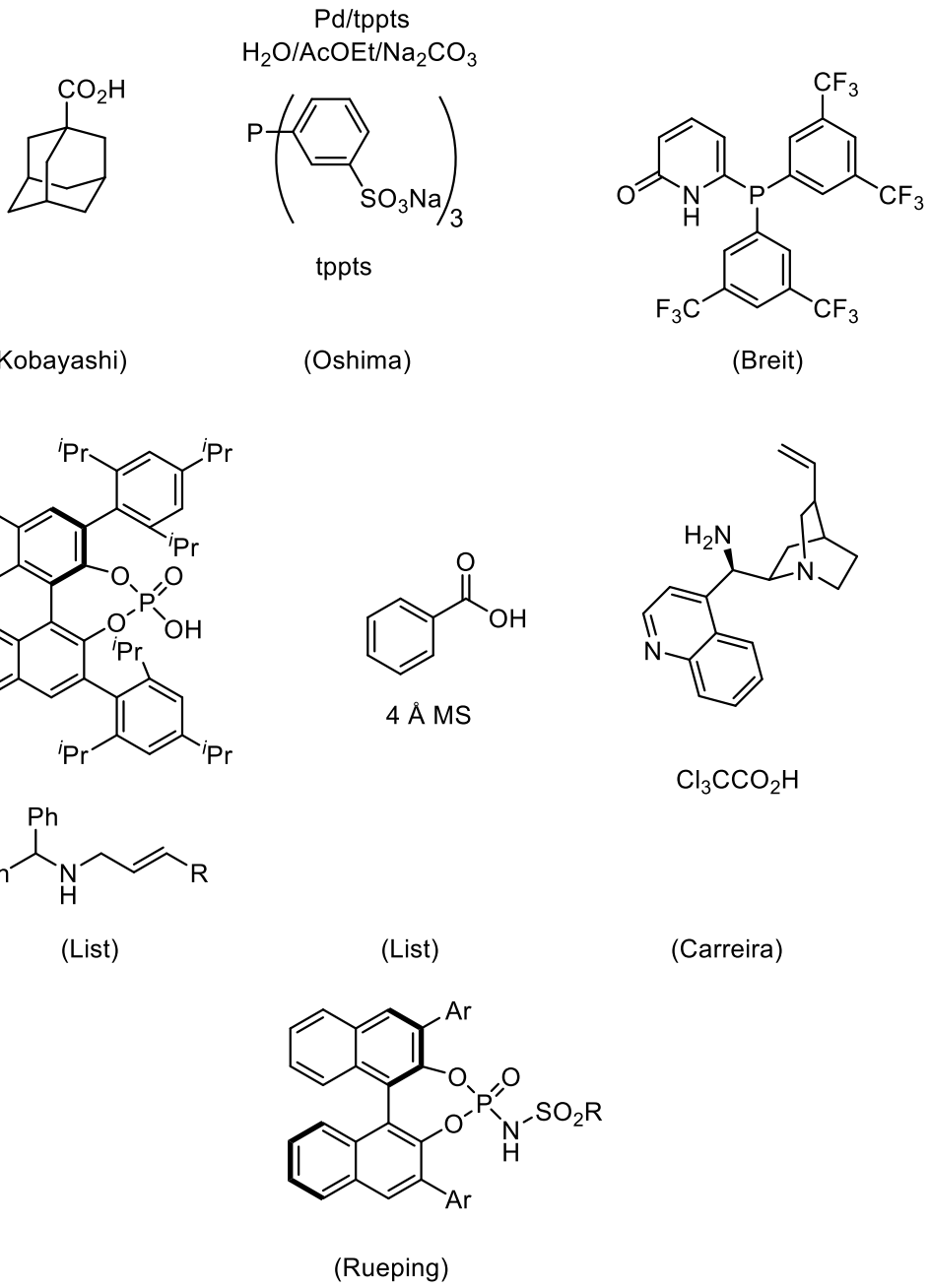

Scheme 66. Pd-catalyzed allylation of active methylenes with allyl alcohol and CO_2

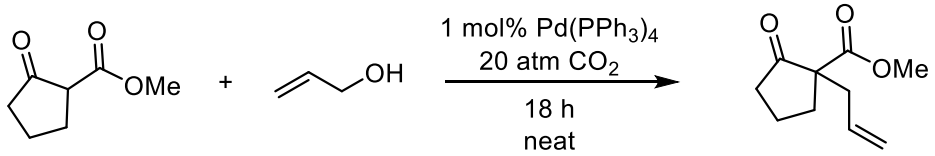

66%

4.3 Activation of Alcohols with Carbon Dioxide

Based on the previous report we imagined the formation of an allylic carbonate *in situ* that would be activated towards oxidative addition. The bicarbonate that forms after addition of palladium could then decarboxylate to form the strong base hydroxide (whose conjugate acid, water, has a pK_a ~30 in DMSO). The desired product forms upon deprotonation of a pronucleophile would then form water and attack on the electrophilic Pd-π-allyl complex (Scheme 67).

Scheme 67. Proposed activation of allylic alcohols with CO_2

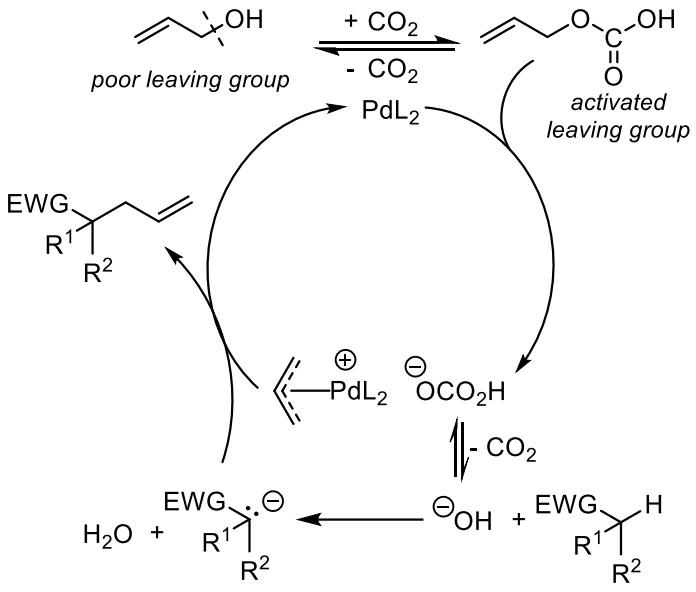

We began our studies using relatively acidic nitroalkanes (pK_a ~ 17 in DMSO).[22] When a sealed vial containing the polar aprotic solvent DMSO, $Pd(PPh_3)_4$, allyl alcohol, and an atmosphere of carbon dioxide was heated at 80 ^oC overnight, the desired allylated product was obtained in a 94% yield. Replacement of the carbon dioxide atmosphere with argon led to no appreciable amount of product formation when the crude reaction mixture was analyzed by ^1H NMR spectroscopy (Scheme 68).

Scheme 68. CO_2-promoted allylation of nitroalkanes with allyl alcohol

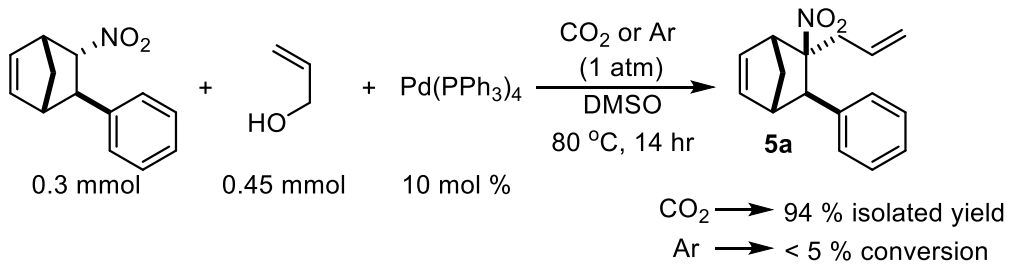

The substrate scope of the allylation reaction was examined with various nitroalkanes derived from Diels–Alder, Henry, and Baylis—Hillman reactions. Cyclic (**5a**, **5c**, **5h**), and acyclic (**5b**, **5d**-**5g**, **5i**, **5k**, **5l**) nitroalkanes were readily allylated under the standard conditions (Scheme 69). Various functional groups including olefins (**5a**, **5c**, **5h**), ethers (**5e**, **5f**), an α,β-unsaturated ester (**5l**) and indole (**5d**) did not interfere with the desired allylation. The desired product was also isolated in high yields when β-methallyl alcohol replaced simple allyl alcohol. Almost identical yields were obtained when the reaction was run for 20 minutes in a microwave reactor at 160 °C, although an additional equivalent of allyl alcohol was required (**5k**).

Good to excellent diastereoselectivities were observed when cyclic nitroalkanes were employed (**5a**, **5c**, **5h**, **5j**). The relative stereochemistry of the major diastereomer was determined by x-ray crystallography of the corresponding amine salt (see appendix). This stereochemistry can be rationalized by considering the most favorable conformation for the nitronate attack on the palladium allyl complex (Scheme 70).

Similar conditions also effectively allylated aldehydes, which are prone to aldol dimerization under standard alkylation conditions. Both acyclic (**6a**-**6g**) and cyclic (**6h**, **6i**) α-aryl aldehydes were allylated rapidly (1-2 h) with 5 mol% of $Pd(PPh_3)_4$ under an atmosphere of CO_2. High yields were obtained when electron-donating (*p*-Me, *p*-OMe) groups and electron-withdrawing (*o*-F, *p*-OCF_3) groups were present on the aryl rings. Aldehydes derived from *N*-methyl carbazole and α-tetralone were also well tolerated. α-Aryl substituents were not explicitly

Scheme 69. CO_2-promoted allylation of nitroalkanes: scope

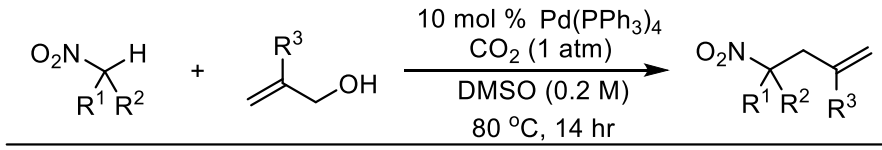

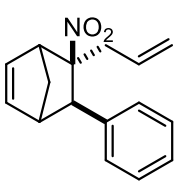

5a
94 %[a] (<5 %)[c]
95 : 5 dr

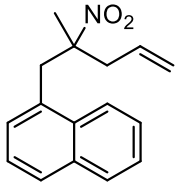

5b
83%[a] (7 %)[c]

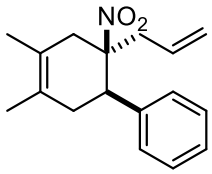

5c
88 %[a]
>95 : 5 dr

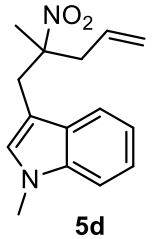

5d
86 %[a]

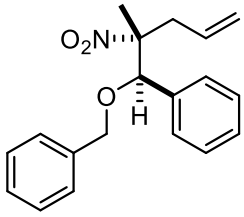

5e
93 %[a]
88 : 12 dr

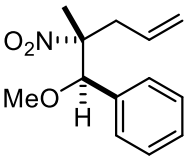

5f
96 %[a]
88 : 12 dr

5g
92 %[a]

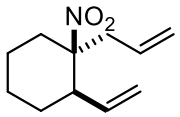

5h
90 %[a]
85 : 15 dr

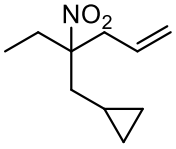

5i
71 %[a]

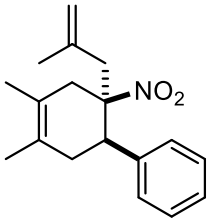

5j
97 %[a]
90 : 10 dr

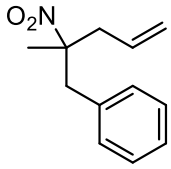

5k
89 %[a]
85 %[d] (7 %)[d,c]

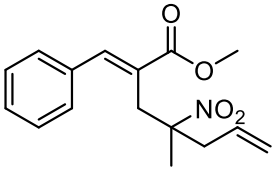

5l
91 %[a]

a) Nitroalkane (0.3 mmol) and allyl alcohol (0.45 mmol) in 1.75 mL DMSO under 1 atm CO_2.
b) Isolated yields. c) Ar replaced CO_2 (% conversion via crude 1H NMR). d) Allyl alcohol (0.9 mmol), 160 °C, 20 min. in a microwave reactor.

Scheme 70. Rational for relative stereochemistry of major diastereomer

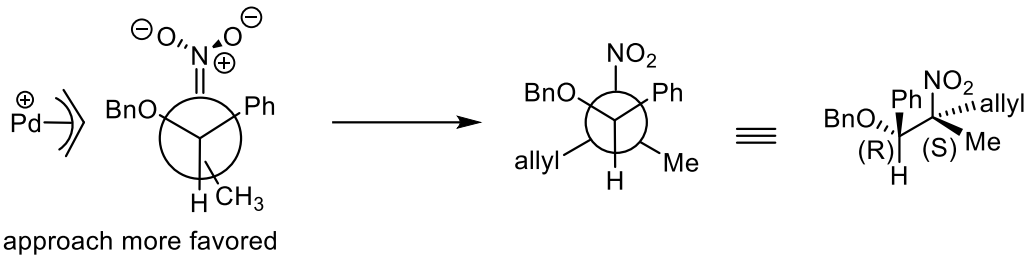

required, as evidenced by the *N*-Boc phenylalanine derivative **6j**, and aldehydes **6k** and **6l**, which contain benzyl substituents. Control experiments revealed that a CO_2 atmosphere was required for synthetically useful yields.The reaction of tertiary nitriles (pK_a ~23-25 in DMSO)[23] was also examined by Theresa Locascio in order to determine the strength of the base generated *in situ*. A variety of tertiary benzyl cyanides with α- methyl, ethyl, and benzyl substituents were successfully allylated with 2.5 mol% $Pd(PPh_3)_4$ under more concentrated conditions and at a slightly higher temperature (Scheme 72). Aryl rings with electron-donating (**7a**, **7d**) and electron-withdrawing (**7b**, **7c**) substituents were allylated in high yields. An *N*-protected indole (**7h**) was tolerated as well as a diaryl (**7f**) ketone. When the steric bulk was increased about the pro-nucleophile, limited conversion was observed (**7g**). When the substrate contained a-diaryl substituents, which are more acidic than the corresponding monoaryl species (**7i**), slightly lower temperature could be employed. Lastly, When an Ar atmosphere replaced CO_2, dramatically lower conversions of starting material were observed.

Scheme 71. Allylation of aldehydes: scope[a,b]

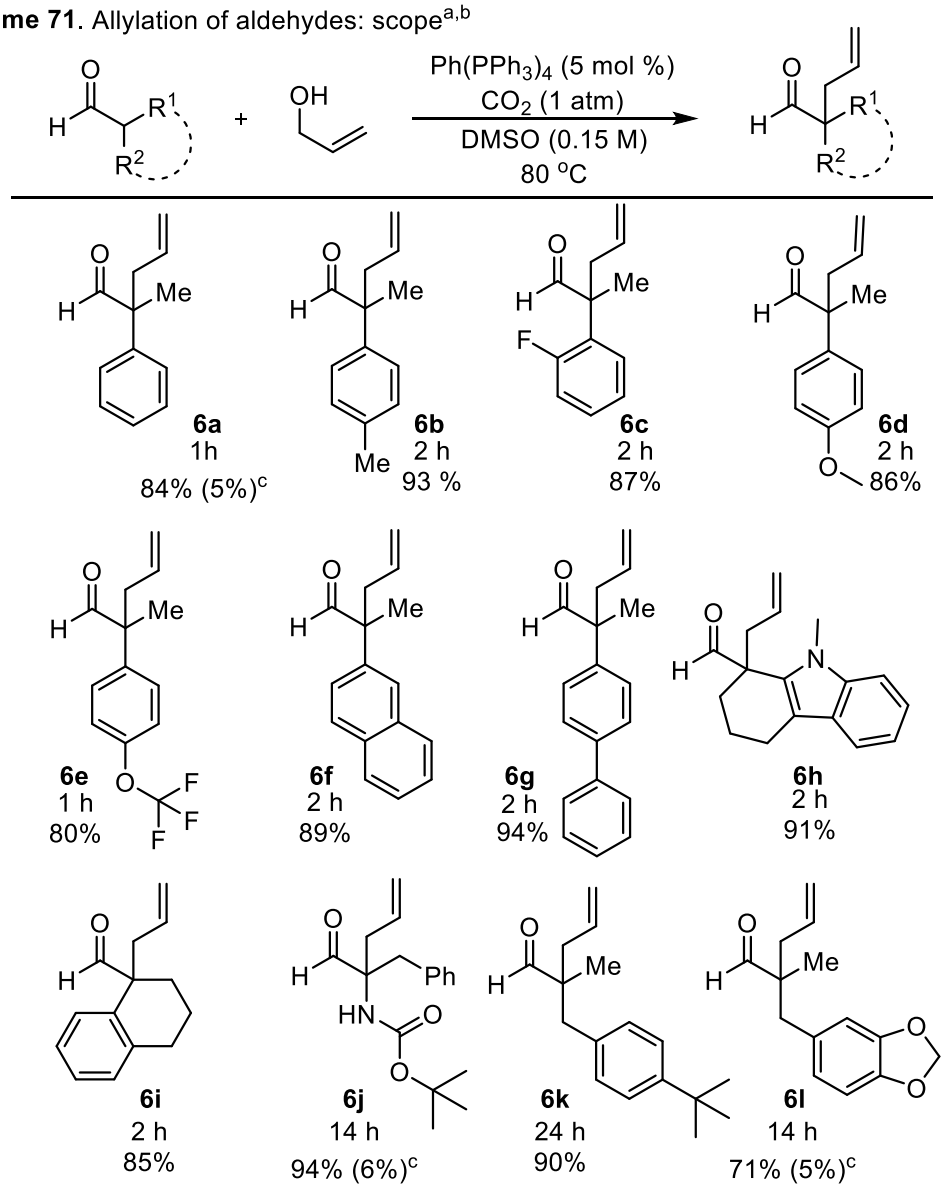

a) Aldehyde (0.30 mmol) and alcohol (0.45 mmol) in 2.0 mL DMSO under 1 atm of CO_2. b) Isolated yields. c) Ar replaced CO_2 (% conversion via GC/MS).

Scheme 72. Allylation of nitriles: scope[a,b]

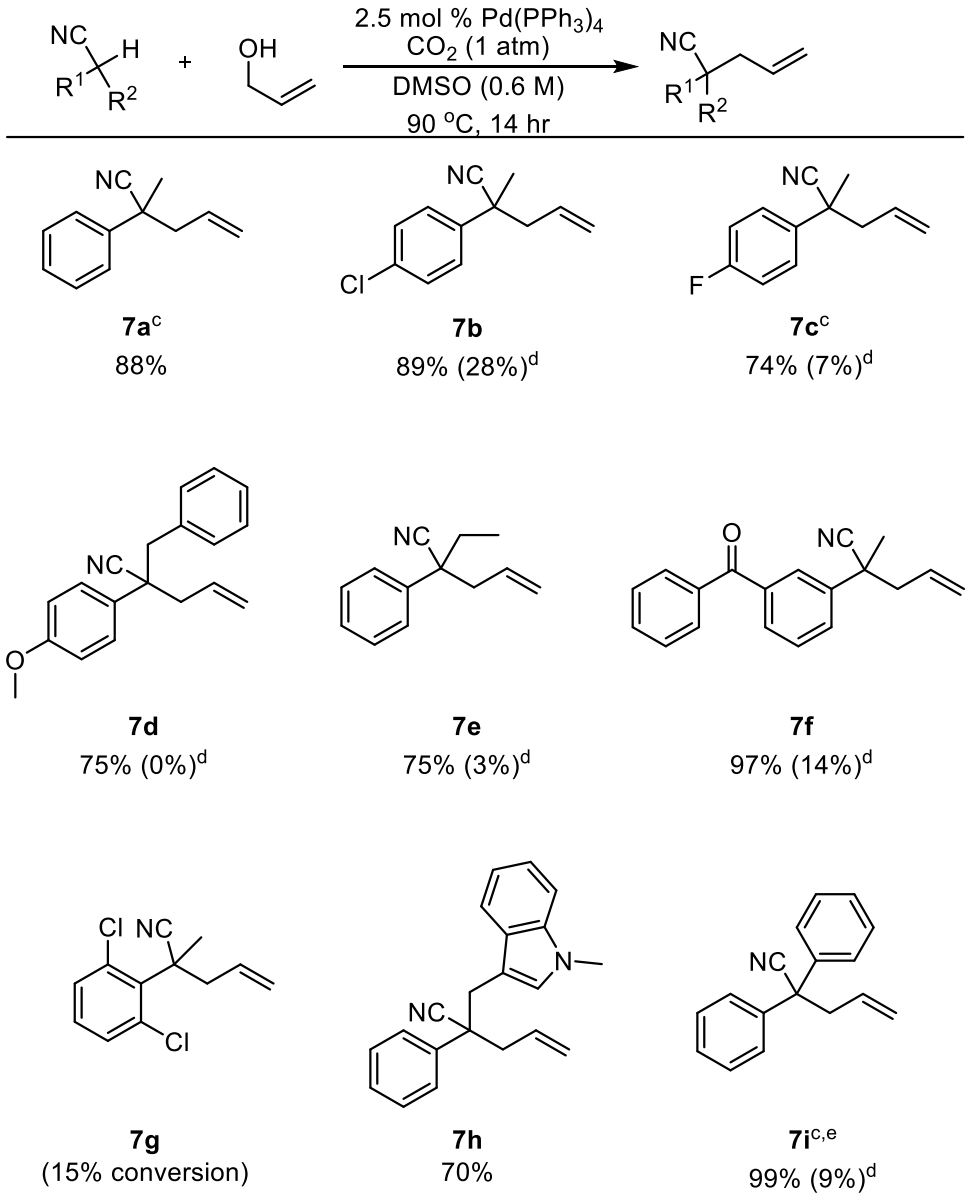

a) Nitrile (0.3 mmol) and allyl alcohol (0.6 mmol) in 0.5 mL DMSO under
b) Isolated yields c) 2 mL of DMSO used d) Ar replaced CO_2 e) 80°C

Next, the scope of alcohols other than simple allyl alcohol were examined for the intermolecular allylation of nitrile and aldehyde pro-nucleophiles. Nitriles were readily allylated with allylic alcohols substituted at the β position with methyl and phenyl substituents (**8a**, **8b**). Alkyl groups α to the alcohol were also well tolerated. Increased linear to branched ratios were

Scheme 73. Scope of allyl alcohols[a,b]

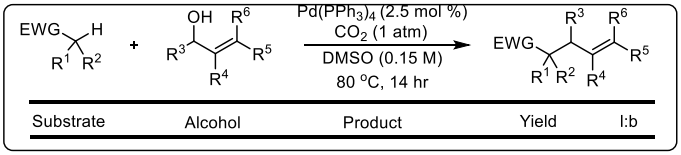

Substrate	Alcohol	Product	Yield	l:b
		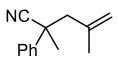 **8a**[b]	94%	--
		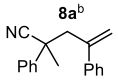 **8b**[b]	79%	--
		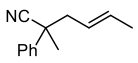 **8c**[b,c]	73%	2:1
		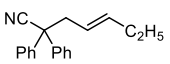 **8d**	99%	10.5:1
		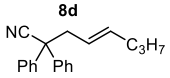 **8e**[d]	99%	11.2:1
		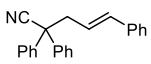 **8f**	94%	>95:5
	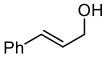	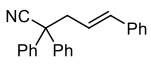 **8g**	79%	>95:5
		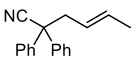 **8h**[e]	99%	1.4:1
		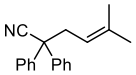 **8i**[f]	0%	--
		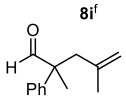 **8j**	77%	--
		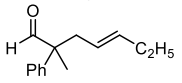 **8k**	79%	93:7
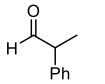	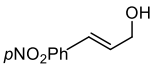	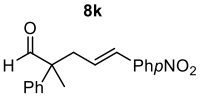 **8l**	79%	86:14
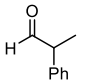	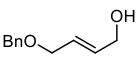	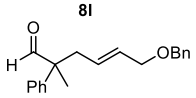 **8m**[g]	73%	>95:5
		8n[h]	70%	>95:5
		8o[i]	79%	>95:5

a) Substrate (0.3 mmol) and allylic alcohol (0.6 mmol) in 2 mL DMSO under 1 atm CO_2. b) Reaction at 90 °C in 0.5 mL DMSO. c) 1 : 2.5 (cis : trans). d) 1 : 14.3 (cis : trans). e) 1 : 4.6 (cis : trans). f) rxn time 4 h. g) rxn time 19 h. 1:5.3 (cis:trans). h) rxn time 8 h, a 23% conversion in the control reaction was observed i) rxn time 7 h.

observed as groups with increasing steric bulk were employed and diphenylacetonitrile was used as the pro-nucleophile (**8c**-**8e**). The linear product was almost exclusively formed (> 95:5) over the branched product when α-vinylbenzyl alcohol was subjected to the reaction conditions (**8f**). Similar selectivity occurred when the isomeric cinnamyl and crotyl alcohols, which form the same Pd-π-allyl intermediates as **8c** and **8f** after oxidative addition were treated with carbon dioxide and the diphenyl acetonitrile pro-nucleophile (**8g**, **8h**). No conversion was detected when allyl alcohol was replaced by prenyl alcohol, presumably due to the increased steric profile which hampers coordination to Pd(0) (**8f**).

2-Phenylpropanal was also allylated with various allylic alcohols. The desired product was isolated in a good yield when β-methallyl alcohols was subjected to the reaction conditions (**8j**). Significantly higher linear:branched ratios were observed with 1-penten-3-ol compared to when the same alcohol was used with a diphenylacetonitrile pro-nucleophile (**8k**). High (>95:5) linear : branched ratios were similarly observed with cinnamyl and *p*-trifluoromethyl cinnamyl alcohols (**8n**, **8o**). The selectivity decreased slightly when *p*-nitro cinnamyl alcohol was used, which may result from the very electron withdrawing group creating an increased partial positive charge on the α-carbon (**8l**). Lastly, a mono protected allylic diol was also compatible with the reaction conditions and provided the desired product in a good yield with > 95:5 linear:branched selectivity (**8m**).

Efforts were also made to effect stereoconvergent allylation. $Pd(PPh_3)_4$ was replaced with common Pd(0) precursors $Pd(OAc)_2$ and Pd_2dba_3 and several popular chiral non-racemic phosphine ligands (Scheme 74). Although several palladium/ligand combinations reached complete conversion after extended times under the standard reactions conditions, good ee's were not observed via chiral HPLC analysis of the products.

Scheme 74. Attempts at stereoconvergent allylation

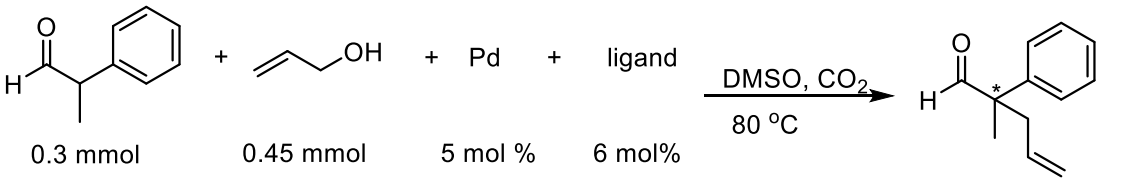

Pd source	Ligand	Time	% conv	%ee
$Pd(OAc)_2$	R-BINAP	15.5 h	full	2-3%
Pd_2dba_3	R-BINAP	15.5 h	20%	nd
$Pd(OAc)_2$	(S,S)-Anden-Phenyl-Trost	12 h	8%	nd
Pd_2dba_3	(S,S)-Anden-Phenyl-Trost	12 h	60%	nd
$Pd(OAc)_2$	(R,R)-DACH-pyridyl-Trost	22 h	none	nd
Pd_2dba_3	(R,R)-DACH-pyridyl-Trost	22 h	none	nd
$Pd(OAc)_2$	DuPhos	24 h	full	no ee
Pd_2dba_3	DuPhos	24 h	5%	nd
$Pd(OAc)_2$	C_3TunePhos	20 h	full	no ee
Pd_2dba_3	C_3TunePhos	20 h	22%	nd
$Pd(OAc)_2$	DACH Phenyl Trost Ligand	24 h	25%	nd
Pd_2dba_3	DACH Phenyl Trost Ligand	24 h	85%	no ee
$Pd(OAc)_2$	t-BuPHOX	14 h	50%	nd
Pd_2dba_3	t-BuPHOX	14 h	full	< 5%
$Pd(OAc)_2$	PhPHOX	14 h	full	9% ee
Pd_2dba_3	PhPHOX	14 h	81%	nd

One potential explanation for the poor levels of enantioenrichment might involve poor control of enolate geometry. Thus, several stereodefined trimethylsilyl enol ethers were subjected to the standard reaction conditions (Scheme 75). Unfortunately, a large quantity of the protonated rather than the allylated adduct was detected via analysis of the crude reaction mixture by GC/MS.

Scheme 75. Reactions of silyl enol ethers

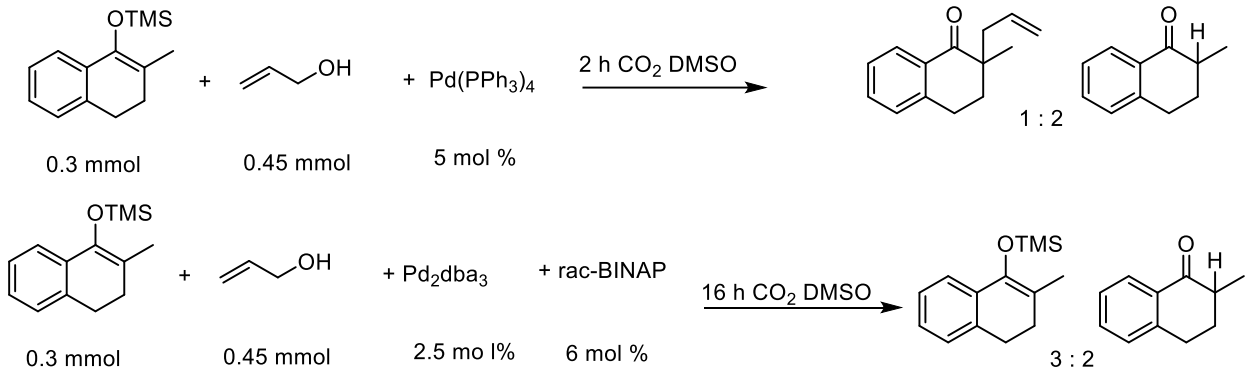

4.4 Conclusion

A wide variety of weakly acidic pronucleophiles were allylated under relatively mild conditions with water produced as the only stoichiometric byproduct. The activation of allylic alcohols with carbon dioxide helped expand the scope of both the electrophile and the nucleophile in the Tsuji–Trost reaction.

4.5 References for Chapter 4

1) Lang, S. B.; Locascio, T. M.; Tunge, J. A. "Activation of Alcohols with Carbon Dioxide: Intermolecular Allylation of Weakly Acidic Pronucleophiles" *Org. Lett.* **2014**, *16*, 4308-4311.

2) Yus, M.; González-Gómez, J. C.; Foubelo, F. "Diastereoselective Allylation of Carbonyl Compounds and Imines: Application to the Synthesis of Natural Products" *Chem. Rev.* **2013**, *113*, 5595-5698.

3) (a) Puentes, C. O.; Kouznetsov, V. "Recent advancements in the homoallylamine chemistry" *J. Heterocycl. Chem.* **2002**, *39*, 595-614 (b) Ding, H.; Friestad, G. K. "Asymmetric Addition of Allylic Nucleophiles to Imino Compounds" *Synthesis* **2005**, 2815-2829 (c) Ramadhar, T. R.; Batey, R. A. "Allylation of Imines and Their Derivatives with Organoboron Reagents: Stereocontrolled Synthesis of Homoallylic Amines" *Synthesis* **2011**, 1321-1346.

4) (a) Vieira, E. M.; Snapper, M. L.; Hoveyda, A. H. "Enantioselectrive Synthesis of Homoallylic Amines through Reactions of (Pinacolato)allylborons with Aryl-, Heteroaryl-, Alkyl-, or Alkene-Substituted Aldimines Catalyzed by Chiral C_1-Symmetric NHC-Cu Complexes" *J. Am. Chem. Soc.* **2011**, *133*, 3332-3335. (b) Silverio, D. L.; Torker, S.; Pilugina, T.; Vieira, E. M.; Snapper, M. L.; Haeffner, F.; Hoveyda, A. H. "Simple organic molecules as catalysts for enantioselective

synthesis of amines and alcohols" *Nature* **2013**, *494*, 216-221 (c) Gandhi, S.; List, B. "Catalytic Asymmetric Three-Component Synthesis of Homoallylic Amines" *Angew. Chem. Int. Ed.* **2013**, *52*, 2573-2576.

5) Trost, B. M. "Pd- and Mo-Catalyzed Asymmetric Allylic Alkylation" *Org. ProcessRes. Dev.* **2012**, *16*, 185-194.

6) Weaver, J. D.; Recio III, A.; Grenning, A. J.; Tunge. J. A. "Transition Metal-catalyzed Decarboxylative Allylation and Benzylation Reactions" *Chem. Rev.* **2011**, *111*, 1846-1913.

7) Mohr, J. T.; Stoltz, B. M. "Enantioselective Tsuji Allylations" *Chem. Asian J.* **2007**, *12*, 1476-1491.

8) Tsuji, J.; Takahashi, H.; Morikawa, M. "Organic syntheses by means of noble metal and compounds. XVII. Reaction of π-allylpalladium chloride with nucleophiles" *Tetrahedron Lett.* **1965**, 4387-4388.

9) Atkins, K. E.; Walker, W. E.; Manyik, R. M. "Palladium catalyzed transfer of allylic groups" *Tetrahedron Lett*. **1970**, 3821-3824.

10) Trost, B. M.; Fullerton, T. J. "New Synthetic Reactions. Allylic Alkylation" *J. Am. Chem. Soc.* **1973**, *95*, 292-294.

11) Trost, B. M.; Dietsche, T. J. "New Synthetic Reactions. Asymmetric Induction in Allylic Alkylations" *J. Am. Chem. Soc.* **1973**, *95*, 8200-8201.

12) Trost, B. M.; Strege, P. E. "Asymmetric Induction in Catalytic Allylic Alkylation" *J. Am. Chem. Soc.* **1976**, *99*, 1649-1651.

13) For example: Trost, B. M.; Van Vranken, D. L. "Asymmetric Transition Metal-Catalyzed Allylic Alkylations" *Chem. Rev.* **1996**, *96*, 395-442.

14) Czako, B.; Kurti, L. *Strategic Applications of Names Reaction in Organic Synthesis* Elsevier Academic Press **2005**, 458-459.

15) (a) Tanigawa, Y.; Nishimura, K.; Kawasaki, A.; Murahashi, S.-I. "Palladium (0)-catalyzed allylic alkylation and amination of allylic phosphates" *Tett. Lett.* **1982**, *23*, 5549-5552 (b) Sakakibara, M.; Ogawa, A. "Pd-catalyzed Allylic Alkylation of Phenylvinylcarbinols with Some Nucleophiles" *Tett. Lett.* **1994**, *35*, 8013-8014.

16) Godula, K.; Sames D. "C-H bond functionalization in complex organic synthesis" *Science* **2006**, *312*, 67-72.

17) Blanksby, S. J.; Ellison, G. B. "Bond Dissociation Energies of Organic Molecules" *Acc. Chem. Res.* **2003**, *36*, 255-263.

18) (a) Itoh, K.; Hamaguchi, N.; Miura, M.; Nomura, M. "Palladium-catalysed Reaction of Aryl-substituted Allylic Alcohols with Zine Enolates of β-Dicarbonyl Compounds in the Presence of Titanium(IV) Isopropoxide" *J. Chem. Soc. Perkin Trans. 1* **1992**, 2833-2835 (b) Stary, I.; Stara, I. G.; Kocovsky, P. "Allylic Alcohols as Substrates for the Palladium(0)-Catalyzed Allylic Substitution" *Tett. Lett.* **1993**, *34*, 179-182 (c) Masuyama, Y.; Kagawa, M.; Kurusu, Y. "Palladium-

Catalyzed Allylic Amination of Allylic Alcohols with Tin(II) Chloride and Triethylamine" *Chem. Lett.* **1995**, 1121-1122 (d) Tamaru, Y.; Horino, Y.; Araki, M.; Tanaka, S.; Kimura, M. "Et_3B-promoted, Pd(0)-catalyzed allylation of active methylene compounds with allylic alcohols" *Tett. Lett.* **2000**, *41*, 5705-5709 (e) Trost, B. M.; Quancard, J. "Palladium-Catalyzed Enantioselective C-3 Allylation of 3-Substituted -1*H*-Indoles Using Trialkylboranes" *J. Am. Chem. Soc.* **2006**, *128*, 6314-6315 (f) Matsubara, R.; Masuda, K.; Nakano, J.; Kobayashi, S. "Direct use of allylic alcohols in the allylation of sulfonylimidates" *Chem. Commun.* **2010**, *46*, 8662-8664.

19) (a) Manabe, K.; Kobayashi, S. "Palladium-Catalyzed, Carboxylic Acid-Assisted Allylic Substitution of Carbon Nucleophiles with Allyl Alcohols as Allylating Agents in Water" *Org. Lett.* **2003**, *5*, 3241-3244 (b) Kinoshita, H.; Shinokubo, H.; Oshima, K. "Water Enables Direct Use of Allyl Alcohol for Tusuji-Trost Reaction without Activators" *Org. Lett.* **2004**, *6*, 4085-4088 (c) Usui, I.; Schmidt, S.; Keller, M.; Breit, B. "Allylation of *N*-Heterocycles with Allylic Alcohols Employing Self-Assembling Palladium Phosphane Catalysts" *Org. Lett.* **2008**, *10*, 1207-1210 (d) Mukherjee, S.; List, B. "Chiral Counteranions in Asymmetric Transition-Metal Catalysis: Highly Enantioselective Pd/Brønsted Acid-Catalyzed Direct α-Allylation of Aldehydes" *J. Am. Chem. Soc.* **2007**, *129*, 11336-11337 (e) Jiang, G.; List, B. "Palladium/Brønstead Acid-Catalyzed α-Allylation of Aldehydes with Allylic Alcohols" *Adv. Synth. Catal.* **2011**, *353*, 1667-1670 (f) Krautwald, S.; Sarlah, D.; Schafroth, M. A.; Carreira, E. M. "Enantio- and Diastereodivergent Dual Catalysis: α-Allylation of Branched Aldehydes" *Science* **2013**, *340*, 1065-1068 (g) Rueping, M.; Uria, U.; Lin, M-Y.; Atodiresei, I. "Chiral Organic Contact Ion Pairs in Metal-Free Catalytic Asymmetric Allylic Substitutions" *J. Am. Chem. Soc.* **2011**, *133*, 3732-3735.

20) Weikel, R. R.; Hallett, J. P.; Liotta, C. L.; Eckert, C. A. "Self-Neutralizing in Situ Acid Catalysis for Single-Pot Synthesis of Iodobenzene and Methyl Yellow in CO_2-Expanded Methanol" *Ind. Eng. Chem. Res.* **2007**, *46*, 5252-5257.

21) Sakamoto, M.; Shimizu, I.; Yamamoto, A. "Activation of C-O and C-N bonds in Allylic Alcohols and Amines by Palladium Complexes Promoted by CO_2. Synthetic Applications to Allylation of Nucleophiles, Carbonylation, and Allylamine Disproprtination" *Bull. Chem. Soc. Jpn*. **1996**, *69*, 1065-1078.

22) Matthews, W. S.; Bares, J. E.; Bartmess, J. E.; Bordwell, F. G.; Cornforth, F. J.; Drucker, G. E.; Margolin, Z.; McCallum, R. J.; McCollum, G. J.; Vanier, N. R. "Equilibrium Acidities of Carbon Acids. VI. Establishment of an Absolute Scale of Acidities in Dimethyl Sulfoxide Solution" *J. Am. Chem. Soc.* **1975**, *97*, 7006-7014.

23) a) Bordwell, F. G.; Cheng, J.-P.; Bausch, M. J.; Bares, J. E. "Acidities of radical cations derived from arylacetonitriles" *J. Phys. Org. Chem.* **1998**, *1*, 209 b) Bordwell, F. G.; Bares, J. E.; Bartmess, J. E.; McMollum, G. J.; Van der Puy, M.; Vanier, N. R.; Matthews, W. S. "Carbon acids. 12. Acidifying effects oh phenyl substituents" *J. Org. Chem.* **1977**, *42*, 321-325.

Chapter 4 Appendix

Experimental methods and spectral analysis for Ch. 4 compounds

Table of Contents

General Information:

TLC analysis was performed (fluorescence quenching or $KMnO_4$ stain) with silica gel HL TLC plates with UV254 purchased from Sorbent Technologies.

Silica gel used for column chromatography (60 Å porosity, 230 x 400 mesh, standard grade) was purchased from Sorbent Technologies (catalog # 30930M-25).

DMSO was purchased from Sigma Aldrich and stored in an Ar-filled glove box.

Allyl alcohol was stored over 3 Å mol sieves.

GC/MS data was obtained using a Shimadzu GCMS-QP2010 SE.

Microwave experiments were run in a Biotage Initiator.

^{1}H, ^{13}C, and ^{19}F NMR spectra were obtained on a Bruker Advance 500 DRX equipped with a QNP cryoprobe or a Bruker Advance 400. ^{19}F NMR spectra were referenced to trifluoromethyltoluene while ^{1}H and ^{13}C NMR spectra were referenced to residual protio solvent signals.

CO_2 was dispensed through a Matheson 3040 series regulator attached to a cylinder purchased from Lindweld.

Scheme 75. Synthesis of nitroalkanes

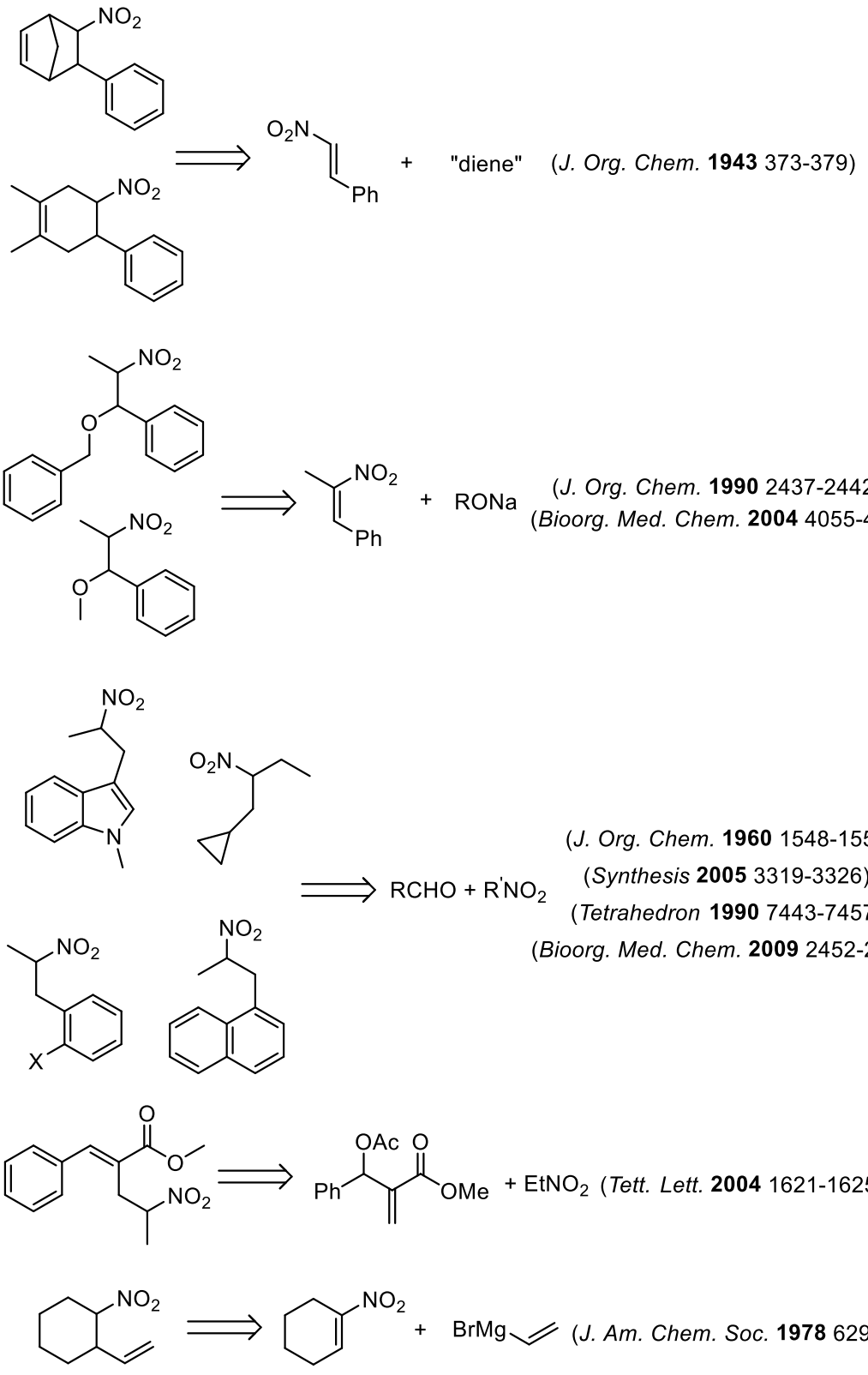

Scheme 76. Synthesis of aldehydes

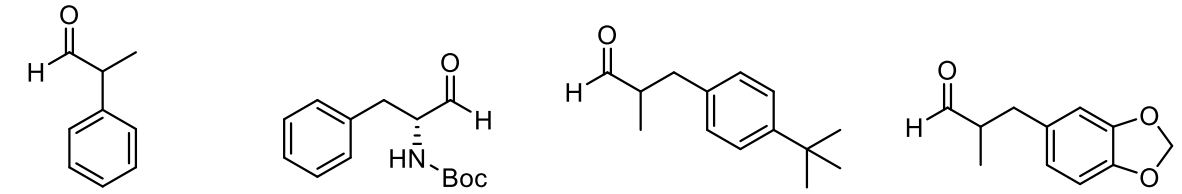

commercially available

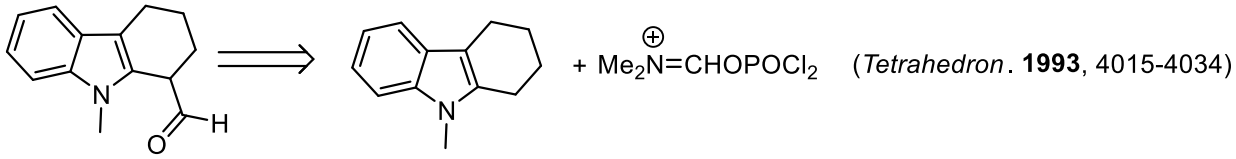

(*Tetrahedron*. **1993**, 4015-4034)

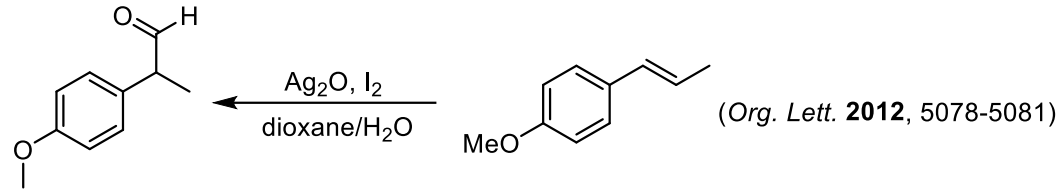

(*Org. Lett.* **2012**, 5078-5081)

The remaining aldehydes were synthesized according to the two step procedure outlined in:

Baumann, T.; Vogt, H.; Bräse. *Eur. J. Org. Chem.* **2007**, 266.

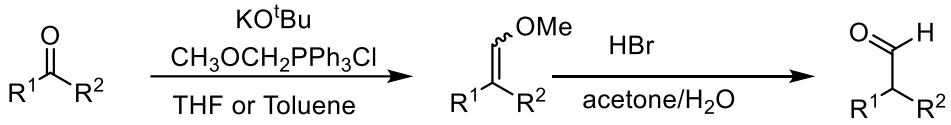

Representative procedure for the CO_2 catalyzed activation of allyl alcohol towards allylation of nitroalkanes: A 2.0 – 5.0 mL microwave vial (Biotage #351521) dried in an oven was charged with a stir bar and taken into a glove box. $Pd(PPh_3)_4$ (10 mol %, 0.035 g) was added along with DMSO (1.75 mL), and the vial capped using a vial cap (Biotage #352298) and a manual cap crimper (Biotage #353671). The vial was removed from the glovebox and substrate (0.30 mmol) and allyl alcohol (0.45 mmol, 0.026 g) were added sequentially via syringe. CO, was then bubbled through the solvent using a long 20 gauge needle connected to a balloon and a

separate 25.5 gauge needle to vent. After 6 min. the vent needle was removed S-4 followed by the CO_2 needle and the top of the vial is wrapped in parafilm “M”. The vial was then placed in an oil bath at room temperature and heated/stirred at 80 ^oC for 14 hours. After 14 hours the vial was removed from the bath, and allowed to cool to room temperature. The contents were taken up in EtOAc (10 mL) and transferred to a separatory funnel and were washed with 30 mL DI water 3x. The organic layer was dried over $MgSO_4$, filtered, and the solvent evaporated in vacuo followed by purification via silica gel column chromatography using 1:20 EtOAc:Pentanes as an eluent unless otherwise noted.

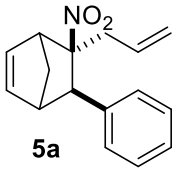

5a

SBL-1-261 0.072g, 94%.

dr = 95:5 ; Stereochemistry assigned by inference. See Grenning, A. J.; Tunge, J. A. *Org. Lett.* **2010**, *12*, 740-742.

^{1}H NMR Spectra (500 MHz, $CDCl_3$): (major diastereomer) δ 7.47 (d, *J* = 7.43 Hz, 2H), 7.37 (t, *J* = 7.40 Hz, 2H), 7.30 (m, 1H), 6.54 (dd, *J* = 5.66, 3.22 Hz, 1H), 6.26 (dd, *J* = 5.67, 2.82 Hz, 1H), 5.57 (m, 1H), 5.04 (dt, *J* = 10.2, 0.95 Hz 1H), 4.90 (dq, *J* = 16.9 Hz, 1.50 Hz, 1H), 3.52 (d, *J* = 2.63 Hz, 1H), 3.41 (s, 1H), 3.12 (s, 1H), 2.29 (ddt, *J* = 15.0, 6.97, 1.20 Hz, 1H), 2.05 (d, *J* = 9.60 Hz, 1H), 1.95 (dd, *J* = 15.0, 7.60 Hz, 1H), 1.85 (dq, *J* = 9.56, 2.07 Hz, 1H).

^{13}C NMR (126 MHz, $CDCl_3$): (major diastereomer) δ 139.8, 138.2, 135.8, 130.2, 127.5, 126.1, 118.7, 100.4, 52.0, 47.1, 45.7, 44.6, 42.1.

GC/MS Data: 255.1 (M^+, 1 %), 66.1, base peak.

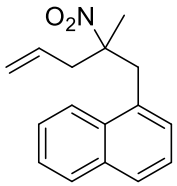

5b

SBL-2-140 0.064g, 83%.

^{1}H NMR Spectra (500 MHz, $CDCl_3$): δ 7.99 (d, *J* = 8.66 Hz, 1H), 7.87 (d, *J* = 8.08 Hz, 1H), 7.80 (d, *J* = 8.40 Hz, 1H), 7.44 (m, 2H), 7.51 (t, *J* = 7.65 Hz, 1H), 7.26 (d, *J* = 6.22 Hz, 1H), 5.71 (m, 1H), 5.21 (m, 2H), 3.78 (d, *J* = 14.7 Hz, 1H), 3.71 (d, *J* = 14.6 Hz, 1H), 3.02 (dd, *J* = 14.2, 6.86 Hz, 1H), 2.57 (dd, *J* = 14.2, 7.76 Hz, 1H), 1.43 (s, 3H).

^{13}C NMR (126 MHz, $CDCl_3$): δ 133.9, 132.7, 131.2, 130.9, 129.0, 128.5, 128.4, 126.3, 125.7, 125.4, 123.6, 120.9, 92.4, 44.4, 41.1, 21.3.

GC/MS data: 255.1 (M^+, 8 %), 141.1, base peak.

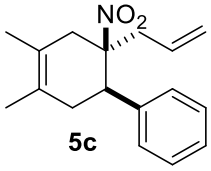

5c

SBL-2-145 0.071g, 88%.

dr > 95:5; Stereochemistry assigned by inference. See Grenning, A. J.; Tunge, J. A. *Org. Lett.* **2010**, *12*, 740-742

^{1}H NMR Spectra (500 MHz, $CDCl_3$): δ 7.23 (m, 3H), 7.11 (m, 2H), 5.63 (m, 1H), 5.14 (m, 2H), 3.47 (d, *J* = 6.82 Hz, 1H), 2.85 (dd, *J* = 14.1, 6.81 Hz, 1H), 2.64 (m, 3H), 2.34 (m, 2H), 1.75 (d, *J* = 10.9 Hz, 6H).

^{13}C NMR (126 MHz, $CDCl_3$): δ 140.3, 131.0, 128.5, 128.3, 127.5, 124.4, 123.7, 120.6, 93.0, 46.8, 41.8, 36.6, 33.4, 19.4, 18.3.

GC/MS data: 225.2 (M – NO_2, 8%), 183.1, base peak.

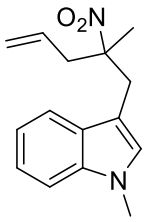

5d
SBL-2-010 0.066g, 86%, 1:10 EtOAc:Hexanes as eluent.

^{1}H NMR Spectra (500 MHz, $CDCl_3$): δ 7.53 (dt, *J* = 7.97, 0.92 Hz, 1H), 7.30 (dt, *J* = 8.31, 0.91 Hz, 1H), 7.23 (ddd, *J* = 8.18, 6.99, 1.11 Hz, 1H), 7.13 (ddd, *J* = 7.99, 6.94, 1.08 Hz, 1H), 6.84 (s, 1H), 5.74 (m, 1H), 5.19 (m, 2H), 3.75 (s, 3H), 3.49 (d, *J* = 14.8 Hz, 1H), 3.24 (d, *J* = 14.8 Hz, 1H), 2.92 (dd, *J* = 14.2, 7.05 Hz, 1H), 2.57 (dd, *J* = 14.1, 7.62 Hz, 1H), 1.51 (s, 3H).

^{13}C NMR (126 MHz, $CDCl_3$): δ 136.6, 131.2, 128.48, 128.45, 121.7, 120.5, 119.3, 118.7, 109.4, 107.5, 92.6, 44.0, 35.6, 32.8, 21.5.

GC/MS data: 258.1 (M^+, 14%) 144.1, base peak.

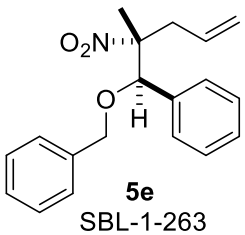

5e
SBL-1-263 0.087g, 93%.

dr = 88:12; Relative stereomchemistry assigned via x-ray structure of corresponding amine salt [pg 197].

^{1}H NMR Spectra (500 MHz, $CDCl_3$): (major diastereomer) δ 7.30 (m, 8H), 7.18 (m, 2H), 5.62 (m, 1H), 5.04 (m, 2H), 4.86 (s, 1H), 4.44 (d, *J* = 11.5 Hz, 1H), 4.20 (d, *J* = 11.5, 1H), 3.01 (dd, *J* = 14.5, 6.63 Hz, 1H), 2.53 (dd, *J* = 14.6, 7.89 Hz, 1H), 1.33 (s, 3H).

^{13}C NMR (126 MHz, $CDCl_3$): (major diastereomer) δ 136.2, 134.2, 130.3, 127.8, 127.4, 127.4, 127.3, 126.9, 119.3, 93.2, 83.7, 70.4, 39.0, 16.7.

GC/MS data: 221.1 (M – toluene, 1%), 91.1, base peak.

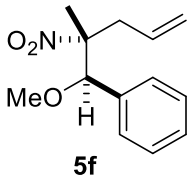

5f

SBL-2-143 0.068g, 96%, 25% to 75% DCM in Pentanes.

dr = 88:12; Relative stereochemistry assigned based on the x-ray structure of the 5e salt.

^{1}H NMR Spectra (500 MHz, $CDCl_3$): (major diastereomer) δ 7.35 (m, 3H), 7.27 (m, 2H), 5.71 (m, 1H), 5.13 (m, 2H), 4.73 (s, 1H), 3.26 (s, 3H), 3.09 (dd, *J* = 14.1, 6.75 Hz, 1H), 2.56 (dd, *J* = 14.5, 7.90 Hz, 1H), 1.38 (s, 3H).

^{13}C NMR (126 MHz, $CDCl_3$): (major diastereomer) δ 135.2, 131.4, 128.8, 128.4, 128.2, 120.3, 94.2, 87.2, 57.8, 39.8, 17.9.

GC/MS data: 121.1 base peak.

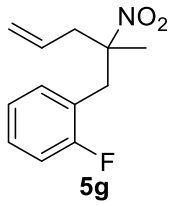

5g

SBL-2-141 0.065g, 92%.

^{1}H NMR Spectra (500 MHz, $CDCl_3$): δ 7.27 (m, 1H), 7.07 (m, 3H), 5.70 (m, 1H), 5.20 (m, 2H), 3.33 (d, *J* = 14.3 Hz, 1H), 3.25 (d, *J* = 14.2 Hz, 1H), 2.89 (dd, *J* = 14.1, 6.93 Hz, 1H), 2.53 (dd, *J* = 14.2, 7.68 Hz, 1H), 1.48 (s, 3H).

^{13}C NMR (126 MHz, $CDCl_3$): δ 161.3 (d, J_{CF} = 246 Hz), 131.8 (d, J_{CF} = 3.91 Hz), 130.7, 129.5 (d, J_{CF} = 8.32 Hz), 124.4 (d, J_{CF} = 3.60 Hz), 121.9 (d, J_{CF} = 15.7 Hz), 120.9, 115.4 (d, J_{CF} = 22.7 Hz), 91.7, 44.0, 38.2, 20.8.

^{19}FNMR (376 MHz, $CDCl_3$): δ -116.75.

GC/MS data: 223.05 (M^+ 0.1 %), 109.1, base peak.

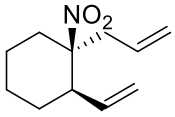

5h

SBL-2-029 0.053g, 90%.

dr = 85:15; Stereochemistry assigned by inference. See Grenning, A. J.; Tunge, J. A. *Org. Lett.* **2010**, *12*, 740-742.

^{1}H NMR Spectra (500 MHz, $CDCl_3$): (major diastereomer) δ 5.98 (m, 1H), 5.62 (m, 1H), 5.13 (m, 4H), 2.80 (dd, *J* = 15.1 Hz, 7.08 Hz, 1H), 2.69 (dd, *J* = 14.1, 7.60 Hz, 1H), 2.55 (m, 1H), 2.23 (ddd, *J* = 13.8, 8.62, 3.78 Hz, 1H), 1.60 (m, 8H).

^{13}C NMR (126 MHz, $CDCl_3$): (major diastereomer) δ 136.2, 130.7, 120.4, 118.2, 93.6, 48.7, 41.6, 29.6, 28.5, 22.1.

GC/MS data: 149.2 (M – NO_2, 5%), 81.1 (base peak).

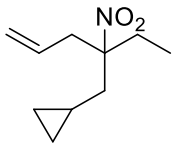

5i
SBL-2-018 0.039g, 71%, 1:10 EtOAc:Pentanes.

^{1}H NMR Spectra (500 MHz, $CDCl_3$):δ 5.63 (ddt, *J* = 17.3, 10.1, 7.30 Hz, 1H), 5.17 (m, 2H), 2.77 (dt, *J* = 7.30, 1.24 Hz, 2H), 2.01 (m, 2H), 1.84 (dd, *J* = 6.8, 1.46 Hz, 2H), 0.87 (t, *J* = 7.45 Hz, 3H), 0.61 (m, 1H), 0.46 (m, 2H), 0.10 (m, 2H).

^{13}C NMR (126 MHz, $CDCl_3$): δ 130.3, 119.0, 93.8, 39.0, 37.7, 28.7, 7.0, 4.6, 2.9, 2.8.

GC/MS data: 154.1 (M – ethyl, 0.4 %), 55.1, base peak.

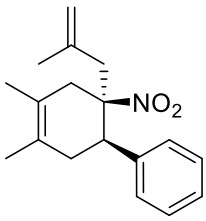

5j
SBL-2-044 0.083g, 97%.

dr = 90:10; Stereochemistry assigned by inference. See Grenning, A. J.; Tunge, J. A. *Org. Lett.* **2010**, *12*, 740-742.

^{1}H NMR Spectra (500 MHz, $CDCl_3$): δ 7.23 (m, 3H), 7.10 (m, 2H), 4.90 (t, *J* = 1.70 Hz, 1H), 4.65 (d, *J* = 1.05 Hz, 1H), 3.44 (d, *J* = 7.17 Hz, 1H), 2.93 (d, *J* = 14.0 Hz, 1H), 2.69 (m, 3H), 2.36 (m, 2H), 1.75 (d, *J* = 13.6 Hz, 6H), 1.63 (s, 3H).

^{13}C NMR (126 MHz, $CDCl_3$): δ 140.3, 139.6, 128.4, 128.3, 127.5, 124.3, 123.9, 116.7, 92.9, 47.3, 44.7, 37.2, 32.6, 23.2, 19.4, 18.3.

GC/MS data: 239.2 (M – NO_2), 197.1 183.1, base peak.

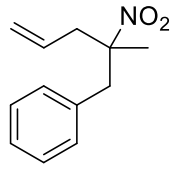

5k
SBL-2-063 0.055g, 89%.

^{1}H NMR Spectra (500 MHz, $CDCl_3$): δ 7.30 (m, 3H), 7.02 (dd, *J* = 7.52, 1.90 Hz, 2H), 5.63 (dddd, *J* = 17.1, 10.2, 7.61, 6.96 Hz, 1H), 5.12 (m, 2H), 3.29 (d, *J* = 13.9 Hz, 1H), 2.98 (d, *J* = 13.9 Hz, 1H), 2.79 (dd, *J* = 14.2, 6.97 Hz, 1H), 2.43 (dt, *J* = 14.2, 7.68, 1.07 Hz, 1H), 1.39 (s, 3H).

^{13}C NMR (126 MHz, $CDCl_3$): δ 134.6, 130.9, 130.1, 128.5, 127.5, 120.8, 91.5, 45.6, 43.8, 21.3.

GC/MS data: 159.1 (M- NO_2, 4%), 91.1, base peak.

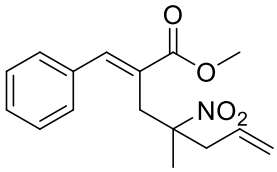

5l
SBL-2-037 0.079g, 91%.

^{1}H NMR Spectra (500 MHz, $CDCl_3$): δ 7.90 (s, 1H), 7.39 (m, 3H), 7.28 (m, 2H), 5.47 (m, 1H), 5.06 (m, 2H), 3.79 (s, 3H), 3.37 (d, *J* = 16.5 Hz, 1H), 3.26 (d, *J* = 14.6 Hz, 1H), 2.73 (dd, *J* = 14.1, 6.78 Hz, 1H), 2.26 (dd, *J* = 14.2, 8.00 Hz, 1H), 1.34 (s, 3H).

^{13}C NMR (126 MHz, $CDCl_3$): δ 168.2, 143.7, 135.1, 130.8, 128.8, 128.7, 128.5, 127.9, 120.7, 90.5, 52.2, 43.9, 35.5, 21.2.

GC/MS data: 289.1 (M^+, 1%), 115.1, base peak.

Representative procedure for the CO_2 catalyzed activation of allyl alcohol towards allylation of aldehydes:

A 2.0 – 5.0 mL microwave vial (Biotage #351521) dried in an oven is charged with a stir bar and taken into a glove box. $Pd(PPh_3)_4$ (5 mol %, 0.014 g) is added along with DMSO (2.0 mL) and the vial is capped using a vial cap (Biotage #352298) and a manual cap crimper (Biotage #353671). The vial is removed from the glovebox and substrate (0.30 mmol) and allyl alcohol (0.45 mmol, 0.026 g) are added sequentially via syringe. CO_2 is then bubbled through the solvent using a 20G needle connected to a balloon and a separate 25.5G needle to vent. After 6 mins the vent needle was removed followed by the CO_2 needle and the top of the vial is wrapped in parafilm “M”. The vial was then placed in an oil bath at room temperature and heated/stirred at 80 ^{o}C until the reaction was complete as shown by GC/MS. The reaction mixture was dry loaded onto silica gel and purified by flash chromatography (1:20 EtOAc:Pentanes unless otherwise noted).

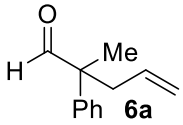

6a

SBL-2-197 0.044g, 84%.

^{1}H NMR Spectra (500 MHz, $CDCl_3$): δ 9.52 (s, 1H), 7.39 (m, 2H), 7.30 (m, 1H), 7.26 (m, 2H), 5.55 (m, 1H), 5.04 (m, 2H), 2.70 (ddt, *J* = 14.2, 6.93, 1.32 Hz, 1H), 2.63 (ddt, *J* = 14.1, 7.72, 1.19 Hz, 1H), 1.45 (s, 3H).

^{13}C NMR (126 MHz, $CDCl_3$): δ 202.0, 139.4, 133.2, 128.9, 127.3, 127.2, 118.6, 53.6, 40.6, 18.8.

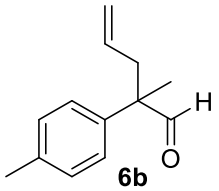

6b

SBL-3-006 0.053g, 93% 1:30 EtOAc:Pentanes.

^{1}H NMR Spectra (500 MHz, $CDCl_3$): δ 9.49 (s, 1H), 7.20 (m, 2H), 7.14 (m, 2H), 5.56 (m, 1H), 5.04 (m, 2H), 2.68 (ddt, *J* = 14.1, 6.91, 1.13 Hz, 1H), 2.61 (ddt, *J* = 14.1, 7.67, 1.13 Hz, 1H), 2.35 (s, 3H), 1.43 (s, 3H).

^{13}C NMR (126 MHz, $CDCl_3$): δ 202.0, 137.1, 136.3, 133.3, 129.6, 127.1, 118.5, 53.3, 40.5, 21.0, 18.8.

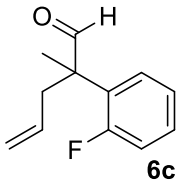

6c

SBL-3-007 0.050g, 87%.

^{1}H NMR Spectra (500 MHz, $CDCl_3$): δ 9.68 (d, *J* = 4.97 Hz, 1H), 7.30 (m, 2H), 7.18 (td, *J* = 7.58, 7.53, 1.35 Hz, 1H), 7.08 (ddd, *J* = 11.8, 8.18, 1.33 Hz, 1H), 5.53 (m, 1H), 5.02 (m ,2H), 2.75 (dd, *J* = 14.0, 6.99 Hz, 1H), 2.63 (dd, *J* = 14.1, 7.77 Hz, 1H), 1.42 (s, 3H).

^{13}C NMR (126 MHz, $CDCl_3$): δ 201.9 (d, *J* = 2.32 Hz), 161.9, 159.9, 132.7, 129.4 (d, *J* = 8.57 Hz), 128.6 (d, *J* = 4.95 Hz), 127.9 (d, *J* = 13.1 Hz), 124.4 (d, *J* = 3.21 Hz), 118.8, 116.1 (d, *J* = 22.8 Hz), 51.9 (d, *J* = 3.15 Hz), 39.2 (d, *J* = 2.50 Hz), 19.2.

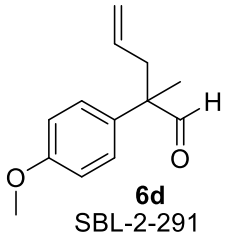

6d

SBL-2-291 0.053g, 86%.

^{1}H NMR Spectra (500 MHz, $CDCl_3$): δ 9.46 (s, 1H), 7.17 (m, 2H), 6.92 (m, 2H), 5.55 (m, 1H), 5.04 (m, 2H), 3.80 (s, 3H), 2.66 (ddt, *J* = 14.1, 6.78, 1.37 Hz, 1H), 2.59 (dd, *J* = 14.2, 7.79, 1.21 Hz, 1H), 1.42 (s, 3H).

^{13}C NMR (126 MHz, $CDCl_3$): δ 201.9, 158.8, 133.3, 131.1, 128.3, 118.5, 114.2, 55.3, 52.9, 40.5, 18.9.

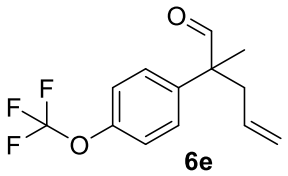

6e

SBL-3-027 0.062g, 80%.

^{1}H NMR Spectra (300 MHz, $CDCl_3$): δ 9.51 (s, 1H), 7.28 (m, 2H), 7.23 (m, 2H), 5.52 (m, 1H), 5.06 (m, 2H), 2.67 (dd, *J* = 10.6, 6.93 Hz, 1H), 2.62 (dd, *J* = 10.8, 7.62 Hz, 1H), 1.45 (s, 3H).

^{13}C NMR (126 MHz, $CDCl_3$): δ 201.4, 148.4 (d, *J* = 2.09 Hz), 138.1, 132.6, 128.7, 121.2, 120.5 (q, *J* = 257 Hz), 119.1, 53.3, 40.7, 19.0.

^{19}FNMR (376 MHz, $CDCl_3$): δ -58.86

HRMS: [M+]: calc: 258.0868, found: 258.0872.

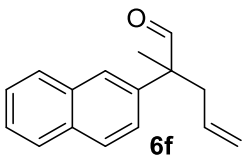

6f

SBL-3-046 0.060g, 89%.

^{1}H NMR Spectra (300 MHz, $CDCl_3$): δ 9.60 (s, 1H), 7.85 (m, 3H), 7.72 (d, *J* = 1.95 Hz, 1H), 7.51 (m, 2H), 7.37 (dd, *J* = 8.60, 1.96 Hz, 1H), 5.57 (m, 1H), 5.06 (m, 2H), 2.83 (ddt, *J* = 14.2, 6.82, 1.29 Hz, 1H), 2.72 (ddt, *J* = 14.1, 7.74, 1.10 Hz, 1H), 1.56 (s, 3H).

^{13}C NMR (126 MHz, $CDCl_3$): δ 202.0, 136.8, 133.3, 133.1, 132.4, 128.6, 128.0, 127.5, 126.4, 126.3, 126.3, 125.0, 118.7, 53.8, 40.5, 18.9.

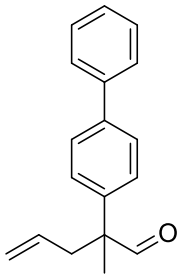

6g

SBL-3-144 0.071g, 94%.

^{1}H NMR Spectra (500 MHz, $CDCl_3$): δ 9.56 (s, 1H), 7.61 (m, 4H), 7.45 (m, 2H), 7.35 (ddt, *J* = 16.9, 8.76, 1.71 Hz, 3H), 5.60 (m, 1H), 5.08 (m, 2H), 2.74 (ddt, *J* = 14.1, 6.87, 1.29 Hz, 1H), 2.67 (ddt, *J* = 14.1, 7.78, 1.16 Hz, 1H), 1.49 (s, 3H).

^{13}C NMR (126 MHz, $CDCl_3$): δ 201.9, 140.4, 140.2, 138.4, 133.1, 128.8, 127.6, 127.5, 127.5, 127.1, 118.7, 53.5, 40.6, 18.9.

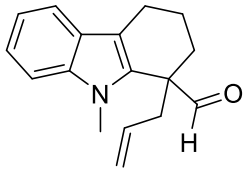

6h

SBL-3-168 0.069g, 91%.

^{1}H NMR Spectra (500 MHz, $CDCl_3$): δ 9.63 (s, 1H), 7.54 (dt, *J* = 7.80, 0.99 Hz, 1H), 7.26 (m, 2H), 7.12 (ddd, *J* = 7.93, 6.77, 1.24 Hz, 1H), 5.61 (m, 1H), 5.12 (dq, *J* = 17.0. 1.61 Hz, 1H), 5.03 (ddt, *J* = 10.1, 2.07, 1.10 Hz, 1H), 3.63 (s, 3H), 2.90 (ddt, *J* = 14.7, 6.95, 1.41 Hz, 1H), 2.81 (t, *J* = 5.9 Hz, 2H), 2.69 (ddt, *J* = 14.8, 7.53, 1.19 Hz, 1H), 1.97 (m, 4H).

^{13}C NMR (126 MHz, $CDCl_3$): δ 201.6, 137.8, 133.7, 131.4, 126.6, 122.1, 119.1, 118.4, 113.9, 108.9, 51.3, 38.1, 31.2, 30.6, 21.2, 19.4.

HRMS: [M+H] calc: 254.1545, found: 254.1535.

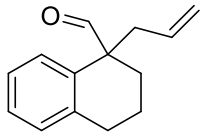

6i

SBL-3-022 0.051g, 85%, 1:50 EtOAc:Pentanes.

^{1}H NMR Spectra (300 MHz, $CDCl_3$): δ 9.55 (s, 1H), 7.18 (m, 4H), 5.60 (m ,1H), 5.05 (m, 2H), 2.78 (t, *J* = 5.65 Hz, 2H), 2.63 (dd, *J* = 7.22, 1.28 Hz, 2H), 2.09 (m, 1H), 1.83 (m, 3H).

^{13}C NMR (126 MHz, $CDCl_3$): δ 200.1, 138.7, 134.0, 133.7, 129.9, 128.3, 127.0, 126.4, 118.5, 53.0, 41.1, 29.9, 27.8, 19.2.

HRMS: [M+Na] calc: 223.1099, found: 223.1103.

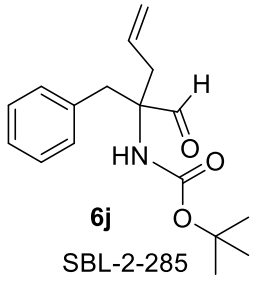

6j

SBL-2-285 0.083g, 94%, 1:3 EtOAc:Hexanes.

^{1}H NMR Spectra (500 MHz, $CDCl_3$): δ 9.40 (s, 1H), 7.18 (m, 3H), 6.99 (d, *J* = 7.08 Hz, 2H), 5.53 (m, 1H), 5.04 (m, 2H), 4.99 (s, 1H), 3.28 (d, *J* = 14.0 Hz, 1H), 3.0 (d, *J* = 14.0 Hz, 1H), 2.79 (dd, *J* = 14.5, 7.48 Hz, 1H), 2.45 (dd, *J* = 14.4, 7.32 Hz, 1H), 1.38 (s, 9H).

^{13}C NMR (126 MHz, $CDCl_3$): δ 200.2, 154.5, 135.4, 131.2, 130.2, 128.3, 127.0, 119.9, 79.8, 66.0, 38.5, 37.7, 28.3.

HRMS: [M+Na] calc: 312.1576, found: 312.1542.

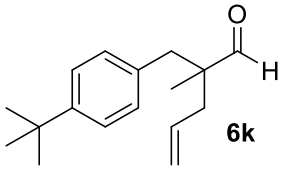

6k

SBL-2-279 0.067g, 90%, 1:30 Diethylether:Pentanes.

^{1}H NMR Spectra (500 MHz, $CDCl_3$): δ 9.60 (s, 1H), 7.28 (d, *J* = 8.28 Hz, 2H), 7.02 (d, *J* = 8.23 Hz, 2H), 5.74 (m, 1H), 5.11 (m, 2H), 2.85 (d, *J* = 13.8 Hz, 1H), 2.72 (d, *J* = 13.7 Hz, 1H), 2.36 (ddt, *J* = 14.2, 7.14, 1.28 Hz, 1H), 2.18 (dd, *J* = 14.2, 7.70, 1.25 Hz, 1H), 1.30 (s, 9H), 1.03 (s, 3H).

^{13}C NMR (126 MHz, $CDCl_3$): δ 206.2, 149.4, 133.5, 133.1, 129.9, 125.1, 118.8, 50.2, 41.4, 39.9, 34.4, 31.4, 18.6.

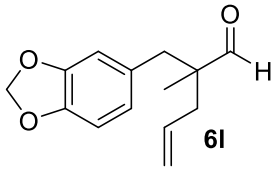

6l

SBL-2-241 0.050g, 71%.

^{1}H NMR Spectra (500 MHz, $CDCl_3$): δ 9.57 (s, 1H), 6.71 (d, *J* = 7.90, 1H), 6.58 (d, *J* = 1.76 Hz, 1H), 6.54 (dd, *J* = 7.95, 1.76 Hz, 1H), 5.92 (s, 3H), 5.72 (m, 1H), 5.11 (m, 2H), 2.81 (d, *J* = 13.9 Hz, 1H), 2.66 (d, *J* = 13.9 Hz, 1H), 2.34 (ddt, *J* = 14.4, 7.32, 1.35 Hz, 1H) 2.17 (dd, *J* = 14.1, 7.73, 1.22 Hz, 1H), 1.02 (s, 3H).

^{13}C NMR (126 MHz, $CDCl_3$): δ 206.0, 147.4, 146.3, 133.0, 130.2, 123.3, 118.9, 110.6, 108.0, 100.9, 50.2, 41.5, 39.9, 29.7, 18.6.

HRMS: [M+H] calc: 233.1178, found: 233.1189.

Representative procedure for the CO_2 catalyzed activation of allylic alcohol towards allylation of nitriles:

A 2.0 – 5.0 mL microwave vial (Biotage #351521) was flame dried and charged with the nitrile substrate (if solid, 0.3 mmol) and a stir bar. In the glove box, $Pd(PPh_3)_4$ (2.5 mol %, 0.0086 g) was added along with DMSO (2 mL) and the vial was capped using a vial cap (Biotage #352298) and a manual cap crimper (Biotage #353671). The vial was then removed from the glove box and substrate (if liquid, 0.3 mmol) and allyl alcohol (0.6 mmol, 0.035 g) were added sequentially via syringe. CO_2 was then bubbled through the solvent using a 20 gauge needle connected to a balloon and a separate 25.5 gauge needle to vent. After 5 minutes, the vent needle is removed followed by the CO_2 needle and the top of the vial was wrapped in parafilm. The vial was then placed in an oil bath at room temperature and heated/stirred at 90 ^oC for 14 hours.

After 14 hours the vial was removed from the bath, and allowed to cool to room temperature. An aliquot was then diluted in DCM and subjected to GC/MS analysis to determine conversion. The remaining solution was subjected to purification via silica gel column chromatography using 1:50 EtOAc:Pentanes as an eluent. Nitrile substrates were prepared by Theresa Locascio.

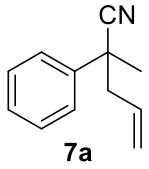

7a

^{1}H NMR Spectra (500 MHz, $CDCl_3$): δ 7.44 (m, 2H), 7.38 (m, 2H), 7.30 (m, 1H), 5.70 (m, 1H), 5.15 (m, 2H), 2.67 (ddt, *J* = 13.9, 6.7, 1.3 Hz, 1H), 2.60 (ddt, *J* = 13.9, 7.8, 1.0 Hz, 1H), 1.7 (s, 3H).

^{13}C NMR Spectra (126 MHz, $CDCl_3$): δ 140.0, 132.1, 129.1, 128.1, 125.8, 123.3, 120.4, 46.5, 42.4, 26.8.

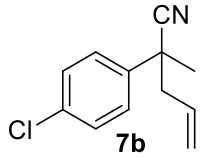

7b

^{1}H NMR Spectra (500 MHz, $CDCl_3$): δ 7.38 (m, 4H), 5.69 (dddd, *J* = 17.0, 10.2, 7.6, 6.9 Hz, 1H), 5.17 (m, 2H), 2.62 (m, 2H), 1.71 (s, 3H).

^{13}C NMR Spectra (126 MHz, $CDCl_3$): δ 138.64, 134.09, 131.75, 129.31, 127.38, 122.99, 120.84, 46.50, 42.09, 26.82.

GC/MS data: 205.1 (M^+), 164.1 (base peak).

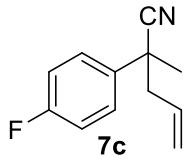

7c

^{1}H NMR Spectra (500 MHz, $CDCl_3$): δ 7.42 (m, 2H), 7.09 (m, 2H), 5.70 (dddd, *J* = 17.0, 10.2, 7.6, 6.9 Hz, 1H), 5.18 (m, 2H), 2.63 (m, 2H), 1.71 (s, 3H).

^{13}C NMR Spectra (126 MHz, $CDCl_3$): δ 163.4, 161.5, 135.9, 135.9, 131.9, 127.8, 127.7, 123.3, 120.8, 116.2, 116.0, 46.8, 42.0, 27.0.

GC/MS data: 189.1 (M^+), 148.1 (base peak).

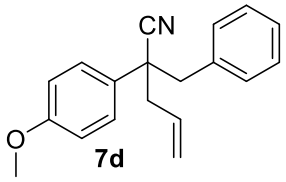

7d

^{1}H NMR Spectra (500 MHz, $CDCl_3$): δ 7.13 (m, 5H), 6.89 (m, 2H), 6.78 (m, 2H), 5.61 (dddd, *J* = 16.9, 10.2, 7.6, 6.5 Hz, 1H), 5.07 (m, 2H), 3.72 (s, 3H), 3.12 (d, *J* = 13.5 Hz, 1H), 3.02 (d, *J* = 13.5 Hz, 1H), 2.68 (m, 2H).

^{13}C NMR Spectra (126 MHz, $CDCl_3$): δ 159.3, 135.2, 132.2, 130.7, 129.6, 128.3, 128.0, 127.5, 122.1, 120.4, 114.2, 55.6, 48.9, 47.3, 43.9.

GC/MS data: 277.2 (M^+), 186.10 (base peak).

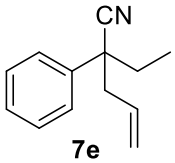

7e

^{1}H NMR Spectra (500 MHz, $CDCl_3$): δ 7.40 (m, 4H), 7.32 (m, 1H), 5.66 (m, 1H), 5.13 (m, 2H), 2.69 (ddt, *J* = 7.0, 2.0, 1.1 Hz, 2H), 2.08 (m, 1H), 1.96 (m, 1H), 0.93 (t, *J* = 7.4 Hz, 3H).

^{13}C NMR Spectra (126 MHz, $CDCl_3$): δ 138.1, 132.3, 129.1, 128.1, 126.5, 122.3, 120.2, 49.1, 45.3, 33.4, 9.9.

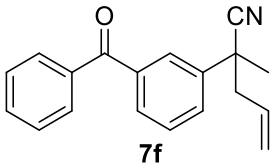

7f

^{1}H NMR Spectra (500 MHz, $CDCl_3$): δ 7.87 (t, *J* = 1.9 Hz, 1H), 7.80 (m, 2H), 7.72 (m, 2H), 7.60 (m, 1H), 7.51 (m, 3H), 5.73 (ddt, *J* = 17.3, 10.3, 7.2 Hz, 1H), 5.18 (m, 2H), 2.68 (m, 2H), 1.75 (s, 3H).

^{13}C NMR Spectra (126 MHz, $CDCl_3$): δ 196.3, 140.6, 138.5, 137.4, 133.0, 131.7, 130.3, 130.1, 129.9, 129.1, 128.7, 127.0, 122.9, 120.9, 46.4, 42.3, 26.7.

GC/MS data: 275.1 (M^+), 234.10 (base peak).

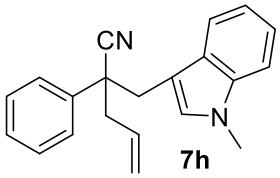

7h

^{1}H NMR Spectra (500 MHz, $CDCl_3$): δ 7.45 (m, 2H), 7.36 (m, 2H), 7.29 (m, 3H), 7.19 (ddd, *J* = 8.2, 6.9, 1.1 Hz, 1H), 7.03 (ddd, *J* = 8.1, 6.9, 1.1 Hz, 1H), 6.85 (s, 1H), 5.68 (dddd, *J* = 17.1, 10.3, 7.6, 6.6 Hz, 1H), 5.12 (m, 2H), 3.73 (s, 3H), 3.44 (d, *J* = 14.7 Hz, 1H), 3.34 (d, *J* = 14.6 Hz, 1H), 2.82 (m, 2H).

^{13}C NMR Spectra (126 MHz, $CDCl_3$): δ 138.7, 136.7, 132.5, 129.1, 129.1, 128.8, 128.1, 126.9, 122.8, 121.8, 120.2, 119.4, 119.0, 109.5, 108.3, 50.2, 43.5, 37.4, 33.1.

GC/MS data: 300.2 (M^+), 144.15 (base peak).

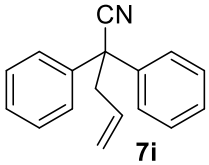

7i

^{1}H NMR Spectra (500 MHz, $CDCl_3$): δ 7.45 (m, 4H), 7.39 (ddd, *J* = 7.8, 6.8, 1.3 Hz, 4H), 7.34 (m, 2H), 5.77 (ddt, *J* = 17.2, 10.2, 7.0 Hz, 1H), 5.23 (m, 2H), 3.19 (dt, *J* = 7.1, 1.2 Hz, 2H).

^{13}C NMR Spectra (126 MHz, $CDCl_3$): δ 139.9, 132.0, 129.1, 128.2, 127.3, 122.2, 120.6, 51.9, 44.1.

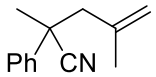

8a

^{1}H NMR Spectra (500 MHz, $CDCl_3$): δ 7.48 (m, 2H), 7.39 (m, 2H), 7.33 (m, 1H), 4.92 (p, *J* = 1.6 Hz, 1H), 4.77 (dq, *J* = 1.8, 1.0 Hz, 1H), 2.64 (t, *J* = 1.0 Hz, 2H), 1.76 (s, 3H), 1.62 (m, 3H).

^{13}C NMR Spectra (126 MHz, $CDCl_3$): δ 140.4, 140.3, 129.1, 128.1, 125.9, 123.9, 116.9, 50.1, 42.0, 27.8, 23.8.

GC/MS data: 185.1 (M^+), 130.1 (base peak).

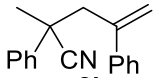

8b

^{1}H NMR Spectra (500 MHz, $CDCl_3$): δ 7.41 (m, 2H), 7.28 (m, 3H), 5.39 (d, *J* = 1.1 Hz, 1H), 5.18 (q, *J* = 1.0 Hz, 1H), 3.12 (d, *J* = 1.0 Hz, 2H), 1.67 (s, 3H).

^{13}C NMR Spectra (126 MHz, $CDCl_3$): δ 143.8, 141.7, 140.2, 129.0, 128.6, 128.0, 127.9, 126.8, 126.0, 123.3, 119.2, 47.5, 43.1, 27.3.

GC/MS data: 247.1 (M^+), 139.1 (base peak).

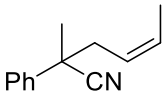

● linear Z diasteromer residues

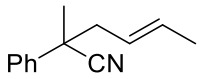

■ = linear E diastereomer residues

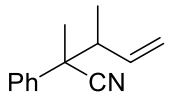

▲ = branched residues (both diastereomers)

8c (l : b, 2 : 1) (cis : trans, 1 : 2.5)

^{1}H NMR Spectra (500 MHz, $CDCl_3$): δ 7.40 (m, 5H (Ph-H_{linear}), 5H (Ph-$H_{branched}$)), 5.89 (ddd, *J* = 16.6, 10.5, 8.8 Hz, 1H branched), 5.68 (m, 1H *cis*-linear), 5.59 (m, 1H (*trans*-linear), 1H (branched)), 5.36 (m, 1H (*cis*-linear), 1H (*trans*-linear)), 5.20 (m, 2H, branched), 5.01 (m, 2H, branched), 2.59 (m, (2H *cis*-linear), (2H *trans*-linear), (1H branched)), 1.66 (d, *J* = 7.1 Hz, 3H,

trans-linear), 1.57 (d, *J* = 7.1 Hz, 3H, *cis*-linear), 1.17 (d, *J* = 6.8 Hz, 3H, branched), 0.94 (d, *J* = 6.8 Hz, 2H, branched).

^{13}C NMR Spectra (126 MHz, $CDCl_3$): δ 140.5, 140.4, 140.1, 139.3, 138.8, 138.2, 131.4, 129.2, 129.1, 128.9, 128.1, 128.0, 126.7, 126.2, 125.98, 125.95, 124.7, 123.9, 123.7, 123.1, 122.3, 118.0, 117.6, 48.7, 47.7, 47.0, 46.7, 45.6, 42.8, 42.6, 39.6, 26.8, 26.6, 24.6, 18.3, 17.2, 16.0, 13.4.

Isomers assigned by TOCSY NMR spectroscopy experiments

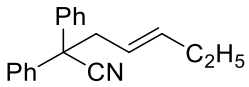

8d (l : b, 10.5 : 1)

^{1}H NMR Spectra (500 MHz, $CDCl_3$): (Major linear diastereomer) δ 7.37 (m, 8H), 7.30 (m, 2H), 5.63 (dtt, *J* = 15.4, 6.5, 1.2 Hz, 1H), 5.31 (dtt, *J* = 15.5, 7.1, 1.6 Hz, 1H), 3.07 (dq, *J* = 7.2, 1.1 Hz, 2H), 1.98 (m, 2H), 0.90 (t, *J* = 7.5 Hz, 3H).

^{13}C NMR Spectra (126 MHz, $CDCl_3$): (Major linear diasteromer) δ 140.3, 138.8, 129.1, 128.1, 127.5, 122.5, 122.3, 52.5, 43.2, 26.0, 13.9.

GC/MS data: 261.2 (M^+), 193.1 (base peak).

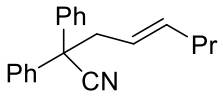

8e (l : b, 11.2 : 1) (cis : trans, 1 : 14.3)

^{1}H NMR Spectra (500 MHz, $CDCl_3$): (Major linear diastereomer) δ 7.38 (m, 8H), 7.30 (m, 2H), 5.58 (dtt, *J* = 15.0, 6.8, 1.3 Hz, 1H), 5.32 (dtt, *J* = 15.4, 7.1, 1.4 Hz, 1H), 3.08 (dq, *J* = 7.1, 1.0 Hz, 2H), 1.94 (m, 2H), 1.31 (h, *J* = 7.3 Hz, 2H), 0.81 (t, *J* = 7.4 Hz, 3H).

^{13}C NMR Spectra (126 MHz, $CDCl_3$): (Major linear diastereomer) δ 140.3, 137.1, 129.1, 128.1, 127.5, 123.5, 122.5, 52.5, 43.3, 34.9, 22.6, 13.8.

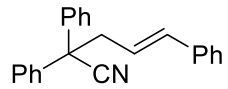

8f

^{1}H NMR Spectra (500 MHz, $CDCl_3$): δ 7.37 (m, 15H), 6.54 (dt, *J* = 15.7, 1.4 Hz, 1H), 6.10 (dt, *J* = 15.7, 7.2 Hz, 1H), 3.31 (dd, *J* = 7.4, 1.3 Hz, 2H).

^{13}C NMR Spectra (126 MHz, $CDCl_3$): δ 140.1, 137.1, 135.5, 129.2, 128.8, 128.3, 127.94, 127.4, 126.7, 123.4, 122.3, 52.4, 43.6.

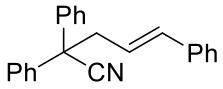

8g

^{1}H NMR Spectra (500 MHz, $CDCl_3$): δ 7.37 (m, 15H), 6.54 (dt, *J* = 15.7, 1.4 Hz, 1H), 6.10 (dt, *J* = 15.7, 7.2 Hz, 1H), 3.31 (dd, *J* = 7.4, 1.3 Hz, 2H).

^{13}C NMR Spectra (126 MHz, $CDCl_3$): δ 140.1, 137.1, 135.6, 129.2, 128.8, 128.3, 128.0, 127.4, 126.7, 123.4, 122.4, 52.4, 43.6.

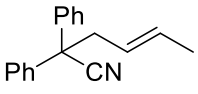

■ = Major linear diastereomer residues

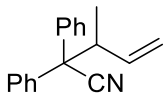

▲ = Branched residues

8h (l : b, 1.4 : 1) (cis : trans, 1 : 4.6)

^{1}H NMR Spectra (500 MHz, $CDCl_3$): δ 7.38 (m, 10H (Ph-H_{linear}), 10H (Ph-$H_{branched}$)), 5.84 (ddd, *J* = 17.1, 10.5, 7.6 Hz, 1H, branched), 5.64 (m, 1H, linear), 5.34 (m, 1H, linear), 5.32 (m, 1H, linear

diastereomer), 5.10 (m, 2H, branched), 3.45 (m, 1H, branched), 3.07 (dt, *J* = 7.3, 1.2 Hz, 2H, linear diatereomer) 2.98 (dt, *J* = 7.0, 1.2 Hz, 2H, linear), 1.64 (dq, *J* = 6.7, 1.2 Hz, 3H, linear), 1.50 (ddt, *J* = 6.9, 1.87, 0.94 Hz, 3H, linear diastereomer), 1.20 (d, *J* = 6.7 Hz, 3H, branched).

^{13}C NMR Spectra (126 MHz, $CDCl_3$): δ 140.3, 139.6, 139.5, 138.5, 131.7, 129.2, 129.12, 129.10, 129.0, 128.2, 128.1, 128.0, 127.9, 127.5, 127.4, 127.1, 124.5, 124.0, 122.5, 121.1, 117.9, 58.2, 52.5, 51.9, 44.5, 43.3, 37.5, 18.4, 17.3, 13.5.

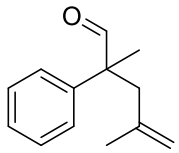

SBL-3-032 0.043g, 77%.

8j

^{1}H NMR Spectra (300 MHz, $CDCl_3$):δ 9.54 (s, 1H), 7.38 (m, 2H), 7.29 (m, 3H), 4.81 (p, *J* = 1.57, 1.53 Hz, 1H), 4.62 (dq, *J* = 1.78, 0.89 Hz, 1H), 2.69 (q, *J* = 13.9 Hz, 2H), 1.47 (s, 3H), 1.40 (s, 3H).

^{13}C NMR (126 MHz, $CDCl_3$): δ 202.0, 141.5, 139.8, 128.8, 127.3, 127.3, 115.4, 53.5, 44.2, 24.2, 18.6.

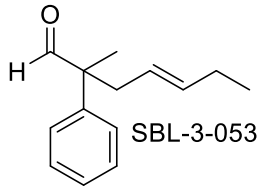

SBL-3-053 0.042g, 79%.

8k

93:7 linear:branched

linear product data reported

^{1}H NMR Spectra (500 MHz, $CDCl_3$): δ 9.45 (s, 1H), 7.30 (m, 2H), 7.19 (m, 3H), 5.42 (m, 1H), 5.09 (m, 1H), 2.53 (dd, *J* = 7.32, 1.16 Hz, 2H), 1.87 (m, 2H), 1.34 (s, 3H), 0.83 (t, *J* = 7.46 Hz, 3H).

^{13}C NMR (126 MHz, $CDCl_3$): δ 202.4, 139.9, 136.5, 128.8, 127.2, 127.1, 123.1, 53.9, 39.26, 25.6, 19.2, 13.8.

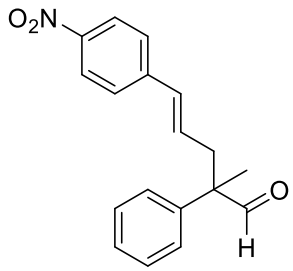

SBL-3-057 0.070g, 79%.

8l

93:7 linear to branched

linear data repoted

^{1}H NMR Spectra (500 MHz, $CDCl_3$): δ 9.55 (s, 1H), 8.11 (d, *J* = 8.76 Hz, 2H), 7.42 (dd, *J* = 8.24, 6.94 Hz, 2H), 7.35 (dd, *J* = 8.12, 6.89 Hz, 3H), 7.28 (m, 2H), 6.44 (d, *J* = 15.8 Hz, 1H), 6.13 (ddd, *J* = 15.8, 7.93, 7.00 Hz, 1H), 2.88 (ddd, *J* = 14.3, 7.01, 1.47 Hz, 1H), 2.81 (ddd, *J* = 14.3, 7.98, 1.28 Hz, 1H), 1.52 (s, 3H).

^{13}C NMR (126 MHz, $CDCl_3$): δ 201.4, 146.7, 143.5, 138.9, 131.7, 130.6, 129.1, 127.7, 127.1, 126.6, 124.0, 54.1, 40.1, 18.9.

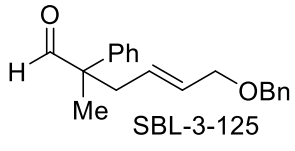

SBL-3-125 0.064g, 73%.

84:16 trans:cis

8m

^{1}H NMR Spectra (500 MHz, $CDCl_3$): δ 9.52 (s, 1H), 7.39 (m, 2H), 7.31 (m, 6H), 7.25 (m, 2H), 5.63 (dtt, *J* = 15.1, 6.17, 1.37 Hz, 1H), 5.47 (dtt, *J* = 14.6, 7.43, 1.24 Hz, 1H), 4.40, (s, 2H), 3.91 (ddd, *J* = 6.27, 2.31, 1.23 Hz, 2H), 2.71 (ddd, *J* = 14.3, 6.96, 1.34 Hz, 1H), 2.64 (ddd, *J* = 14.2, 7.70, 1.17 Hz, 1H), 1.46 (s, 3H).

^{13}C NMR (126 MHz, $CDCl_3$): δ 201.9, 139.3, 138.2, 130.6, 128.9, 128.6, 128.4 127.8, 127.6, 127.4, 127.2, 71.8, 70.4, 53.8, 39.1, 18.9.

HRMS: [M+Na] calc: 317.1512, found: 317.1515.

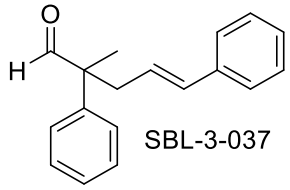

SBL-3-037 0.053g, 70%.

8n

96:4 linear:branched

linear product data reported

^{1}H NMR Spectra (300 MHz, $CDCl_3$): δ 9.58 (s, 1H), 7.41 (m, 2H), 7.28 (m, 6H), 7.20 (m, 2H), 6.41 (dt, *J* = 15.7, 1.33 Hz, 1H), 5.94 (dt, *J* = 15.2, 7.44 Hz, 1H), 2.81 (m, 2H), 1.50 (s, 3H).

^{13}C NMR (126 MHz, $CDCl_3$): δ 202.0, 139.4, 137.2, 133.6, 128.9, 128.5, 127.4, 127.3, 127.2, 126.1, 124.9, 54.1, 40.0, 19.0.

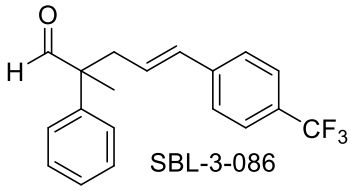

SBL-3-086 0.075g, 79%.

8o

^{1}H NMR Spectra (500 MHz, $CDCl_3$): δ 9.56 (s, 1H), 7.50 (d, *J* = 8.12 Hz, 2H), 7.42 (dd, *J* = 8.21, 6.96 Hz, 2H), 7.33 (m, 3H), 7.28 (dd, *J* = 8.37, 1.30 Hz, 2H), 6.41 (d, *J* = 16.0 Hz, 1H), 6.04 (ddd, *J* = 15.4, 7.93, 7.07 Hz, 1H), 2.86 (ddd, *J* = 14.2, 7.06, 1.45 Hz, 1H), 2.79 (ddd, *J* = 14.2, 7.92, 1.27 Hz, 1H), 1.51 (s, 3H).

^{13}C NMR (126 MHz, $CDCl_3$): δ 201.7, 140.6, 139.1, 132.3, 129.1 (q, *J* = 33.3 Hz), 129.0, 128.0, 127.6, 127.1, 126.2, 125.4 (q, *J* = 3.88 Hz), 124.2 (q, *J* = 271.82 Hz), 54.1, 40.0, 18.9.

Procedure for the reduction of compound 1e (Wurz, R. P.; Charette, A.B.; *J. Org. Chem*. **2004**, *69*. 1262-1269) and formation of the corresponding amine salt.

In a 50 mL round bottom flask equipped with a stir bar, compound **1e** (0.185 g, 0.59 mmol) was dissolved in 12 mL isopropanol. To this solution 1.5 M HCl (6.0 mL) and zinc dust (0.740 g, 11.3 mmol) were added and the solution was stirred at 50 ^{o}C for 2 hours. Saturated aq K_2CO_3 (8.0 mL) was added after the solution cooled to rt. The reaction mixture was filtered though a pad of celite and extracted 3x with 25 mL $CHCl_3$ washes. The combined organic layers were washed with 20 mL brine and dried over $MgSO_4$.

The dried solution was filtered and concentrated *in vacuo* to afford the corresponding amine as a colorless oil (0.072 g, 43%). 2.0 M HCl in diethyl ether (5.0 mL) was added to the amine and the solvent removed *in vaccuo* to provide a white solid which was re-crystallized from EtOAc to provide suitable crystals of the HCl salt.

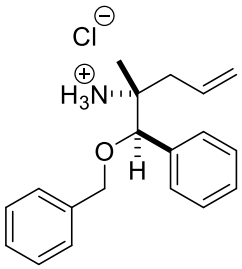

Major diastereomer shown.

^{1}H NMR Spectra (500 MHz, $CDCl_3$): Major diastereomer δ 8.55 (s, 3H), 7.36 (m, 10H), 5.98 (ddt, *J* = 16.4, 11.4, 7.49 Hz, 1H), 5.19 (m, 2H), 4.90 (s, 1H), 4.62 (d, *J* = 11.4 Hz, 1H), 4.33 (d, *J* = 11.4 Hz, 1H), 2.69 (dd, *J* = 14.6, 7.02 Hz, 1H), 2.17 (dd, *J* = 14.6, 7.73 Hz, 1H), 1.31 (s, 3H).

^{13}C NMR (126 MHz, $CDCl_3$): Major diasteromer δ 137.7, 135.3, 130.9, 128.7, 128.6, 128.4, 128.3, 128.06, 127.6, 127.5, 84.9, 71.3, 60.3, 37.6, 21.0.

HRMS: [$C_{19}H_{24}NO$]: calc: 282.1858, found: 282.1855

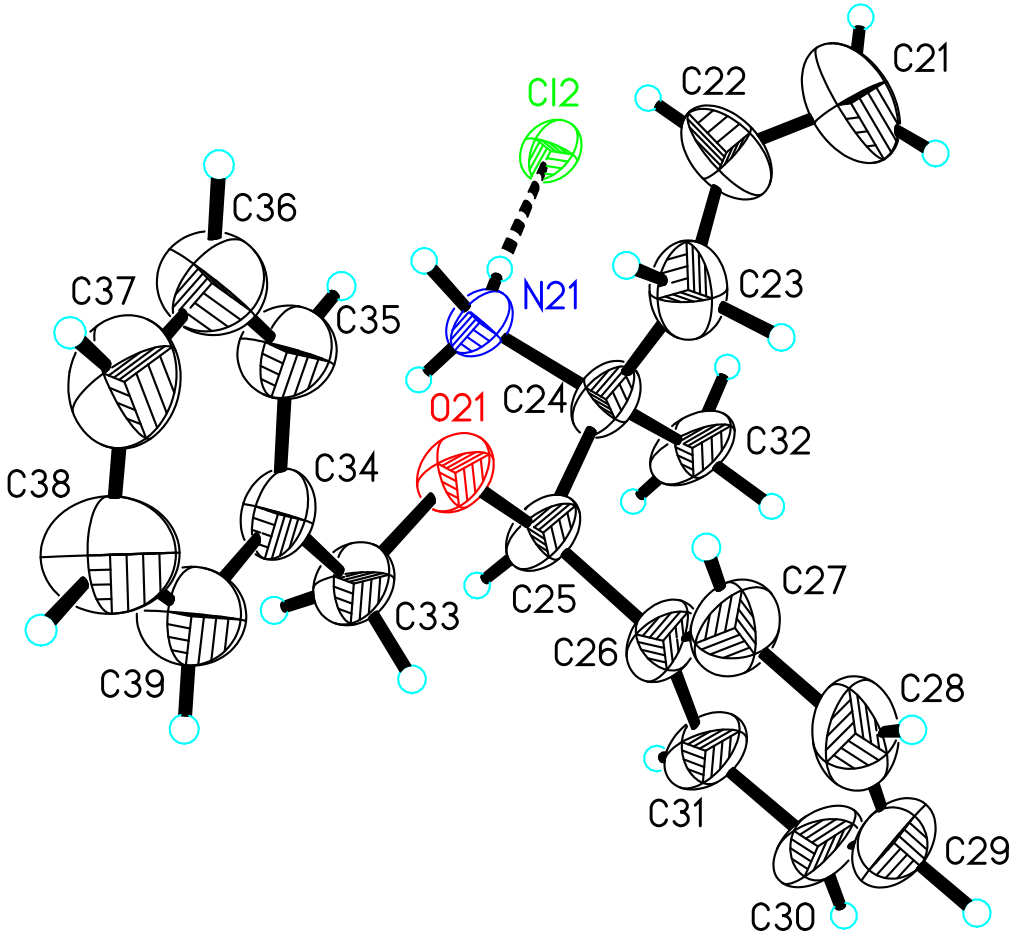

See: http://pubs.acs.org/doi/suppl/10.1021/ol502023d for .cif file.

Detailed description of x-ray crystal structure determination for $[C_{19}H_{24}NO][Cl]$:

The alignment reflections for determining the preliminary unit cell for the crystal of $[C_{19}H_{24}NO][Cl]$ (**1)** indexed quite well as a C-centered monoclinic lattice. The crystal was therefore believed to utilize a monoclinic space group and intensity data were collected accordingly. The monoclinic R_{sym} was 0.105 and the most probable space group appeared to be centrosymmetric C2/m. When the structure would not solve in C2/m, the intensity data were further analyzed and

this indicated the possible presence of a c-glide. The structure solved straightforwardly in the centrosymmetric space group C2/c with an asymmetric unit containing two $[C_{19}H_{24}NO][Cl]$ cation/anion pairs. When this structure failed to refine below $R_1 = 0.153$, the possibility of it being a triclinic structure that was pseudomerohedrally twinned to look monoclinic was considered. This turned out to be the case and the final centrosymmetric triclinic asymmetric unit has four nearly identical, but crystallographically-independent $[C_{19}H_{24}NO][Cl]$ cation/anion pairs, related by non-crystallographic pseudosymmetry. The crystals utilize the centro-symmetric triclinic space group $C\bar{1}$ [a nonstandard setting of $P\bar{1} - C_i^1$ (No. 2)] with lattice constants at 100K of: ***a*** =26.96214(19)Å, ***b*** = 12.68483(10)Å, ***c*** = 21.88641(18)Å, α = 90.4219(6)°, β = 104.5435(4)°, γ = 89.7970(4)°, V = 7245.3(1)Å^3 and Z = 16 $[C_{19}H_{24}NO][Cl]$ moieties. The crystals are pseudomerohedrally (68%/32%) twinned with the two domains related by a 180° rotation about the ***b*** axis.

The final centrosymmetric triclinic asymmetric unit contains four cation/anion pairs. All nonhydrogen atoms were included in the structural model with variable anisotropic thermal parameters. All twelve hydrogens for the protonated amine groups were located from difference Fourier syntheses and incorporated into the structural model as individual isotropic atoms whose parameters were allowed to vary in least-squares refinement cycles. Mild restraints were applied to the anisotropic thermal parameters of two carbon atoms [C(78) and C(79)] and three of the ammonium hydrogens were fixed at values 1.2 times the equivalent isotropic thermal parameter of their nitrogen atom. The remainder of the hydrogen atoms were placed at idealized sp^2- or sp^3-hybridized positions with C-H bond lengths of 0.95 - 1.00 Å and isotropic thermal parameters fixed at values 1.20 (nonmethyl) or 1.50 (methyl) times the equivalent isotropic thermal parameter of the carbon atom to which they are bonded. Methyl groups were placed at idealized “staggered” positions. The terminal ethylene group for the first cation is 57%/43% disordered between two conformations and both of these were restrained to have metrical parameters similar to that group in the fourth cation.

The final least-squares refinement cycles for **1** in space group $C\bar{1}$ utilized anisotropic thermal parameters for all nonhydrogen atoms, isotropic thermal parameters for all hydrogen atoms, 867 variables, 51 restraints and 11861 reflections having $2\theta(CuK\alpha) < 140.10°$. Final agreement factors at convergence for **1** are: R_1(unweighted, based on F) = 0.078 for 10457 independent absorption-corrected "observed" reflections having $2\theta(CuK\alpha) < 140.10°$ and $I>2\sigma(I)$; R_1(unweighted, based on F) = 0.086 and wR_2(weighted, based on F^2) = 0.213 for all 11861 independent absorption-corrected reflections having $2\theta(CuK\alpha) < 140.10°$. The largest shift/s.u. was 0.000 in the final refinement cycle. The final difference map had maxima and minima of 0.59 and -0.56 $e^-/Å^3$, respectively.